

# AIRCRAFT ACCIDENT REPORT 1/2023



Report on the accident to  
**Leonardo AW169, G-VSKP**  
at King Power Stadium, Leicester  
on 27 October 2018





**Air Accidents Investigation Branch**

---

---

Report on the accident to  
Leonardo AW169, registration G-VSKP  
at King Power Stadium, Leicester  
on 27 October 2018

---

This investigation has been conducted in accordance with  
*Annex 13 to the ICAO Convention on International Civil Aviation,*  
*EU Regulation No 996/2010 and*  
*The Civil Aviation (Investigation of Air Accidents and Incidents) Regulations 2018.*

The sole objective of the investigation of an accident or incident under these Regulations is the prevention of future accidents and incidents. It is not the purpose of such an investigation to apportion blame or liability.

Accordingly, it is inappropriate that AAIB reports should be used to assign fault or blame or determine liability, since neither the investigation nor the reporting process has been undertaken for that purpose.

---

© *Crown Copyright 2023*

This report contains facts which have been determined up to the time of publication. This information is published to inform the aviation industry and the public of the general circumstances of accidents and serious incidents.

Extracts may be published without specific permission providing that the source is duly acknowledged, the material is reproduced accurately and it is not used in a derogatory manner or in a misleading context.

Cover picture courtesy of JML.

Published: 6 September 2023.

**Printed in the United Kingdom for the Air Accidents Investigation Branch**

---



1.6.12	Cabin configuration .....	49
1.6.13	Health and Usage Monitoring System (HUMS) .....	49
1.6.14	Air-Data Attitude Heading Reference System (ADAHRS) – data bus limits .....	53
1.6.15	Flight Control Computer (FCC) .....	54
1.6.16	Crew alerting system .....	54
1.7	Meteorological information.....	54
1.8	Aids to navigation.....	54
1.9	Communications .....	54
1.10	Aerodrome information .....	55
1.10.1	Aerodrome .....	55
1.10.2	LCFC training ground.....	55
1.10.3	King Power Stadium .....	55
1.11	Recorded information.....	55
1.11.1	Flight recorder.....	56
1.11.2	Avionics.....	57
1.11.3	Witness videos and imagery .....	59
1.11.4	Personal electronic devices .....	60
1.11.5	Radar and air traffic control radio transmissions .....	60
1.11.6	Accident flight.....	60
1.11.7	Previous flights.....	66
1.11.8	HUMS .....	68
1.11.9	Comparison of recorded data with published limitations.....	70
1.12	Wreckage and impact information .....	71
1.12.1	Initial site inspection.....	71
1.12.2	Results of the initial forensic laboratory investigation .....	73
1.12.3	Results of the in-depth forensic laboratory investigation .....	78
1.12.4	Post-accident continued airworthiness response .....	86
1.12.5	Investigation of other failed bearings identified by emergency checks .....	88
1.13	Medical and pathological information.....	100
1.14	Fire.....	101
1.15	Survival aspects.....	101
1.15.1	Certification requirements .....	101
1.15.2	AW169 crashworthiness .....	103
1.15.3	Examination of wreckage related to crashworthiness .....	104
1.16	Tests and research.....	106
1.16.1	Engineering tests and trials.....	106
1.16.1.1	Post-accident bearing tests .....	106

1.16.1.2	Investigation requested endurance rig test .....	107
1.16.1.3	Manufacturer's subsequent rig test .....	109
1.16.1.4	Review of AW169 flight test and rig test bearing contact pressures .....	120
1.16.2	Impact assessment .....	126
1.16.3	Flight simulator trials .....	128
1.16.4	Manufacturer's additional flight mechanics analysis .....	129
1.17	Organisational and management information .....	130
1.17.1	Requirements for non-commercial operations with complex aircraft .....	130
1.17.1.1	Complex helicopters .....	130
1.17.1.2	Part-NCC Operator requirements .....	130
1.17.2	Congested area operations .....	131
1.17.3	Operational oversight .....	132
1.18	Additional information .....	132
1.18.1	AW109 Cat A profile .....	132
1.18.2	Reported drone sightings .....	133
1.18.3	Research regarding pilot response to helicopter tail rotor emergencies .....	133
1.18.4	Startle and surprise .....	134
1.18.5	Critical Part .....	134
1.18.6	Rolling Contact Fatigue (RCF) .....	135
1.18.7	Grease lubrication .....	137
1.18.8	Dark Etched Region .....	142
1.18.9	Avionics simulator – yaw rate effects .....	142
1.18.10	Flight mechanics simulation .....	143
1.18.11	Vibration monitoring of the duplex bearing .....	143
1.18.12	Previous accidents .....	146
1.18.13	Rule Making Tasks (RMT) 128 and 712 .....	149
1.18.14	Certification Specifications for Engines (CS-E) .....	150
<b>2</b>	<b>Analysis .....</b>	<b>151</b>
2.1	General .....	151
2.2	Helicopter operation .....	151
2.3	Stadium departure .....	152
2.4	Emergency handling .....	153
2.5	External operational factors .....	157
2.6	Accident flight recorded data .....	157
2.7	Loss of tail rotor control .....	158

2.8	Crashworthiness and survivability.....	160
2.9	Duplex Bearing failure .....	162
2.9.1	Investigation-requested endurance rig test .....	165
2.9.2	Manufacturer's subsequent rig test.....	165
2.9.3	Conclusions from the bearing investigation .....	167
2.9.4	Associated factors.....	184
2.10	Safety Actions .....	193
2.11	Operational oversight.....	195
2.12	HUMS .....	195
<b>3</b>	<b>Conclusions.....</b>	<b>197</b>
3.1	Findings .....	197
3.2	Causal Factors.....	204
3.3	Contributory Factors .....	204
<b>4</b>	<b>Safety Recommendations and Actions.....</b>	<b>205</b>
4.1	Safety Recommendations.....	205
4.2	Safety action .....	207

## APPENDICES

Appendix A - Summary of the accident pilot's flying experience.....	211
Appendix B - AW169 flight simulator trials .....	212
Appendix C - Summary of pilot response times from previous accidents .....	220
Appendix D - Flight recorder issues .....	221
Appendix E - AW169 flight test load survey and contact pressure analysis.....	231
Appendix F - Certification Specification E.515 - Engine Critical Parts .....	234
Appendix G - Notice of proposed Amendment 2022/01 .....	249
Appendix H - Extracts from EASA Certification Specification 29 Amendment 2.....	255
Appendix I - Changes to Certification Specification 29 Amendment 11 .....	271
Appendix J - Flight mechanics analysis information provided by the helicopter manufacturer .....	277
Appendix K - Comments of the ANSV representing the State of Design and Manufacture.....	280

## GLOSSARY OF ABBREVIATIONS USED IN THIS REPORT

AAIB	Air Accidents Investigation Branch	CIVP	Continued Integrity Verification Programme
Accrep	Accredited Representative	CIVPP	Continued Integrity Verification Programme Plan
agl	above ground level	CIVPR	Continued Integrity Verification Programme Report
AC	Advisory Circular (FAA)	CMR	Critical Maintenance Requirements
AD	Airworthiness Directive	CRD	Comment Response Document
ADAHRS	Air-Data Attitude Heading Reference System	CS	Certification Specification
ADAHRU	Air-Data Attitude Heading Reference System Units	CS-E	Certification Specifications for Engines
AEH	Airborne Electronic Hardware	CT	Computed Tomography
AFCS	Automatic Flight Control System	CTO	Continued Takeoff Speed
AHRS	Attitude Heading Reference System	DAFR	Data Acquisition Flight Recorder
ALS	Airworthiness Limitations Section	daN	Decanewton
AMC	Acceptable Means of Compliance	daNm	Decanewton metre
AMMC	Aircraft and Mission Management Computers	DER	Dark Etched Region
AMPI	Approved Maintenance Planning Information	DSN	Download Sequence Number
ANSV	Agenzia Nazionale per la Sicurezza del Volo – Italy	DTD	Data Transfer Device
AoA	Angle of Attack	EASA	European Union Aviation Safety Agency
AOC	Air Operator's Certificate	ED	EUROCAE Document
AP	Autopilot	EDAX	Energy-Dispersive Analysis of X-rays
ASB	Alert Service Bulletin	EHL	Elastohydrodynamic Lubrication
ATC	Air Traffic Control	EMI	Electromagnetic Inteference
ATD	Anthropomorphic Test Dummy	ES	Engineering Simulator
ATPL(H)	Airline Transport Pilot's Licence (Helicopters)	ESUM	Reference to continuously recorded flight parameters in the DTD
ATS	Above the Takeoff Surface	EUROCAE	European Organisation for Civil Aviation Equipment
ATT	'Attitude hold' autopilot mode	Fa	Axial load
AUW	All-up Weight	FAA	Federal Aviation Administration
AVSR	Adaptive Variable Speed Rotor	FCC	Flight Control Computer
BBJ	Boeing Business Jet	FDM	Flight Data Monitoring
BEA	Bureau d'Enquêtes et d'Analyses pour la sécurité de l'aviation civile	FDR	Flight Data Recorder
CAA	Civil Aviation Authority	FFS	Full Flight Simulator
CAM	Cockpit Area Microphone	FMEA	Failure Modes and Effects Analysis
Cat A or B	Category A or Category B	FSTD	Flight Simulation Training Device
CCTV	Closed Circuit Television	ft	Feet
CCU	Cockpit Control Unit		
CG	Centre of Gravity		

**GLOSSARY OF ABBREVIATIONS USED IN THIS REPORT cont**

ft/min	Feet per minute	NTSB	National Transportation Safety Board
FY	Radial load	NVM	Non-volatile Memory
FZ	Axial load	OEI	One Engine Inoperative
g	Acceleration due to gravity	OTL	Operating Time Limit
GM	Guidance Material	PC	Performance Class
GPS	Global Positioning System	PIC	Pilot in Command
HEMS	Helicopter Emergency Medical Services	PFD	Primary Flight Display
HI	Health Index or Health Indicator	p/n	Part number
HIC	Head Injury Criteria	POD	Probability of Detection
hrs	Hours	PSE	Principal Structural Elements
HQ	Headquarters	PV	Reference indicator of bearing duress
HTL	High Temperature Limit	PVmax	Highest value of PV
HTPL	High Temperature Performance Limit	QPD	Qualified Products Database
HUMS	Health and Usage Monitoring System	RCF	Rolling Contact Fatigue
KEAS	Knots Equivalent Airspeed	RIPS	Recorder Independent Power Supply
kg	Kilograms	RFM	Rotorcraft Flight Manual
kHz	Kilohertz	RT	Radio Transmission
KIAS	Knots Indicated Airspeed	rpm	Revolutions per minute
kN	Kilonewtons	RMT	Rule Making Task
lbs	Pounds	SB	Service Bulletin
LCF	Low-cycle Fatigue	sec	Second(s)
LCFC	Leicester City Football Club	SEM	Scanning Electron Microscope
LTE	Loss of Tail Rotor Effectiveness	SFE(A)	Simulator Flying Examiner (Aircraft)
LTL	Low Temperature Limit	SFI(A)	Simulator Flying Instructor (Aircraft)
LTPL	Low Temperature Performance Limit	SMS	Safety Management System
m	Metres	s/n	Serial number
M	Moment	SUSA	Small Unmanned Surveillance Aircraft
mm	Millimetres	TAS	True Airspeed
MRB	Maintenance Review Board	TCAS	Traffic Alert and Collision Avoidance System
ms	Milliseconds	TCDS	Type Certificate Data Sheet
MSG	Maintenance Steering Group	TDH	Tie Down Helicopter
MTOW	Maximum Takeoff Weight	TDP	Takeoff Decision Point
N	Newtons	TC	Type Certificate
NCC	Non-commercial operations with complex motor-powered aircraft	TGB	Tail Rotor Gearbox
Ng	Rotational speed - gas generator stage	TP	Test Pilot
Nm	Newton metres	TQ	Torque
NPA	Notice of Proposed Amendment	TRA	Tail Rotor Actuator
N <sub>R</sub>	Rotational speed - rotor	TRE	Type Rating Examiner
		TRI	Type Rating Instructor
		TSB	Transportation Safety Board of Canada

## GLOSSARY OF ABBREVIATIONS USED IN THIS REPORT

TVM	Transmission Vibration Monitoring	$^{\circ}/s$	Degrees per second
		$^{\circ}M$	Degrees Magnetic
UTC	Coordinated Universal Time	$\eta_{oil}$	Grease base oil viscosity
$V_{NE}$	Never-exceed speed	$h_R$	Grease thickener boundary layer thickness
$V_{TOSS}$	Takeoff safety speed		Grease base oil
$V_Y$	Speed for best rate of climb	$h_{EHL}$	elastohydrodynamic lubrication boundary layer thickness
$V_{DAM}$	Vibration Data Acquisition Module		Grease total film thickness
VIP	Very Important Person		
VHM	Vibration Health Monitoring	$h_T$	

**Intentionally left blank**

## Air Accidents Investigation Branch

Aircraft Accident Report No:	1/2023 (AAIB-25398)
Registered Owner:	Foxborough Limited (Isle of Man)
Registered Operator:	Starspeed Limited
Aircraft Type:	Leonardo AW169
Nationality:	British
Registration:	G-VSKP
Place of Accident:	King Power Stadium, Leicester
Date and Time:	27 October 2018 at 1937 hrs (All times in this report are UTC)

## Introduction

The Air Accidents Investigation Branch (AAIB) became aware of this accident during the evening of 27 October 2018. In exercise of his powers, the Chief Inspector of Air Accidents ordered an investigation to be carried out in accordance with the provisions of Regulation (EU) 996/2010 and the UK Civil Aviation (Investigation of Air Accidents and Incidents) Regulations 2018.

The sole objective of the investigation of an accident or incident under these regulations is the prevention of future accidents and incidents. It shall not be the purpose of such an investigation to apportion blame or liability.

In accordance with established international arrangements, the Agenzia Nazionale per la Sicurezza del Volo (ANSV) of Italy, representing the State of Design and Manufacture of the helicopter, appointed an Accredited Representative (Accrep) to participate in the investigation. The Transportation Safety Board (TSB) of Canada, representing the State of Design and Manufacture for the helicopter's engines, the National Transportation Safety Board (NTSB) of the USA, representing the State of Design and Manufacture of the tail rotor actuator and the Bureau d'Enquêtes et d'Analyses pour la sécurité de l'aviation civile (BEA) of France representing the State of Design and Manufacture of the tail rotor duplex bearing, also appointed Accreps.

Experts<sup>1</sup> were appointed by the Aircraft Accident Investigation Committee of Thailand and the State Commission on Aircraft Accidents Investigation of Poland.

The helicopter, bearing, tail rotor actuator and grease manufacturers, the operator, the European Union Aviation Safety Agency (EASA), and the UK Civil Aviation Authority (CAA) also assisted the AAIB investigation.

## Summary

At 1937 hrs the helicopter, carrying the pilot and four passengers, lifted off from the centre spot of the pitch at the King Power Stadium. The helicopter moved forward and then began to climb out of the stadium on a rearward flightpath while maintaining a northerly heading and with an average rate of climb of between 600 and 700 ft/min. Passing through a height of approximately 250 ft, the pilot began the transition to forward flight by pitching the helicopter nosedown and the landing gear was retracted. The helicopter was briefly established in a right turn before an increasing right yaw rapidly developed, despite the immediate application of corrective control inputs from the pilot. The helicopter reached a radio altimeter height of approximately 430 ft before descending with a high rotation rate. At approximately 75 ft from the ground the collective was fully raised to cushion the touchdown.

The helicopter struck the ground on a stepped concrete surface, coming to rest on its left side. The impact, which likely exceeded the helicopter's design requirements, damaged the lower fuselage and the helicopter's fuel tanks which resulted in a significant fuel leak. The fuel ignited shortly after the helicopter came to rest and an intense post-impact fire rapidly engulfed the fuselage.

The investigation found the following causal factors for this accident:

1. Seizure of the tail rotor duplex bearing initiated a sequence of failures in the tail rotor pitch control mechanism which culminated in the unrecoverable loss of control of the tail rotor blade pitch angle and the blades moving to their physical limit of travel.
2. The unopposed main rotor torque couple and negative tail rotor blade pitch angle resulted in an increasing rate of rotation of the helicopter in yaw, which induced pitch and roll deviations and made effective control of the helicopter's flightpath impossible.
3. The tail rotor duplex bearing likely experienced a combination of dynamic axial and bending moment loads which generated internal contact pressures sufficient to result in lubrication breakdown and the balls sliding across the race surface. This caused premature, surface initiated rolling contact fatigue damage to accumulate until the bearing seized.

---

<sup>1</sup> Representing States which suffered fatalities to its citizens in the accident.

The investigation found the following contributory factors for this accident:

1. The load survey flight test results were not shared by the helicopter manufacturer with the bearing manufacturer in order to validate the original analysis of the theoretical load spectrum and assess the continued suitability of the bearing for this application, nor were they required to be by the regulatory requirements and guidance.
2. There were no design or test requirements in Certification Specification 29 which explicitly addressed rolling contact fatigue in bearings identified as critical parts; while the certification testing of the duplex bearing met the airworthiness authority's acceptable means of compliance, it was not sufficiently representative of operational demands to identify the failure mode.
3. The manufacturer of the helicopter did not implement a routine inspection requirement for critical part bearings removed from service to review their condition against original design and certification assumptions, nor were they required to by the regulatory requirements and guidance.
4. Although the failure of the duplex bearing was classified as catastrophic in the certification failure analysis, the various failure sequences and possible risk reduction and mitigation measures within the wider tail rotor control system were not fully considered in the certification process; the regulatory guidance stated that this was not required.

AAIB Special Bulletin S1/2018, published on 14 November 2018 and AAIB Special Bulletin S2/2018, published on 6 December 2018, provided initial information on the circumstances of this accident.

During the course of this investigation and as a result of the findings made, the helicopter manufacturer has issued sixteen Service Bulletins and EASA has published nine Airworthiness Directives for the continued airworthiness of the AW169 and AW189 helicopter types.

Eight Safety Recommendations have been made in this report. These have been made to EASA to address weaknesses or omissions identified in the regulations for the certification of large helicopters - Certification Specification 29. The recommendations address the main findings of the investigation and include: validation of design data by suppliers post-test; premature rolling contact fatigue in bearings; life limits, load spectrum safety margin and inspection programmes for critical parts; and assessment and mitigation of catastrophic failure modes in systems.

**Intentionally left blank**

## 1 Factual information

### 1.1 History of the flight

#### 1.1.1 Background

G-VSKP was a corporately owned Leonardo AW169 helicopter operated out of Fairoaks Airport, Surrey, UK.

The helicopter was used to support the business and personal transportation requirements of the staff of one of the corporate owner's sister companies. It was operated in the single-pilot role under the requirements for non-commercial operations with complex motor-powered aircraft<sup>1</sup>.

A regular task undertaken by the helicopter was to convey corporate personnel and guests to football matches and business meetings in Leicester. Two landing sites routinely used for flights to the city were Leicester City Football Club's (LCFC) training ground and the King Power Stadium (Figure 1), both under the control of the helicopter's owner. G-VSKP's operations at these two sites were within the scope of the helicopter operator's delegated congested areas permission, granted by the CAA.

The pilot was the primary pilot for G-VSKP and conducted most of its flights but was not directly employed by the owner of the helicopter. While not a regulatory requirement, G-VSKP was regularly operated with a second person, who was a pilot but not necessarily qualified to fly a helicopter, in the cockpit. This second pilot was classified as a passenger but assisted with lookout and VIP passenger handling. The second pilot<sup>2</sup> for the accident flight was a commercially licensed fixed wing pilot and regularly flew the owner's corporate aircraft.

#### 1.1.2 Previous flights on 27 October 2018

##### *Fairoaks to Leicester training ground*

On 27 October 2018, G-VSKP was scheduled to fly corporate personnel to and from Leicester to allow them to attend a football match at the King Power Stadium.

The pilot, accompanied by the front seat passenger, arrived at the airfield approximately 40 minutes before departure. Air Traffic Control records show that the helicopter took off from Fairoaks at 1342 hrs with two people on board and flew to London Heliport.

1 Established in Annex VI (Part-NCC) of Commission Regulation (EU) No 965/2012.

2 Hereinafter called the 'front seat passenger'.



**Figure 1**

G-VSKP landing sites in Leicester (image ©2018 Google)

G-VSKP arrived at London Heliport at 1402 hrs and picked up three corporate passengers, before departing for Leicester at 1415 hrs. It landed at the LCFC training ground at 1459 hrs and all five occupants travelled onward to the King Power Stadium by car.

#### *Training ground to stadium*

While the pilot was at the stadium, he was observed checking weather and planning the onward flights. He and the front seat passenger left the stadium before the end of the match and returned to the helicopter. CCTV footage showed that they passed through the training ground security post at 1835 hrs and walked the short distance to where the helicopter was parked.

The match ended at 1815 hrs and by 1835 hrs the stadium had been declared clear of spectators. The match-day coordinator liaised with the police operations team to ensure that their small, unmanned surveillance aircraft (SUSA)<sup>3</sup> was clear of the area. They then gave permission for the flight into the stadium. A football club official relayed the flight clearance to the pilot by mobile phone at 1837 hrs.

At 1844 hrs the helicopter lifted off for the short flight to the King Power Stadium, 1 mile to the north. The approach into the stadium was made at 1847 hrs. After landing, the helicopter was parked on the centre spot facing the north-easterly goal. The pilot and front seat passenger both left the helicopter.

### 1.1.3 Accident flight

The onward flight was planned to London Stansted Airport, where a corporate aircraft was waiting for the three rear-cabin passengers. Between 1900 hrs and 1933 hrs the original five occupants returned to and boarded G-VSKP. No other persons were seen to have approached close to the helicopter.

In conversations captured on cockpit voice recordings prior to departure, the pilot sounded relaxed and unhurried during cockpit preparation and engine start.

At 1935 hrs, the main rotor started to turn and at 1937 hrs the helicopter lifted from the centre spot of the pitch. The helicopter moved forward and then began a climb on a rearward flightpath while maintaining a northerly heading and with an average rate of climb of between 600 and 700 ft/min. Passing through a height of approximately 250 ft the pilot began pitching the helicopter nose-down through 15° over a period of six seconds. During the pitch down he called “GEAR UP PLEASE” and shortly afterwards the landing gear began retracting. Roll and yaw changes consistent with entry to a gently banked right turn were observed as the helicopter climbed through approximately 300 ft. The helicopter briefly stabilised in the turn before an increasing right yaw rapidly developed (Figure 2). The pilot immediately started to apply left pedal and full deflection was reached after about one second. At that point an exclamation of “HEY, HEY, HEY” came from the rear cabin, after which the pilot said, “I’VE NO IDEA WHAT’S GOING ON”. Four seconds after the onset of the uncommanded yaw, the pilot uttered an exclamation. A ROTOR LOW warning occurred. The pilot began to lower the collective lever about five seconds after full left pedal was applied and it was fully lowered over a two second period. The helicopter reached a radio altimeter height of approximately 430 ft before descending with a high rotation rate which peaked at 209°/s. Pitch and roll oscillations accompanied the high yaw rate. At approximately 75 ft the collective was fully raised to cushion the impact.

<sup>3</sup> Commonly referred to as a ‘drone’.

The helicopter struck the ground on a stepped concrete surface, while still rotating and with the landing gear retracted (Figure 2). It came to a stop and then rolled onto its left side and was rapidly engulfed in an intense post-impact fire. Stadium staff and emergency services were quickly at the scene but were not able to gain access to the helicopter because of the intensity of the fire.

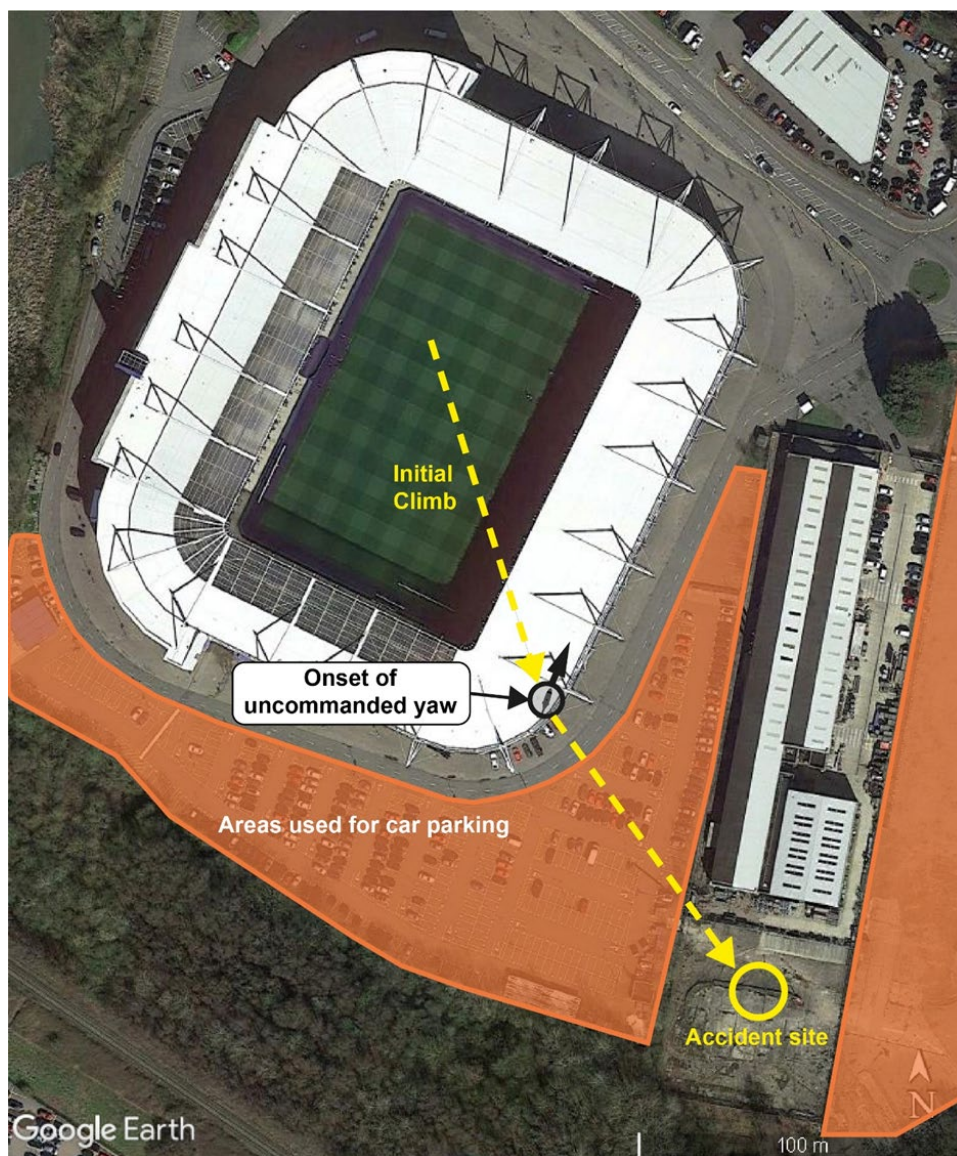


**Figure 2**

Approximate trajectory of G-VSKP on the accident flight  
Map data © 2021 Google

## 1.2 Injuries to persons

Injuries	Crew	Passengers	Others
Fatal	1	4	0
Serious	0	0	0
Minor/None	0	0	4*

(\*heat injuries sustained by first-responders)

## 1.3 Damage to the aircraft

The helicopter was severely damaged both in the initial impact with the ground and the subsequent fire.

### *Impact damage*

The tail section separated from the main wreckage at the end of the tail boom during the impact. The main rotor blades were damaged and sections of individual blades had separated at differing lengths; from the whole blade to approximately two thirds of the blade length. The sections of released blade were distributed some distance from the main wreckage location. The tail rotor blades were also damaged. This ranged from tip removal to loss of the full blade from close to the blade root.

The four doors had been ejected from the fuselage. The cabin windows had also been broken in various places, but the cockpit windscreen initially remained intact. The fuselage structure around the fuel tank was damaged and the integrity of the fuel tank was compromised.<sup>4</sup>

### *Fire damage*

The carbon fibre fuselage was largely destroyed by the post-impact fire. Most of the cockpit structure had been completely consumed including both the carbon fibre and aluminium elements. The passenger cabin and rear fuselage retained more of its structural shape, but most of the resin within the carbon fibre had been consumed resulting in a loss of structural rigidity.

The metallic components and structure, particularly the high strength materials used in the landing gear, engines, gearboxes and transmission system, main and tail rotor hubs, hydraulic flight control actuators and the engine deck survived the fire largely intact. The avionics boxes and wiring were severely heat damaged but remained identifiable.

<sup>4</sup> See 'survival aspects', [section 1.15.3](#) for a more detailed description.

## 1.4 Other damage

There was some structural damage to the small wall which formed the edge of the step which the aircraft struck. There was also extensive contamination of the ground with fuel and products of combustion.

## 1.5 Personnel information

### 1.5.1 Pilot

Age:	53 years
Licences:	Airline Transport Pilot's Licence (Helicopters) Airline Transport Pilot's Licence (Aeroplanes)
Licence expiry date:	Valid for life
Pilot proficiency check:	Valid until 31 October 2019 (AW169)
Class 1 medical examination:	14 March 2018
Flying experience:	Total on all types: 12,947 hours Total on helicopters: 4,784 hours Total on type: 177 hours Last 90 days: 41 hours Last 28 days: 7 hours Last 24 hours: 2 hours
Previous rest period:	The pilot had not flown during the week prior to the accident.

### 1.5.2 Background information

#### 1.5.2.1 Pilot

The pilot was the primary pilot for G-VSKP and conducted most of its flights but was not directly employed by the owner of the helicopter. He was qualified on, and regularly flew, the owner's AW109 helicopter and their Boeing B737-7EI Business Jet (BBJ). During 2018 he had flown 55 hours in G-VSKP, 17 hours in AW109 helicopters as well as 74 hours in the BBJ and other Boeing 737 aircraft. The pilot was a type rating instructor (TRI) on AW109 and AW169 helicopters and was a type rating examiner (TRE) for the Boeing 737 family of aircraft, which included the BBJ. A summary of the accident pilot's flying experience and instructor ratings is included at [Appendix A](#).

#### 1.5.2.2 Front seat passenger

The front seat passenger was a pilot who flew the helicopter owner's fixed wing aircraft and, with the accident pilot as her instructor, she had completed over 55 hours of Private Pilot's Licence training on Robinson R22 helicopters. It was planned that she would become qualified on the AW169 in due course but had yet to begin formal training on type. Cockpit voice recordings indicated that, under the pilot's supervision, on the day of the accident she flew the departure from Fairoaks and from the training ground. On both these flights there were no others on board the helicopter and the pilot took control for the approach and landing. The investigation was not able to determine if she had flown G-VSKP on previous occasions.

#### 1.5.3 Training and checking

The pilot undertook initial type conversion training on the AW169 in October 2016. This training was conducted at the helicopter manufacturer's facility in Italy. The course syllabus included discussion, demonstration and practise of the Loss of Tail Rotor Effectiveness (LTE) emergency procedure. The pilot's training report form showed that he achieved a 'Very Good' standard when practising the LTE and autorotation drills. Because it was not a certification requirement, the course did not include training for the specific mode of failure experienced on the accident flight.

Training for the Category A (Cat A) '*Ground and Elevated Heliport/Helideck Variable Takeoff Decision Point (TDP) Procedure*'<sup>5</sup> takeoff profile required for operations from the stadium was also not included in the pilot's AW169 type rating course syllabus.

In October 2017 the pilot successfully completed the manufacturer's TRI course conducted on G-VSKP. His AW169 TRI rating was valid until 31 October 2020.

The pilot completed a proficiency check with an examiner for the revalidation of his AW169 type rating eight days before the accident flight. The examiner reported that during the revalidation they discussed and practised Cat A departure profiles as appropriate for the King Power Stadium. The recorded flight data from the check flight revealed that three rearward climb profiles were carried out. The first profile showed a maximum rate of climb of 400 ft/min and a level-off at 130 ft agl. The second and third profiles showed a maximum rate of climb of 300 ft/min and were levelled-off at 120 ft agl. All three profiles were terminated with a return to the takeoff surface; transition to forward flight was not practised. A simulated tail rotor control malfunction, with tail rotor at fixed pitch, was also practised. The helicopter was landed successfully following this simulated emergency.

---

5 See [section 1.6.7](#) Helicopter performance.

## 1.6 Aircraft information

### *General*

Manufacturer:	Leonardo S.p.A. <sup>6</sup>
Type:	AW169
Engines:	2 Pratt & Whitney PW210A turboshaft engines
Manufacturer's serial number:	69018
Year of manufacture:	11 July 2016
Certificate of Airworthiness:	Issued 11 July 2016
Certificate of Registration:	Issued 20 July 2016
Airworthiness Review Certificate:	Expiry date 10 July 2019
Last maintenance check:	Bi-weekly check 22 October 2018
Total airframe hours:	330.9 hours
Total airframe landings:	1,034 landings

Two voyage reports were identified which recorded the takeoff weight for two earlier stadium departures as 4,550 kg, with 410 kg fuel, and 4,580 kg, with 510 kg of fuel respectively. The aircraft system recorded a total fuel mass of 510 kg for the accident flight. Based on these figures the helicopter's all-up weight for the accident flight was estimated as being between 4,500 kg and 4,600 kg.

### 1.6.1 Maintenance and bearing manufacturing process review

The helicopter was compliant with all applicable airworthiness requirements, had been correctly maintained and was appropriately certified for release to service prior to the accident flight. The records showed that on 6 July 2017 G-VSKP had been modified, in accordance with Leonardo Technical Bulletin 169-024, to operate at a higher maximum takeoff weight of 4,800 kg.

The tail rotor duplex bearing manufacturing process was also reviewed to assess the implications of findings from a quality audit conducted by the helicopter manufacturer after the accident and to consider the potential for contamination of the bearing during manufacture. The audit findings were reviewed and found to be administrative in nature. They were rectified by administrative updates, with no material change to the manufacturing process. No evidence was found that contamination was a significant risk during manufacture, with various precautionary safeguards taken to prevent this.

---

6 The helicopter manufacturer was called AgustaWestland at the time of the AW169 type certificate issue and the manufacture date of the accident helicopter. On 28 July 2016 AgustaWestland S.p.A. was renamed Leonardo S.p.A. which was the name of the company at the time of the accident.

## 1.6.2 Aircraft description

The AW169 is the most recently certified model in the AW family of helicopters, which includes the AW139 and AW189. It formally started development in February 2011 and was granted a type design certificate in July 2015.

The helicopter is 14.65 m long, 2.53 m wide, 4.5 m high and has a normal maximum gross weight of 4,600 kg. It is certified for a maximum of 11 passengers and one or two crew operation, but in executive passenger configuration the cabin is more typically equipped to carry six or seven passengers, as was the case with the accident aircraft. It has an endurance of 4 hours 20 minutes and a range of 440 nm.

The helicopter has a predominantly carbon fibre fuselage, with a retractable tricycle landing gear and hydraulically powered flight controls, with mechanical control linkages. It has a glass cockpit and a four-axis digital Automatic Flight Control System (AFCS).

The helicopter is twin-engined and has a conventional main gearbox which drives a five blade main rotor, and a three blade tail rotor via a tail rotor gearbox.

The AW189 has the same tail rotor control system as the AW169 but uses a larger four blade tail rotor that operates at a different rotational speed. The AW139 has a similar tail rotor to the AW189, with four tail rotor blades, but has small differences in the design of the control system compared to the AW169 and AW189.

The AW139 was the first of the three models to be introduced. Formally starting development in March 1999 and being granted a type design by ENAC<sup>7</sup> in June 2003. The subsequent EASA type certification approval date was September 2003. The AW139 has a certified Maximum Takeoff Weight (MTOW) of 6,400 kg, which can be increased to either 6,800 or 7,000 kg when the helicopter is operated in accordance with the relevant Rotorcraft Flight Manual (RFM) supplement, and the appropriate mod kit is embodied. It has an operating ceiling of 20,000 ft.

The AW189 was the second of the three models to be introduced into service. It was initially developed as the military AW149, before a civilian version was launched in May 2011 for EASA certification under the AW189 name. It was granted a type design certificate in February 2014. The AW189 has a certified maximum takeoff weight of 8,300 kg, which can be increased to 8,600 kg when operating to RFM Supplement 2. It has an operating ceiling of 15,000 ft.

<sup>7</sup> Ente Nazionale per l'Aviazione Civile – Italian national airworthiness authority.

The AW169 has a certified maximum takeoff weight of 4,600 kg, which can be increased to 4,800 kg when the helicopter is modified in accordance with Technical Bulletin 169-024. It has an operating ceiling of 15,000 ft.

The Type Certificate Data Sheet for the AW169, No EASA.R.509<sup>8</sup>, states that the AW169 helicopter type was certified in accordance with EASA Certification Specification (CS) 29 Amendment 2<sup>9</sup>, dated 17 November 2008. CS 29 details the design and test requirements for certification of large helicopters.

#### *Description of the yaw control system*

Helicopters can manoeuvre in three axes: pitch, roll and yaw. The yaw axis runs through the axis of rotation of the main rotor blades, with yaw rotation occurring around it. Movement about this axis is controlled by a set of opposing foot pedals, which change the tail rotor blade pitch. Pressing the right pedal forward pushes the left pedal back and rotates the nose to the right, pressing the left pedal forward, pushes the right pedal back and rotates the nose to the left (Figure 3).

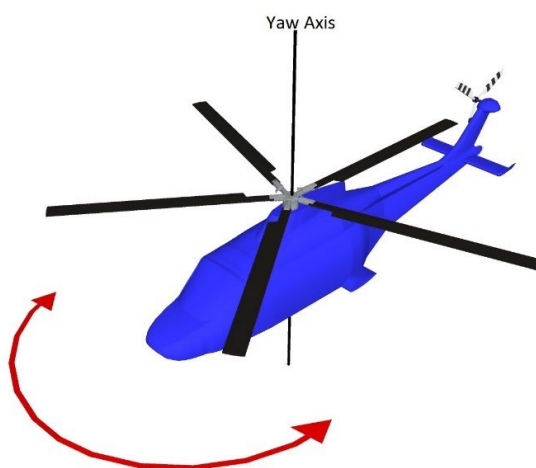


**Figure 3**

Helicopter yaw axis

In helicopters such as the AW169, with a single main rotor system that turns anti-clockwise (looking down from above), a torque couple is created when the rotor blades rotate under power from the engines, this causes the nose of the helicopter to yaw to the right.

8 <https://www.easa.europa.eu/sites/default/files/dfu/AW169-TCDS%20R-509%20Issue1.pdf> (Accessed 3 July 2023).

9 <https://www.easa.europa.eu/document-library/certification-specifications/cs-29-amendment-2> (Accessed 3 July 2023).

To resist this tendency, for example when the pilot wishes to keep the helicopter straight or to yaw to the left, a smaller rotor system is fitted to the tail of the helicopter. This tail rotor generates a torque around the yaw axis which can match the torque couple from the main rotor, thus keeping the helicopter pointing forward or if required exceed it, resulting in the helicopter yawing to the left. The tail rotor blades rotate at a relatively constant speed. To increase or decrease the force generated by the tail rotor system, the angle at which the rotor blades travel through the air relative to their path of rotation (pitch), is adjusted on all the blades at the same time. Increasing the angle increases the force, reducing the angle reduces the force. The normal range of blade pitch angle is  $+25^{\circ}$  to  $-10^{\circ}$ <sup>10</sup> and is limited by the primary yaw stops. The control input load required to change the angle of the blades on large helicopters such as the AW169, is too large for a pilot to achieve by moving a simple direct mechanical linkage. A hydraulic system is therefore used to translate the pilot's control inputs on the pedals into changes in the tail rotor blade pitch angle.

On the AW169, the yaw pedals in the cockpit are connected to the tail rotor control system by a flexible cable running on ball bearings within an outer sheath, whereas the AW189 uses a mechanical rod to achieve this. The cable on the AW169 is routed along the length of the fuselage to the tail, where it connects to a control rod and a bellcrank. The range of movement of the bellcrank is limited in each direction by the primary control stops for the yaw system (Figure 4). The bellcrank is then connected to a longer rigid control rod.

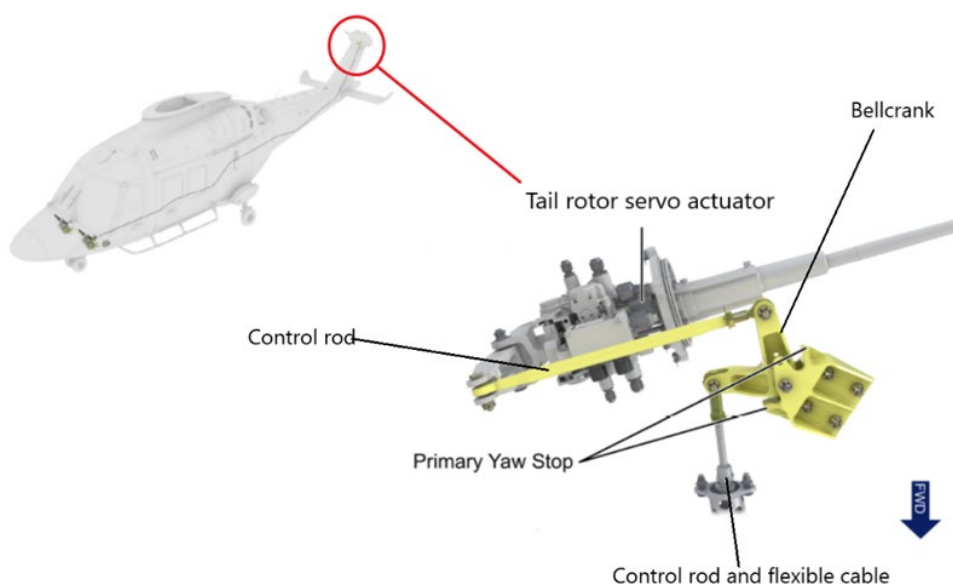


**Figure 4**

AW169/AW189 tail rotor control yaw stops<sup>11</sup>  
(original image courtesy of the manufacturer)

<sup>10</sup> Measured at the 75% tail rotor blade radius.

<sup>11</sup> Note the AW189 does not have the flexible cable used on the AW169.

The other end of the control rod is connected to one end of a lever mechanism which forms part of the tail rotor servo actuator, this is the same arrangement of components on both the AW169 and AW189. The middle of the lever is connected via rods and a lay shaft to the hydraulic servo main control valve (not visible in Figure 5), and the other end of the lever is connected to the tail rotor actuator control shaft by a connecting pin and pin carrier.

The pin carrier is secured to the shaft by a castellated lock nut which, at the time of the accident, attached to a threaded section on the end of the shaft using a conventional right hand thread. The nut has a torque load applied before a split pin is fitted between the castellations of the nut and through a hole in the shaft. It is also wire locked in place (Figure 5 & 6).

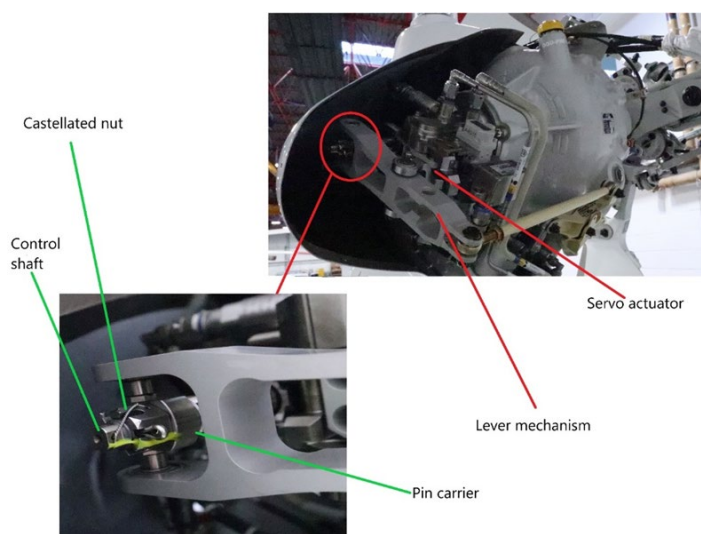


**Figure 5**

Tail rotor actuator control input mechanism

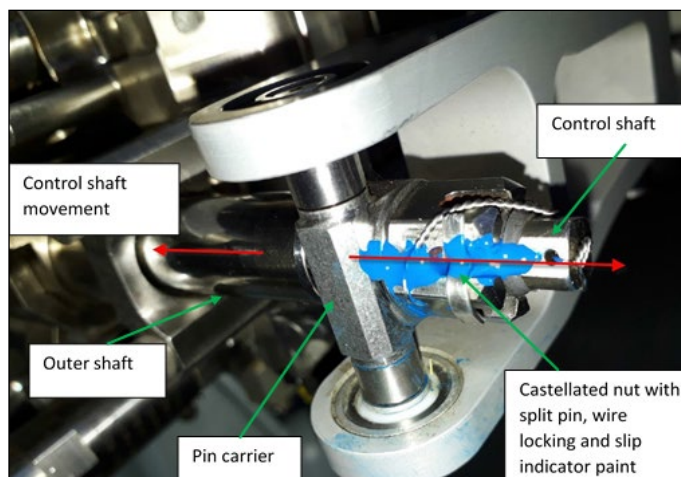


**Figure 6**

Reverse view of actuator system showing pin carrier and lock nut

The AW139 has the same basic arrangement, but rather than a separate pin carrier and nut, the connection to the actuator uses a one-piece pin carrier and nut arrangement. This is secured to the shaft using a left-hand thread. Although similar in design and function, the actuator is a different component from the AW169/AW189, produced by a different manufacturer.

The control shaft passes through an outer shaft, which forms part of the tail rotor hydraulic actuator piston, continues through a tunnel in the tail rotor gearbox and passes through the inner race of a duplex bearing installed in the tail rotor slider/spider assembly (Figures 7 and 8). The inner race of the bearing is locked in place on the control shaft by a spacer and a second, larger castellated nut and split pin.

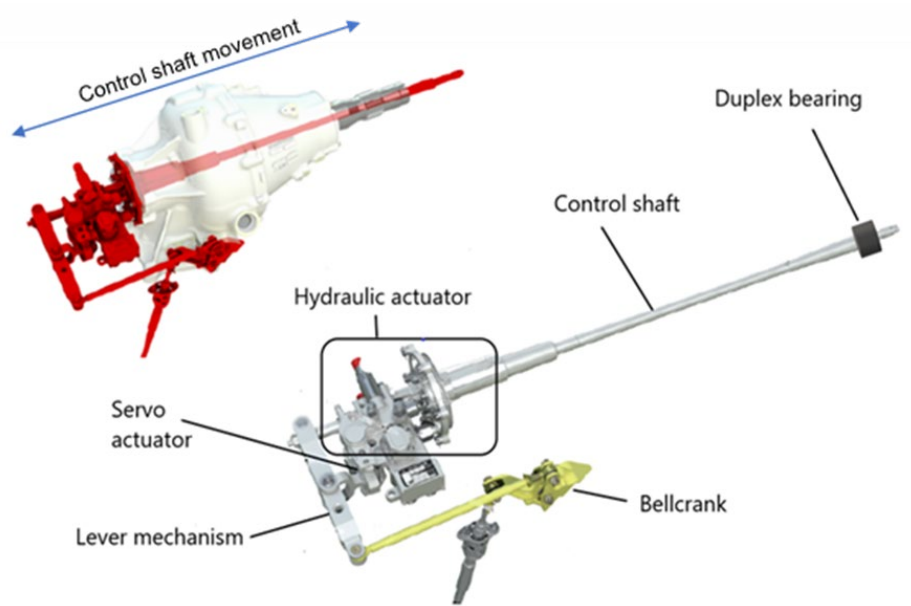


**Figure 7**

AW169/AW189 tail rotor actuator and duplex bearing  
(Original image courtesy of the manufacturer)

The spider is a rotating hub which holds the slider and duplex bearing. The slider guides the movement of the spider as it is extended and retracted by the control shaft. Each of the three arms of the spider is connected by a rod (pitch link) to the rear of a tail rotor blade. The spider/slider assembly is attached to the tail rotor hub by the scissor assemblies and rotates with the outer race of the duplex bearing, while the control shaft attached to the inner race remains stationary (Figure 8).

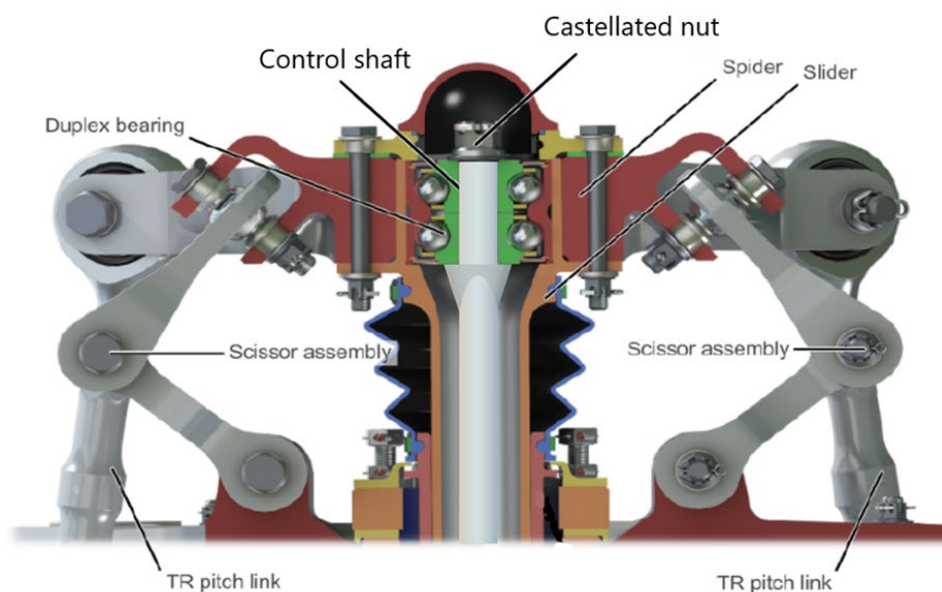


**Figure 8**

Tail rotor spider and pitch link assembly  
(Original image courtesy of the manufacturer)

#### *Tail rotor control operation*

When the pilot applies a yaw pedal input, it moves the control cable rotating the bellcrank. The movement is transferred to the tail rotor hydraulic actuator lever mechanism by the control rod. The lever mechanism pivots around the pin and carrier connection at the control shaft end and creates a demand on the hydraulic system via the main control valve. The hydraulic piston and control shaft of the actuator then move in the demanded direction under hydraulic pressure. Movement of the control shaft is transmitted to the tail rotor blades via the spider/slider assembly and the pitch links, which alter the tail rotor blade pitch (angle) to meet the pilot's demand. As the control shaft moves, it also moves the lever mechanism connected to it, which now pivots around the connection to the control rod attached to the bellcrank. This action closes the main control valve and stops movement of the actuator when the tail rotor blade pitch matches the control input demand from the pilot.

#### *Adaptive Variable Speed Rotor (AVSR)*

During original development the AW169<sup>12</sup> was equipped with a variable speed main rotor system which allowed the pilot to select the algorithm used to control the main rotor speed ( $N_R$ ). This was intended to improve the fuel economy of the helicopter by reducing the required torque from the engines during periods

<sup>12</sup> This system is not fitted to the AW189.

where the demand for lift from the main rotor blades is reduced, whilst still providing full lift from the rotor when required during low-speed manoeuvres or at high forward speeds.

The design of the AVSR system had two normal modes 'ECO' and 'PLUS' and a fixed speed 'BACKUP' mode which the system will revert to if it detects a fault. The intention was that the pilot could alternate between ECO and PLUS mode using the 'N<sub>R</sub> MODE' push button on the collective grip. The selected mode and the N<sub>R</sub> maximum and minimum limits are then displayed. The selected mode is also annunciated when changed (Figure 9).

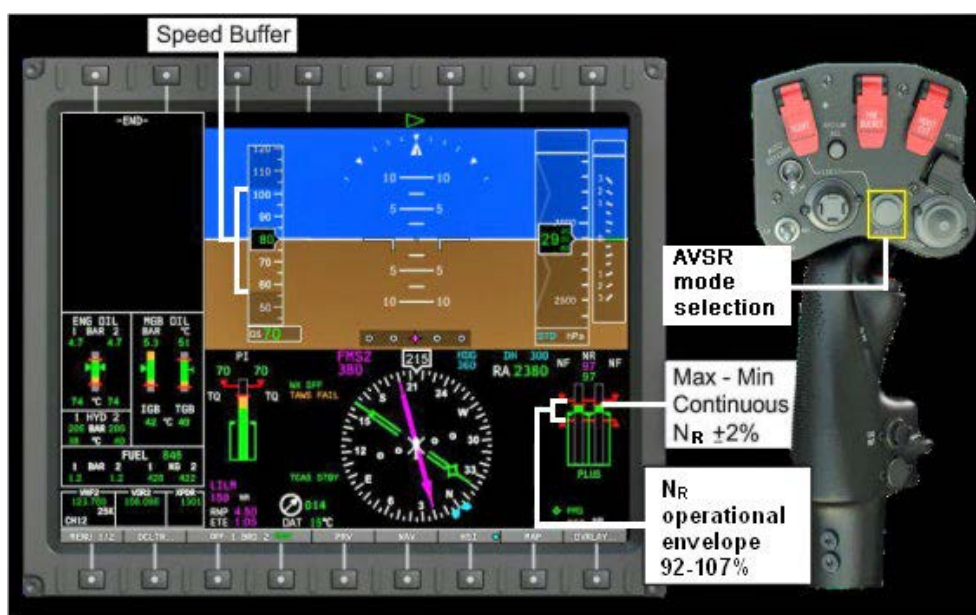


**Figure 9**

AVSR controls and primary flight display as anticipated during development  
(Original image courtesy of the manufacturer)

Depending on the airspeed and altitude, the selected mode would have varied the N<sub>R</sub> between 94% and 103%. The graph shown in Figure 10 shows how the N<sub>R</sub> was intended to vary in each mode. In BACKUP mode the system reverts to the blue line giving a fixed N<sub>R</sub> of 103%.

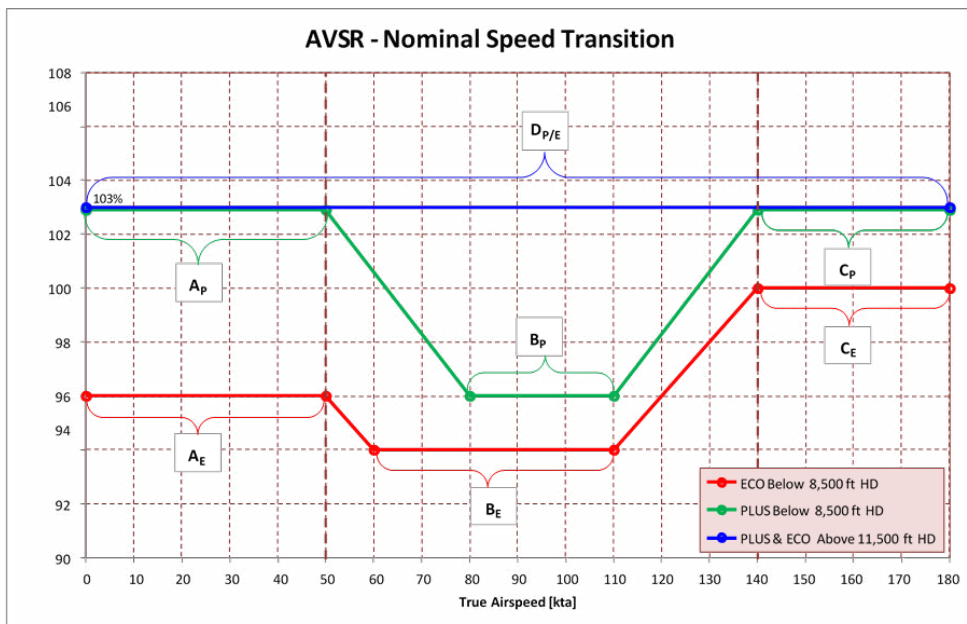


**Figure 10**

Intended AVSR variation in NR with true airspeed and altitude in each mode during original development (Original image courtesy of the manufacturer)

The main rotor is driven by the helicopter main gearbox. This gearbox also drives the tail rotor, which means there is a fixed ratio between main rotor speed and tail rotor speed. At 100%  $N_R$  the tail rotor rotates at 1,586 revolutions per minute (rpm). At 103%  $N_R$  this increases to 1,633 rpm.

Although used for some flight testing, the ECO mode of the AVSR system was never certified for operation under the type design approval granted for entry into service of the AW169. As such, this mode is disabled on production helicopters and only PLUS and BACKUP modes are operational. As a result, only the blue and green lines shown in Figure 10 are possible giving a variation in  $N_R$  of between 96 and 103% with both engines operating normally<sup>13</sup>.

*Duplex bearing*

The duplex bearing is required to connect the rotating slider and spider assembly (outer race) to the static tail rotor actuator control shaft (inner race). As the shaft moves in two directions (in/out), the bearing is required to have two rows positioned back-to-back to support the axial load in each direction. In order to support loads in both the axial ( $F_z$ ) and radial ( $F_r$ ) directions, the running surfaces of each row are angled at approximately 30°. The control

13 Normal operation is limited to the range 96%-103% NR, but this limit automatically increases to 105% with one engine inoperative. NR is permitted to drop to 94% or rise to 107%, providing this is only transitory.

shaft also experiences a bending moment ( $M$ ) which is transferred to the bearing (Figure 11).

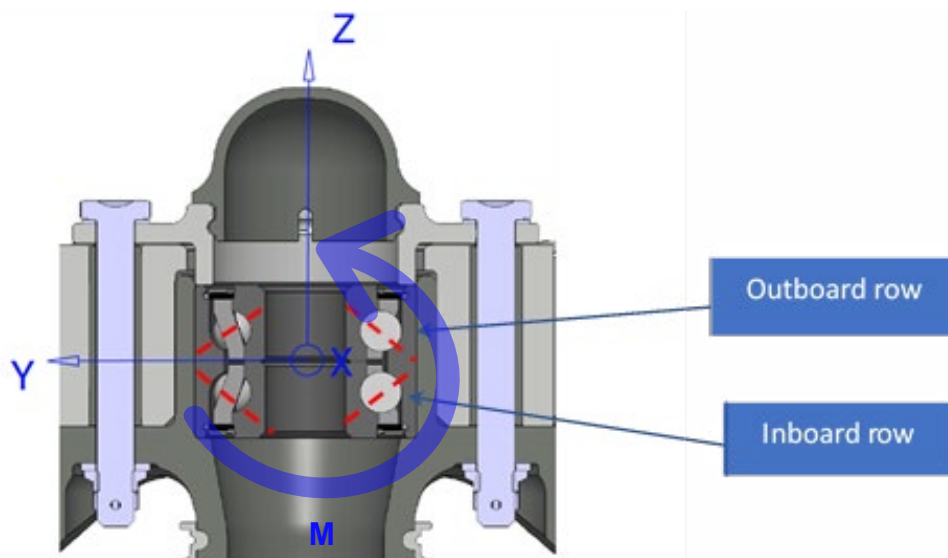


**Figure 11**

Diagram (with control shaft removed) showing two halves of the bearing (inboard and outboard) and the 30° orientation. (Original image courtesy of the manufacturer)

The two halves of the bearing are referred to as the inboard and outboard rows based on their relative position to the helicopter centreline. The inner races are clamped together on the control shaft by the castellated nut. The internal design of the bearing in combination with the torque setting on the nut ensures the correct preload is applied to the bearing. The correct preload gives a consistent baseline contact pressure which is necessary so that the ball bearings roll rather than skid along the running surfaces. By applying a constant installed load, it also reduces the amount of deflection within the bearing when external operational loads are applied.

The bearing consists of a steel one-piece outer housing, which forms the two outer races (running surfaces) of each half of the bearing, two steel inner races, two sets of nine silicon nitride ceramic ball bearings and two bronze alloy cages. The cages sit between the inner and outer races of the bearing to locate the ball bearings, ensuring the balls are in contact with the races in the correct position. An elastomeric seal on each end of the bearing prevents entry of contaminants and debris.

The AW169/AW189 bearing internal free space is completely filled with grease which weighs 6 g in total. The bearing manufacturer stated they typically fill 25 to 35% of the free space on sealed bearings, but a 100% fill was specified

for this bearing. The AW139 bearing drawing has recently been amended from requiring 100% to specifying a minimum 33% fill, which equates to 2 g of grease in total.



**Figure 12**

Bearing in new condition - (A) Housing and outer race, (B) inner race, cage and balls assembled, (C) cage, seal and inner race disassembled

Figure 12 shows the housing and the outboard row, outer race in image A. Image B shows the inner race, cage and balls as they have been removed from the housing in image A and turned over (the top surface in view is normally located in the middle of the bearing). Image C shows the inner race, cage and seal after they have been disassembled and the balls removed. The other row of the bearing is identical but is installed the opposite way around (mirror image).

The combination of steel races with ceramic ball bearings is referred to as a hybrid bearing. Use of ceramic ball bearings provides several benefits over traditional all steel bearings.

These include weight reduction, a wider operating temperature range, allowing higher rotational speeds, better resistance to corrosion and they are electrically isolating. However, as the silicon nitride material is exceptionally hard, it is also more brittle and can be susceptible to shock loads. The relative hardness of the ceramic ball compared to a steel ball bearing also reduces the contact area with the races, resulting in approximately 12% higher contact pressure<sup>14</sup> applied to the race material under the same load.

<sup>14</sup> The figure of 12% is quoted by a number of research papers including: Lorösch, H.K., Vay, J., Weigand, R., Gugel, E., Kessel, H., (1980). Fatigue Strength of silicon nitride for high-speed rolling bearings, Transactions of ASME, J. of Engineering for Power, vol. 102, 128-131.), A figure of 12.8% is also quoted by NASA paper NASA/TM-2005-213061.

### 1.6.3 Tail rotor duplex bearing development history

Hybrid bearings have been used in various industry applications for around 40 years but are less common in aerospace applications, particularly in critical safety functions.

The helicopter manufacturer first introduced the hybrid duplex bearing design on the AW139 tail rotor control system as p/n 3G6430V00151. This was subsequently modified in 2006 by a minor modification to facilitate assembly, which changed the part number to 3G6430V00153. The bearing is manufactured and delivered as a sealed unit by the bearing manufacturer, and is then assembled onto the tail rotor actuator control shaft by the helicopter manufacturer. The AW139 bearing has accumulated 3,699,826<sup>15</sup> hours in service across both part numbers.

Dimensionally and functionally, the p/n 3G6430V00153 bearing is identical to the bearing which was subsequently used in the AW169 and AW189 tail rotor system. However, the original steel specification for the race material was changed to CHROMEX 40 on the AW189/AW169 bearing to address corrosion issues experienced in service on the AW139 bearing.

Original certification of the bearing on the AW139 considered it to be an 'on condition' part. This meant it had no scheduled removal time and remained operating in service until it required replacement due to deterioration of its performance.

The condition of the bearing in operation was assessed by a tactile check of the bearing's rotational smoothness, achieved by disconnecting the spider from the rotor blades and rotating it by hand. This check was scheduled every 600 flying hours or one calendar year, whichever came first. At 2,400 flying hours or four calendar years the bearing was removed from the spider, and the spider assembly visually inspected, before the bearing was refitted. If bearings were rejected due to roughness during these routine maintenance checks, they were disposed of by the operator and a new bearing fitted. Data provided to the investigation from a retrospective assessment of UK and Italian AW139 operators' records by the UK and EU airworthiness authorities has confirmed that a number of bearings were being rejected across a range of operating hours for roughness and axial play, as a result of these inspections.

---

<sup>15</sup> As of March 2023.

### *2012 AW139 bearing serious incident*

In 2012 an operator based in Qatar suffered a loss of yaw control incident on an AW139. This was found to have been caused by a failure of the duplex bearing (p/n 3G6430V00151). Evidence of rotation of the tail rotor actuator control shaft confirmed that the bearing had seized at some point. However, as the control shaft had a left-hand thread, the pin carrier had tightened onto the actuator shaft, rather than unscrewing. This transferred the torque load back into the bearing, forcing rotation until the bearing components became so heavily worn that the bearing failed completely, to the extent that it no longer provided any resistance to the movement of the hydraulic actuator. Effectively no longer attached to the control system, the tail rotor blades moved to, and remained at, a positive blade pitch angle of approximately 10° with no means of changing the blade position possible by pilot action. The helicopter started to turn under the influence of the main rotor torque couple, but the loss of tail rotor control occurred while the helicopter was in forward flight. The reduced engine torque demand, the vertical tail surface aerodynamically contributing to the yaw control and the force generated by the default blade position, were sufficient to allow the pilot to maintain forward flight and perform a 'run on' landing without any additional damage occurring to the helicopter.

#### *Manufacturer's response*

The 2012 AW139 loss of yaw control event wasn't subject to an independent Annex 13 investigation, and the operator, helicopter manufacturer and local airworthiness authority assessed that the bearing was too badly damaged to conduct a meaningful failure analysis.

As a precautionary response to the bearing failure, the manufacturer applied two new requirements to the AW139 bearing. The first was an amendment to the approved maintenance manual stating bearings shall not be refitted after removal from the spider assembly. The second was to apply a discard life of 3,000 hours. Once a bearing reached this life in service it was discarded by the operator and a new bearing fitted<sup>16</sup>. This change was only introduced by a Service Bulletin from the manufacturer. The airworthiness authority did not issue an Airworthiness Directive, as such the discard life was not mandated as an airworthiness requirement. A selection of seven bearings across a range of service lives from 98 to 7,000 hours were removed and sent back to the bearing manufacturer for assessment of their condition. No abnormal wear was identified. The bearing manufacturer's stated conclusion from this assessment was that they supported a discard life of 2,400 hours (rather than 3,000 hours), in addition to the 600 hour rotational inspections.

<sup>16</sup> In practice this meant that bearings should have been discarded at 2,400 hours life due to the maintenance requirement at this time. However, evidence collected following the second incident suggests operators were confused by the 3,000-hour life and were routinely refitting bearings after the 2,400 hour inspection to achieve the maximum time in service.

Only the AW139 was certified and in service in 2012. However, the operational load spectrum and discard life for the AW169/189 bearing were being assessed in the design acceptance phase for both the AW169 and AW189 helicopters around this time. The usage and load spectrum for the AW169/189 bearing, although different from the AW139 spectrum, was developed using experience from the AW139 as a reference and resulted in the same recommended discard life and inspection period from the bearing manufacturer.<sup>17</sup>

#### *2022 AW139 bearing incident*

A second AW139 bearing failure was identified by a UK operator on the ground during post-flight checks in June 2022. Although the bearing failure was found before it resulted in an in-flight incident, the circumstances and nature of the failure were similar to the 2012 AW139 occurrence. The bearing life at removal was 2,750 hours. This incident is currently under investigation by the AAIB as a separate investigation case<sup>18</sup>.

The helicopter manufacturer has taken several safety actions on the AW139 fleet following this failure event, including various inspection and replacement requirements for installed bearings and reducing the discard life to 2,400 hours to match the maintenance task interval requiring the bearing to be removed. While not the stated reason for the change, this also aligned it with the bearing manufacturer's recommended discard life for the AW139 and AW169/AW189 bearings.

This limit is still considered a discard life rather than an airworthiness limitation, despite removal from service of bearings over 2,390<sup>19</sup> hours being mandated by EASA Airworthiness Directive No 2022-0182-E.

#### 1.6.4 AW169 and AW189 tail rotor design and certification

Up until 2023 and at the time of certification of the AW169 and AW189, there were no requirements at all in CS 29 specifically covering bearing design or fatigue tolerance requirements relating to any form of rolling contact fatigue (RCF)<sup>20</sup>. As a result, bearings are not individually certified but are considered as part of a system. The assessment of bearing performance in drivetrain or control applications during the certification process has typically been based on review of the condition of bearings after completion of an endurance test specified by CS 29.923 and following development and certification flight test campaigns.

<sup>17</sup> See [section 1.6.5.3](#) for more detail.

<sup>18</sup> AAIB case reference AAIB-28373.

<sup>19</sup> The AD allows 10 hours for implementation, giving a total limit of 2,400 hours.

<sup>20</sup> See [section 1.18.13](#) A new AMC has been introduced to 29.571 directing manufacturers to consider RCF as part of their analysis.

The tail rotor duplex bearing and the tail rotor actuator control shaft onto which it fits are separated into two different systems in the design of the helicopter. The applicable regulations quoted by the helicopter manufacturer in their certification report for the AW169 tail rotor system, which includes the duplex bearing, were CS 29.547 and CS 29.602. These covered the design safety assessment and identification of critical parts. The tail rotor control actuator was assessed against CS 29.1309 and CS 29.602 as it forms part of the tail rotor control system. These also cover the design safety assessment and critical parts.

The design system safety assessment completed by the helicopter manufacturer identified failures at a system level, which meant the effect of failures of the duplex bearing and the Tail Rotor Actuator (TRA) were assessed separately and covered in different reports.

The TRA reports were completed by the actuator manufacturer and provided to the helicopter manufacturer. The Failure Modes and Effects Analysis (FMEA) which the TRA manufacturer conducted, only considered the potential failure of the component parts of the actuator itself. They stated that they were not informed about the effect of failures within other connected components that could adversely impact the actuator parts, for example rotation of the shaft driven by gearbox torque. These were considered by a system level assessment and therefore stated as being outside of the scope of the TRA manufacturer's analysis. As such, rotation of the nut to allow disconnection from the input/feedback lever was not identified in the FMEA as a potential failure mode. They informed the investigation that the thread direction was not specified for the actuator end locking nut in the design specification, and they did not have access to the design of the AW139 TRA at the time for comparison. However, the TRA manufacturer did identify that loss of control of the actuator due to a structural failure of the position feedback was catastrophic.

In a separate report the helicopter manufacturer identified that failure of the tail rotor to provide the necessary variable thrust was catastrophic and that this would result from seizure of the duplex bearing. It was anticipated by the helicopter manufacturer's analysis that in the event of a failure of the bearing, the control shaft would fracture.

Analysis of the failure and loss of retention capability of the castellated locking nuts at both the bearing end and the actuator end of the control shaft, were also classed as catastrophic. Though these were also considered separately as the actuator end nut formed part of the TRA assembly, whereas the bearing end nut was considered part of the tail rotor assembly. The duplex bearing and both the locking nuts were identified as critical parts<sup>21</sup>.

---

21 Critical parts are explained in [section 1.18.5](#).

The airworthiness authority responsible for certification of the AW169 and AW189 confirmed that once the system safety assessment identifies the failure of a component as catastrophic, then there is no requirement for the manufacturer to consider the associated implications of that failure.

The locking nuts at both ends of the control shaft were also certified as compliant with CS 29.607, which required two separate locking features for safety critical fasteners.

#### 1.6.5 Duplex bearing design and load analysis

##### 1.6.5.1 Factors contributing to tail rotor control loads

There are three main factors which determine the magnitude of the axial load ( $F_z$ )<sup>22</sup> on the tail rotor bearing. The amount each factor contributes to the overall load varies depending on the operating conditions and the manoeuvre being flown, but the broad ranges are:

Inertial Loads	50% - 60%
Elastomeric Loads	30% - 40%
Aerodynamic Loads	10% - 15%

##### *Inertial Loads*

These are loads which are generated by the inherent physics of a tail rotor blade rotating at speed. As described in section 1.6.2, the tail rotor blades can be adjusted using the control system to rotate each blade around its longitudinal axis, this changes the pitch (angle) of the blade relative to the plane of rotation. The centrifugal loads on the blade as it rotates circumferentially inherently drive the blade towards a flat ( $0^\circ$ ) pitch angle; this load would be present even if the blade was operating in a vacuum.

To change and then maintain a different pitch angle on the blades, the control system must apply an opposing load sufficient to move the blades to the required angle and then maintain an equal and opposite load to the inertial load. The faster the tail rotor rotates, the greater the inertial load on the blades.

##### *Elastomeric Loads*

To allow the tail rotor blades to rotate in pitch about their longitudinal axis relative to the fixed attachment to the tail rotor hub, they are fitted with a bearing. As the blade is only required to rotate in a range between  $-10^\circ$  and  $25^\circ$  on the AW189 and AW169, this is achieved by twisting a flexible elastomeric material, rather

<sup>22</sup> See [Figure 11](#) for definition of loads and directions.

than using a conventional mechanical bearing. This approach has a number of advantages but requires a force to be applied to overcome the inherent stiffness of the elastomer in order to deform it. The stiffness of the elastomer varies with temperature, so the control load required to move the blade increases as the material cools and reduces as it warms up. The force required to continue to rotate the blade also increases the more the elastomer becomes twisted as pitch angle increases.

### *Aerodynamic Loads*

The amount of lift generated by a rotor blade depends on several factors. Those which can vary during operation are:

- Speed of the airflow over the blade: a combination of the speed of the blade through the air (driven by the torque produced by the engines), the speed of the moving helicopter and the relative wind speed.
- Density of the air: this changes with altitude and temperature.
- Angle of attack (AOA) between the airflow and the blade: the angle between the blade and the direction of the airflow as it meets the blade.

As these three factors increase, the amount of lift generated also increases.

As the amount of lift increases, so too does the amount of drag. Lift and drag are referred to as aerodynamic forces as they are generated by the blade interacting with the surrounding air. Aerodynamic forces are lowest when the blades have a zero angle of attack to the airflow over them. As the angle of attack increases an increasing aerodynamic moment created by the drag force tries to return the blade to the lowest drag attitude. To increase the amount of lift for a given airflow, the tail rotor control system must apply an opposing load sufficient to overcome this aerodynamic moment and must maintain an equal and opposite load to sustain it.

#### 1.6.5.2 Factors affecting the demand for tail rotor lift<sup>23</sup>

Main rotor blades must produce sufficient lift to overcome the weight and drag of the helicopter to allow it to take off, hover and manoeuvre. In the hover the helicopter is stationary, so airflow over the blades depends on the rotation of the rotor blades and the wind speed and direction. The heavier the helicopter, the lower the positive contribution from the wind speed or the lower the air density, the greater the blade pitch angle required to generate sufficient lift to maintain the hover.

<sup>23</sup> This section references information contained in the FAA Helicopter Flying Handbook FAA-H-8083-21B.

At low altitude the helicopter benefits from 'ground effect'. This is caused by the interaction with the ground of the downwash generated by the main rotor. For most helicopters, it occurs up to a height of approximately one rotor diameter (measured from the ground to the rotor disk). It has the effect of making the rotor system more efficient by decreasing the downward airflow velocity. This increases the blade AOA without changing the pitch angle, thereby reducing the drag for the same amount of lift. Above this height, the effect is lost, and the required AOA must be achieved by increasing the blade pitch angle.

The greater the blade pitch angle, the more drag the blades create and the greater the torque which must be generated by the engines to overcome it. Any increase in the torque required to rotate the main rotor blades creates a larger torque couple, which must then be countered by an increase in lift<sup>24</sup> generated by the tail rotor blades.

The direction of the wind can also increase the amount of force required from the tail rotor. Tailwinds and crosswinds will attempt to weathervane the nose of the aircraft into the relative wind by acting on the fuselage and vertical fin, requiring greater tail rotor control inputs to counter them.

Further complications can occur in the hover and when the wind direction relative to the tail rotor blades comes from an adverse direction, as this can reduce the aerodynamic effectiveness of the blades, for example:

- Airflow and downwash generated by the main rotor blades can interfere with the airflow entering the tail rotor.
- A high main rotor pitch angle demand can induce considerable main rotor blade downwash and hence more turbulence.
- Main rotor blade tip vortices can enter the tail rotor causing it to operate in an extremely turbulent environment.
- Wind at velocities of about 10 to 30 kt from the left front will cause the main rotor vortices to be blown into the tail rotor.
- During a turn, the tail rotor will experience a reduction in control force as it comes into the area affected by the main rotor blade tip vortices.
- Turbulent air from the surroundings and other natural phenomena can affect the airflow around the tail rotor, particularly during a confined area takeoff.

<sup>24</sup> Given the orientation of the tail rotor, lift generated by the blades acts as a horizontal force rather than vertical and may also be referred to as thrust.

Aerodynamically the tail rotor works in the same way as the main rotor in that a low positive contribution from the windspeed and low air density means a higher blade pitch angle is required to generate sufficient control force, increasing the amount of drag. Reduced aerodynamic efficiency of the rotor due to operation in disrupted air results in a similar increased blade pitch demand.

As a result of these factors, higher tail rotor control loads can be experienced when operating at high gross weight, hovering out of ground effect, at high altitude or high ambient temperatures, in still air or with the wind from unfavourable directions, in turbulent air and from asymmetric manoeuvres requiring large and prolonged control inputs.

### 1.6.5.3 Duplex bearing specification and load spectrum development

The specification for a hybrid tail rotor duplex bearing was originally produced by the helicopter manufacturer during development of the AW139, with the basic load spectrum shown in Table 1. Of note are the lower axial Fz load, and the much higher bending moment load (M) for the highest load conditions (highlighted in yellow), compared to the subsequent AW169/AW189 spectrum shown in Table 3 (also highlighted). The AW139 sits between the AW169 and AW189 in terms of size and MTOW.

Condition	FZ (daN)	FY (daN)	M (daNm)
<b>Static limit loads</b>			
1	1,247	0	0
2	650	200	30.6
<b>Fatigue loads</b>			
1	200	0	6.2
2	80	0	6.2
3	240	0	13.2
4	-80	0	5

**Table 1**  
AW139 load spectrum

The tail rotor bearing specification for the AW149<sup>25</sup> was developed in December 2008. This was passed to the bearing manufacturer who selected a bearing against the axial (Fz)<sup>26</sup> load spectrum provided by the manufacturer, shown in Table 2. This work assumed a bearing preload of 129 daN in operation, a nominal operating speed of 1,410 rpm and a maximum speed of 1,438 rpm.

25 The AW149 was a prototype developed as a derivative of the AW139 for use in military applications. It was never subject to civilian certification requirements.

26 See [Figure 11](#) for definition of load directions.

Condition <sup>27</sup>	Occur. (%)	Fz Static (daN)	Fz Dynamic (daN)	Fz Total (daN)
1	0.95	-781.6	190.7	-972.3
2	4.25	-458.2	237.2	-695.4
3	11	-324.8	290.0	-614.8
4	50	-166.8	217.5	-384.3
5	11	152.3	111.4	263.7
6	12	261.0	215.5	476.5
7	4	362.5	172.3	534.8
8	2	546.7	285.7	832.4
9	4.6	635.1	142.1	777.2
10	0.2	785.0	145.0	930.0

**Table 2**

Original development load spectrum for the AW149

In February 2009, the bearing manufacturer issued a design document for a bearing based on the one used in the AW139, using 100C6 steel for the bearing races. The design estimated a fatigue life ( $L_{10}$ )<sup>28</sup> of 25,530 hours using the loads provided. In December 2009 the bearing race material was changed to CROMEX 40 to give it better corrosion resistance. This was done to address in-service problems experienced on the AW139 bearing. The bearing was given the part number 4F6430V00551 and assessment of the new material using the same loads resulted in a reduction in the L10 life by the bearing manufacturer to 16,791 hours.

Further analysis of the tail rotor component parts determined that the loads generated by the stiffness of the elastomeric bearings used on the tail rotor blade pitch mechanism were higher than originally expected, these were anticipated to increase further in cold weather. In October 2010 the bearing was fitted to the instrumented AW149 Tie Down Helicopter rig for initial load assessment trials. The testing confirmed that the tail rotor control loads were higher than anticipated by the original load spectrum. The AW149 was a military rather than civil programme, so it was not necessary to meet civil certification requirements. As such, the loads analysis conducted at this stage was only required to validate the safety case for conducting prototype flight test trials.

<sup>27</sup> 'Condition' is the manufacturer's terminology for the reference points used to define the load spectrum.

<sup>28</sup> Bearing L10 life is explained in [section 1.18.6](#).

Coinciding with this work, in 2010 a specification document was issued for a tail rotor duplex bearing for the AW169. The load spectrum supplied to the bearing manufacturer to design the bearing is shown in Table 3. This assumed a bearing preload of 113 daN in operation, a nominal operating speed of 1,586 rpm and a maximum speed of 1,666 rpm.

Condition	Occur. (%)	Fz Static (daN)	Fz Dynamic (daN)	Fz Total (daN)	M (daNm)
1	0.5	-1,080	250	-1,330	3.43
2	2	-890	150	-1,040	3.94
3	11	-700	100	-800	3.73
4	25	-510	110	-620	4.24
5	57	-320	110	-430	4.19
6	4	130	110	240	3.41
7	0.5	250	110	360	3.67

**Table 3**

Original development load spectrum for the AW169

As the stiffness of elastomeric material is affected by temperature, and based on the AW149 experience, the helicopter manufacturer elected to apply a conservative 'stiffening factor' to the elastomer components to anticipate operation at very low temperatures. This stiffening factor contributed between 18% and 25% of the axial Fz total load, resulting in higher loads in the AW169 spectrum than in the AW149 spectrum, despite the AW169 being a smaller helicopter. The actual loads would be assessed by cold temperature trials during the flight test programme and use of a conservative factor was intended to avoid the need for disruptive redesigns at a later stage in the development process. A bearing, part number 6F6430V00351, was then developed by the bearing manufacturer to meet this specification.

In May 2011, the helicopter manufacturer applied to the European Union airworthiness authority for type certification of the AW189 to begin. The AW189 was essentially the same helicopter as the AW149 but certified to CS 29 standards for civil use. By 2012, it was identified that the higher bearing loads measured on the AW189 would likely be enveloped by the load spectrum being used for the AW169 bearing development. In July 2012 the helicopter manufacturer requested that the bearing manufacturer assess the AW149/189 bearing (part number 4F6430V00551) against the AW169 load spectrum, with a view to using this bearing in both applications. In September 2012, the bearing manufacturer issued a design document summarising the conclusion of this work.

Using a preload of 120 daN and a rotational speed of 1,586 rpm, they determined that the bearing (p/n 4F6430V00551) as defined for the AW189 application was also acceptable for operation with the AW169 load spectrum, though this resulted in a reduced  $L_{10}$  life of 12,882 hours.

In the bearing manufacturer's design document, the summary stated:

*'Hertz stress<sup>29</sup>: Hertz stress values for dynamic conditions are quite high, out of the range in which bearing life could be assumed as infinite. Under overload conditions, the Hertz stress values are up to 3795 MPa, what is acceptable, but very close to the maximum allowable stress for this kind of conditions, i.e. close to plastic deformation of the bearing raceways.*

*Hertz stress under overload condition is acceptable, bellow[sic] the maximum allowable limit.*

*Hertz stress under ultimate load is above current limits for standard conditions, but no problem of bearing destruction is to be expected. The bearing will be submitted to slight plastic deformation, what is acceptable for an ultimate load.*

*Ball excursion values are within acceptable range.*

*Hoop stress values are within acceptable range.*

*In order to contain the contact ellipsis within the shoulder and avoid truncation<sup>30</sup>, the cage design is on "Z" shape.*

*The calculated life (12882h) is a pure cyclic fatigue life of the material and doesn't account for bearing environment (grease, pollution...)*

*The investigations after operating tests on similar bearings show with confidence an operating time limit (OTL) at 2400 hours.*

*To verify that the bearing works properly and to guarantee the continuous airworthiness, we advice[sic] to make a roughness check after every 600 hours operating.'*

---

29 Hertz stress is explained in [section 1.18.6](#).

30 Truncation occurs when the whole of the normal contact area between the ball and the race is no longer supported within the running surface of the race, for example if the ball is running partially over the shoulder at the edge of the running surface where the geometry changes. This can result in significantly increased stress on the ball where it contacts the corner edge of the race.

The percentage of operating time at the various load levels shown in the design load spectrum was estimated based on experience with other helicopters and the various role profiles that the helicopter was designed to be used for. These were then combined into an overall usage spectrum. The spectrum assumed most of the flight time is spent in the cruise, where engine torque demand is reduced and the aerodynamic force generated by the vertical fin offsets some of the force required from the tail rotor to maintain a heading. Conversely, the highest axial load case is anticipated to be experienced for only 0.5% of the life of the bearing.

The  $L_{10}$  life for the bearing of 12,882 hours was based on theoretical optimised conditions which would allow the bearing to reach its maximum fatigue life, it did not, for example, account for any degradation of the grease. A recommended discard time for the bearing of 2,400 hours was then proposed to account for any adverse conditions and the inherent variability within the  $L_{10}$  life calculation. Finally, a repetitive 600 hours in situ rotation check of the tail rotor was recommended by the bearing manufacturer. This was subsequently reduced to 400 hours by the helicopter manufacturer, in line with the AW169 Maintenance Review Board report.

The full load spectrum used to confirm acceptability of the bearing in both applications, as stated in the bearing manufacturer's design report, is shown below in Table 4. The highlighted values indicate the highest considered values for dynamic axial load, bending moment and Hertz Stress (contact pressure) in normal operation.

#### 1.6.5.4 Control of bearing discard life and inspection tasks

The manufacturer published an Approved Maintenance Planning Information (AMPI) manual for the helicopter to comply with the continued airworthiness instructions requirement CS 29.1529. For the AW189 and AW169 a process was used called a Maintenance Review Board (MRB). This is a standardised process accepted by EASA, the FAA and Transport Canada as an acceptable means of compliance for the regulation. It involved a review board comprised of representatives from the manufacturer, certifying airworthiness authorities and operators. They used the latest Maintenance Steering Group (MSG-3) methodology<sup>31</sup> as a tool to assess what scheduled maintenance was required to maintain the airworthiness of the AW169 in service, based on candidate tasks submitted by the helicopter manufacturer. The output of this review process was an MRB report which contained the recommended minimum initial scheduled maintenance requirements. This report was then considered in combination with the output of the regulatory compliance activity by the helicopter manufacturer to determine the final content of the AMPI.

31 MSG-3 logic is owned by A4A. It is reviewed and updated by a Maintenance Programs Industry Group and approved by the International MRB Policy Board.

## PRELOAD UNDER OPERATING CONDITIONS

Preload [N]: 1200  
Preload [mm]: 0.033

## OPERATING LOADS

## Flight Cycle

Cond.	% Time	Outer ring Speed [rpm]	Mean Cubic Power		Max	
			F <sub>z</sub> [N]	M [N.m]	F <sub>z</sub> [N]	M [N.m]
1	0.5	1,586	-11,080	22.34	-13,300	34.3
2	2	1,586	-9,020	25.88	-10,400	39.4
3	11	1,586	-7,070	24.21	-8,000	37.3
4	25	1,586	-5,216	27.51	-6,200	42.4
5	57	1,586	-3,378	27.33	-4,300	41.9
6	4	1,586	1,658	22.35	2,400	34.1
7	0.5	1,586	2,722	23.9	3,600	36.7

## Overload

Cond.	% Time	Outer ring Speed [rpm]	F <sub>z</sub> [N]	M [N.m]
Overload	-	-	24,000	0
Ultimate	-	-	36,000	0

## HERTZ STRESS\* &amp; CONTACT GEOMETRY\*

## Max Power - Loaded Row

Cond.	Hertz Stress		Contact Ellipse				Ball Trip (mm)
	Inner Ring (MPa)	Outer Ring (MPa)	Inner Ring (deg)		Outer Ring (deg)		
1	3340	3160	7.7	72.2	17.2	62.7	0.22
2	3170	2990	8.4	69.2	17.3	60.3	0.21
3	2980	2800	9.1	65.7	17.4	57.4	0.20
4	2850	2670	9.5	63.3	17.3	55.5	0.18
5	2655	2475	10.0	59.8	17.2	52.6	0.15
6	1960	1795	9.7	45.5	14.8	40.4	<0.1
7	2030	1855	8.0	45.2	13.4	39.9	<0.1

## Overload and Ultimate Load - Loaded Row

Cond.	Hertz Stress		Contact Ellipse				Ball Trip (mm)
	Inner Ring (MPa)	Outer Ring (MPa)	Inner Ring (deg)		Outer Ring (deg)		
Overload	3795	3595	2.9	77.6	14.2	66.3	-
Ultimate	4250	4060	0	85.8	13.2	72.45	-

\* On the most loaded ball

**Table 4**

Certification load spectrum for the tail rotor duplex bearing

CS 29.1529 also directs manufacturers to include a separate Airworthiness Limitations Section (ALS) in their instructions for continued airworthiness. This section must be formally approved by EASA at certification and again each time it is subsequently amended.

CS 29.571 and CS 29.573 which address fatigue and damage tolerance require mandatory latent failure inspections and component replacement times

identified as necessary for continued airworthiness of Principal Structural Elements (PSE) to be specifically listed in the ALS. There are currently no other regulations in CS 29 which explicitly direct component life limitations to be listed in the ALS as airworthiness limitations.

The AMPI produced by the manufacturer has two chapters relating to replacement of components at specific service intervals. Chapter Four listed components were assessed to comply with CS 29.571, where inspection and/or replacement of PSE at a specific service life was considered an airworthiness requirement. These lives were agreed with the airworthiness authority and cannot be changed without their approval. They are based on a defined helicopter usage profile and variation in service will result in penalty life reductions. This chapter met the regulatory requirement for an ALS. The limitations listed within Chapter Four were not subject to review under the MRB process.

Chapter Five of the AMPI dealt with scheduled maintenance. While these tasks are also necessary to ensure the continued airworthiness of the helicopter, they do not have the same status as the airworthiness limitations in the Chapter Four ALS<sup>32</sup>. Chapter Five contained a section entitled '*Time Limits*'. The introduction for this section stated, '*This section gives the recommended time limits requirements for the components of the helicopter*'. Within this was a sub-section entitled '*Discard Time Schedule*', which stated, '*This sub-section gives the indication of the number of hours/months/years at which the component must be discarded.*'

The tail rotor duplex bearing Operating Time Limit (OTL) and inspection interval were recommended by the bearing manufacturer<sup>33</sup>. These were then used by the helicopter manufacturer in the output of the design assessment process completed by them to comply with CS 29.547 and raised as candidate preventative maintenance tasks. These candidate tasks were then discussed and agreed with EASA. The conclusion of this process was that the OTL would be included in Chapter Five of the AMPI as a discard time of 2,400 flight hours.

The MRB process operates independently of the regulatory compliance process. The manufacturer then compared the output from both processes to determine the final content of the AMPI. This resulted in a variation of the bearing inspection interval from the bearing manufacturer's recommended 600 hours to 400 hours.

The method by which the AMPI for the AW139 was developed differed slightly from the AW189/169, as it did not use the MRB process. However, the results

32 Scheduled maintenance task intervals are typically permitted to be extended by the Continuing Airworthiness Maintenance Organisation (CAMO) within limits set by the manufacturer and detailed in the approved maintenance programme.

33 Refer to [section 1.6.5.3](#).

gave the same approach of applying a Chapter Five discard life rather than a Chapter Four airworthiness limitation<sup>34</sup>.

#### 1.6.6 AW189 and AW169 flight test load surveys

The AW189 flight loads were measured during a load survey campaign, performed using two flight test prototypes and spanning 47 flights between 19 September 2012 and 20 June 2013. The AW169 load survey was conducted over 47 flights between April 2013 and November 2015.

The AW169 and AW189 flight test campaigns were designed to measure the loads on a large number of the helicopter's components when flown in routine configurations and to the limits, or corner points, of the operating envelope with respect to gross weight, longitudinal and lateral CG positions and altitude. For the AW169, tests were conducted at two main airfield elevations, sea level and 5,000 ft, and up to 15,000 ft inflight. Some near ground manoeuvre testing was also done at airfield altitudes of 10,000 ft, 12,000 ft and 14,000 ft, though gross weight was limited to 4,600 kg at 10,000 ft and above, and 4,200 kg at 14,000 ft.

Some additional cargo hook testing was done at an airfield elevation of 7,000 ft on the AW169. For the AW189, testing was done at airfield elevations of sea level and 8,000 ft. In-flight altitudes up to 20,000 ft were also tested. Not all test manoeuvres were repeated at every variation of altitude and gross weight and the shape of the CG envelope meant the forward CG limit moved further aft at higher gross weights. Some of the test points were repeated to explore aspects such as the variable rotor rpm system on the AW169, cabin strengthening modifications on the AW189 and the vibration control systems on both helicopters. Comparison of loads at extreme hot and cold air temperatures was conducted. Load assessments for specialist role equipment were also carried out, including rescue hoists for search and rescue and a cargo hook for underslung loads. All the test points were flown to a defined and repeatable procedure and the static and dynamic loads were recorded by the installed instrumentation on the prototype airframes. The test points were typically short in duration, commonly with a 20 seconds 'entry' to achieve the required test criteria, 20 sec at the 'steady' state test point and 20 sec to 'exit' back to the pre-test condition.

This data was assessed post-test primarily for fatigue purposes using alternating fatigue loads, which were typically lower than the maximum and minimum loads recorded for each test point. Some assessment was done regarding absolute load figures, but this was primarily a sample assessment of a select number of key parameters to determine how critical the variations in altitude, CG location and air temperature were to the loads encountered.

<sup>34</sup> Refer to [section 1.6.3](#)

For the AW169, the summary of findings from the flight test load survey activity was documented in the helicopter manufacturer's report 169F0290T001/2/01. With regard to altitude variations, it concluded:

*'Flight loads measured at 5,000 ft are generally higher than those measured above 5,000 ft for all considered components and parameters.'*

For loads specifically related to airfield manoeuvres, it reported:

*'The flight loads registered on AW169P3 helicopter during flight at field altitude 5,000 ft are lower or at least similar to those recorded at sea level (0 ft). For the key parameters loads recorded at sea level (Core Load Survey) are in several cases higher or at least similar to those gathered at 10,000 ft HD. Flight loads at 12,000 ft HD are generally less critical than those coming from lower field altitudes. Plots show that the weight limitation applicable at 14,000 ft HD it is sufficient to obtain loads similar to what[sic] measured previously.'*

For the loads related to use of the rescue hoist, it stated:

*'The investigation of the effects of the lateral CG, typical of the Rescue Hoist configuration, on the flight loads is done by comparison between Basic data and Rescue Hoist data. From the analysed flight conditions and key parameters it can be concluded that there is no significant difference between Basic and Rescue Hoist configurations from an aerodynamic point of view.'*

For comparison of internal vs external load carrying using the cargo hook, it concluded:

*'No significant differences are shown confirming that helicopter flight loads depend only on the total weight of the aircraft. For conditions performed at field sea level and field high altitude the data show no significant differences between Basic and Cargo Hook configurations.'*

The two key parameters relevant to validation of the bearing load spectrum were axial load (Fz), which was measured using strain gauges at a single point on the tail rotor actuator control shaft, labelled TH1. The other was bending moment. As it was not possible to measure this at the bearing itself, it was measured at two points on the actuator control shaft labelled 'BB1' and 'BB2', and in two planes at 90° to each other labelled 'PRL' and 'NRL', using arrays of strain gauges (Figures 13 and 14).

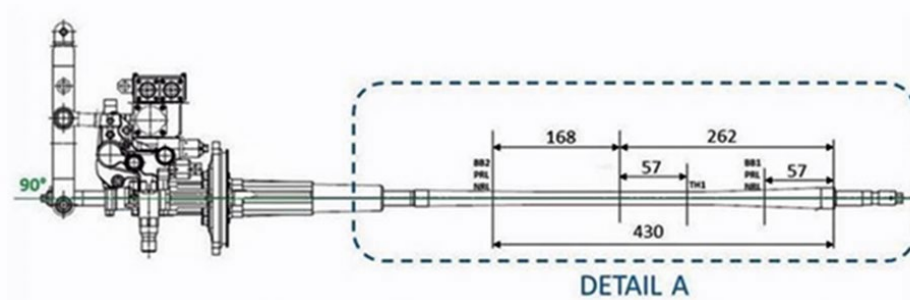


**Figure 13**

AW169 flight test instrumentation location of sensors to measure axial load and bending moment  
(Original image courtesy of the manufacturer)

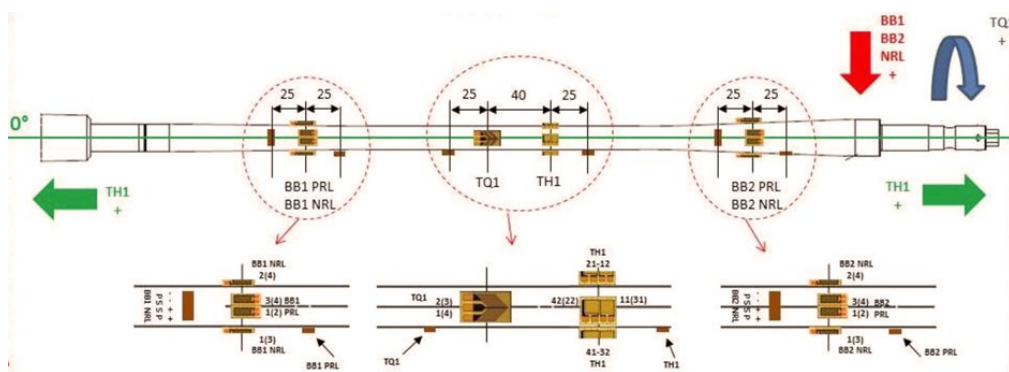


**Figure 14**

AW169 flight test instrumentation to measure axial load and bending moment  
(Original image courtesy of the manufacturer)

A sign convention was used by the helicopter manufacturer to identify load direction. For axial load, extension of the control shaft away from the hydraulic pack was negative and retraction towards the pack was positive<sup>35</sup>. For bending moment, right to left (looking vertically down) was positive for ‘PRL’ and top to bottom was positive for ‘NRL’.

The load surveys carried out during the AW169 flight testing recorded highest tail rotor axial loads that were lower than the development load spectrum (Table 3) had predicted. The manufacturer stated that they considered this was due to the conservatism used in the elastomer stiffening factor, which cold temperature trials confirmed was not as severe as originally anticipated. The AW189 uses different elastomer materials than the AW169 and the loads were similar to those in the spectrum.

35 The annotation for TH1 in Figure 14 shows both directions as positive in error. The right arrow should indicate negative load direction.

The results of the flight test load survey were not shared with the bearing manufacturer to validate the original bearing suitability assessment.

The test data was requested by and provided to the investigation for detailed assessment.

#### 1.6.7 Tail rotor certification testing

The assessment of bearing performance in drivetrain applications during the certification process for the AW169 and the AW189 was, with the agreement of the certification authority, based on review of the condition of bearings after completion of an endurance test and following development and certification flight test campaigns.

##### 1.6.7.1 Tie down helicopter rig endurance test

For both the AW169 and AW189 an endurance test was carried out in accordance with CS 29.923, using a test rig called the Tie Down Helicopter (TDH). As the name suggests, this was a fully functional helicopter airframe restrained to the ground to prevent it from moving during testing. The test schedule, specified by CS 29.923<sup>36</sup>, included 20 equal duration cycles of 10 hours or more at various power settings used in normal operating conditions, plus a number of abnormal condition operating periods such as main rotor overspeed and overtorque, with the torque from both engines or with one inoperative. One phase of the test included three hours of operation at main rotor maximum continuous torque and speed. During this period the yaw controls had to be cycled at least 15 times each hour through maximum left turn, neutral, to maximum right turn. The full yaw pedal input was held for 10 seconds at each extreme. During the rest of the test the control inputs in yaw replicated the following scenarios in sequence:

- Max vertical thrust (20% of time)
- Max forward thrust (50% of time)
- Max left thrust (10% of time)
- Max right thrust (10% of time)
- Max rearward thrust (10% of time)

The manufacturer confirmed that the airframe was fully instrumented during the test. Whilst the test specification was primarily intended to endurance test the main mechanical components of the drivetrain system, the instrumentation also recorded the tail rotor actuator loads during these simulated manoeuvres.

<sup>36</sup> The full text of the requirement can be found in [Appendix H](#).

As such, the tail rotor loads achieved were a product of the test, rather than the test being intended to achieve specified tail rotor load targets.

Given the high sampling rate and the large volume of data this generated, it was not practical for the investigation to obtain all the data recorded or to analyse the bearing bending moments. However, representative samples for axial load from each phase of the test were provided by the manufacturer and were reviewed. The sampling rate of 1 kHz meant that extremely transient short duration loads were captured. Although absolute load magnitudes are quoted these may have only occurred for fractions of a second. The load data showed significant variation in the absolute values over the 20 second duration of the samples provided, which the manufacturer confirmed was partly due to 'noise' within the data. This was particularly evident on the AW189 dataset.

From the data provided, the highest absolute tail rotor axial loads on the AW169 test were generated during the maximum continuous power test, at 100%  $N_R$  when full left yaw pedal was applied, and an axial load of 9,738 N was recorded. This load was reasonably consistent and repeatable for the four 10 second periods that this pedal position was held in the data sample provided. A total of 45 pedal applications were made during this phase of the test, resulting in the load being applied for 7.5 minutes. The highest consistent axial load in any other test phase was during the 6 minute overspeed power test 'right flight' at 105%  $N_R$ , when an average load of 6,836 N was recorded. All the other loads in the data provided were lower than this.

On the AW189 the highest load was recorded during the overspeed power test 'left flight' at 105%  $N_R$ , when a transient figure of 18,488 N was recorded.

However, the peak-to-peak values recorded in this 20 second sample gave a range of 11,225 N and the manufacturer stated this maximum figure was likely to have just been noise in the data rather than a genuine load. Given the noise limitations in several of the recorded data samples it was difficult to determine with precision the highest consistent load for the AW189. A 20 second sample from the 12 minute long 'hover' section of the maximum continuous power one engine inoperative test phase at 104%  $N_R$  was reasonably consistent and gave an average of 9,127 N but most of the average loads where the magnitude range was more consistent were below 5,000 N.

The tests ran for 383 hours on the AW169 and 334 hours on the AW189. At the end of the respective tests each tail rotor bearing, along with all the other drivetrain components, was disassembled and in this case inspected by the bearing manufacturer. No visual evidence of RCF damage was identified in either case, allowing the bearings to pass the certification test. No laboratory investigations to assess the material microstructure were carried out, as these

were not required by CS 29.923. The inspection did confirm that for the AW169 test, the bearing contained 3.62 g of grease when disassembled compared to the original 6 g when new. There was no evidence of damage or displacement of the bearing seals. On the AW189, 3.14 g of grease remained from the original 6 g: no damage to the seals was noted.

#### 1.6.7.2 Flight test programme

Tail rotor bearings were fitted to nine helicopters used during the certification flight test programmes of the AW189 and AW169. A snapshot of the record of flight hours performed on each bearing was quoted by the manufacturer in email correspondence (Table 5)<sup>37</sup> up to the point when the new post-accident modified bearings<sup>38</sup> were installed.

The columns should be read vertically, with the five-digit numbers in row two referring to the individual flight test helicopter serial numbers. The duplex bearings fitted to each airframe during its life are indicated by the serial number in brackets. The last two rows report the amount of flight hours performed pre-certification and post-certification.

The original duplex bearing part number shown in column one was 4F6430V00551. MM6430V00151 is the part number for the new bearing introduced following the accident, which has been fitted to a number of flight test helicopters as shown.

The manufacturer advised that only two duplex bearings, fitted during the original certification flight testing, were removed for reasons relevant to the investigation.

For helicopter s/n 69004, bearing s/n 12112 was removed on 22 November 2013, as a slight roughness in operation was detected during a scheduled 25 flight hour inspection<sup>39</sup>. The roughness was not confirmed once an axial force was applied to the races while rotating the bearing and no further investigation was carried out.

For helicopter s/n 69004, bearing s/n 13108 was removed on 19 June 2014 due to the presence of grease on the bearing face during visual inspection. The bearing was considered serviceable after removal and no further investigation was carried out.

<sup>37</sup> Flight hours accrued as of 5 April 2021.

<sup>38</sup> In response to this accident the helicopter manufacturer replaced the existing bearing with a new bearing type. See [section 1.12.4](#) for details of the modification.

<sup>39</sup> Maintenance requirements for prototypes are different from in-service maintenance requirements.

P/N	AW169 (T.C. Issued 15/07/2015)				AW189 (T.C. Issued 07/02/2014)				
	69002	69003	69004	69005	49002	49003	49004	49005	49006
4F6430V00 551	(12111) 760h 40'	(13128) 783h 40'	(12112) 82h 45'	(13127) 553h 50'	(10103) 850h 15'	(10105) 122h 25'	(10109) --		(12104) 505h 40'
	(19121) 149h 15'	(18122) 291h 15'	(13108) 54h 05'	(20175) 28h 35'		(10106) 638h 45'	(17115) 0	(10107) 1128h 00'	
	Installed P/N MM6430V0 0151		(14128) 684h 10'	Installed P/N MM6430V0 0151		(19154) 51h 50'	(10109) 1192h 10'	Installed P/N MM6430 V00151	
			(19268) 24h 05'			(14110) 475h 05'	Installed P/N MM6430V0 0151		
			Installed P/N MM6430 V00151			Installed P/N MM643 0V00151			
<b>FH pre T.C.</b>	469h 30'	307h 00'	408h 50'	277h 45'	558h 40'	561h 20'	395h 55'	235h 55'	147h 45'
<b>FH post T.C.</b>	440h 25'	767h 55'	436h 15'	304h 40'	291h 35'	726h 45'	796h 15'	892h 05'	357h 55'

**Table 5**

Flight hours accumulated on the tail rotor duplex bearings used in flight test, up to introduction of the new post-accident bearing

After type certification was granted, the respective duplex bearings remained fitted to the flight test aircraft for continued operation on flight test duties. No bearings were removed after pre-certification flight testing was completed specifically to confirm their condition for certification purposes. When the new post-accident bearing was fitted, the old standard bearings were disposed of without being inspected.

### 1.6.7.3 Tail rotor actuator certification testing

The Tail Rotor Actuator (TRA) was designed to work with dual independent hydraulic systems to provide redundancy. In normal operation both systems are pressurised and the operating force is combined. In single hydraulic system operation either system should still be capable of controlling the movement of the tail rotor blades. The helicopter manufacturer's safety assessment for the TRA stated that in normal operation with both hydraulic systems pressurised, the stall load in both extension and retraction was 25,780 N. For a single hydraulic system, it was 12,760 N in both extension and retraction. It also listed unrestricted linear movement (loss of control) of the TRA as catastrophic and confirmed the castellated locking nut as a single point of failure.

### *Stall load test*

The tail rotor actuator was tested in extension and retraction using each of the single hydraulic systems in turn.

For hydraulic system 1 the stall loads in extension and retraction were 1,281 kg (12,567 N) and 1,300 kg (12,753 N) respectively. For system 2, they were 1,284 kg (12,596 N) in extension and 1,327 kg (13,017 N) in retraction.

#### 1.6.8 Tail rotor system failure emergency procedures

The AW169 RFM contains a single consolidated emergency procedure to cover all tail rotor system failures, the LTE drill.

##### *AW169 LTE emergency procedure*

The preamble to the AW169 LTE emergency procedure states that losing tail rotor effectiveness *'will result in a rapid yaw to the right and a loss of yaw control.'* It explains that the severity of the initial yaw would depend on the helicopter's airspeed and main rotor torque settings at the time of failure. The aerodynamic stabilising effect of the helicopter's fin and airframe would increase with airspeed while increased torque settings would lead to higher de-stabilising forces.

Guidance in the RFM is that *'severe yaw rates will result in large yaw angles within a very short period of time and, depending on the flight conditions at the time of failure, it is possible that yaw angles in excess of 30° will be experienced.'* The RFM further states that *'very high yaw rates will produce aircraft pitching and rolling making retention of control difficult without the use of large cyclic inputs, which are structurally undesirable.'* Due to the disorientating effects on the pilot, the RFM recommends taking prompt action to prevent post-failure yaw rates from reaching *'unacceptably high levels.'*

The RFM emergency procedure lists two LTE scenarios: in the hover and in forward flight (Figure 15). In both scenarios the first required action is to reduce the de-stabilising main rotor torque using the collective lever. With an anti-clockwise rotating main rotor, uncommanded right yaw requires the collective to be lowered, left yaw requires it to be raised.

For the hover scenario, if time permits, pilots should shut down both engines to remove engine torque. In forward flight, if possible, the helicopter's speed should be altered to generate a balancing aerodynamic stabilising force.

Lowering the collective lever reduces main rotor pitch angle, and thereby lift, leading to a descent. With the collective fully lowered any rate of descent would rapidly increase. The drill does not offer guidance as to how to judge at what point the collective should be raised to arrest rates of descent generated through application of the procedure.

<b>In Hover</b>	
<ul style="list-style-type: none"> <li>- Lower collective to <b>LAND IMMEDIATELY</b> while maintaining attitude and minimizing lateral translation with the cyclic control;</li> <li>- Select both <b>ENG MODE</b> knobs to <b>OFF</b> if time available.</li> </ul>	
<b>In Forward Flight</b>	
<ul style="list-style-type: none"> <li>- Move collective immediately to minimize yaw rate (lowering the collective to reduce yaw right / increasing the collective to reduce yaw left);</li> <li>- Establish a suitable airspeed/rate of descent/attitude combination to reach a stable condition;</li> <li>- At landing site assess running landing capability;</li> </ul>	
Approved	Issue 2 Page 3-49

**Figure 15**

AW169 RFM LTE emergency procedure  
(Courtesy of the manufacturer)

The LTE emergency procedure was not designed to address tail rotor pitch control runaway and was not required to because this was considered, in certification terms, a catastrophic failure<sup>40</sup>. Nonetheless, the most suitable initial course of action for a pilot in response to a tail rotor pitch control runaway would be to follow the RFM LTE emergency procedure guidance.

#### 1.6.9 Helicopter performance

Under the EASA regulatory framework, helicopters operate in Performance Classes, but they are certified according to their engine failure capability.

##### *Performance Classes*

Operational regulations are specified according to the single engine failure capability of the helicopter in a defined area of operations. These are designated as Performance Classes.

<sup>40</sup> One for which it is not possible to design an RFM emergency procedure that would enable the pilot to regain control and achieve continued safe flight and/or a safe landing.

- In areas where Performance Class 1 (PC1) operations are planned the helicopter must be able to safely continue the flight or land within the rejected takeoff or landing area.
- Performance Class 2 (PC2) requires that the helicopter should be capable of either being safely flown away or executing a forced landing during takeoff and landing.
- Performance Class 3 (PC3) operations are those where, should an engine fail, a forced landing will be required.

Note: for both PC2 and PC3 operations there must be a reasonable expectation that no injuries would arise from a forced landing.

Due to the limited availability of alternative emergency landing sites, PC1-compliant procedures were applicable when operating at the King Power Stadium.

#### *Certification categories*

Helicopters certified to CS 29 are either in performance Category A, Category B or both. The two categories are:

- Category A (Cat A). To be certificated in Category A helicopters must have critical engine failure performance capability sufficient for continued flight or a safe rejected takeoff. Certification in Category A requires that the helicopter has the capability, performance data and procedures necessary to conduct PC1 and PC2 operations.
- Category B (Cat B). Category B helicopters are not required to have a guaranteed capability to continue safe flight in the event of an engine failure.

The AW169 was certificated in performance Categories A and B.

#### *King Power Stadium departure profile*

To comply with the regulatory requirement for a PC1-compliant departure from the King Power Stadium an approved Cat A procedure was required. The appropriate profile to be flown was the 'Ground and elevated heliport/helideck variable TDP<sup>41</sup> procedure' (Figure 16) as specified in the RFM.

---

41 The takeoff decision point (TDP), is defined in the AW169 RFM as 'The first point in the takeoff path from which a continued takeoff (CTO) capability is assured and the last point from which a rejected takeoff (RTO) is assured, within the rejected take off distance.' The TDP value represents a height above the takeoff surface.

The Cat A profile is designed such that should one engine fail between lifting-off and reaching the TDP the helicopter can safely return to the takeoff position. Once above TDP height a rejected takeoff is no longer assured and the pilot is required to continue the takeoff by lowering the helicopter's nose to commence an accelerating transition to climbing forward flight with due regard to obstacles on the planned departure track.

RFM performance data used for calculating TDPs assume a minimum 80 ft height loss during a continued takeoff after an engine failure at TDP and require a minimum planned obstacle clearance of 35 ft. The maximum permitted crosswind for the departure was 10 kt. The Cat A procedure performance data also includes a table which allows pilots to calculate the effect on one-engine climb performance of turns undertaken when above 200 ft ATS<sup>42</sup> and climbing to 1,000 ft ATS at the speed for best rate of climb ( $V_y$ ).

Turns at speeds below  $V_y$  are not explicitly prohibited by the RFM but could adversely affect climb performance following an engine failure. Specifically, turns below the takeoff safety speed ( $V_{TOSS}$ ) could compromise the helicopter's ability to achieve the required 35 ft minimum obstacle clearance height during a single-engine continued takeoff (CTO) manoeuvre. The manufacturer's expectation is that turns will not be flown below  $V_y$  and it does not publish performance data to support them.

The RFM contains the following caution related to the variable TDP procedure:

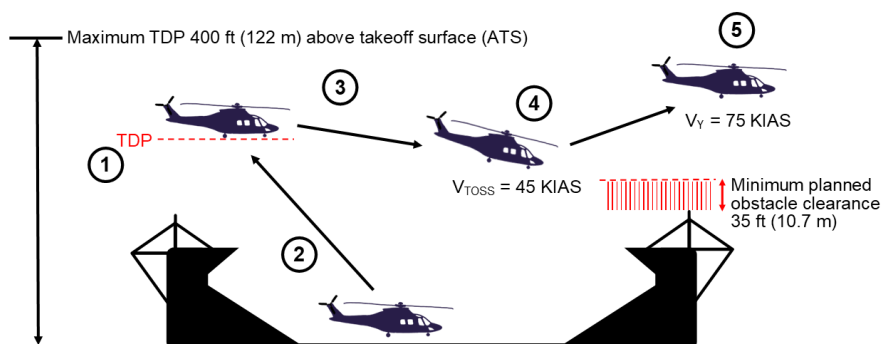
*'If this procedure is modified, it may not be possible, if an engine fails in the Take-Off path, to carry out a safe OEI<sup>43</sup> landing or achieve the scheduled OEI performance.'*

The investigation found that the performance analysis<sup>44</sup> used to support the initial application for G-VSKP to use the King Power Stadium as a landing site had assumed an incorrect maximum relevant obstacle height of 70 ft ATS. Documents provided to the investigation showed that, while the stadium canopy was 70 ft above the pitch, the roof support structure was approximately 95 ft high. The performance analysis dated back to 2016 and, using an assumed height loss of 85 ft and taking 35 ft as the minimum obstacle clearance height, calculated a TDP of 190 ft, which was then rounded up to 200 ft.

42 Above the takeoff surface.

43 One Engine Inoperative.

44 Undertaken by a previous Operator.



- ① Pilot takes into account environmental conditions and known relevant obstacles on the departure track when calculating the TDP during pre-flight planning
- ② Rearward climb established at  $\leq 300$  fpm rate of climb, pilot maintains sightline to the takeoff point between the yaw pedals
- ③ Once above TDP the pilot lowers the helicopter's nose by  $15^\circ$  to start the transition to forward flight and the helicopter is committed to a continued takeoff (CTO)
- ④ On passing takeoff safety speed ( $V_{Toss}$ ) the pilot begins accelerating towards climb speed ( $V_Y$ ) and climbs to 1,000 ft ATS
- ⑤ When above 200 ft ATS and  $V_Y$  has been reached, the landing gear can be raised and the after takeoff checks completed

**Figure 16**

Overview of variable TDP procedure for the AW169

The investigation found evidence to indicate that the pilot had measured the support posts' height when he re-surveyed the site in October 2017<sup>45</sup>, but did not find a subsequently updated version of the performance analysis. Using the assumptions from the original performance analysis, but based on the height of the roof support structure, the minimum TDP height for the stadium would have been 215 ft. The investigation was not able to confirm what TDP height the pilot was using on the accident flight.

#### 1.6.10 Bird strike protection

The AW169 is certified as a Category A large rotorcraft. The Certification Standards for bird strike protection, CS 29.631, state that a helicopter in this category must be capable of continued safe flight and landing after an impact with a 1 kg bird at  $V_{NE}$ <sup>46</sup> which, for the AW169, is 165 kt.

45 To satisfy the NCC operator's requirement for site survey periodicity, see section 1.17.3 regarding operational oversight.

46 The published never-exceed speed for the helicopter.

### 1.6.11 Fuel tanks

The AW169 is fitted with two 1,130 litre capacity fuel tanks in the rear of the passenger cabin. Each fuel tank consists of an internal bladder made from tear and abrasion resistant rubber impregnated fabric, which is encased in a composite structure (Figure 17). The bladders are positioned within the supporting structure by fuel resistant high-density foam, to prevent liner abrasion of the bladder material. A pipe connects the two fuel tanks allowing fuel to flow between both tanks.



**Figure 17**

AW169 fuel tank arrangement  
(original image courtesy of the manufacturer)

### 1.6.12 Cabin configuration

In order to allow the AW169 to meet different role requirements it can be fitted with several alternative cockpit and cabin configurations. G-VSKP had been fitted with a VIP interior during manufacture, which allowed up to seven passengers to be carried in the passenger cabin, four in rearward facing seats located at the forward cabin bulkhead and three in forward facing seats to the rear of the cabin.

### 1.6.13 Health and Usage Monitoring System (HUMS)

The maintenance of a helicopter can be enhanced by analysing occurrences such as system faults and looking for changes in the vibration levels of the rotating components. This is done using helicopter systems to gather data, the manufacturer's on-line system to process the HUMS data (Heliwise), and

personnel to review the results and take action where necessary. This description focuses on the aspects of the system associated with vibration monitoring.

As vibration monitoring systems are not developed or certified to meet the requirements of a primary safety warning system, the manufacturer must demonstrate that the helicopter still meets the airworthiness requirements for reliability and risk mitigation, without relying on vibration monitoring to achieve this. As G-VSKP was used for Non-Commercial Complex (NCC) operations HUMS usage was not an operational requirement.

#### *General system overview*

Two Aircraft and Mission Management Computers (AMMCs) form the core of the data gathering system. These receive data from the other onboard systems and incorporate the vibration monitoring system. Vibrations are sensed using accelerometers distributed around the helicopter, and partially processed in the AMMCs.

Some of the data, such as the raw vibration data, is stored in the Data Transfer Device (DTD) and other data is stored in the AMMCs. When required, the AMMC data is transferred to the DTD and then the data is transferred from the helicopter to the Heliwise system. Each transfer of data to Heliwise is given a Download Sequence Number (DSN) for that helicopter. As well as other HUMS tasks Heliwise compares the vibration data with previously downloaded results to assess trends. Heliwise provides feedback which can be used for maintenance purposes.

Different levels of manufacturer support are available for analysing the Heliwise results. G-VSKP was supported under a 'Standard Support' arrangement which meant that the customer was responsible for reviewing the results of the Heliwise processes which highlight issues, such as increasing vibration trends and recorded faults. The helicopter manufacturer's HUMS support team would then reply to queries raised by the customer.

Heliwise was only used during maintenance inputs for this helicopter. More regular transfers of data to Heliwise during normal operations, such as at the end of a day of flying, can add a further layer of health monitoring such as identifying increased vibration levels associated with specific components. This was not a requirement for NCC operations.

#### *Occurrence logging*

The AMMCs record a log of when significant events occur. These include cautions and warnings issued to the crew, system faults and torque limits being exceeded.

### *Usage monitoring*

HUMS can generate summaries of how the helicopter and its systems are being used. Engine usage and helicopter utilisation as well as more detailed aspects of the operation can then be assessed to influence maintenance decisions.

### *Vibration Health Monitoring (VHM)*

Rotating parts such as bearings and meshing gears generate vibrations. Degradation in these parts leads to changes to the vibration characteristics. The vibrations can be monitored over time to identify trends that indicate a developing problem with a component. These trends can be used to trigger corrective maintenance.

The vibrations are sensed using accelerometers located to detect vibrations of targeted components. The accelerometer outputs are not recorded or monitored all the time as their vibration levels will vary under different power or flight conditions. In order to allow for accurate comparison of vibration levels, data is only collected when certain conditions are met. The sample rate for the accelerometers and the types of signal processing carried out on the collected data must also be tuned to the particular component they are monitoring. The component type and specific design details affect the optimal monitoring configuration. In the case of bearings, the frequencies of interest are governed by how fast the parts are rotating and the dimensions of key bearing parts.

Different methods for processing the data are used to identify different types of degradation. The result of this process is called a Health Index or Health Indicator (HI). It is changes in these HI values over time that trigger corrective action.

Figure 18 illustrates the A13 accelerometer mounted on the tail rotor gearbox for vibration monitoring.

There is also a biaxial accelerometer on the tail rotor gear box for the purpose of monitoring the rotor track and balance. None of these were positioned to monitor for problems in the duplex bearing as there was no requirement to do so. The location of the accelerometer meant that vibrations generated by the duplex bearing were obscured by the vibration of other components between the bearing and accelerometer.

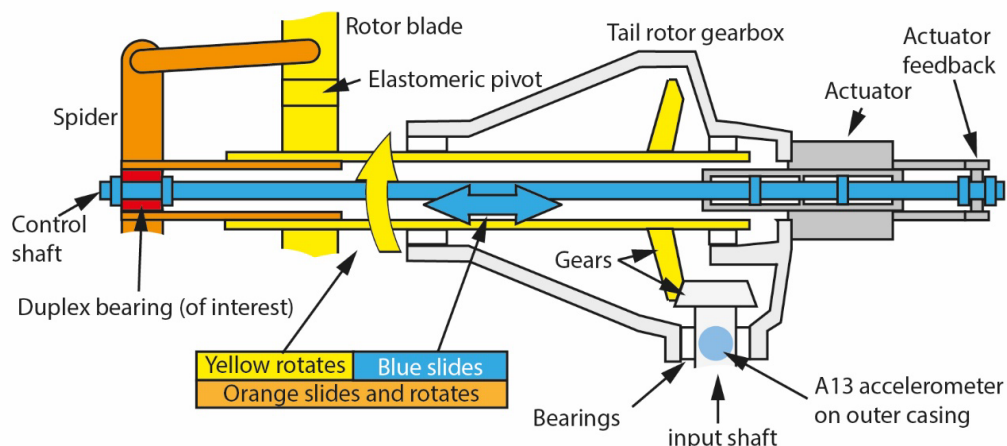


**Figure 18**

Simple schematic of the tail rotor gearbox showing the relative locations (viewed from forward looking aft) of the vibration sensing accelerometer and the failed critical duplex bearing. Not to scale.

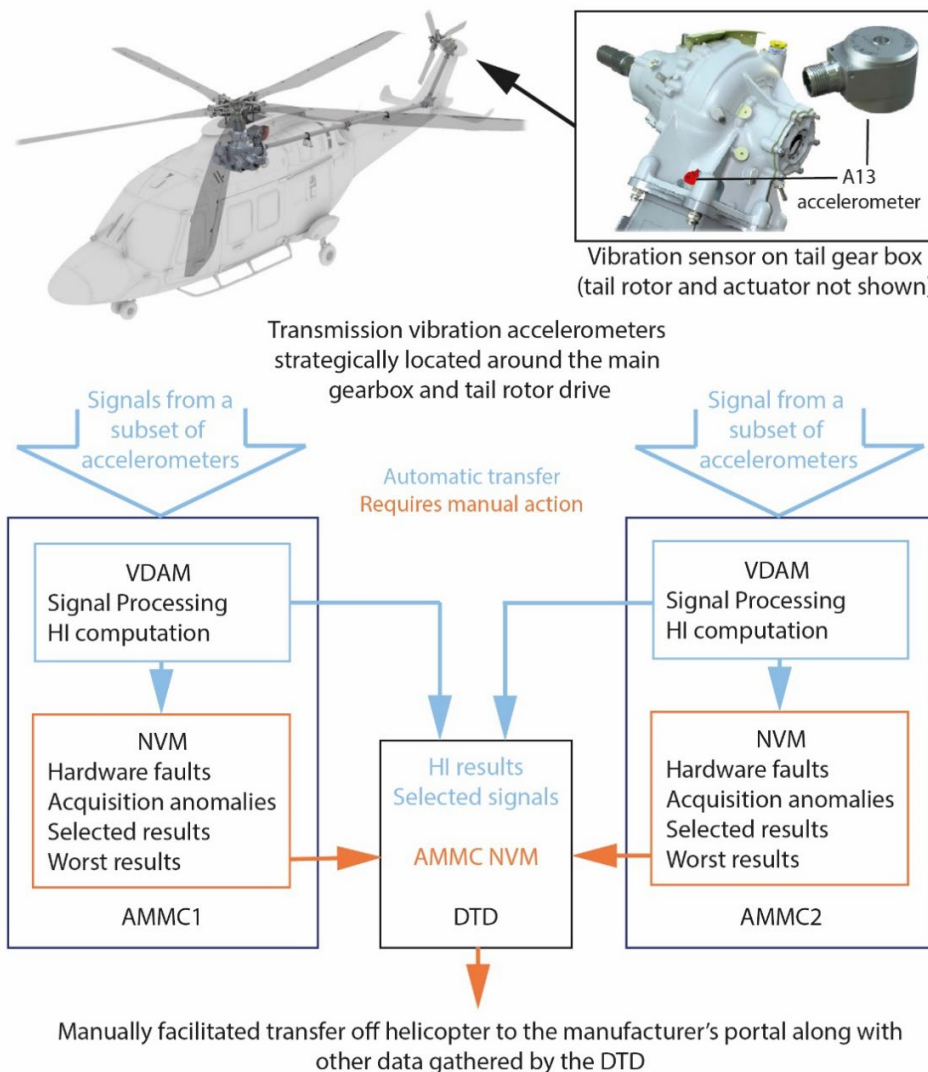
Figure 19 provides an overview of how the Transmission Vibration Monitoring (TVM) data passes through the helicopter systems. Vibration is sensed using accelerometers in various locations around the transmission system. Vibration data is gathered and partially processed by the two Vibration Data Acquisition Module (VDAM) boards in the AMMCs.

The AMMCs store some of the results in their Non-Volatile Memory (NVM) but other results and the raw vibration data itself are stored in the Data Transfer Device. Some of the transfer of data from the AMMC to the DTD is automatic and some requires manual action.

The AMMCs store some of the results in their Non-Volatile Memory (NVM) but other results and the raw vibration data itself are stored in the Data Transfer Device. Some of the transfer of data from the AMMC to the DTD is automatic and some requires manual action.

A continuous recording of a number of flight parameters, referred to as 'ESUM' data, is also recorded in the DTD.

The transfer of data from the DTD to the Heliwise system is not an automatic process and must be manually initiated.



Factual Information

**Figure 19**

Transmission vibration monitoring data flow (original image courtesy of the manufacturer)

1.6.14 Air-Data Attitude Heading Reference System (ADAHRS) – data bus limits

The two ADAHR Units (ADAHRUs) use various internal and external sensors to generate location, motion and orientation data for the cockpit instruments and the AFCS. The data is communicated over data buses. The format of the data buses is such that yaw rates above 128°/s cannot be represented so, if a higher yaw rate is sensed, the ADAHRU flags the yaw rate data as invalid.

The ADAHRUs store fault data in NVM associated with internal ADAHRU issues. They do not store faults relating to the ADAHRS function of providing data to the aircraft systems. For example, if the yaw rate exceeds 128°/s the

ADAHRUs would not log a fault because they are capable of managing yaw rates greater than 128°/s. The ADAHRUs would however flag the data as invalid due to the limitations of other systems.

Crew alert messages relating to the attitude data use the abbreviation AHRS.

#### 1.6.15 Flight Control Computer (FCC)

The FCC is the core of the AFCS. The FCC is located in the nose of the helicopter. It contains processing boards which are functionally split into two channels, one for each autopilot. Each channel has two lane modules that carry out the same autopilot functions but are of a different design to each other to add robust redundancy and independence.

Each lane module stores data relating to the health of the module hardware and equipment software. It does not store health data relating to the autopilot software it is running or other hardware within the AFCS. An example of this is how the system handles invalid yaw rate information from the ADAHRS. The AFCS software generates a caution to the crew which is logged in the AMMC NVM and recorded by the Data Acquisition Flight Recorder (DAFR). However, it would not be logged into the FCC NVM because it only records faults with its own internal systems and these would be operating normally.

#### 1.6.16 Crew alerting system

Warnings and cautions trigger visual indicators above each pilot's Primary Flight Display (PFD). They also add to the list of alerts on the PFDs in a prioritised order. Some alerts also have an audible sound and/or message. The triggering of all the alerts are recorded in the AMMC NVM, and many are recorded by the DAFR.

### 1.7 Meteorological information

The accident occurred at night. At the time of the accident the weather was clear with a surface wind of 10 to 12 kt from a north to north-westerly direction in the vicinity of the King Power Stadium. There was no significant cloud below 2,500 ft.

### 1.8 Aids to navigation

No relevant information.

### 1.9 Communications

No relevant information.

## 1.10 Aerodrome information

### 1.10.1 Aerodrome

No relevant aerodrome information.

### 1.10.2 LCFC training ground

The LCFC training ground, located 1 mile south of the King Power Stadium, is owned by the club and was regularly used as a landing site for G-VSKP. It is a secure access-controlled facility with motion-activated CCTV coverage.

### 1.10.3 King Power Stadium

The King Power football stadium is of an enclosed design with covered seating and an open roof. It is situated in the south of Leicester.

Helicopter flights into the stadium began after the owner of G-VSKP bought the football club. The operation originally used an AW109 before switching to G-VSKP in 2016. Flights in and out of the stadium were coordinated through the LCFC match-day control room.

LCFC had developed their own risk assessment for the helicopter operation which considered ground-based risks to the aircraft as well as risks posed to personnel on the ground.

## 1.11 Recorded information

The helicopter was fitted with a flight recorder and other avionics equipment that stored data in Non-Volatile Memory (NVM). External sources of recorded information considered by the investigation included radar recordings, Air Traffic Control (ATC) Radio Transmission (RT) recordings and image recordings. The imagery came from CCTV cameras, witness mobile phones, body worn cameras, car mounted cameras and a camcorder. Historical data from the helicopter previously uploaded to the helicopter manufacturer's Heliwise system was also reviewed.

The following sections describe the information recovered from the above sources where pertinent, followed by an amalgamated description of the accident flight and a review of the available HUMS data.

### 1.11.1 Flight recorder

The helicopter was fitted with a Data Acquisition Flight Recorder (DAFR). This had suffered heat damage, but the memory module was intact and was successfully downloaded at the AAIB. This recorded two hours of audio and 25 hours of data. The recordings continued for a period after impact, powered by its Recorder Independent Power Supply (RIPS).

The audio recording captured most of the flight from Fairoaks to London Heliport on the day of the accident. It recorded the subsequent flights to the training ground, the stadium and finally the accident flight. Four channels of audio were recorded, one from each of the two cockpit headsets, one from the Cockpit Area Microphone (CAM) and one from the cabin intercom system.

The CAM channel suffered from periodic brief dropouts throughout most of the recording with a significant amount of disruption during the accident sequence. This is discussed further in the 'Cockpit Area Microphone channel audio quality' section of [Appendix D](#).

Spectrum analysis of the CAM did not find any anomalies across the broad spectrum generally or specifically in the tail rotor signatures before the departure from controlled flight. Tail rotor signatures did not show anomalies after the departure from controlled flight; though the analysis was compromised in this period due to the quality issues discussed above and in [Appendix D](#).

Spectrum analysis enables identification of rotating parts that create vibrations with sufficient energy to affect the audio recorded by the area microphone in the cockpit. Gear meshing and fan blade motion transfer large amounts of energy and create larger vibrations than smaller, less energetic sources such as bearings. Fluctuations in the spectrum at the frequencies associated with the tail rotor duplex bearing were observed with extreme spectrum analysis configurations but they were not distinguishable from other seemingly random fluctuations at other frequencies. The CAM and recording system are not designed for the purpose of tracking the conditions of bearings in the tail rotor; finely tuned monitoring of an accelerometer in the tail section is required for that.

The recorded data captured the accident flight and the previous 34 flights dating back to 1 September 2018.

The main source of data recorded by the DAFR in this installation design were the two AMMCs. As well as the aircraft parameters, each provided time data from their own internal clocks. Due to issues with the sampling method for the data, the AMMC2 timeline included repeated timestamps. The time recordings from both AMMCs were not stable in the middle of the accident sequence,

starting at approximately 1937:52 hrs. For the purpose of the investigation, a stable timeline was extrapolated from the stable AMMC1 timestamps for the initial climb out of the stadium, based on the assumption that the recording rate remained consistent.

The yaw rate parameter saturated at the 128°/s limit of the databus carrying the data. This not only affected the recorded yaw rate parameter but also generated a failure in the ADHRS system. Recorded magnetic heading data was used to derive the yaw rate past this limit. However, the time between the heading samples is subject to jitter (Section 1.18.12.1) so some smoothing of the parameter was carried out to show the general trend.

As the yaw rate increased, the longitudinal acceleration parameter reached and remained above its 1 g limit because the accelerometer was located some distance from the centre of rotation and so was subjected to a large centrifugal acceleration.

The GPS position parameters had become highly inaccurate by the end of the accident sequence so there was no accurate source of flightpath data.

#### 1.11.2 Avionics

A number of avionics units were identified as potentially containing useful recordings in NVM. These suffered various degrees of heat damage.

The DTD would have contained raw vibration sensor data from the accident flight and more comprehensive data from previous flights not yet downloaded from the helicopter. However, it suffered unrecoverable damage to the memory chips of the solid-state hard drive.

Data was recovered from the two AMMCs, the FCC and the two ADAHRUs by chip removal and download at the AAIB.

Further decoding of the downloaded data was carried out by the manufacturers and further detail about how the units store data was provided to the AAIB to corroborate the processes.

The two AMMCs recorded HUMS related information, the results of the onboard vibration analysis activities and logs of different aspects of the operation including faults, exceedances and crew alerts. The FCC and ADHRS record less useful information but were downloaded due to the faults flagged with these systems during the accident sequence.

Some of these logged events could be correlated to the timeline by the GPS timestamps recorded. However, the source of GPS time data became unreliable

during the accident sequence. This was corrected for using the DAFR recording of the GPS time. Some of the times recorded in the avionics were elapsed times since power was applied to the unit. The helicopter systems are not designed to enable the DAFR to capture the time when power is applied to the downloaded units, but analysis of previous flights along with power-up timing information from the manufacturers of the various units enabled correlation of the recorded elapsed times with the accident timeline.

### *AMMCs*

Three files were recovered from the data from each of the two AMMCs, relating to logged issues/events, transmission vibration results and helicopter usage.

The first of these contained logged faults, exceedances, alarms and events against timestamps. The data recovered from the accident AMMCs contained many logged entries associated with the accident as well as many nuisance log entries. Nuisance records are those that reflect an expected system status at the time of logging rather than a problem. An example of this would be logging a system as failed when it has not yet had time to boot-up during flight preparations.

The AMMC software is continually being developed. Nuisance logs are designed out of the system at each successive software revision.

The AMMCs fitted to G-VSKP were operating on Phase 3 software. Downloads from other helicopters with the same software revisions were reviewed and all faults considered by the manufacturer as nuisance were found in some if not all other recordings.

The AMMC logged data corroborated the DAFR recordings in terms of crew alerts and flagged issues during the accident sequence.

The information in the recovered files relating to usage and vibration were also analysed and are discussed in section 1.11.7.

### *Flight Control Computer (FCC)*

The FCC NVM was investigated to establish the health of at least part of the flight control system. The fault logs were downloaded. They contained a mixture of nuisance faults associated with many flights and genuine faults associated with the accident flight. Considering power-up times and aligning the logs to each other and to the DAFR recording, the genuine faults occurred at or after the initial impact. No faults were associated with the helicopter whilst in flight. *Air-Data Attitude Heading Reference System (ADAHRS).*

The AMMC and DAFR recorded in-flight issues associated with the two ADAHRS, so data was recovered from the two ADAHRUs.

The units were installed in the nose electronics bay, however this had suffered significant heat damage such that the components were no longer in a structure. The ADAHRUs were recovered from locations that indicated which was ADAHRU1 and which was ADAHRU2.

The NVM of both ADAHRUs contained faults relating to the accident flight. The ADAHRU timings indicate that the first faults in each occurred approximately one second apart, ADAHRU2 followed by ADAHRU1. The uncertainty in timing indicates that the ADAHRU2 failure could have been triggered at any time in the two seconds leading up to and including the impact.

The DAFR recorded a failure from ADHARS1 approximately two seconds before impact and from ADAHRS2 slightly after impact.

The NVM and DAFR timings appear to contradict each other, however, the NVM is linked to internal errors, and the DAFR recording is triggered by the application software interacting with the aircraft systems. It is therefore possible that the DAFR recorded issues were not linked to the ADAHRU NVM data. It is also possible the position they were found in at the accident site was not indicative of where they were fitted.

### 1.11.3 Witness videos and imagery

The stadium CCTV camera system captured the aircraft's arrival, most of the time the helicopter was on the ground in the stadium, and the departure of the accident flight whilst within the confines of the stadium but not above the stadium roof height. The recording was not continuous but triggered by motion within the camera's field of view.

Other sources of CCTV captured the helicopter after the helicopter cleared the stadium roof but from a distance. Videos recorded on mobile phones from the side of the pitch captured the takeoff, the start of the accident sequence and the descent until the helicopter disappeared behind the stadium roof line. These images corroborated recorded data and provided visual evidence of the flightpath of the helicopter in a period when the recorded flightpath lost accuracy.

The witness videos also showed particles such as grass swirling in the air in the turbulent helicopter downwash. These are more prominent when the camera view does not include the stadium lights. Such particles closer to the camera appear larger, more prominent and move faster in the image frame

than items further away. There was some speculation regarding the possible interaction between an object and the helicopter captured by one of the witness videos. This object interaction was not apparent on any of the other witness videos taken from the same general pitch-side location at the same time. This object was indistinguishable from the many other particles visible in the videos, in terms of its colour, shape (sometimes a dot, sometimes more grass like) and erratic motion. The object was most likely a piece of grass, or similar small debris, much closer to the camera than the helicopter, moving in the turbulent air.

Videos recorded on police cameras and by the fire service were also reviewed. The police cameras had times embedded in the video. Aligning the video content showed that the different sources of time agreed. Assuming the time sources were correct, the blue lights of the first police car to arrive on scene were switched on within four seconds of the impact time. Within a minute, the accident site came into view of the police car camera. A significant fire had already taken hold.

#### 1.11.4 Personal electronic devices

Mobile phones, tablets and a laptop were recovered from the accident site, with varying degrees of damage. Data was recovered from the laptop, informing the operational aspects of the investigation. Other items were not functional or not related to the operation of the helicopter.

#### 1.11.5 Radar and air traffic control radio transmissions

Radar and Air Traffic Control Radio Transmissions recordings were gathered relating to the flights of the day. They corroborated the DAFR recordings.

#### 1.11.6 Accident flight

The majority of the data in this section is from the DAFR recording. Other recordings corroborated or expanded on this.

##### *Takeoff and climb*

The helicopter lifted to a low hover at 1937 hrs, manoeuvred forward, stopped and then lifted vertically out of the stadium whilst also moving slowly backwards. The helicopter climbed at an increasing rate, reaching 500 ft/min passing a radio altimeter height of 50 ft. The climb rate peaked at approximately 730 ft/min passing a radio altimeter height of 225 ft. After this it reduced to approximately 650 ft/min.

Figure 20 shows the accident flight from climbing through a height of approximately 150 ft to just after impact. The pressure altitude is approximately

the same as the radio altimeter height during the initial climb. As the helicopter climbed out of the stadium the radio altimeter tracked stronger signal returns from the stadium roof and possibly some of the seating, rather than the ground, indicated by the deviation from the general pressure altitude trends.

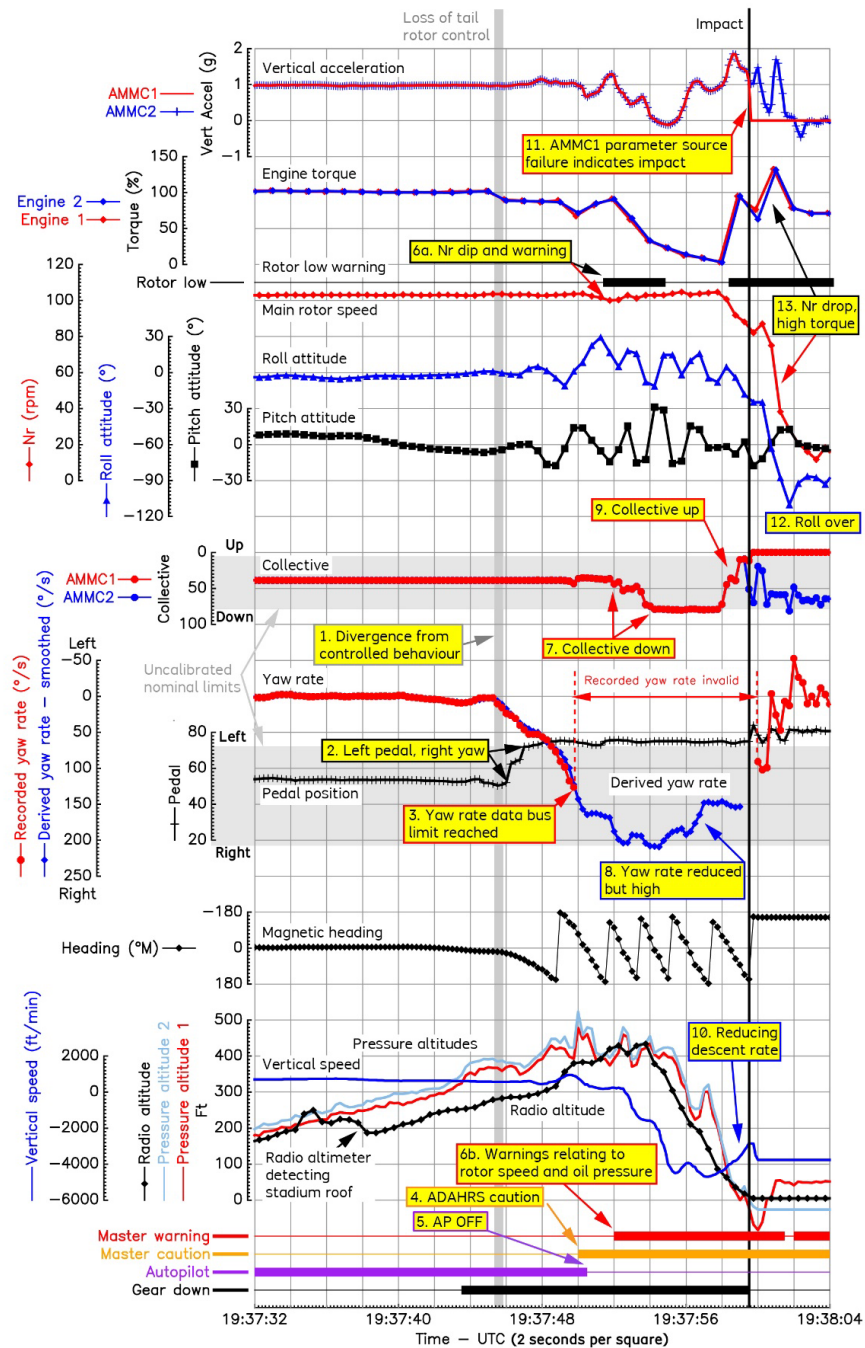


Figure 20

Pertinent extracts from the flight recorder

Factual Information

Passing approximately 300 ft, a heading change to the right was initiated and stopped followed by another heading change in the same direction (note 1 in Figure 20) which carried on accelerating despite opposite pedal being applied (note 2 in Figure 20).

The recorded GPS position was highly inaccurate by the end of the flight. Analysis of the recorded imagery shows that at the onset of the loss of yaw control, the recorded GPS position was relatively accurate and the helicopter was above or close to being above the stadium roof as shown in Figure 21. The difference between the recorded radio height and barometric altitude also indicated that there was a structure underneath the helicopter when yaw control was lost.

After the yaw rate reached  $128^{\circ}/s$  (note 3 in Figure 20), the recorded yaw rate became invalid. ap ahrs 1 fail, ap ahrs 2 fail (note 4 in Figure 20) and 1-2 ap off (note 5 in Figure 20) cautions were recorded.

The yaw rate derived from the magnetic heading showed that it carried on increasing. The helicopter was not level and as the yaw rate increased, the pitch and roll deviations increased. The recorder sample rate was not sufficient to capture the peaks of motion in pitch and roll but the data shows a change in pitch of more than  $43^{\circ}$  and a change in roll of more than  $25^{\circ}$  both in half a second. The smoothed derived yaw rate peaked at  $209^{\circ}/s$ .

There was a small movement in the collective at the same time as the yaw rate became invalid, followed by a very slight increase. At this point the yaw rate was in excess of  $160^{\circ}/s$  and the rotor speed decayed to a recorded value of 99.75% after previously having been holding at approximately 103% (this equates to 348 rpm or nearly  $2,100^{\circ}/s$ ). A ROTOR LOW warning was triggered (notes 6a and 6b of Figure 20). The collective was partially lowered for approximately one second and then fully lowered (note 7 of Figure 20). The rotor speed recovered.

Low main gearbox oil pressure alerts were triggered at approximately the same time as the low rotor rpm warning. These were followed by engine oil pressure warnings. Each engine has its own self-contained oil system, not connected to the helicopter gearbox oil system.

The radio altimeter height had peaked at about 430 ft agl. The yaw rate started to reduce and plateaued at about  $150^{\circ}/s$  (note 8 of Figure 20).

The helicopter did not pick up sufficient forward speed to create valid airspeed information.



**Figure 21**

Location at the point that yaw control was lost.  
 The original video and CCTV images are shown cropped  
 Map data © 2021 Google

*Descent*

After the collective was lowered the helicopter started to descend. The descent rate increased and stabilised at approximately -4,000 ft/min until the collective was pulled up prior to impact (notes 9 and 10 of Figure 20). There was then an associated drop in rotor speed and engine output speed with increased engine torques.

The last attitude data recorded before impact, averaged across the two sources, indicated that the helicopter was pitched 2° nose up with a left roll of 18°, with a heading of approximately 155°M.

These values were rapidly changing until that point, pitching up and rolling left whilst continuing to yaw right. The sample rates of the attitude parameters are insufficient to accurately represent the dynamic impact sequence.

The final descent rate significantly affects the impact forces. Vertical speed parameters were recorded, and the descent rate can be derived from the radio altimeter data but these sources have issues in this instance.

The vertical speed parameters from the AMMCs were showing a reducing trend prior to impact but they disagreed by as much as 400 ft/min during the descent. The last recorded vertical speed from AMMC1 and AMMC2 was -2,517 ft/min and -2,855 ft/min respectively. The vertical speed parameter is derived by the onboard systems from sources including the static pressure. These differences were possibly due to the high yaw rate of the aircraft affecting the static pressure measurements.

Vertical speed can be derived from the radio altimeter data. The last two radio altimeter heights recorded by the AMMCs for radio altimeter 1 before impact were 35.625 ft and 17.750 ft. The recording system is designed such that the latest values from the AMMCs are recorded every 500 ms. However, these latest values are updated by the AMMCs every 320 ms. With this difference in the time between updates and recording values, it is possible that there was either one or two AMMC updates between two successive recorded values. The last two recorded radio altimeter heights were either 320 ms or 640 ms apart. This means that the descent rate between the last two radio altitudes was either 3,352 ft/min or 1,676 ft/min. The values from radio altimeter 2 generate equivalent descent rate values of 2,461 ft/min and 1,231 ft/min respectively. Errors associated with radio altimeter readings in this location under these conditions are also likely to result in large errors in the point-to-point derivation of altitude rate from samples less than a second apart.

### *Impact*

The recorded accelerometer data did not provide a clear spike associated with the impact.

However, loss of AMMC1 data is likely associated with the impact sequence, which occurred at approximately 1937:59 hrs (note 11, Figure 20).

### *Post-impact*

The recorder has its own independent 10-minute power supply. The recorder carried on operating after impact, as did AMMC2 but AMMC1 stopped on impact. The integrity of AMMC 2 and the systems supplying it with data, as well as that of the audio related parts of the system is not known. The ensuing fire progressively degraded these further. Therefore, the validity of the recorded content post-impact is not robust.

The audio recording stopped 5 minutes and 28 seconds after impact. No sound attributable to an occupant was recorded post-impact. Less than a second after initial impact, mechanical sounds likely relating to the rotors striking the ground were briefly recorded. The pilot channels carried on recording automated warnings for 1 minute and 19 seconds. These are directly injected into the audio system rather than being sound sensed by a microphone.

The DAFR did not receive data from AMMC1 for approximately 60 seconds after impact. All parameters from both AMMCs stopped updating approximately 78 seconds after impact. The DAFR stopped recording at 1943:01 hrs, just over 5 minutes after impact.

After ground contact the helicopter rolled left (note 12, Figure 20) and pitched up, with a peak left roll of 110° and a nose-up attitude of 13° recorded two seconds after impact. It then rolled back to 83° of left roll and pitched to 6° nose-down in a similar time frame.

The quick roll over correlated with a recorded audio associated with the rotors striking the ground. The small reversion of pitch and roll ceased approximately as the sounds of the rotor strikes ceased. A sharp drop in rotor speed and increases in engine torque values were also recorded during this period (note 13, Figure 20).

Further gradual changes in the attitude of the helicopter were recorded until the recording stopped but the helicopter remained on its left side.

The cockpit, cabin and baggage compartment doors were recorded as open at the point of initial impact.

The engine Ng<sup>47</sup> values dropped to approximately 50% until about 35 seconds after impact when the Ng values for Engine 2 dropped off, as did the Engine 1 values 30 seconds after that.

---

47 Engine rotational speed gas generator stage.

The data indicated the presence of smoke in the baggage bay 13 seconds after impact. This was initially intermittent but overall lasted for one minute before indicating normal conditions for the last five seconds before the AMMC2 parameters froze. An Engine 1 (left engine) fire was indicated approximately 58 seconds after impact. Both of the fire indication parameters had an initial intermittent period. The only other fire detection parameter, associated with Engine 2 (right engine), did not trigger. Engine fire detection is designed to trigger when the temperature in an area of the engine compartment that normally does not get excessively hot exceeds 450°C. The integrity of these systems at that time is not known.

#### *Forces imparted on the pilot in the descent*

The yaw rate of the helicopter imparted longitudinal forces on the occupants. These forces increase with increasing yaw rate and distance of the occupant from the centre of rotation of the helicopter. Simplistic calculations of the longitudinal acceleration at the pilot location due to the yaw rate show a rapidly increasing force pushing the pilot forward in his seat. This peaked at just above 3 g.

#### 1.11.7 Previous flights

The DAFR recording of the previous flights were reviewed to establish the range of yaw rates experienced during normal flight operations. The recorded yaw rates during the flights prior to the day of the accident ranged from -38.5°/s to 32.9°/s. This provides some context for comparison to the extreme yaw rates that occurred during the accident flight and to the 128°/s ADHARS data bus limit.

The previous flights were also reviewed to establish how the AVSR affected the tail rotor speed.

The AVSR mode parameter confirmed that as expected, PLUS mode was in operation for all the flights. Figure 22 shows the relationship between the tail rotor rpm and CAS during these flights. AVSR uses TAS rather than CAS to drive system behaviour but the focus here is on the resultant spread of tail rotor speeds and so the difference between CAS and TAS is not relevant. The observed relationship matches the expected PLUS mode behaviour for the majority of the flights. Deviations from this are associated with training flight activity using the one-engine-inoperative training mode or the approach to landing captured right at the start of the recording, though some transient reversions to BACKUP mode may also have occurred.

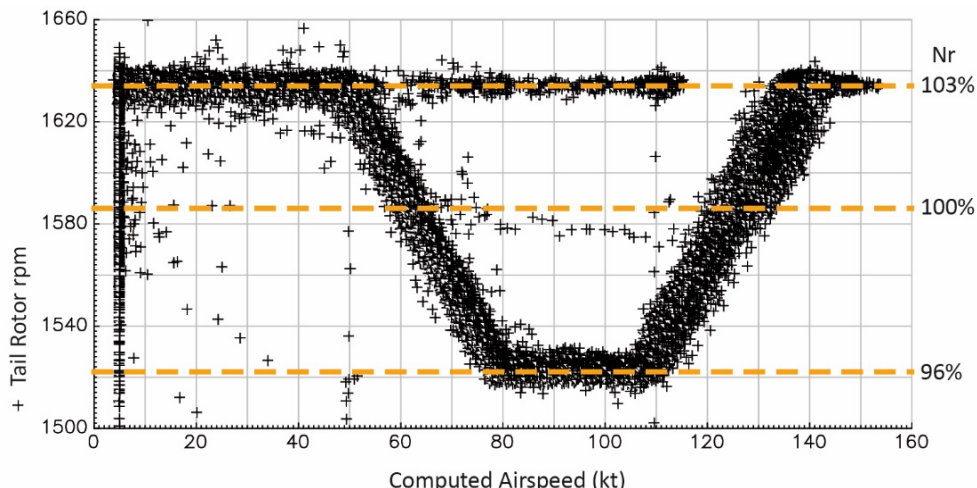


**Figure 22**

Comparison of Tail Rotor rpm with Computed Airspeed when the weight-on-wheels sensor was not active, for all flights captured by the flight recorder

Figure 23 is a histogram of the same tail rotor rpm data. This shows that nearly 75% of the flying was with rotor speeds above 100%  $N_R$ . 37% of the flying was at 103%  $N_R$ .

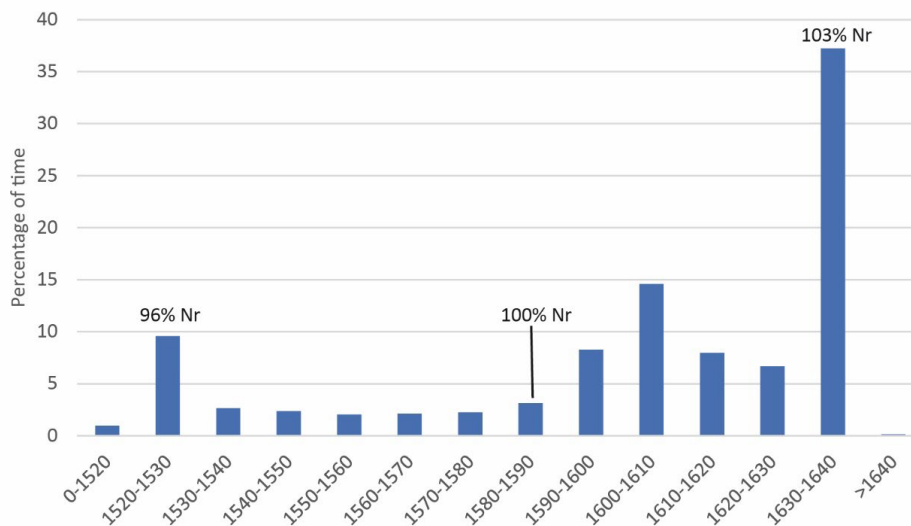


**Figure 23**

Histogram of the Tail Rotor rpm when the weight-on-wheels sensor was not active, for all flights captured by the flight recorder

The previous flights were also compared to helicopter limitations ([section 1.11.9](#)).

Factual Information

1.11.8 HUMS

The Heliwise standard service contract for this helicopter required the customer to review the Heliwise data with the manufacturer available to answer any queries. The manufacturer stated that no query had been raised against this aircraft.

Factual Information

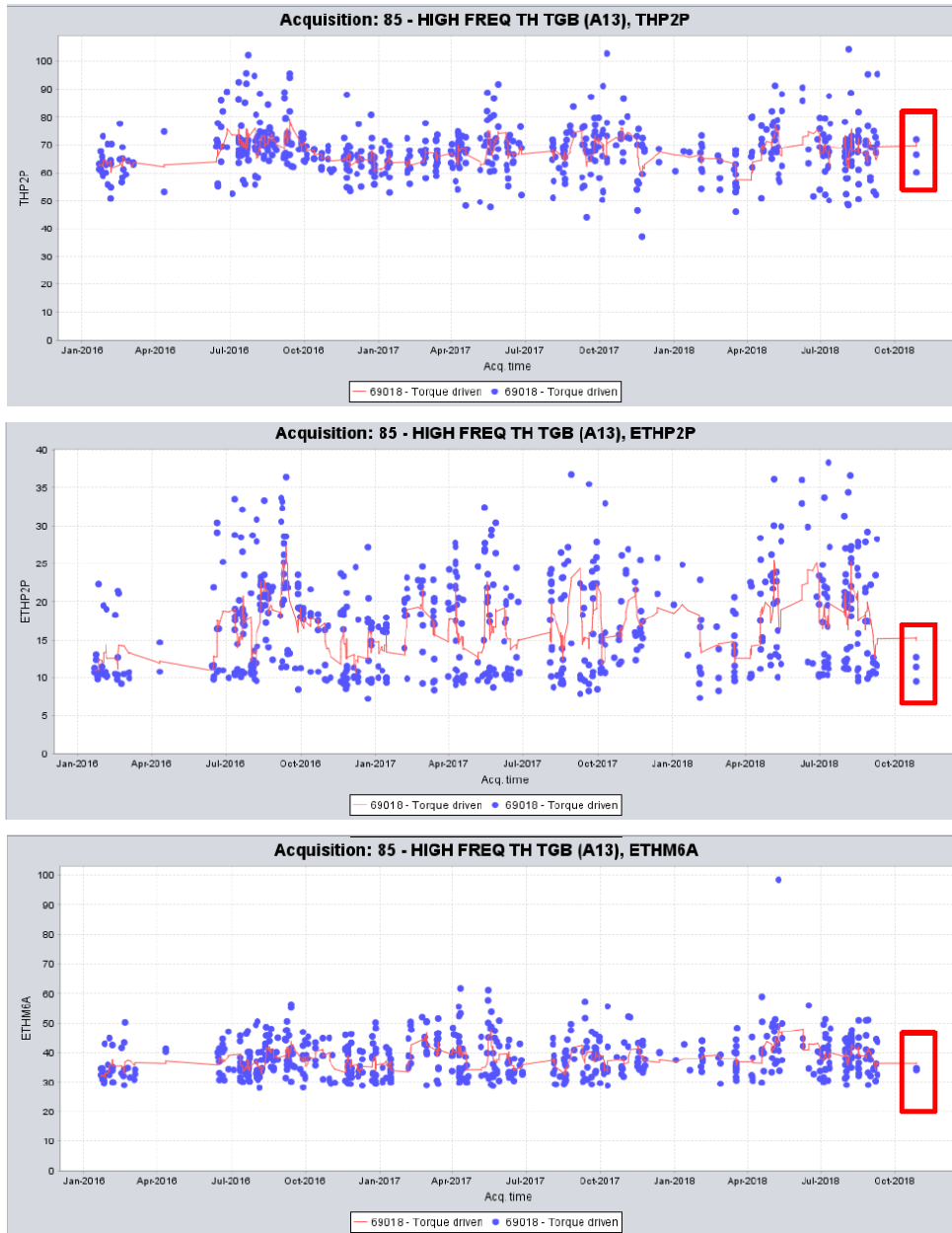


**Figure 24**

Example TGB Accelerometer A13 derived HI trends. The red box highlights the results from the accident flight

The last data that was transferred to the Heliwise system was for the period of 11 September 2018 to 28 September 2018 and tagged as DSN 173. The laptops used for maintenance were searched for possible data from after that period, but none was found. The AMMC recovered files contained some of the relevant data relating to the most recent activity, including the accident flight. It is likely that the bulk of the data from the period between 28 September 2018 and the accident was contained in the DTD, which was unrecoverable.

The manufacturer was asked to review the available historical HUMS data along with the recovered AMMC data.

### *Vibration*

The AMMCs recorded data acquisitions targeting the Tail rotor GearBox (TGB) components during the day of the accident, including two just prior to lift-off of the accident flight.

The important factor is not the absolute value of these but how they change over time. Examples of this, using different HIs acquired using the TGB A13 sensor are shown in Figure 24.

The analysis performed on the TGB acquisition results did not highlight behaviour outside of the fleet average. More generally, the manufacturer stated that there were no significant TVM arisings that indicated problems that needed addressing.

### *Rotor Track and Balance analysis*

No anomalies were highlighted in any of the data relating to the rotor track and balance.

### *Failure monitoring*

Outstanding arisings were already open on the system. The manufacturer assessed them as being triggered by obsolete triggers. They stated that flagged issues were negligible and would have rejected them with no further action required had they been consulted at the time.

### *Overall assessment of historical HUMS data for this helicopter*

Outstanding issues had been flagged by Heliwise but were not showing as being progressed. The manufacturer assessed these arisings as not genuine issues. They were triggered before Heliwise had refined the trigger thresholds. The last upload, DSN 173, had not triggered any new arisings.

The manufacturer concluded that the historical and AMMC data would not have flagged a need for any additional maintenance.

### *ESUM data*

Archived ESUM data was also compared to helicopter limitations (section 1.11.9).

#### 1.11.9 Comparison of recorded data with published limitations

Helicopter operational limitations for the helicopter, such as maximum airspeeds, are documented in Rotorcraft Flight Manual (RFM) Document No 169F0290X001 and Supplement 30.

The flights recorded in the flight data recorder and ESUM recordings, recovered from the manufacturer's Heliwise archive, enabled comparisons of flight activities with some of the RFM limitations. The two sources recorded different parameters at different rates. These differences meant that they could not assess an identical subset of limitations, but both enabled some level of assessment.

The datasets did not always allow simple comparisons of recorded parameters with stated limitations. Layers of derivation were sometimes required, and some of the recorded parameters on which these were based, such as windspeed, were not robust under all conditions (such as lower speed flight). To aid in the understanding of whether some of the exceedance activity was associated with actual flight or issues with the data, it was useful to compare activity before and after the Certificate of Airworthiness and Certificate of Registration were issued.

With a few exceptions, discussed below, the recorded flights were within the limitations checked.

The flight recorder data covered 34 flights involving approximately 12 hours of in-air activity. This was from the 1 September 2018 to the accident flight. A review of the data found a single exceedance, an instance of a gear operation speed being exceeded by approximately 4 kt (5%).

The ESUM data spanned the period between 1 December 2015 and 25 April 2018, just under 216 hours of which was in-flight. Some of this was from before G-VSKP had been issued with its Certificate of Registration and Certificate of Airworthiness.

The airspeed limitations are quoted as Indicated Air Speed (IAS) limitations but True Air Speed (TAS) is recorded in the ESUM dataset. Equivalent Air Speed

(EAS) was derived from the ESUM data and used as a close approximation to IAS for the purpose of the assessment. This was valid for the limited range of altitudes and temperatures encompassed by the dataset.

The ESUM data showed 12 events above 100 % TQ (when above 90 KEAS) for more than 10 seconds. Seven of these events occurred before the Certificate of Airworthiness was issued and five after. The maximum transient torque limit is 125% for a maximum duration of 10 seconds.

The maximum torque recorded was 109%, lower than the 125% TQ transient limit but for a longer duration. The RFM does not provide any intermediate limitations between the transient limit (125% torque for 10 seconds) and the maximum continuous limit (100% torque) above 90 KIAS. The AW169 Type Certificate Data Sheet<sup>48</sup> states a transmission limitation of 111% for 5 minutes with both engines operating regardless of air speed. The Approved Maintenance Manual for the AW169 has no unscheduled maintenance requirements for torque excursions below 111% of any duration.

The assessment of the maximum allowable windspeed/groundspeed/airspeed azimuth envelope requires layers of calculations based on recorded parameters that themselves are not robust during periods of interest (eg recorded wind data with little or no forward airspeed being sensed). The derived data crosses limitation boundaries during dynamic flight. The majority, but not all, of these occurrences were recorded after the issue of the Certificate of Airworthiness.

Assuming that autorotation is associated with flight with less than 10% total TQ, exceedances of the minimum airspeed for autorotation occurred for a few seconds on five occasions.

Two of the rotor speed data points recorded in flight fell below the minimum transient rotor speed limitation of 90%. One occurred in the climb and one in the flare on landing. These were marginal exceedances for very brief moments.

## 1.12 Wreckage and impact information

### 1.12.1 Initial site inspection

The main helicopter wreckage was located within an enclosed secure compound to the southeast of the football stadium. On match days the two gates of the compound were opened to allow foot access between the rough ground to the east, which was used as a temporary staff car park, and the stadium. The site consisted of a concrete surface on two levels with a 0.5 m step between them, formed by a small brick wall.

48 <https://www.easa.europa.eu/sites/default/files/dfu/AW169-TCDS%20R-509%20Issue1.pdf> (Accessed 3 July 2023).

The helicopter's initial impact with the ground was diagonally across the step with the nose of the helicopter pointing on a heading of approximately 155°<sup>49</sup>, although it was still rotating at high speed as it struck the ground. There was significant structural damage to the fuselage in the region where the fuel tanks were located.<sup>50</sup>

After the rotation in yaw stopped, the helicopter rolled onto its left side and came to rest in this attitude on a heading of approximately 050°. Sections of the main rotor blades detached from the helicopter as they contacted the ground and were found over a wide area of the temporary staff car park and surrounding treeline. Witnesses reported that fuel was seen to leak from the helicopter along the ground before it ignited, resulting in an intense fire which rapidly engulfed the whole helicopter. This resulted in significant fire damage to the fuselage structure, with the front section almost entirely consumed.

An initial inspection of the site was conducted by the AAIB during the night of the accident. Action to recover the victims was then initiated the following morning. Work to recover the wreckage to the AAIB HQ at Farnborough was eventually completed five days after the accident took place.

#### *Tail wreckage*

Initial evidence obtained from video footage of the accident, focussed attention on the tail rotor of the helicopter. The tail section of the helicopter where the tail rotor was located was less damaged by the fire than other sections of the helicopter. Onsite inspection of the tail rotor control mechanism identified that the servo actuator lever mechanism was no longer attached to the TRA control shaft. The castellated nut and pin carrier were found bonded to each other but detached from both the lever mechanism and the control shaft and lying in the remains of the vertical tail carbon fibre skin panel (Figure 25).

A more detailed inspection of the tail rotor control system was conducted with the manufacturer in attendance once the wreckage had been recovered. The locking nut and pin carrier, tail rotor actuator control shaft, and spider/slider/bearing assembly were removed from the tail wreckage and sent for further forensic laboratory analysis by specialists at nC<sup>2</sup> Engineering Consultancy within the University of Southampton. During disassembly, the locking nut on the bearing end of the control shaft was found to have a torque load significantly higher than the required assembly value.

49 Based on recorded data.

50 See 'survival aspects', [section 1.15.3](#) for a more detailed description.

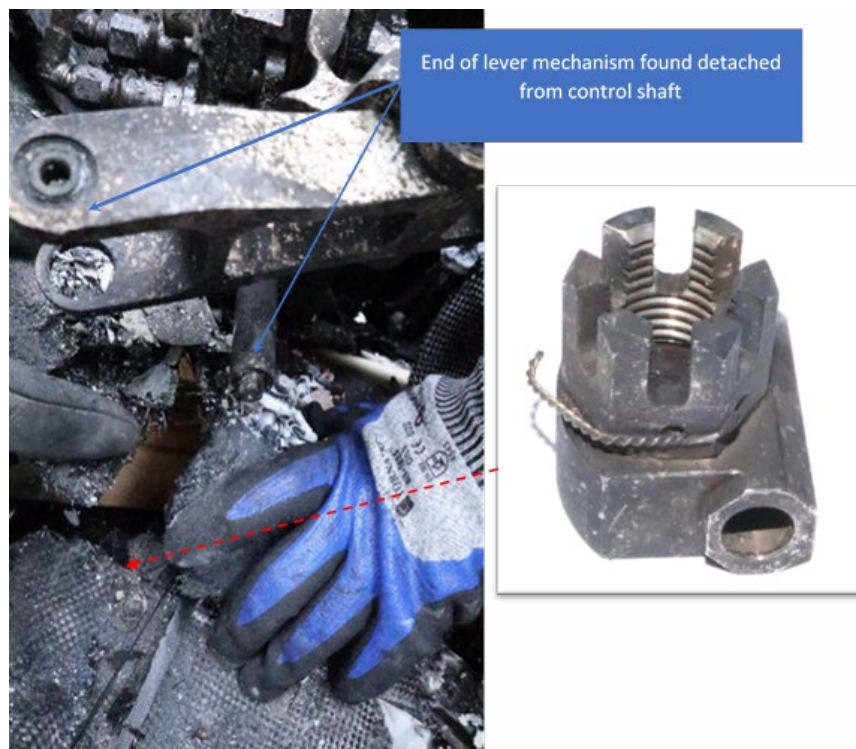


**Figure 25**

Disconnected lever mechanism, TRA control shaft and detached but fused nut and pin carrier

#### 1.12.2 Results of the initial forensic laboratory investigation

##### *Locking nut and pin carrier*

Inspection of the thread on the nut confirmed it was undamaged.

Use of a stereo microscope to view the component, identified wear debris between the nut and the pin carrier and deformation of the nut consistent with softening of the material. The inspection also confirmed the presence of an impression mark on the edge of one of the castellations on the nut, consistent with the size and shape of a split pin. The pin carrier and nut were then scanned using an X-ray Computed Tomography (CT) Scanner based at the facilities of  $\mu$ -VIS X-ray Imaging Centre at the University of Southampton. This passes X-rays through components from different angles to produce multiple cross-sectional images, which are then combined as a 3-D model. The model allowed the interface between the two components to be 'virtually sectioned'. This confirmed areas of fusion and evidence of rotation (Figure 26).

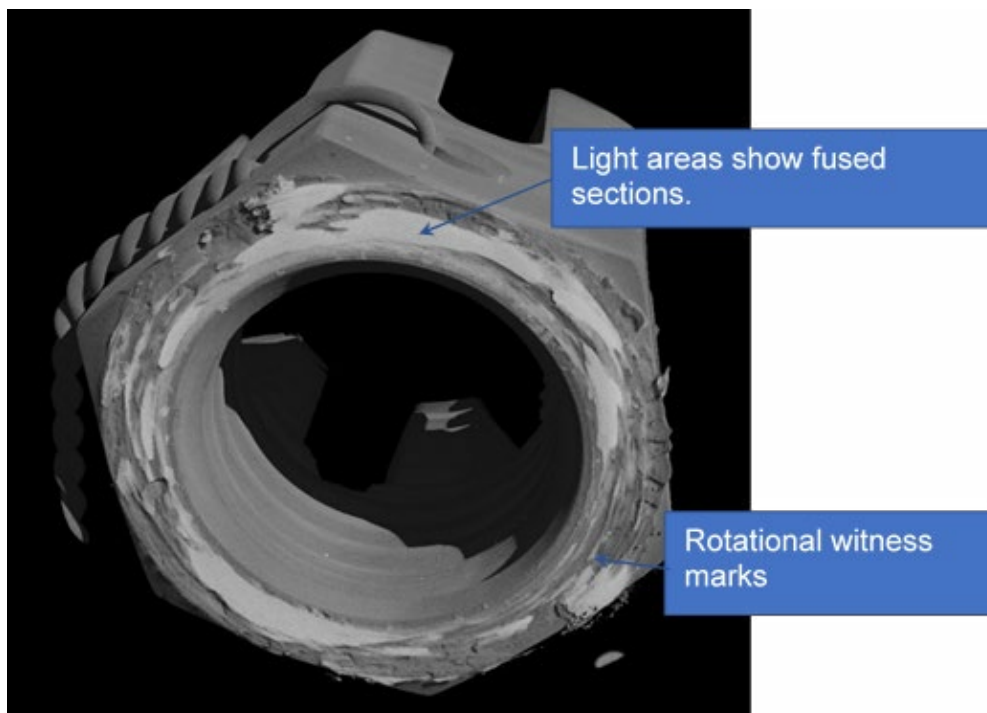


**Figure 26**

Virtual cut through joint between the nut and pin carrier

#### *Tail rotor actuator control shaft*

Initial inspection showed no evidence of the split pin which should have retained the locking nut and pin carrier to the threaded section of the control shaft at the actuator end. The threaded section itself had been drawn inside the outer shaft during the extraction process and was no longer visible.

The shaft was imaged using the CT scanner, which confirmed the threaded portion of the control shaft was inside the outer shaft and contained the remains of the split pin. The top and bottom of the split pin had been sheared off in rotation (Figures 27 and 28).

At the other end of the control shaft, the section adjacent to the duplex bearing face showed evidence of burnt-on grease and was discoloured along its length (Figure 29).

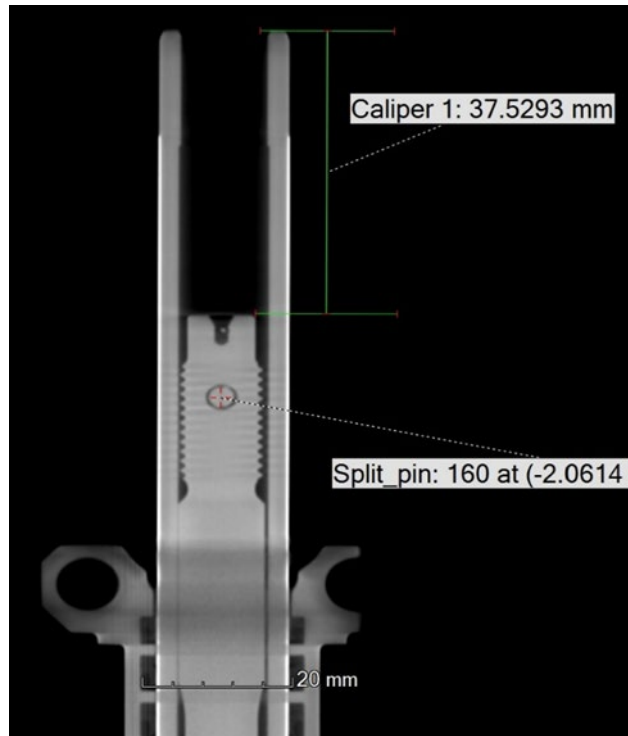


**Figure 27**

CT scan of threaded section of control shaft and split pin

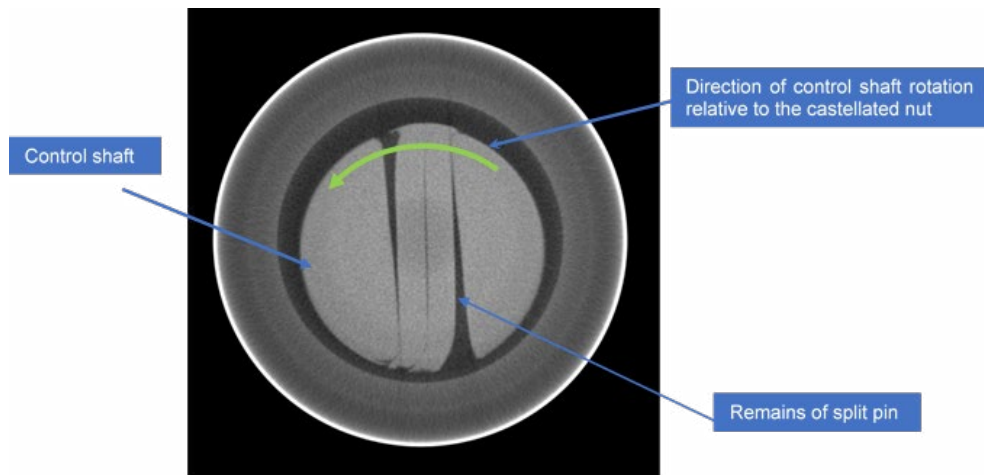


**Figure 28**

CT scan through tail rotor actuator control shaft (viewed from bearing end)

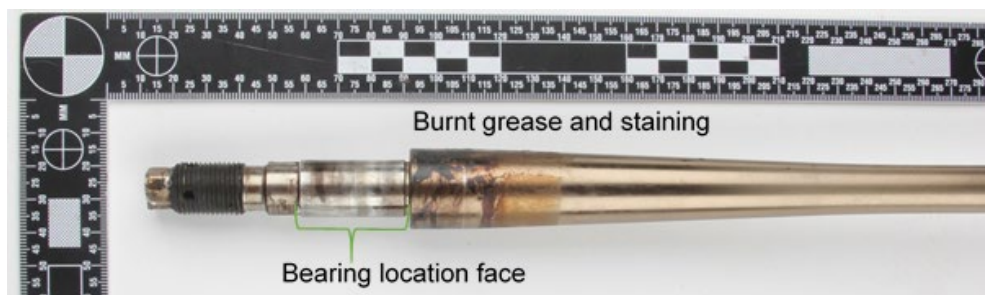
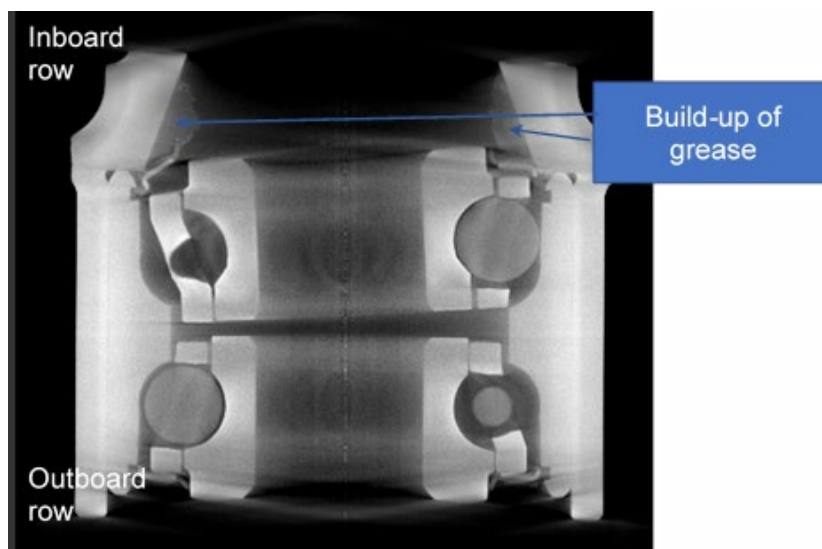


**Figure 29**

Duplex bearing location on tail rotor actuator control shaft after removal of the bearing

#### *Spider/slider/bearing assembly*

Following removal from the control shaft, the inner races of the bearing could only be rotated a few degrees in either direction by hand. There was also a small build-up of black grease inside the slider unit around the inboard face of the duplex bearing. The spider assembly was removed, and the slider/bearing assembly was CT scanned<sup>51</sup> (Figure 30).

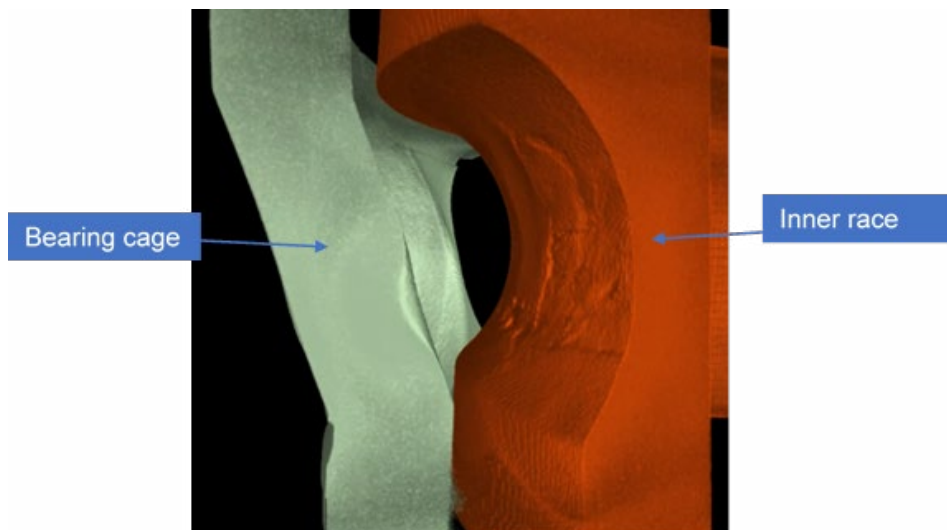


**Figure 30**

CT scan of bearing/slider assembly

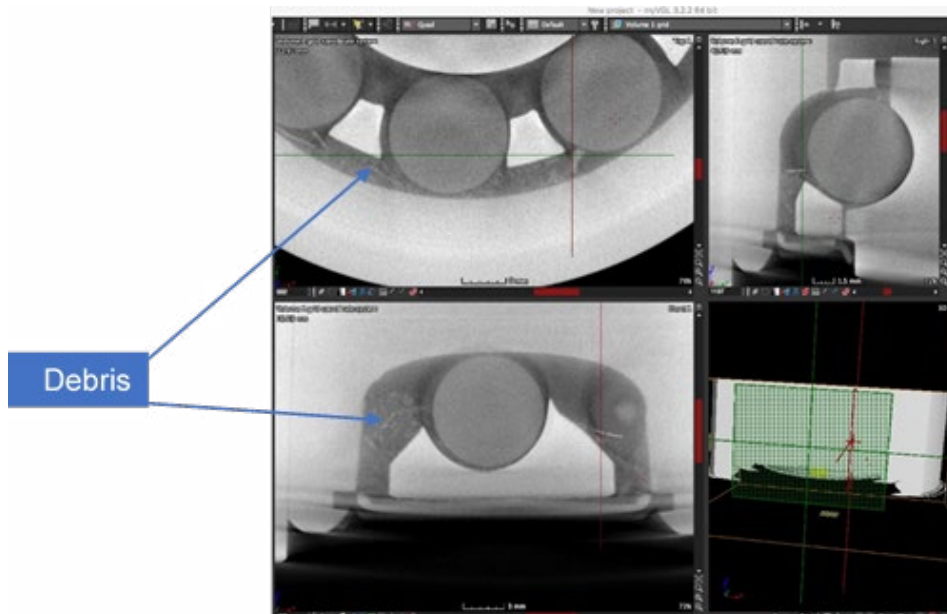
The scan of the bearing showed fractures to the bearing cages and significant damage to the surface of the inner bearing races, the damage being worse on the inboard inner bearing race (Figure 31) where there was evidence of sub-surface damage.

<sup>51</sup> The misalignment of the inboard inner race was an unavoidable consequence of the extraction process from the wreckage.

**Figure 31**

CT imagery of duplex bearing inboard inner ring surface damage

The scan also showed evidence of debris accumulating in the bearing raceways (Figure 32).

**Figure 32**

Scan images of duplex bearing showing debris accumulation

#### *Duplex Bearing (s/n 14126)*

The bearing was then removed from the sliding unit and disassembled, revealing evidence of relative rotation between the sliding unit and the bearing

outer ring. The debris present on the CT scan was identified as a combination of black dust and metallic particles. No grease, in its original form, remained in the bearing but there was black dust in and around the bearing races and cage (Figure 33). The seal on the inboard side of the bearing exhibited wear marks on its inner surface from contact with the cage. Visual inspection of the surface of the bearing races confirmed the extent of the damage seen in the CT scans. The surface of each of the balls from both sides of the bearing was crazed and exhibited areas of matt white surface finish, but none of the balls were spalled.



**Figure 33**

(A) Inboard row, outer race (B) inboard row inner race and fractured cage  
(C) inboard row inner race

### 1.12.3 Results of the in-depth forensic laboratory investigation

#### *Non-destructive examination techniques*

The duplex bearing was subjected to a sequence of detailed analysis techniques to document its condition. Initially the surface of the inner and outer races was scanned using a high resolution, non-contact, optical scanning technique to record the topography of the running surfaces (Figure 34). This was combined with higher resolution CT scans to identify the extent of the damage. The inner races were examined further using a Scanning Electron Microscope (SEM). This confirmed the presence of step-like features with striations, indicating that they were formed by a cyclic failure mechanism consistent with rolling contact fatigue.

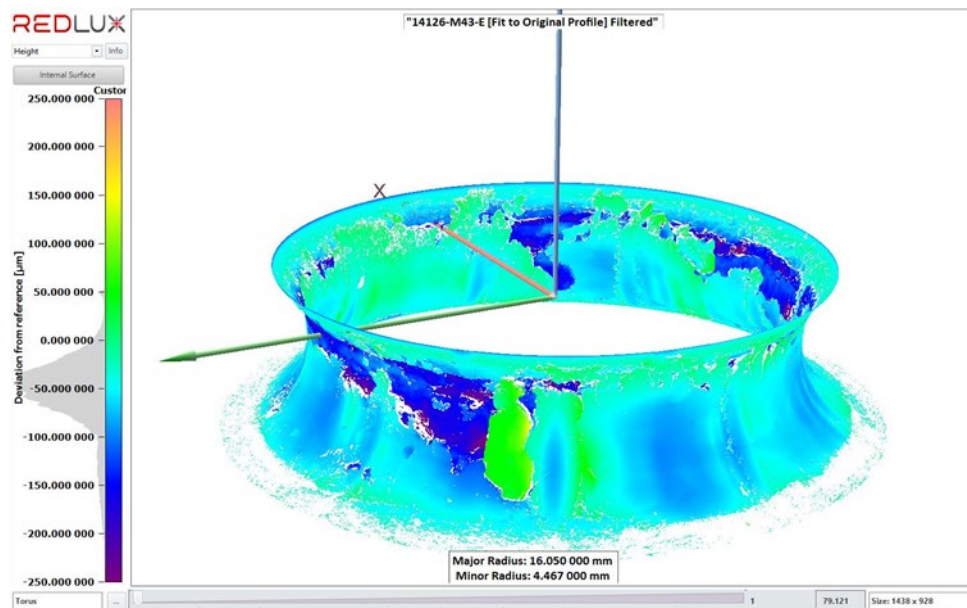


**Figure 34**

Optical measurement of the rolling surface of the inner race showing heavy wear, with large pits (blue areas), but also areas raised higher than the original surface (green/yellow)

The SEM scans confirmed several features on the inboard inner race surface which showed consistent characteristics (Figure 35). The features:

- were orientated normal to the rolling direction;
- were edged by adhered debris;
- contained flattened debris within the feature;
- displayed large segments of material; and
- showed the presence of long shear cracks, normal to the rolling direction and secondary cracking in the rolling direction.

#### *Destructive examination techniques*

In order to document the subsurface condition of the race material, sections were cut out both radially and circumferentially. Of the two races the inboard row showed the most extensive damage, and the inner race exhibited more damage than the outer race.

The outboard row inner race was typified by repeating inclined cracks. The cracks had a depth and angle typical of a rolling contact fatigue damage mechanism and had initiated from the surface, with material released at the initiation point of the cracks. (Figure 36).

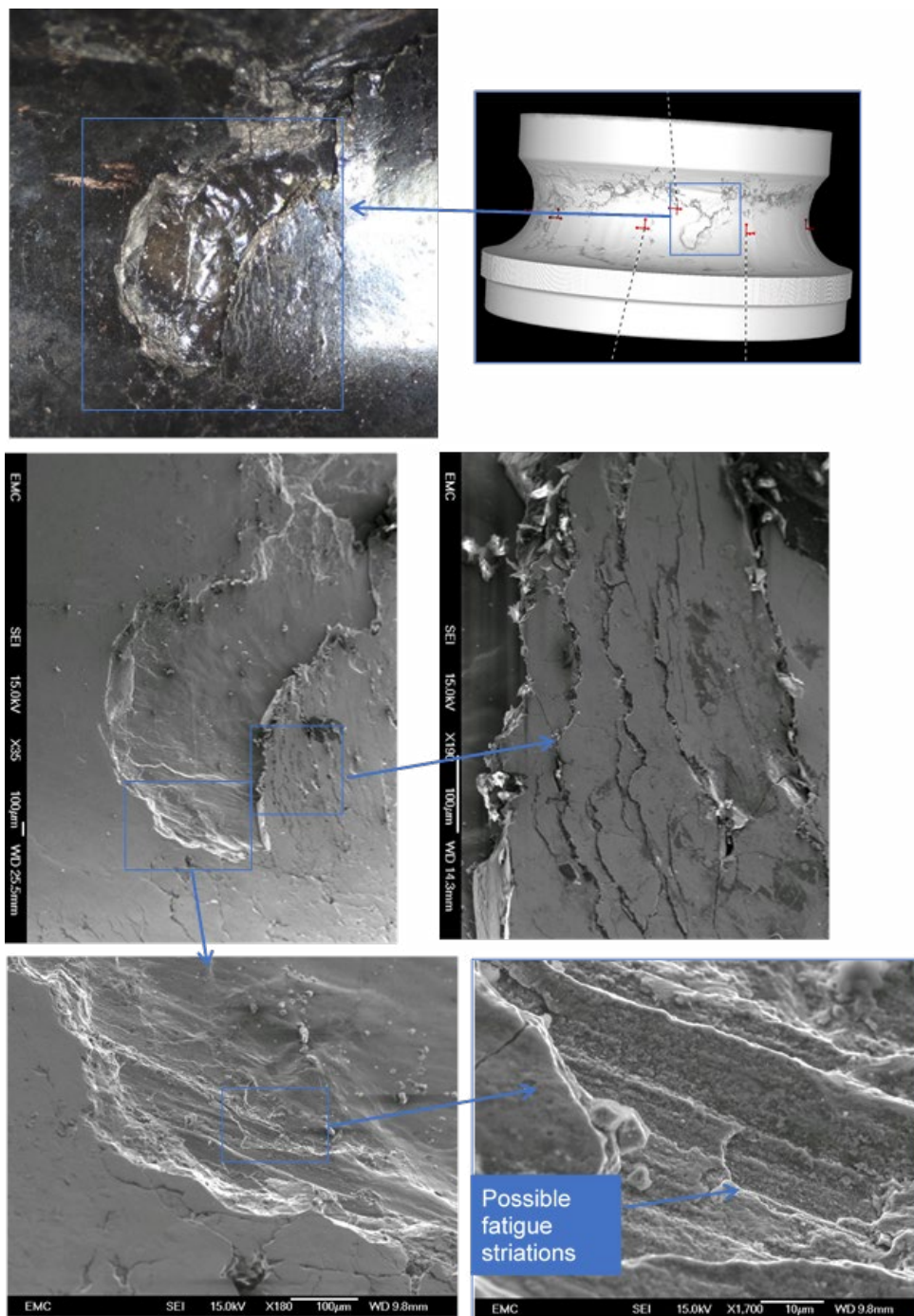


**Figure 35**

SEM images showing the large pit with fatigue and secondary cracking

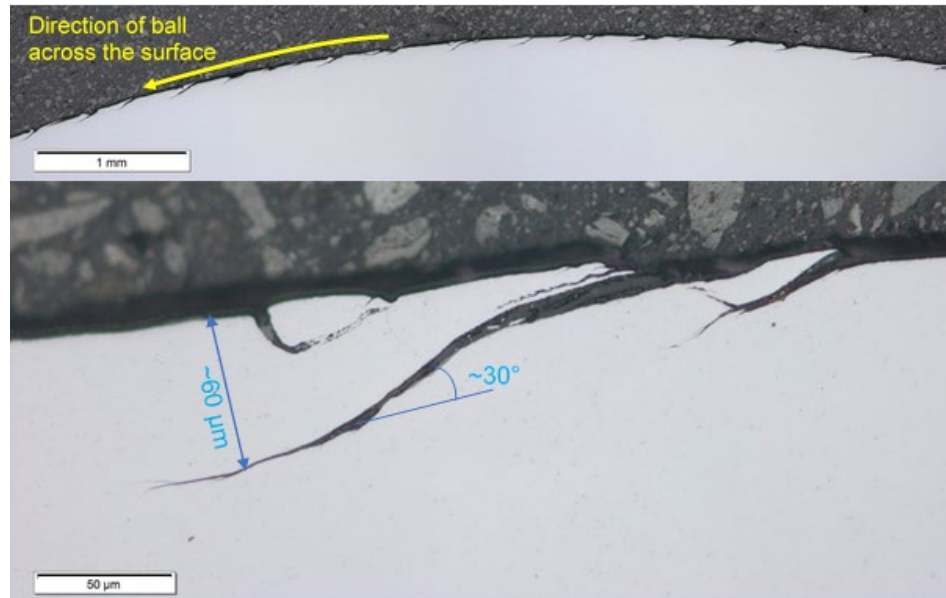


**Figure 36**

Optical microscopy views showing surface cracking on the circumferential section of the inner race from the outboard row<sup>52</sup>

The sections were then polished and viewed under an optical microscope (Figure 37). On the inboard inner race this revealed that the surface in the centre of the race, down to a depth of approximately 0.5 mm, had a swirling, layered structure with extensive cracks in many locations (Figure 38). The surface of the polished sections were then etched using various reagents and again viewed under an optical microscope.

The outboard inner race showed evidence of a heat affected zone and a Dark Etched Region<sup>53</sup> (DER) below the surface. A combination of the reagents used and EDAX<sup>54</sup> analysis confirmed that the various layers on the inboard inner race were formed from different materials including carbon, steel and copper, which had been deposited and compressed (Figure 39).

Below this layer of mixed material, was the original bearing steel material. However, use of etchant on the section surface identified a heat affected zone where the material microstructure had changed (Figure 40). Microhardness profiling was conducted both radially and circumferentially. The results confirmed that the steel had softened compared to a new bearing, but closest to the surface the material had rehardened. This suggested that the temperature at

52 In all the images of bearing sections used in the report the 'mottled' black and grey section is a mounting material used to hold the bearing section. The bearing section is seen as a mostly consistent block of colour, in this example light grey.

53 For further explanation of DER see [section 1.18.8](#).

54 EDAX is Energy-Dispersive Analysis of X-rays, using an additional sensor in scanning electron microscopes to allow identification of component materials.

the surface of the race had reached austenitising<sup>55</sup> temperatures of over 980°C, reducing to temperatures of 600°C at the lowest level of the heat affected zone which had only a tempering effect.



**Figure 37**

Optical microscopy view of circumferential slice from inboard inner race of bearing following polishing to show the layered surface

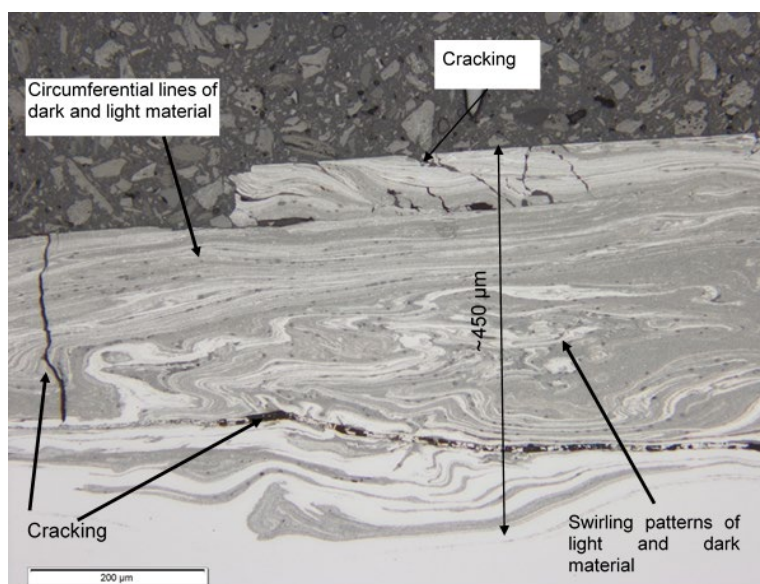


**Figure 38**

Magnified view of inboard inner race of bearing showing cracking of material

<sup>55</sup> Changing the microstructure of the steel by heating it until it enters the austenite phase. Austenite is a solid solution of carbon and other constituents in a particular form of iron known as  $\gamma$  (gamma) iron.

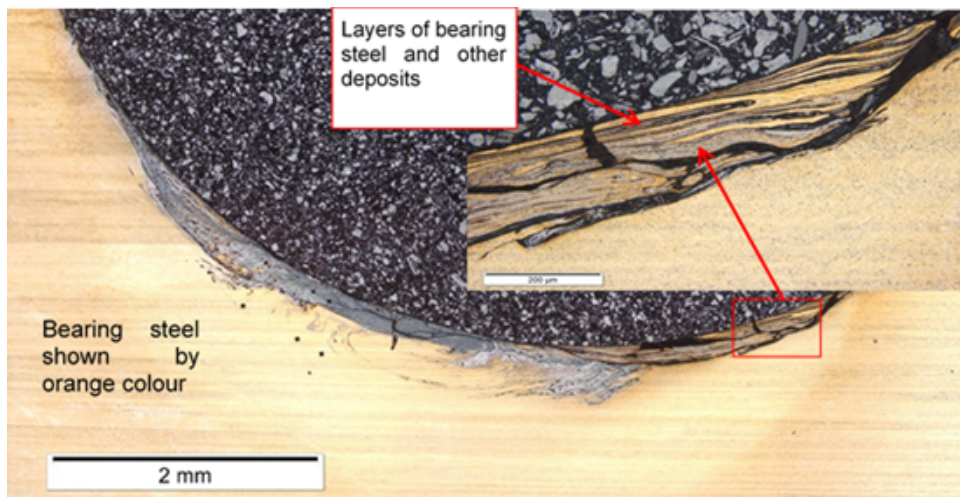


**Figure 39**

Optical microscopy views of etched (Murakami’s reagent) radial slice from inboard, inner race showing mix of materials in the layer

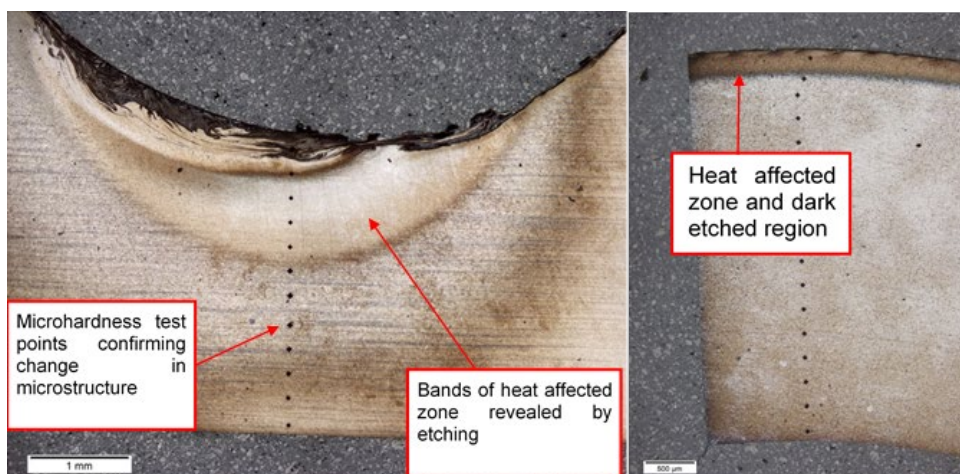


**Figure 40**

High magnification light microscopy views of etched (Vilella’s reagent) radial slice of inboard inner race (left) and circumferential slice of outboard inner race (right), showing heat affected zones, DER and microhardness testing points

*Cage damage and wear*

The inboard cage had fractured across the top and bottom of two pockets, resulting in the cage breaking into two pieces. The outboard cage had three fractures, but remained in one piece. The inspection of the cages using CT scanning, SEM and optical imaging showed distinctive wear patterns. These included wear within the individual cage pockets on both inboard and outboard

cages (Figure 41 and 42), but also a wear lip on the inner running surface of the wide end of the cages (Figure 43). On the inboard cage there was also a wear scar on the outside of the narrow end of the cage (Figure 44).

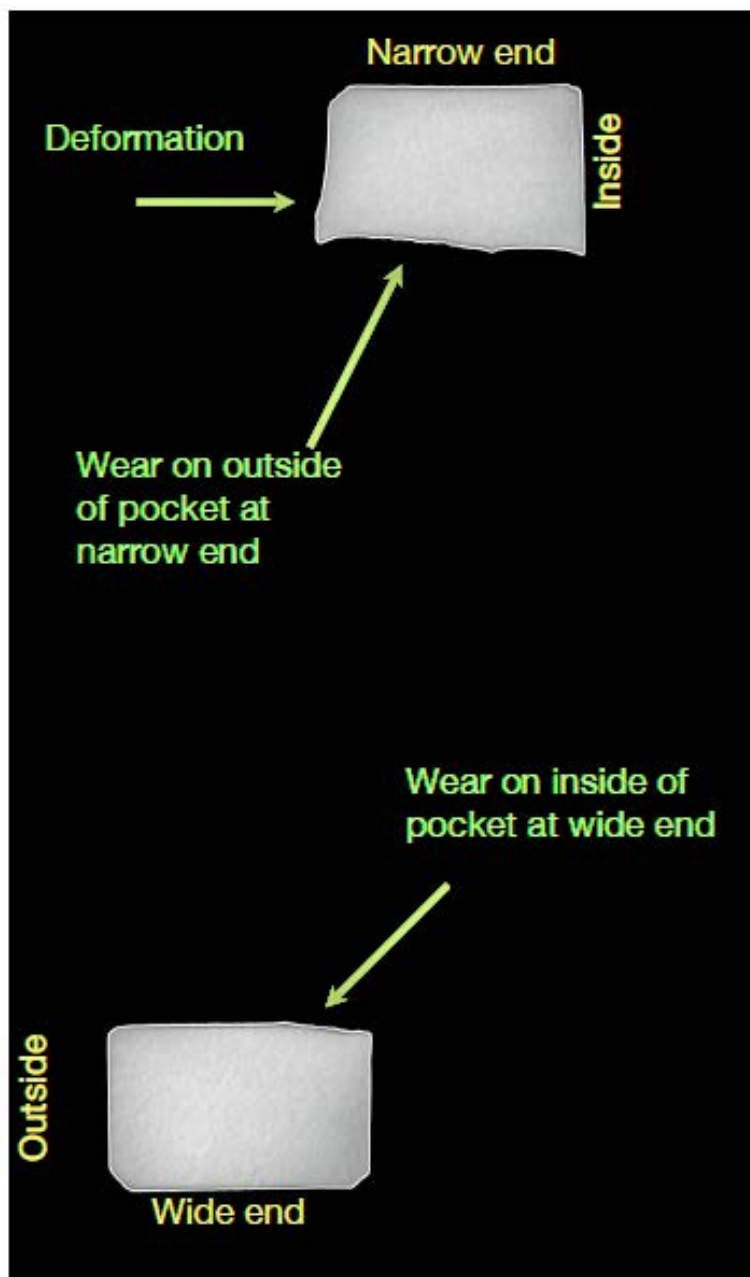


**Figure 41**

CT scan cross section of pocket on inboard cage showing wear on the top and bottom surfaces

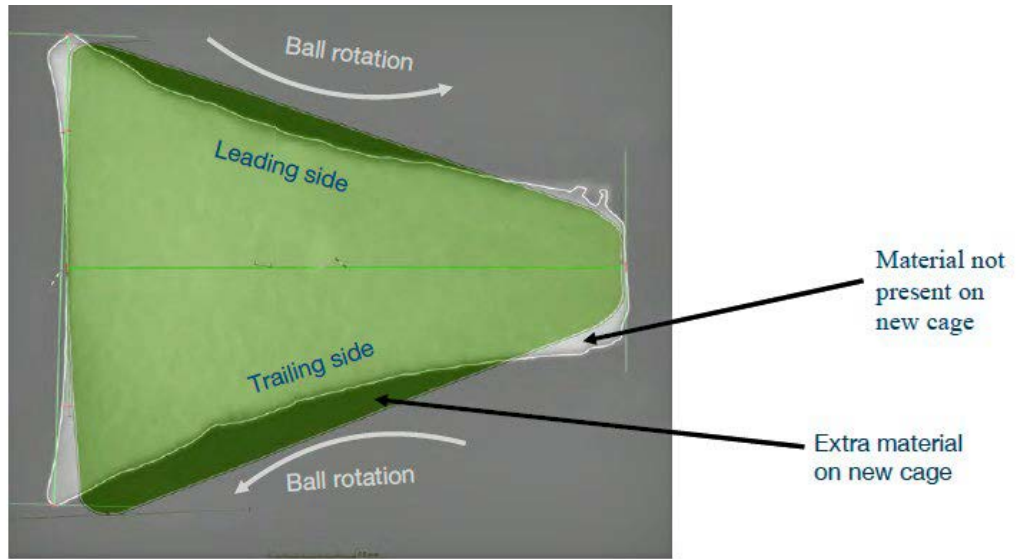


**Figure 42**

Material removal and displacement relative to a new cage (shown in green) on the cage section between ball pockets

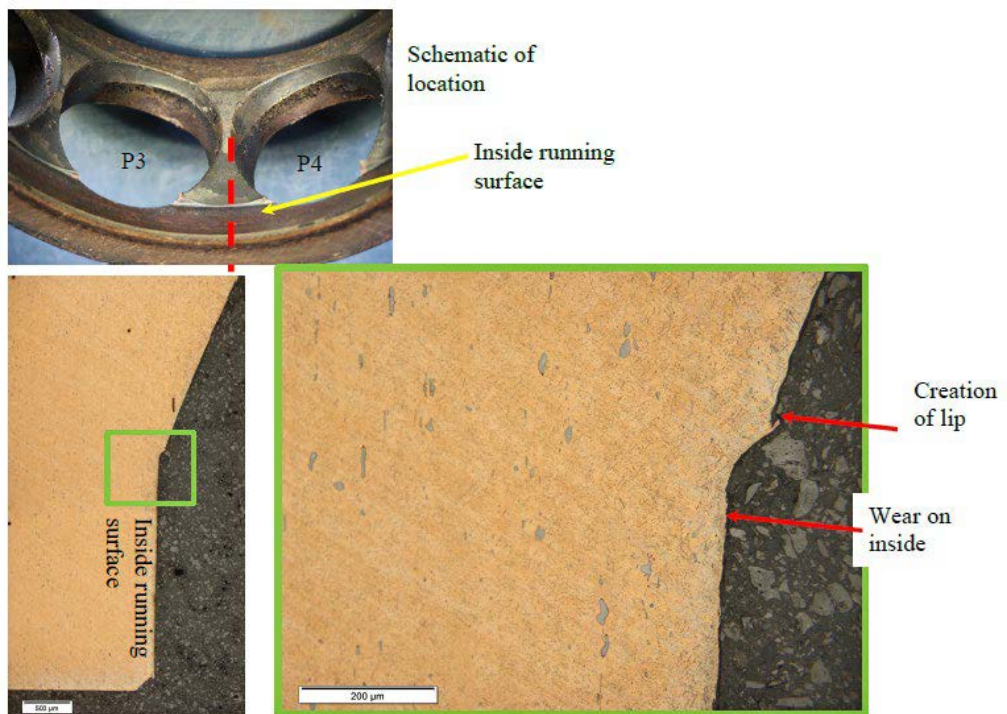


**Figure 43**

Optical and SEM images of wear on the inside of the wide end of the outboard cage

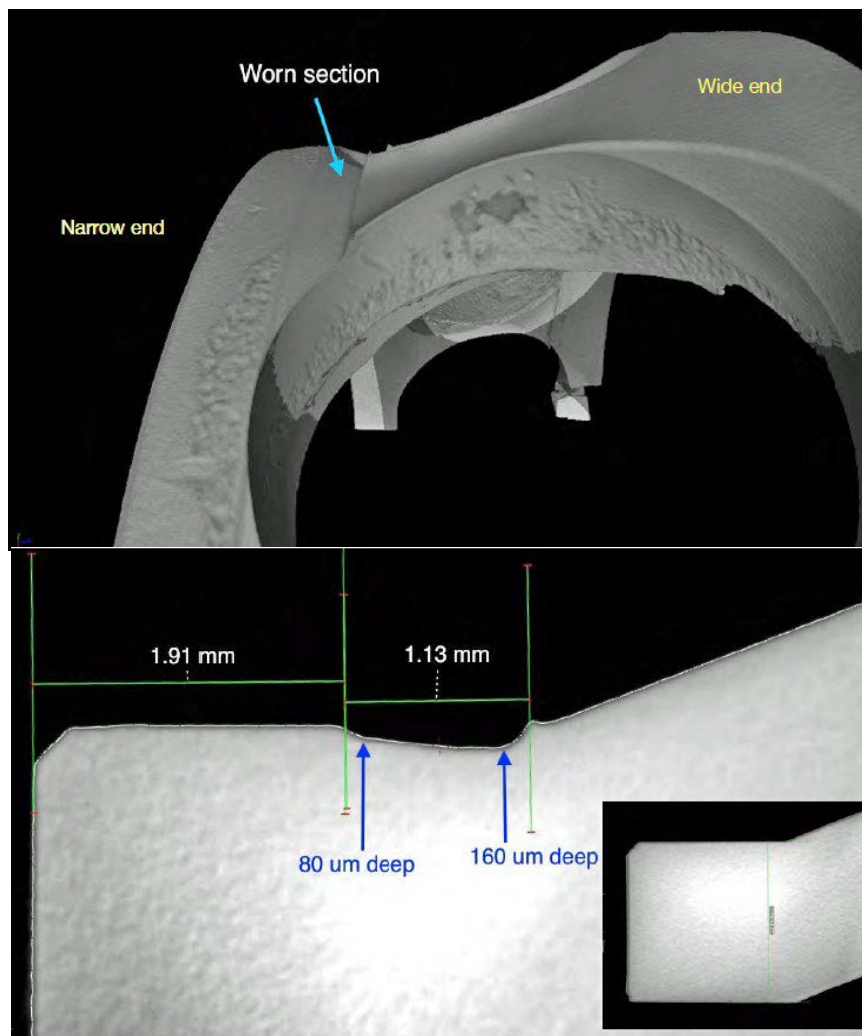


**Figure 44**

CT scan images showing wear on outside of the narrow end of the inboard side

#### 1.12.4 Post-accident continued airworthiness response

As the same part number duplex bearing and tail rotor control system were fitted to the AW189, soon after the accident the helicopter manufacturer introduced a number of emergency inspection measures on both the AW169 and AW189. These were introduced by Alert Service Bulletins (ASB) which were subsequently mandated by the EASA in a combination of emergency and standard Airworthiness Directives (AD).

The first of these was Emergency AD 2018-0241-E, issued on 7 November 2018 and referenced ASB 169-120 and 189-213, which were issued on 5 and 6 November 2018 respectively. It mandated a one-time visual inspection of the servo-actuator installation. The AD was then superseded by emergency

AD 2018-0250-E on 19 November 2018. In addition to the requirements of the first AD, a precautionary one-off inspection of the duplex bearing was added. This resulted in an initial number of bearings being rejected from helicopters in service, some of which were sent to the AAIB for further investigation.

The helicopter manufacturer then published ASB 169-125 and ASB 189-214 on 21 November 2018. Consequently, EASA issued Emergency AD 2018-0252-E to mandate them. This introduced a one-time inspection and breakaway torque check of the duplex bearing and inspection and reinstallation of the servo-actuator castellated locking nut.

The manufacturer and airworthiness authority then determined that repetitive inspections of the duplex bearing were necessary for continued monitoring of the fleet. The helicopter manufacturer published ASB 169-126 and ASB 189-217 accordingly, and EASA issued Emergency AD 2018-0261-E in November 2018 to mandate these inspections. A steady number of bearings were removed from service and were sent to the bearing manufacturer. Some were selected for further investigation, using a standardised process agreed with the AAIB.

In the period following the introduction of these inspections, tail rotor system rig tests were being conducted by the helicopter manufacturer (see [section 1.16.1](#)). The test results showed that as the duplex bearing degraded, its operating temperature increased consistently. A modification was therefore developed to install and repetitively inspect a thermal strip, as an additional warning indicator of the condition of the duplex bearing. This was introduced by the helicopter manufacturer in ASB 169-135 and ASB 189-224 and mandated by EASA through the issue of AD 2019-0023 on 1 February 2019.

Operator feedback from the repetitive tail rotor inspections allowed improved techniques to be developed and the helicopter manufacturer published ASB 169-148 and 189-237, to provide instructions for more in-depth inspections of the duplex bearing. EASA issued AD 2019-0121 on 3 June 2019<sup>56</sup> to require accomplishment of these actions.

After AD 2019-0121(R1) was issued, the helicopter manufacturer introduced into service a modification to the Vibration Health Monitoring (VHM) system fitted to the AW169 and AW189. The modification relocated an existing accelerometer sensor on the tail to the servoactuator control lever, to allow monitoring of the vibration signature of the duplex bearing and provide an optional aid for the continued airworthiness of the fleet.

Whilst the modification itself was not mandated, the reporting of data from helicopters with the modification installed, was mandated. This requirement

---

<sup>56</sup> This was reissued later in June 2019 as R1 to correct inconsistencies between the AD and the ASB.

was included in a new AD 2019-0193 issued 7 August 2019, which also included revisions to the other inspection requirements and superseded AD 2019-0121(R1).

In early 2020, the helicopter manufacturer issued modification Service Bulletins 169-153 and 189-249. These introduced a new standard of tail rotor actuator. The control shaft now has a left-hand thread on the castellated lock nut and an additional washer fitted to the actuator end of the shaft. The EASA then issued Airworthiness Directive 2020-0048 on 6 March 2020, which superseded AD 2019-0193.

This AD mandated the fitment of the new standard control actuator, with one-way interchangeability<sup>57</sup>. Fitting of the modified actuator alleviated the requirement to conduct an inspection of the castellated lock nut every 10 flight hours. All the other mandatory inspections were retained in the new AD.

The final change by the manufacturer was to develop a new tail rotor duplex bearing introduced into service by mandatory Service Bulletins 169-162 and 189-254 on 4 August 2020. Replacement with the new bearing was required within 400 flight hours or 4 calendar months of the SB issue date. The new bearing replaced the ceramic balls with steel balls. The new bearing had an introductory life limit of 400 flight hours. The Service Bulletin also required time expired bearings to be returned to the manufacturer for inspection following replacement.

None of these safety actions were applied to the AW139 fleet, as the helicopter manufacturer considered it was not affected by this issue.

#### 1.12.5 Investigation of other failed bearings identified by emergency checks

Several bearings were removed from service globally as a result of inspections carried out to comply with the ASB and AD requirements. Most of these bearings were returned to the bearing manufacturer for further investigation, but several of them were selected for further investigation by the AAIB. Some of the total number of rejected bearings inspected were found not to show any visible damage. However, some of the bearings exhibited levels of distress that were inconsistent with their time since new and could potentially have resulted in the same in service failure had they not been detected by the emergency inspections.

The removed bearings showing evidence of distress, were subjected to in-depth forensic laboratory investigation using the same techniques applied

---

<sup>57</sup> The old part number actuator can be replaced by the new part number actuator, but not the other way around.

to the accident bearing. The following serial numbers are reported as exemplars of the various stages of deterioration of the bearing but were not the only bearings confirmed to have damage.

*Serial number 14134*

This bearing was removed in service from an AW189 during the initial AD inspection requirement. It had accumulated 1,117 flying hours since new. The operator identified that the bearing rotation was 'notchy' when turned by hand, so rejected it for further investigation. This was done on behalf of the AAIB by nC<sup>2</sup> at the University of Southampton.

Once the bearing had been weighed and CT scanned, it was opened for detailed inspection. Visually there was evidence of degradation of the grease. The grease on the outboard inner race appeared brown but still moist, suggesting the presence of lubricating oil but no longer in the solid grease form. The inboard inner race was also brown but with a tacky rather than moist residue over the race surface (Figure 45). There was no evidence of any damage to the balls, but the cages showed evidence of wear in the ball 'pockets' and witness marks indicating a 'running line' around the circumference where the cage had been in contact with the inner race.

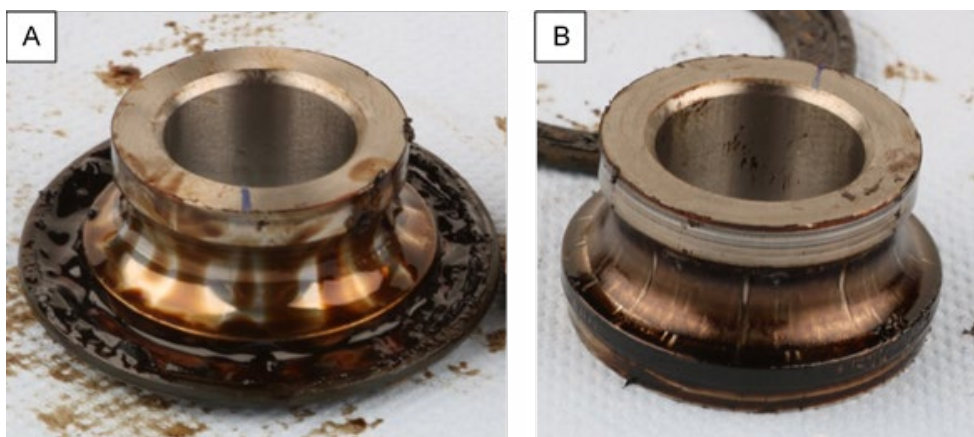


**Figure 45**

A) Outboard inner race of bearing showing evidence of moist lubricant residue. B) Inboard inner race showing tacky residue coating the race surface

*Non-destructive examination*

Following ultrasonic cleaning, both the inner races were examined by visual microscopy. This confirmed a clear track where the balls had been running, which was consistent with the intended design position.

The races were then scanned using the non-contact optical scanning technique (RedLux OmniLux). This allowed the identification of raised features in the worn running path on the inboard inner race (Figure 46).

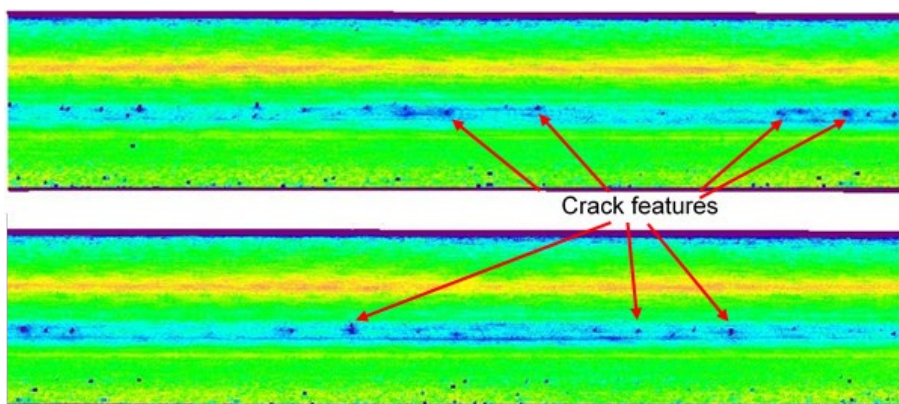


**Figure 46**

Optical scan of inboard inner race on a +5 µm to -10 µm colour scale showing distribution of raised crack features

The inner races were inspected using an SEM, with the images then processed using MeX software to create height maps. The outboard inner race showed evidence of the original manufacturing grinding marks across the race surface, except for the running area band, where they had been worn smooth. The inboard inner race exhibited crack features, which displayed the same orientation and aspect ratio but varied in size (Figures 47 and 48).

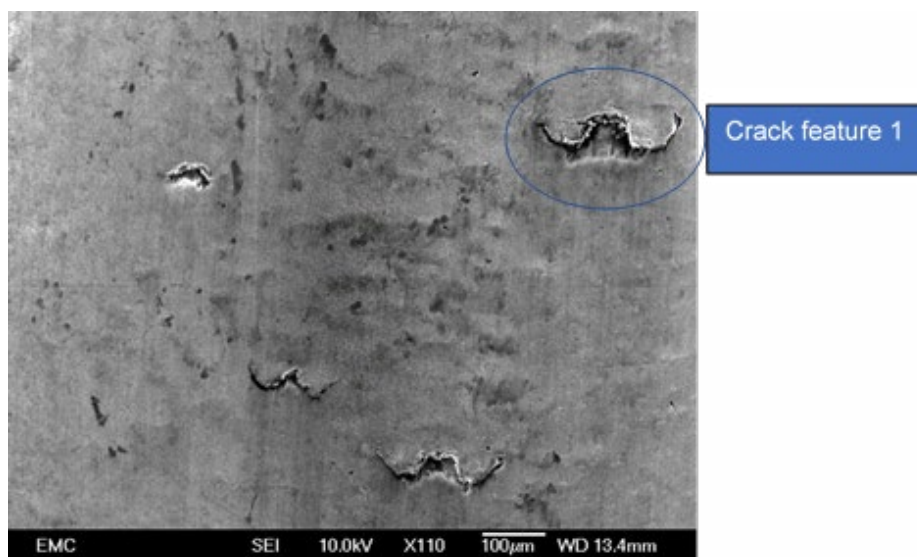


**Figure 47**

SEM image of inboard inner race showing variation in crack sizes

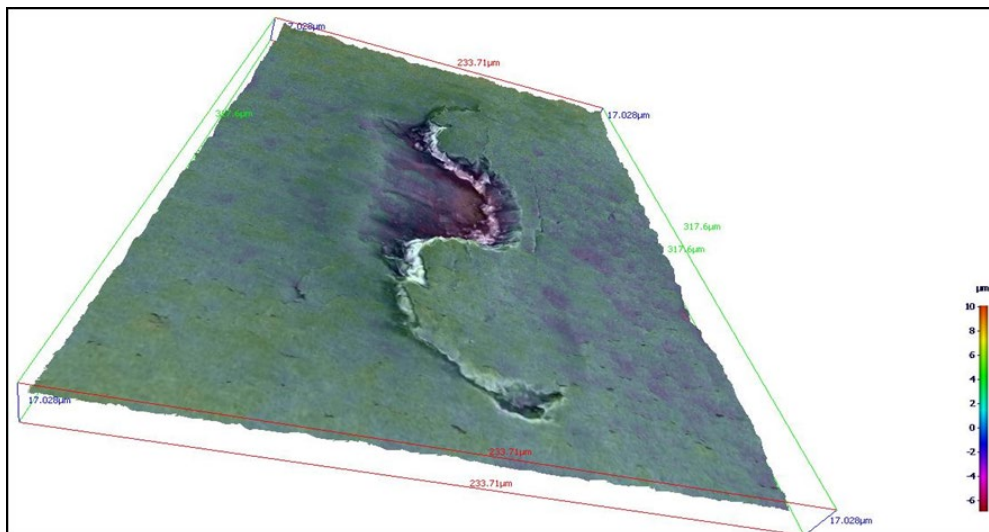


**Figure 48**

MeX height map of crack feature 1 showing measurements and pitting

*Destructive examination*

A circumferential and radial section was cut from the inboard inner race and inspected using the SEM. This showed that the larger cracks extended to a depth of 50  $\mu\text{m}$  and were consistent with those seen on the accident bearing (Figure 49).

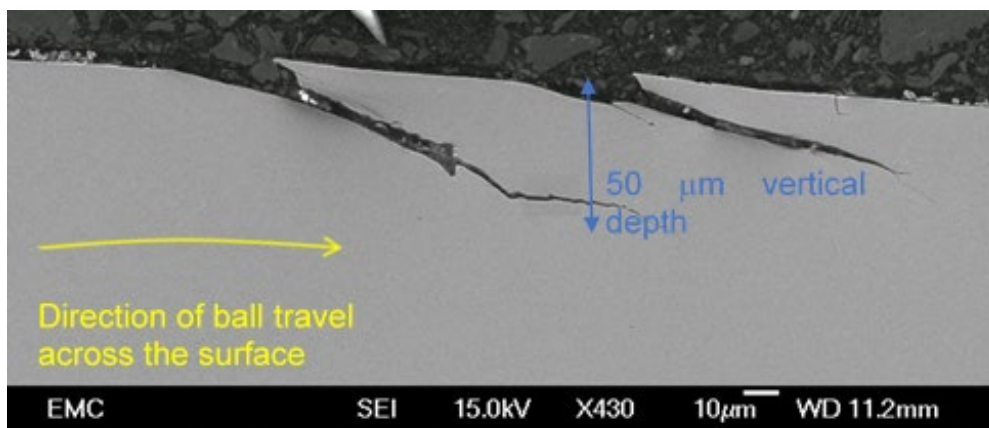


**Figure 49**

SEM image of circumferential section showing crack depth and orientation

Etching of the sections from both the inboard and outboard inner rings confirmed a DER of microstructural change within a band from the surface to 0.2 mm down. (Figure 50). Nano hardness testing confirmed a reduction in hardness through this region. The area of microstructural change on the inboard race was deeper and more consistent than on the outboard race, but both showed

evidence of change consistent with the early stages of a surface origin, rolling contact fatigue mechanism.

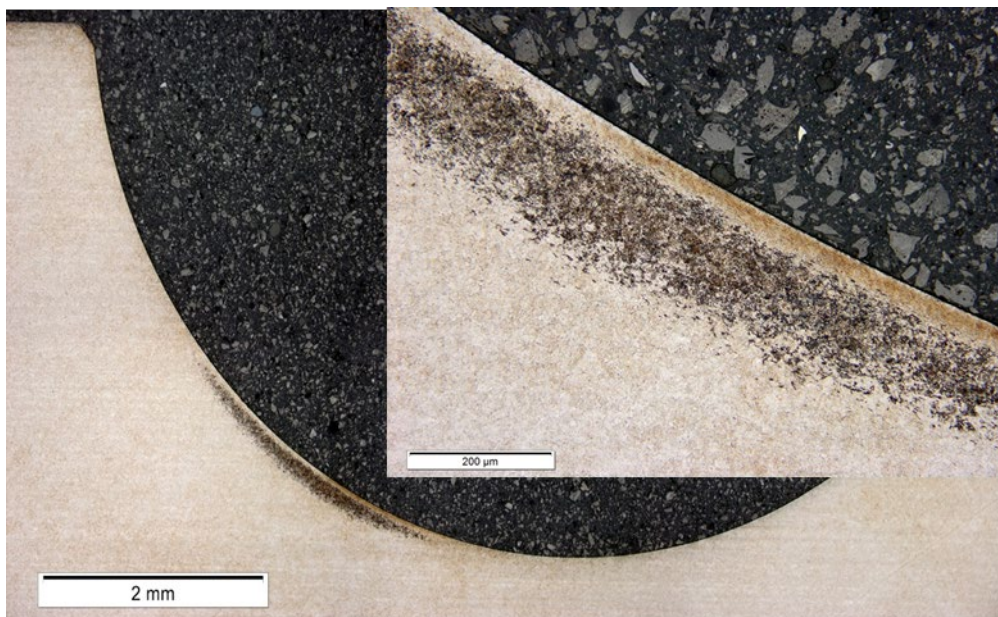


**Figure 50**

Etched radial section from inboard inner race showing area of microstructural change (DER)

*Serial number 15119*

This bearing was removed from an AW169 during the post-accident repetitive inspection programme. It had accumulated 663 flying hours in service. Initially it was opened and inspected by the bearing manufacturer, after which components were provided for further forensic assessment by nC<sup>2</sup> at the University of Southampton and the bearing manufacturer's failure analysis specialist, in order to independently compare the findings.

*Non-destructive examination*

Initial inspection showed burnt grease residue and heavy damage to both the inner races. Two balls from the outboard race exhibited spalling damage, with the other balls showing evidence of crazing. The cage from the inboard row was cracked completely through in one location and partially cracked in another. There was also wear in various ball pockets from contact with the balls. The bearing components were CT scanned and cleaned, before being inspected by optical microscope (Figure 51).

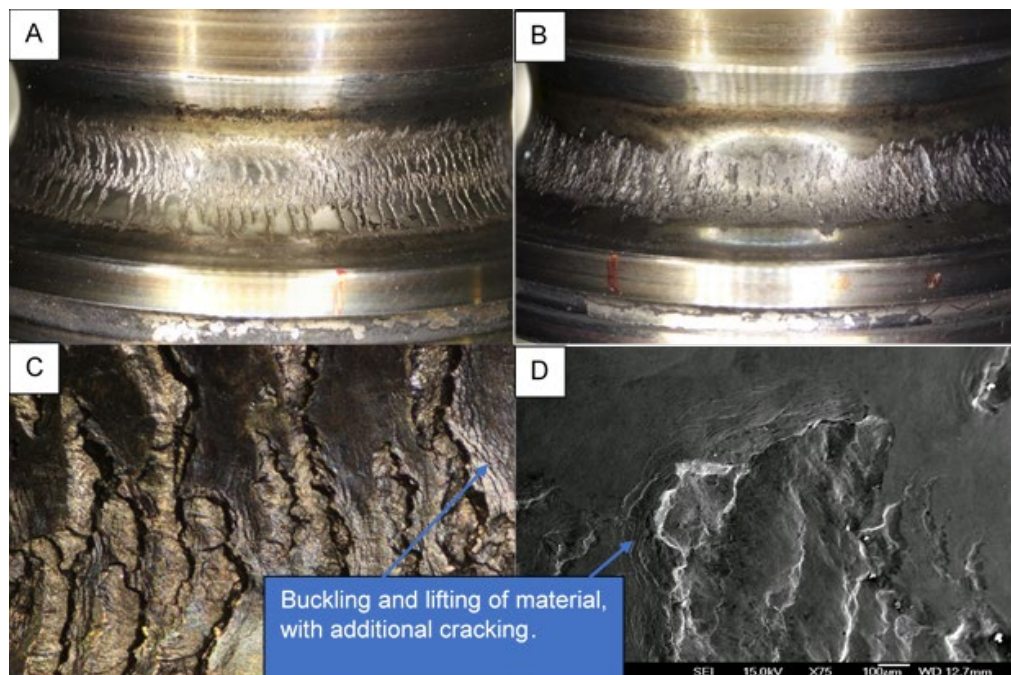


**Figure 51**

- A) Damage to inboard inner race. B) Damage to outboard inner race.  
C) Magnified image of damage showing macropitting on inboard inner race.  
D) SEM image of macropitting

#### *Destructive examination*

The inboard and outboard inner races were sectioned both radially and circumferentially to assess the subsurface cracking. This showed angled, surface initiated cracks consistent with the other bearings that had been analysed but showing evidence of additional material loss to create macropitting (Figure 52). Etching of the radial section and hardness testing confirmed the presence of a DER of microstructural change extending approximately 0.2 mm downwards from the surface (Figure 53). The radial section from the outboard inner race showed some initial material transfer from the cage to the surface of the race. The damage on this race extended over a larger arc of the running surface compared to that seen on bearing s/n 14134.

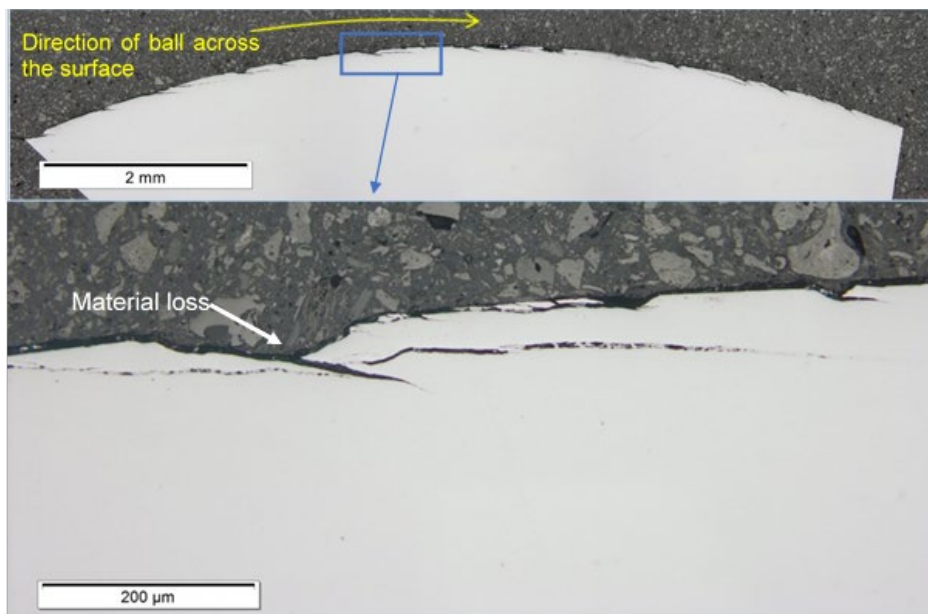


**Figure 52**

Microscope view of circumferential section from inboard inner race showing angled, surface initiated cracking with material loss

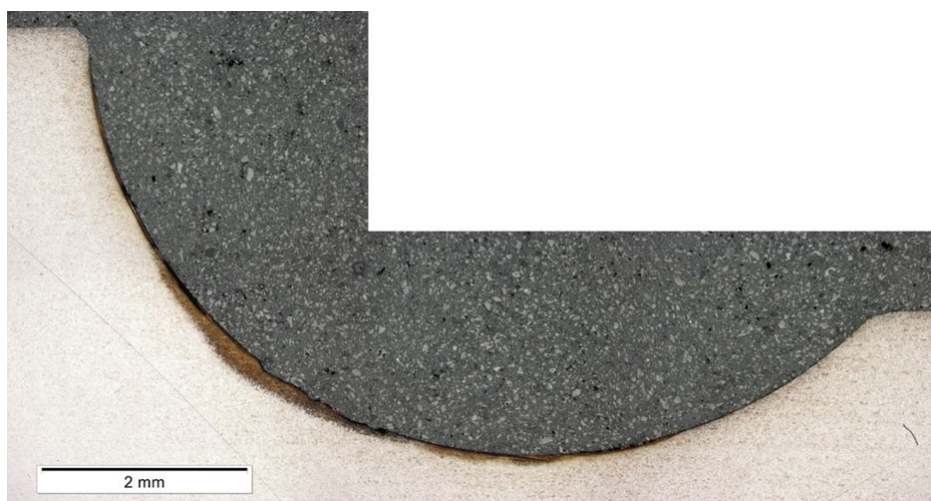


**Figure 53**

Macroscopic view of etched (Vilella) radial section from outboard inner race, showing change in microstructure (DER)

#### *Cage damage and wear*

The inboard cage had two fractures in pockets on the narrow end and one on the wide end, but remained in one piece. Both the cages from this bearing had a wear lip on the inside surface of the wide end of the cage (Figure 54).

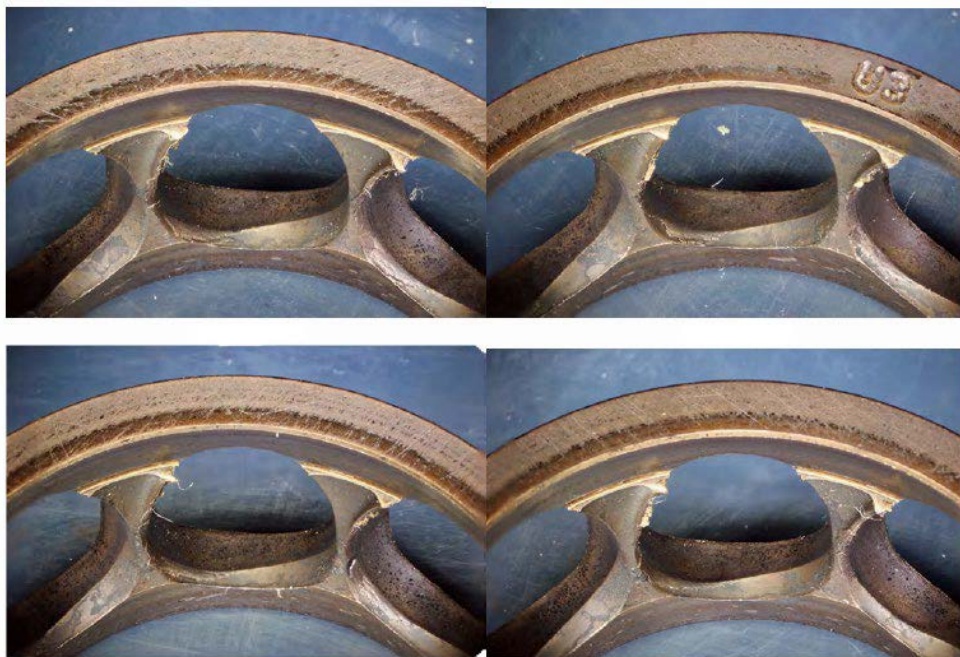


**Figure 54**

Wear lip on the inner surface of the wide end of the outboard cage

*Serial number 13123*

This bearing was removed from service by an operator in May 2019 due to the presence of black powder around the bearing and an increase from one mandatory inspection to the next, in the measured torque required to turn the bearing, although the torque measured was still well within the rejection limits. The bearing had operated 1,695 hours since new. Following removal, it was inspected by the bearing and helicopter manufacturer's failure investigation laboratories.

*Non-destructive examination*

When the bearing was opened, it was found to have significant damage over the whole running surface of the bearing on the inboard row, inner and outer races (Figure 55). Material had been displaced from a wear path the same radius as the radius of the balls and pushed up above the shoulder of the race (Figure 56).

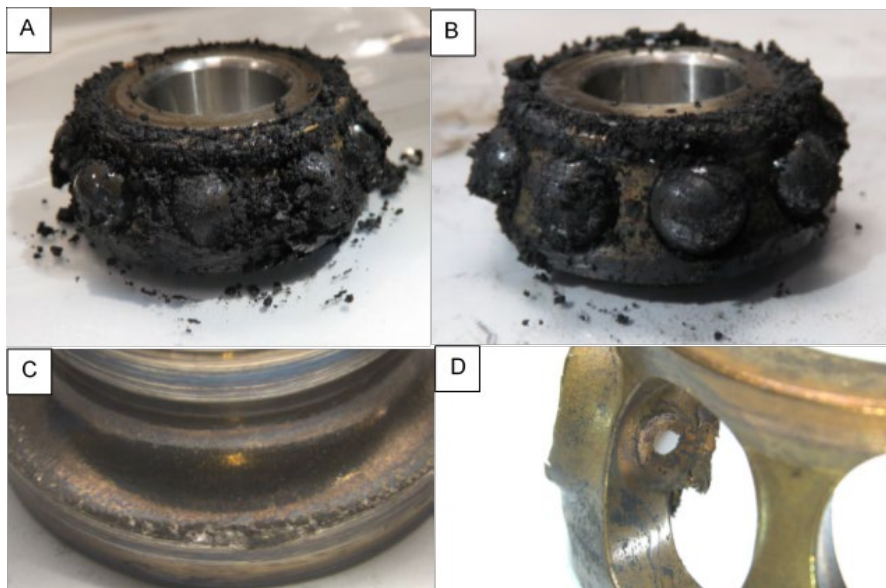


Figure 55

- A) Outboard inner race, cage and balls. B) Inboard inner race, cage and balls.
- C) Damage to inboard inner race. D) Wear to inboard cage pocket

The outboard row races exhibited less damage than the inboard row.

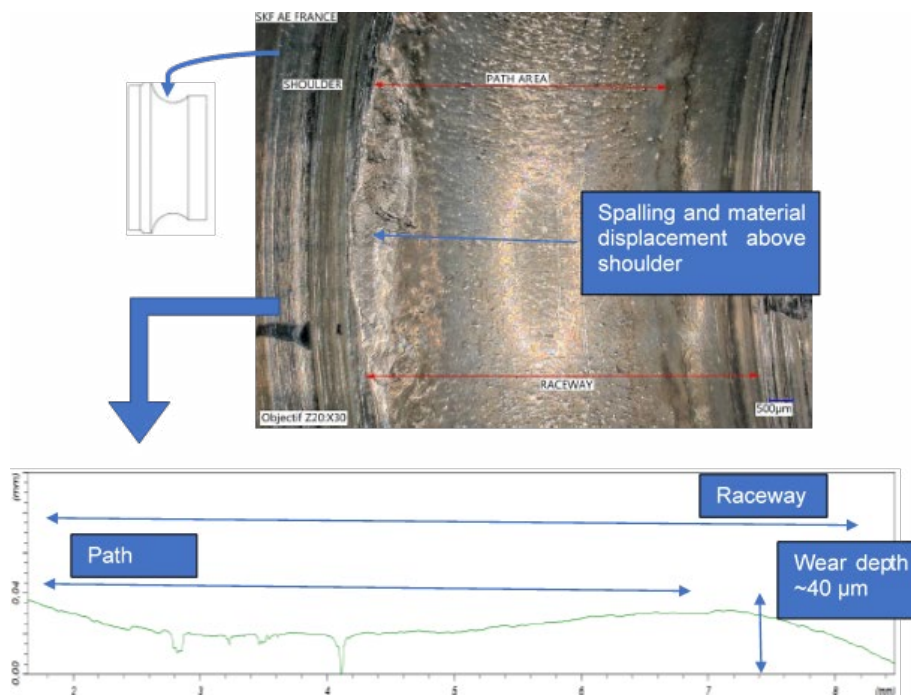
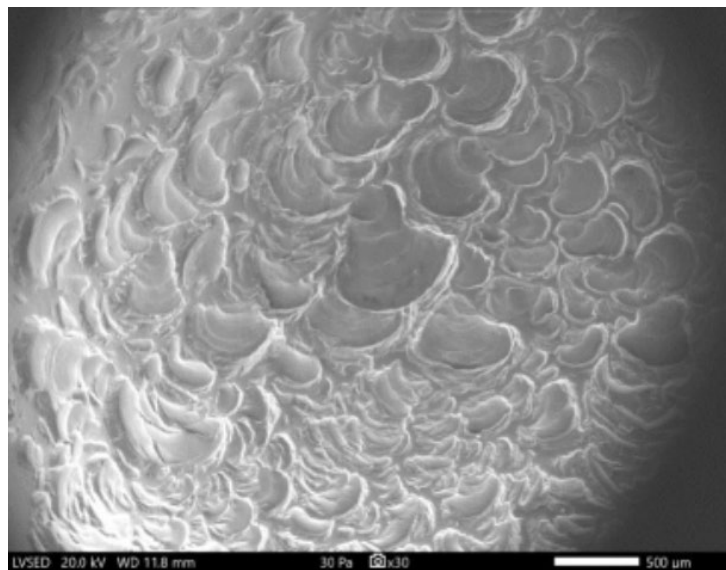


Figure 56

Inboard inner race showing wear path created by the balls and material displacement

The inboard cage showed evidence of heavy wear predominantly to one of the cage pockets, where the wall was holed. One of the balls from the inboard row had heavy spalling, with wear scarring to the neighbouring ball as well, potentially caused by contact between the balls through the pocket wall.

The ball had spalled over 50% of its surface area. The bearing manufacturer's report stated that although the estimated initiation point of the spalling was identified, the cause could not be determined (Figure 57). The helicopter manufacturer's laboratory investigation report stated that a 3D particle was identified embedded in the spalled area of the ball. EDAX analysis of the particle suggested it was iron oxide, which the report identified was used as an additive during the sintering<sup>58</sup> and/or hipping<sup>59</sup> process. The bearing manufacturer refuted this, stating that iron oxide is not used in either of these processes and that the material was likely adhered debris rather than an inclusion. The helicopter manufacturer's report stated the particle was 'embedded' with ball material partially covering it. They considered it likely that this particle was originally below the surface of the ball material.



**Figure 57**

Magnified view of the spalling on the surface of the ball

### *Destructive examination*

The inner and outer races were sectioned and etched with Vilella's reagent to identify any material microstructure change. The inboard inner and outer races showed surface initiated cracking at an angle of approximately 20° to the

58 Process of creating a solid from powder using heat and compression.

59 Hot isostatic processing (HIPping) involves the application of high gas pressure at an elevated temperature to components to completely remove internal porosity and voids.

surface and extensive micropitting (Figure 59). However, there was no DER below the surface as found on the other bearings (Figure 58).

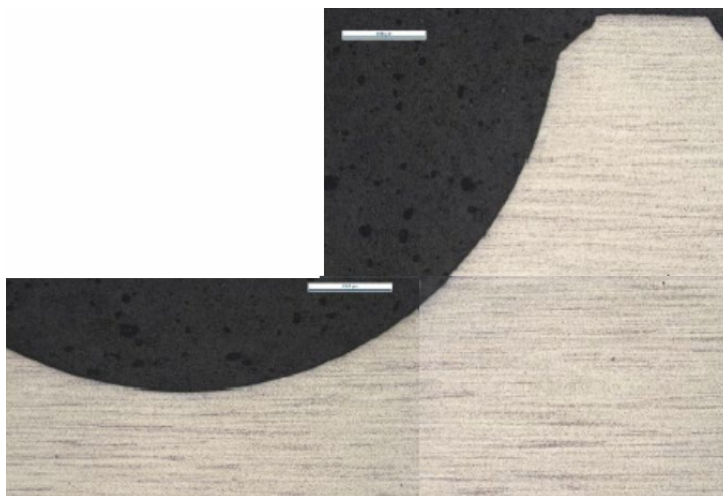


**Figure 58**

Inboard inner race radial section with no evidence of DER

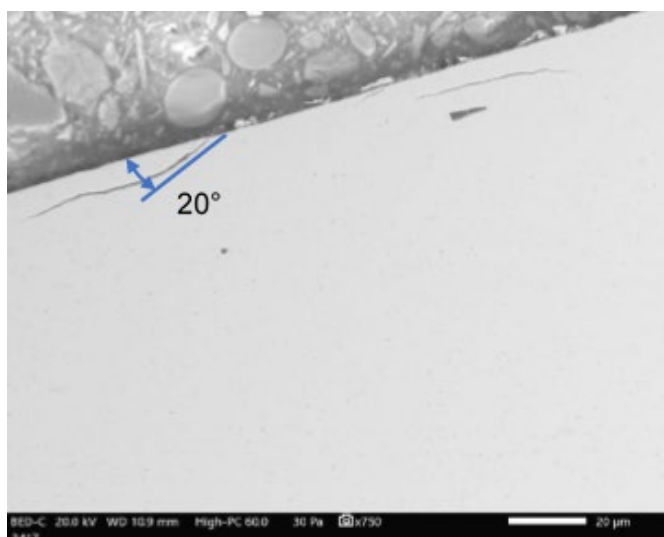


**Figure 59**

Inboard inner race surface initiated cracking

#### *Serial Number 17115*

This bearing was removed from service in 2018 after just 23 flight hours due to the presence of black dust, during one of the Service Bulletin inspections. During the subsequent lab inspection, the grease was observed to be black in colour, but consistently distributed in the bearing.

The inner and outer race on one side of the bearing was found to be damaged with significant spalling and material loss on both the races and on one of the balls (Figure 60).

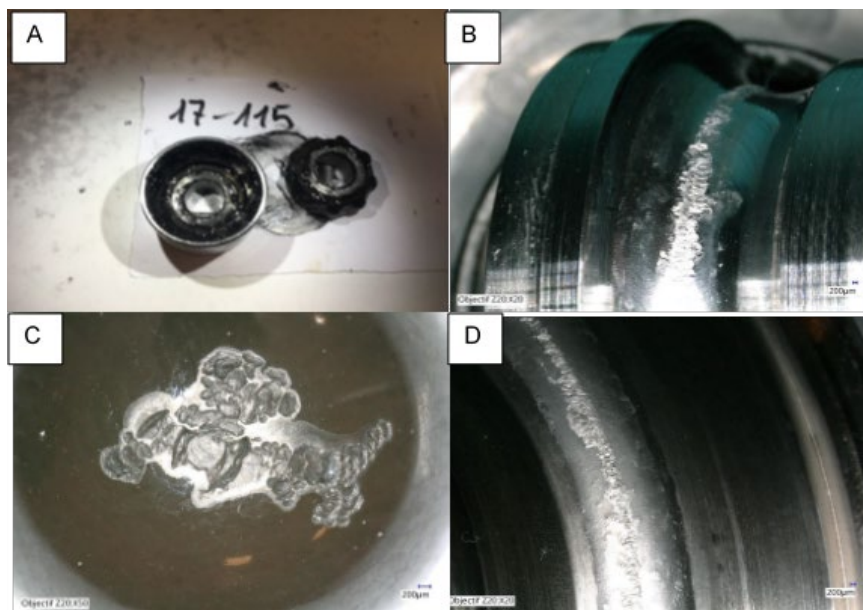


**Figure 60**

A) Bearing with one side removed showing black grease.  
B) Inner race damage. C) Spalled ball. D) Outer race damage

Forensic investigation by the bearing manufacturer confirmed that the ball had spalled due to a large iron silicide inclusion in the ceramic material (Figure 61).

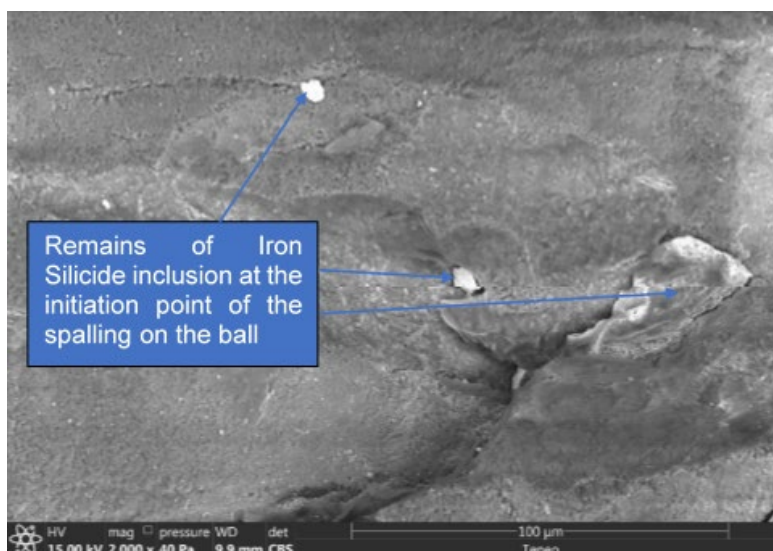


**Figure 61**

Remains of inclusion on the spalled ball

### *Serial number 14125*

This bearing was reported to the AAIB in January 2020 by the helicopter manufacturer, as having been removed from an AW169 during the postaccident repetitive inspection programme. It had accumulated 454 flying hours in service. It was then assessed by the bearing manufacturer's failure specialists, who issued a laboratory report in February 2021. The bearing was not assessed independently by the investigation and the factual information provided below is based solely on the manufacturer's report.

#### *Non-destructive examination*

Initial inspection showed burnt grease residue on the outside of the seal on one side of the bearing (0.11 g). Both seals were present and showed evidence of wear consistent with contact with the cages. CT scans showed that the cage on one side of the bearing had displaced outwards due to wear from contact with the inner race at the wide end, the same as seen on various bearings inspected, but most noticeably on bearing s/n 16141, used in the manufacturer's final rig test. Once opened, the bearing was found to contain grease which had fully degraded to black powder. One of the cages had also completely fractured into two pieces. There was also wear in various ball pockets from contact with the balls. The balls had a matt white surface finish. One ball from the side of the bearing where the cage was displaced exhibited spalling damage, with the other balls all showing evidence of crazing. The outer races showed signs of wear and damage, whilst the inner races exhibited heavy damage with spalling across the normal running path of the balls, but with additional evidence of damage across a broader width of the race.

#### *Destructive examination*

The inboard and outboard inner races were sectioned both radially and circumferentially to assess the subsurface cracking. This showed angled, surface initiated cracks consistent with the other bearings that had been analysed with evidence of material loss to create macropitting. Etching of the radial section and hardness testing confirmed the presence of a DER, microstructural change and carbide flow. The inner races also showed some initial material transfer from the cage to the surface of the race. As with the other bearings, the fracture surfaces on the cages confirmed the cage failed in fatigue.

## **1.13 Medical and pathological information**

All five occupants of the helicopter suffered significant and disabling injuries when the helicopter struck the ground. Post-mortem reports indicated that

four of the occupants survived the initial impact but died as a result of breathing products of combustion from the resulting fire. One occupant was likely to have died from injuries sustained during the ground collision.

Four first responders were treated for the effects of heat following their attempts to rescue the occupants of the helicopter.

## 1.14 Fire

Shortly after rising above the stadium the helicopter was seen by two police officers in a car near to the stadium. They saw the helicopter begin to rotate and descend from view followed by the sound of an impact.

They reported the accident to their control room and drove to the scene, arriving at 2039 hrs<sup>60</sup>, approximately one minute after the helicopter struck the ground. They found the helicopter resting on its left side with a significant fire already visible towards the rear of the fuselage. In their statements, the officers reported that as they approached the helicopter the fire was rapidly moving from the rear towards the front of the helicopter and increasing in ferocity. One officer also reported that they could hear one or both of the helicopter's engines running. The officers could not reach the right side door apertures due to their height from the ground, so attempted to break the helicopter's windscreen using their batons and other handheld equipment, which was unsuccessful. Body worn camera footage showed that by 2041 hrs the fuselage was completely engulfed by the fire.

Approximately 13 seconds after impact, the helicopter's baggage compartment smoke detection system began to trigger intermittently and one minute after impact the helicopter's automated warning system was recorded by the CVR announcing "ENGINE ONE FIRE".

Approximately nine minutes after impact the Fire Service began extinguishing the fire. The fire was largely extinguished within six minutes of water being applied, but periodic flare-ups were observed for a further eight minutes after which no flames were visible.

## 1.15 Survival aspects

### 1.15.1 Certification requirements

The AW169 was certified in accordance with EASA CS 29 Amendment 2<sup>61</sup>. The current version is CS 29 Amendment 11.

60 Time recorded on police car camera.

61 <https://www.easa.europa.eu/document-library/certification-specifications/cs-29-amendment-2> (accessed 28 July 2023).

The certification requirements related to passenger protection and emergency evacuation are defined in CS 29 Book 1, Emergency Landing Conditions, CS 29.561 through CS 29.563 and Personal and Cargo Accommodations CS 29.771 through CS 29.863.

A review of all the changes between CS 29 Amendment 2 and CS 29 Amendment 11 confirmed that the only changes to the certification standards for passenger protection and emergency evacuation concern the introduction of additional measures relating to landing on water which are not relevant to this accident.

The emergency landing conditions, which must be achieved by a helicopter design, are defined in CS 29.561 (b) which states:

*'(b) The structure must be designed to give each occupant every reasonable chance of escaping injury in a crash landing when:*

- (1) Proper use is made of seats, belts and other safety provisions*
- (2) The wheels are retracted (where applicable); and*
- (3) Each occupant and each item of mass inside the cabin that could injure an occupant is restrained when subject to the following ultimate inertial load factors relative to the surrounding structure*
  - (i) Upward - 4 g*
  - (ii) Forward - 16 g*
  - (iii) Sideward - 8 g*
  - (iv) Downward - 20 g, after the intended displacement of the seat device*
  - (v) Rearward - 1.5 g'*

Subpart (c) of CS 29.561 also states that the helicopter's structure must be capable of restraining significant items of mass, which are attached to the structure, such as the engines and main rotor transmission at downward loads of up to 12 g.

The dynamic conditions which a helicopter must withstand during an emergency landing are defined in CS 29.562.

This states that a helicopter, although it may be damaged in a crash landing, must reasonably protect each occupant when exposed to a range of forces. CS 29.562 (b) requires that the seats installed in a helicopter must demonstrate by testing their ability to provide protection from a peak floor deceleration of not less than 30 g over a period of no more than 0.031 seconds with the longitudinal axis of the floor inclined upward at 60° to the direction of deceleration. The tests are conducted with a 77 kg test dummy secured to the seat.

The helicopter's fuel system must also meet the crash resistance standards defined in CS 29.952. This states that fuel tanks located in the helicopter cabin must be capable of resisting an ultimate downward inertial load factor of 20 g. The ability of the fuel system to meet dynamic load requirements is verified by carrying out a 'drop test' from a height of at least 15.2 m.

#### 1.15.2 AW169 crashworthiness

In order to meet the emergency landing dynamic conditions of CS 29.562 the cockpit and passenger seats installed in the AW169 are fitted with an impact absorption mechanism. Two L shaped legs secure the seats to the cabin floor and carry the seat pan. A slide is fitted to each side of the seat pan which engages in a rail in each seat leg. This allows vertical adjustment of the seat pan and allows downward movement of the seat pan against an energy absorption system during severe vertical loads. The energy absorption system consists of sheet metal straps positioned between the slides and seat rails. These bend progressively under load, decreasing the forces experienced by the occupant. A 'stroke index mark' is located on the side of each seat leg (Figure 62). The stroke index mark must remain visible with the seat pan at its lowest position. If the mark is not visible or partially obscured, this is an indication that the seat's impact absorption system has operated. The seats were designed, and certified, to mitigate vertical decelerations of up to 30 g.



**Figure 62**

Generic AW169 cockpit seat (original image courtesy of the manufacturer)

The helicopter manufacturer provided documentation which confirmed that the AW169, and the interior configuration installed in G-VSKP, met the cabin and passenger safety requirements defined in CS 29 Amendment 2. Documentation was also provided which confirmed that, during the certification process, the fuel tank installation and fuselage structure met the design and drop test requirements of CS 29.

The design of most helicopter's, including the AW169, does not allow for the provision of emergency exits in the top, bottom or rear of the fuselage. If the helicopter comes to rest on its side during an accident, the only practical means of escape for the occupants would be to leave by the doors and exits on the uppermost side of the helicopter. This would require them to climb up to the highest side of the helicopter using seat arms and internal fittings as hand and foot holds.

### 1.15.3 Examination of wreckage related to crashworthiness

Damage observed to the lower fuselage of the helicopter showed evidence of buckling and failure in the region directly below the main fuel tanks. It was consistent with this section of the fuselage striking the raised step on the accident site. Examination of the damage showed evidence that parts of the fuselage structure had been driven into the fuel tank structure as a result of impact forces (Figure 63).



Location of fuel tank

**Figure 63**

Lower fuselage and fuel tank damage

After recovery of the helicopter to the AAIB, an examination of the helicopter's cabin was carried out to locate the cockpit and passenger seat impact absorption features and to determine if they had operated correctly during the accident. Due to the damage caused by the post-impact fire it was not possible to identify specific components of the two cockpit seats. The four rearward facing seats in the passenger cabin had been extensively damaged, but the lower sections of the seats remained in-situ. The level of damage to the seats did not allow reference to the stroke index marks to determine if the seat impact absorption systems had operated. However, examination of the position of the seat pan sliders within the seat leg rails, confirmed that the impact absorption system of the two outboard seats had operated and seat pan slides had exceeded the limit of their downward travel (Figure 64).

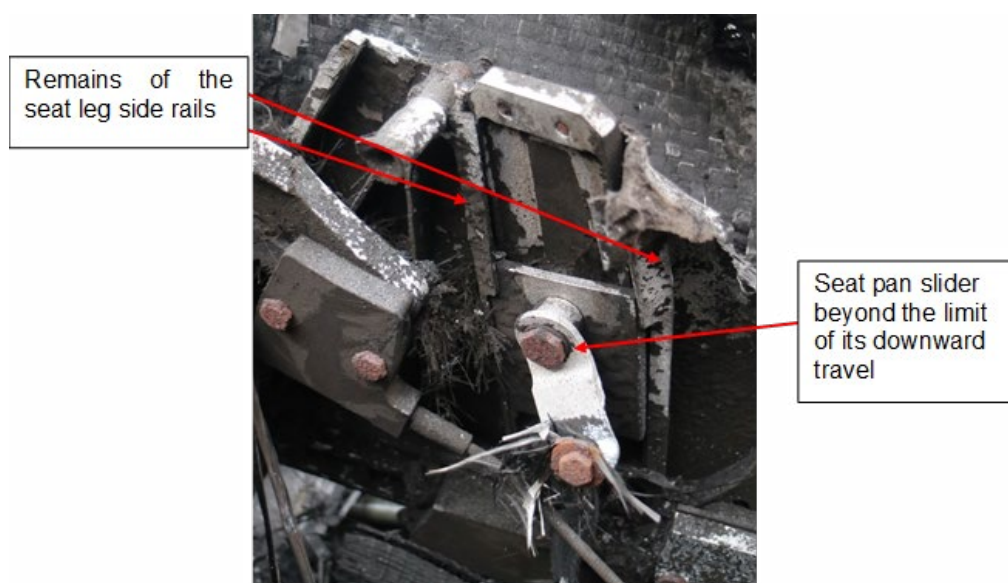


**Figure 64**

Rearward facing passenger seat impact absorption mechanism

Examination of the remains of the three forward facing passenger seats confirmed that the impact absorption mechanism of the central seat had also operated, and the seat pan slides had reached the downward limit of their range of movement.

## 1.16 Tests and research

### 1.16.1 Engineering tests and trials

#### 1.16.1.1 Post-accident bearing tests

The helicopter manufacturer utilised three test rigs, two in Italy and one in the UK. These were used to conduct a series of fifteen tests for both investigation and continued airworthiness purposes. A fourth test rig at the bearing manufacturer's facility was used to conduct a further investigation test. The rigs used production standard TRA control shafts to apply an axial load to the bearing. The rig in the UK also allowed a bending moment load to be applied. The control shafts were instrumented to measure temperature, vibration and torque. Specific temperature, vibration and torque limits were defined as stop conditions for the testing in order to protect the rigs. In practice, observation of a torque reading on the control shaft became the limiting factor which resulted in the tests being stopped, as it demonstrated that the bearing was starting to seize.

The test scenarios explored a range of possible factors including:

- Standard and modified bearings with different operating loads applied.
- Standard and modified bearings with different preloads.
- Standard and modified bearings with the grease degraded or removed.
- Intentionally incorrectly installed bearings.
- Continued running of bearings that had been removed from service with initial signs of distress.
- Continued running of bearings that had been removed from service with heavy damage.

The tests demonstrated that as the axial load changed direction (control shaft moved to the left or right) the side of the bearing carrying the load changed and the temperature in that part of the bearing increased. The tests with different preloads did not result in any damage to the bearing, as such the manufacturer did not consider this to be a significant factor in isolation.

The tests which continued operation with existing heavy race damage (TSDD-DB-4&6) and those where the grease was completely removed (TSDD-DB-1&2), were conducted to try to understand the duration and sequence of the final failure of the bearing, rather than to replicate the initiating cause of bearing failure.

These tests ran until a stop condition was reached and identified that the temperature of the bearing (measured at the control shaft) rose significantly and consistently in the final stages of operation prior to failure (seizure), peaking around 600°C. The incipient seizure of the bearing was replicated in two of the rig tests. Both confirmed that seizure of the bearing resulted in a torque load being transferred to the control shaft. On one of the tests this also resulted in movement of the servo end locking nut relative to the shaft.

A separate rig test (TSDD-DB-16) was completed replicating the removal of the seal and grease on one side of the bearing as with the earlier test but using an AW139 bearing, this bearing subsequently failed in the same manner<sup>62</sup>.

The helicopter manufacturer's test card for one test (TSDD-DB-05) recorded the finding that 'typical' grease loss was present in the form of a ring of grease on the external face of the seal. In this test the bearing was operated with intact seals and nominal grease content. It ran for 1,037 hours with no damage identified when the bearing was disassembled.

#### 1.16.1.2 Investigation requested endurance rig test

This test was carried out on the rig at the bearing manufacturer's facility and was a 1,000 hour endurance test, undertaken at the request of the investigation. The continuous run test was conducted on a new bearing (s/n 19189), with a constant load in the same direction of 8,000 N axially and 16 Nm bending load<sup>63</sup>, recommended by the manufacturer to replicate the maximum certification static flight load case for the AW169.

Except for two minor stoppages due to technical difficulties, the test ran continuously for 1,000 hours. During this time, the temperature of the bearing, measured by a thermocouple on the outside of the inner race, varied between approximately 72°C and 82°C. At the end of the test the bearing was still able to rotate freely.

#### *Lab forensic investigation*

The endurance test bearing (s/n 19189) was removed from the test rig and sent to nC<sup>2</sup> at the University of Southampton for the same forensic examination as the accident bearing.

62 At the time of publication, two tail rotor bearings have been reported as having failed on the AW139 fleet. These are being investigated as a separate but linked AAIB investigation. None of the emergency AD inspections or modifications issued for the AW169/AW189 are applicable to the AW139, which are covered by separate inspection requirements.

63 The rig test couldn't mechanically apply bending moment, so a calculated equivalent load was applied.

### *Non-destructive examination*

Comparison of the pre and post-test bearing mass showed that 1.4 g had been lost during the test. The bearing was opened to separate the component parts.

The grease was found to be black in colour, with some separation of the oil and the matrix. It had also become sticky and lumpy in consistency, indicating a change of condition due to ageing (Figure 65).



**Figure 65**

Condition of the grease in the endurance test bearing s/n 19189

The races of the loaded side of the bearing showed evidence of a wear line created by the balls, but no evidence of fatigue damage. The balls also exhibited a 'run' line, which was off centre, but no spalling (Figure 66). The cages had witness marks in the pockets, which were more pronounced on the loaded side of the bearing, but no significant damage.



**Figure 66**

Wear on inner race and balls of the loaded side of the test bearing

### *Destructive examination*

Sectioning, etching and SEM inspection of the race material, confirmed there was no evidence of rolling contact fatigue damage or a heat affected zone of

material properties change on any of the races. The inboard race of the loaded side of the bearing did, however, exhibit a DER below the race surface, where the wear line showed the balls had been running (Figure 67).



**Figure 67**

DER under the running surface of the inner race on the loaded side of the bearing

#### 1.16.1.3 Manufacturer's subsequent rig test

The manufacturer conducted a further rig test on the test rig based in the UK. This test utilised the same certification endurance test profile to test the hybrid bearing as was used for the approval of the new all steel replacement bearing. The hybrid bearing selected for the test was s/n 16141. This bearing had been removed from service in November 2018 with 138 flight hours, after being rejected for rough operation following the additional in-service inspections (SB 169-125). The bearing was inspected visually and found serviceable, so it was reconditioned with fresh grease by the bearing manufacturer and sent for use on the test rig. However, a decision was made by the helicopter manufacturer to completely remove the seal on the inboard side of the bearing, to test how this would affect the performance of the bearing. The test rig was instrumented with sensors to measure axial load, bending moment, temperature and torque.

The test spectrum used for the certification endurance test was based on the highest axial loads recorded during the original certification flight testing of the AW189, (Figure 68) combined with the highest bending moment from the development spectrum.

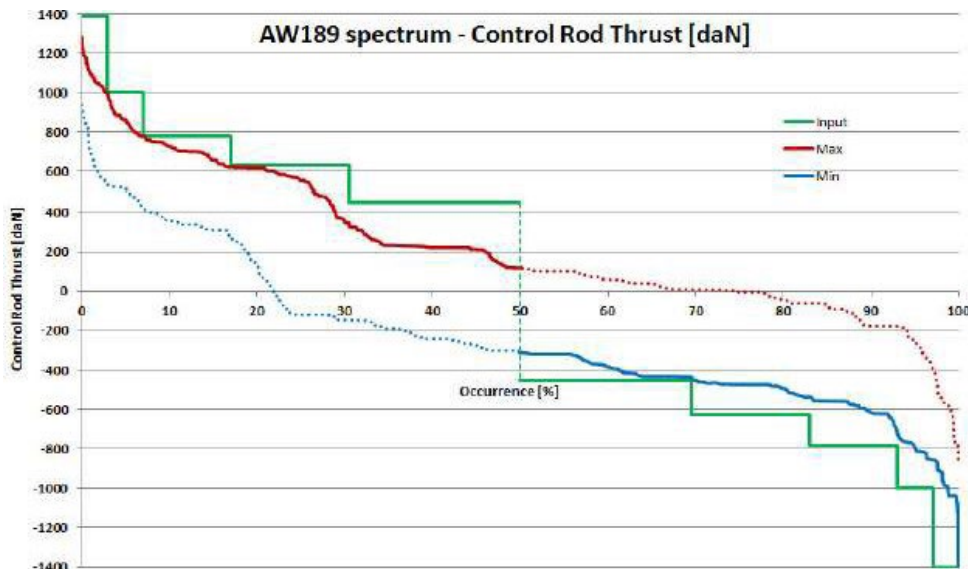


**Figure 68**

AW189 flight loads used to create the certification endurance test for the new all steel bearing.  
(original image courtesy of the manufacturer)

This was translated into a test profile by alternating the loads at each step (green line in Figures 68 and 69) to create a test block.

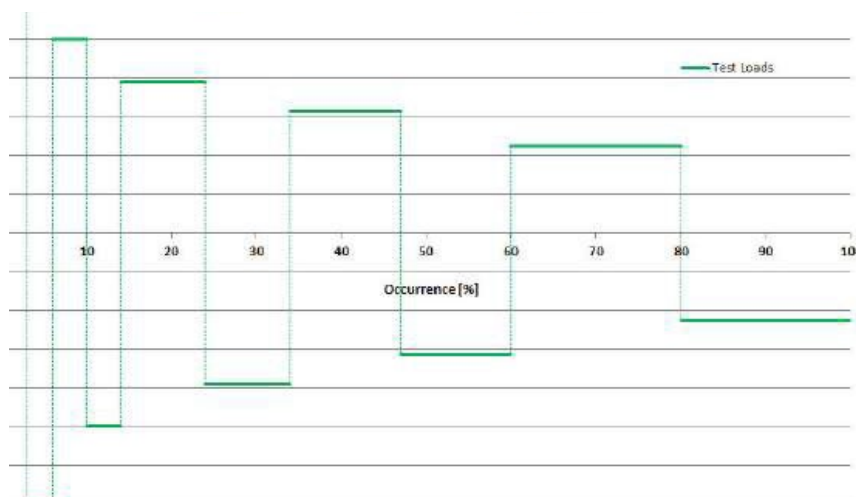


**Figure 69**

Load profile for certification endurance test  
(original image courtesy of the manufacturer)

Factual Information

Each test block consisted of a total of five hours of running time under load, distributed at the loads and durations shown in Figure 70, followed by two hours at a complete stop. The test was also conducted at the AW189 tail rotor rotation speed of 1,406 rpm, rather than the AW169 tail rotor rotation speed of 1,633 rpm, used for the other rig tests.

Control Rod Thrust [daN]	Duration [%]	Duration [min/block]	RPM	Control Rod BB [daNm]
1400	3	9	1406	4.2
-1400	3	9	1406	
1000	4	12	1406	
-1000	4	12	1406	
780	10	30	1406	
-780	10	30	1406	
630	13	39	1406	
-630	13	39	1406	
450	20	60	1406	
-450	20	60	1406	

**Figure 70**

Test block for certification endurance test  
(original image courtesy of the manufacturer)

The hybrid bearing rig test finished on 10 December 2020 after a total of 145 test blocks had been conducted, resulting in an elapsed time of 1,015 hours and an operating time of 725 hours.

The test had been halted at various points through its progression. The first was at 290 hours to replace the thermal indicator strip which was showing an erroneously high temperature. The second stop occurred when the rig temperature sensor warning was triggered to indicate the bearing sensor had reached 130°C. The warning threshold was progressively raised to 200°C, then 300°C and then 400°C to allow the test to continue. The test was eventually stopped when the torque alarm was triggered at 10 Nm, indicating that the bearing was starting to transfer drive torque through to the control shaft.

The inspection conducted at the first stop indicated that a 'collar' of grease extruded from the bearing had built up around the inboard bearing face where the seal had been removed (Figure 71). The volume of grease remained the same throughout the test.



**Figure 71**

Grease extruded from the bearing during the first 290 hours of testing.  
(original image courtesy of the manufacturer)

The actual axial and bending moment loads recorded during the testing were provided to the investigation for further analysis. This data was sampled once a minute. In many cases the test point recorded loads did not exactly match the planned test loads shown in Figure 70. The top three positive and negative load cases were considered during this analysis as they were above a threshold where damage could potentially be incurred from the resulting contact pressures. The data for each test point was then extracted and averaged to give a representative spectrum for the whole test. The approximate bearing bending moments were then calculated<sup>64</sup> (Table 6).

Target axial load (N)	Average Axial load (N)	Approx. bearing bending moment NRL (Nm)	Approx. bearing bending moment PRL (Nm)
14,000	13,834.01	-10.5	-2.25
-14,000	-10,684.60	20.4	-20.6
10,000	9,703.20	-5.9	-9.5
-10,000	-7,605.67	15.6	-19.6
7,800	7,956.77	-4.64	-10.4
-7,800	-5,980.96	12.7	-18.1

**Table 6**

Averaged actual loads applied during the rig test for highest load cases

<sup>64</sup> For more information on bending moment sensors and PRL and NRL locations see [section 1.16.2](#)

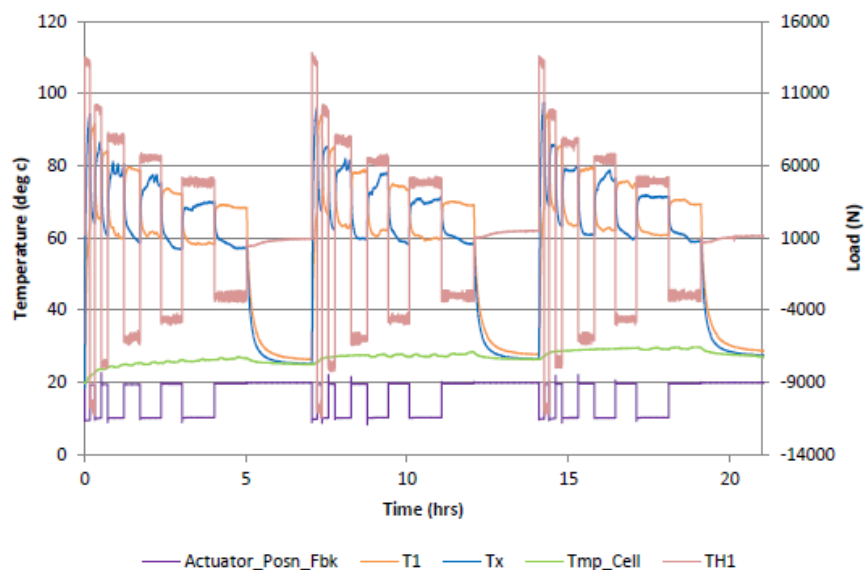


**Figure 72**

Graph showing temperature increase with load application during three blocks of the rig test (original image courtesy of the manufacturer)

Plotting the load and temperature sensor readings showed that the temperature on each side of the bearing increased proportionately to the load magnitude and direction applied. Figure 72 shows the two temperature sensors T1 and Tx and the load being applied TH1.

Towards the end of the test the temperature increase seen each time the load was applied began to increase significantly more than seen at the start of the test, until the torque alarm was triggered, and the test was stopped (Figure 73).

The bearing was removed from the test rig and collected by the AAIB for further investigation by nC<sup>2</sup> at the University of Southampton using the same agreed procedure used for examining the other bearings. The extruded grease was recovered and weighed at 3.3 g. Following initial visual and SEM inspections, the bearing was cut in half, to allow one half to be examined separately by the helicopter manufacturer. Prior to disassembly of the bearing, it was CT scanned. This showed that the cage on the outboard side of the bearing had moved, relative to its intended running location.

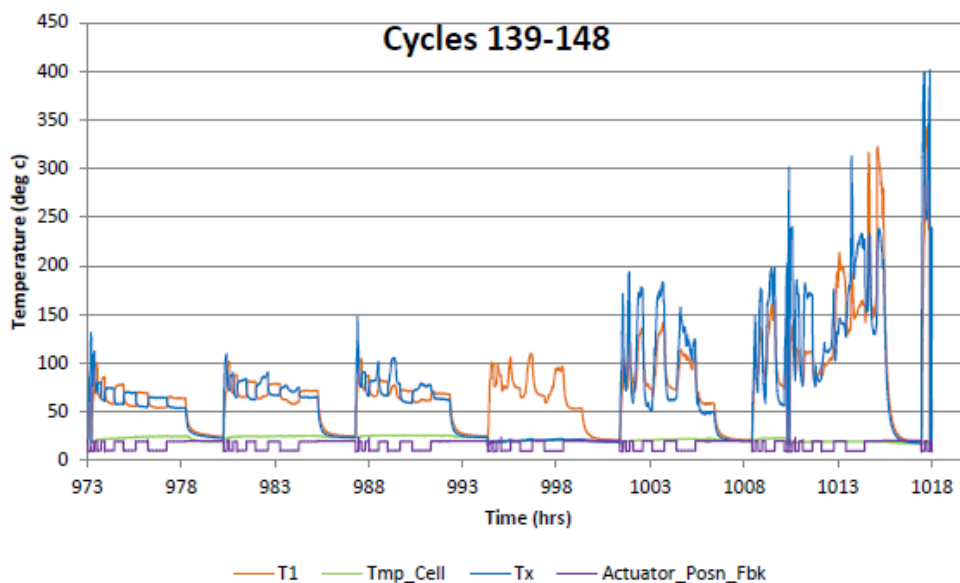


**Figure 73**

Graph showing rise in temperature increase with load application at the end of the test (original image courtesy of the manufacturer)

A groove had been worn in the cage and a lip worn on the race where they were in contact (Figure 74). Large amounts of debris were also seen within the bearing races.

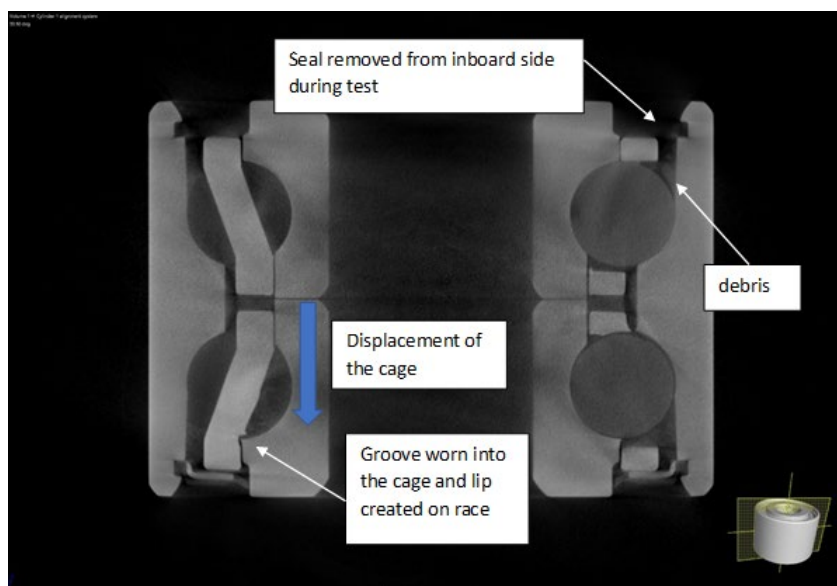


**Figure 74**

CT scan of bearing 16141 showing wear interaction on the outboard cage and race

### *Non-destructive examination*

The inboard side of the bearing, which had operated with the seal removed, was disassembled and inspected. The grease had degraded to the extent that it was black, dry and powdery but it was still present (Figure 75).



**Figure 75**

Condition of the inboard side of the bearing which was operated with the seal removed

The inner race of the inboard side showed discrete areas of macropitting and high temperature induced permanent change in colour (Figure 76).

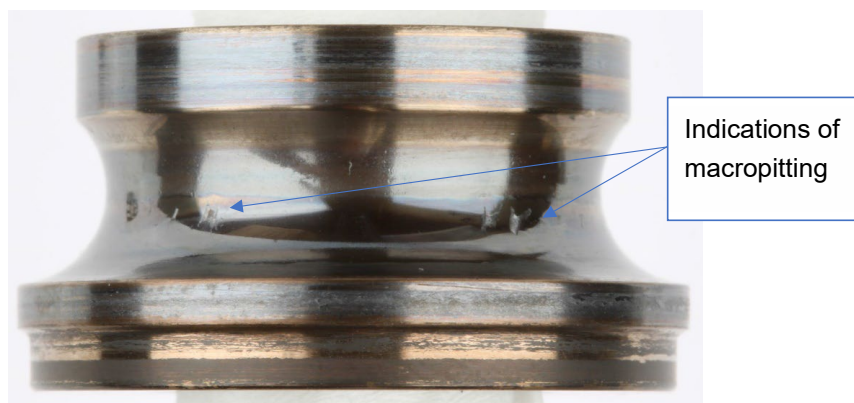


**Figure 76**

Inboard inner race showing discrete areas of macropitting and permanent colour change

The grease on the outboard side was in a similar condition to that of the inboard side (Figure 77).



**Figure 77**

Condition of the outboard side of the bearing operated with the seal in place

The cage could be rotated independently but not separated from the inner race due to the groove and lip worn into the cage and race (Figure 78).

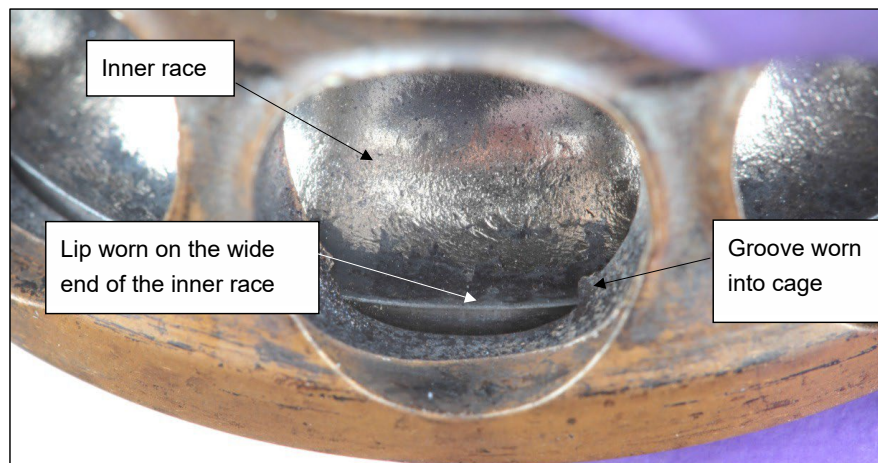


**Figure 78**

Image showing the groove and lip worn into the cage and inner race of the outboard side of the bearing and the damage to the race running surface (post-cleaning)

The race surface of the outboard inner race was more heavily damaged than the inboard side, with the level of damage consistent all around the circumference. The balls from both halves of the bearing were examined

visually and using an SEM. Both sets of balls were found to be surface crazed in a similar way to that seen on the accident bearing. There was no evidence of spalling on the balls.

The cages on both sides of the bearing were also visually inspected using a stereo microscope. On the inboard side (no seal) the pockets were worn in a consistent manner, with more wear on the leading side than the trailing side of the pockets. On the outboard side, the cage pockets were more heavily worn than the inboard side, again with the leading side of each pocket worse than the trailing side. The heaviest wear occurred where the groove had been cut into the cage by the lip on the inner race. This wear feature was also seen to a lesser extent on the accident bearing.

The damage to the outer races mirrored that of the respective inner races, with the inboard side showing individual discrete macropits in the middle of the rolling surface, while the outboard race had consistent surface damage all the way around its circumference and across the width of its running surface.

#### *Destructive examination*

The outer race was sectioned to allow inspection using an SEM. The inboard side displayed growing RCF damage from a series of surface initiated cracks. Copper deposits were also identified on the rolling surface. The outboard side had more extensive micropitting resulting in an undulating surface. Copper transfer was also identified to a greater extent on this surface. Etching and polishing of the sections identified microstructural change below the surface but no DER.

The inner races from both sides of the bearing were also sectioned and inspected using an SEM. The inboard side (no seal) showed discrete micro and macropitting consistent with surface initiated RCF. The cross sections were etched and polished to show a DER was present below the surface of the race (Figure 79), with compression and deformation of the microstructure immediately below the surface. Shallow angle surface initiated cracks were also present.

The outboard inner race sections confirmed surface damage all over, with large amounts of copper transfer. The race showed evidence of heat treatment during the etching process, which was confirmed by the presence of a DER and heat affected zone below the surface. The microstructure also showed evidence of flow lines consistent with plastic deformation. Shallow angle, surface initiated cracks were also present, although these were more closed than seen on the outer race and previous bearings inspected (Figure 80).

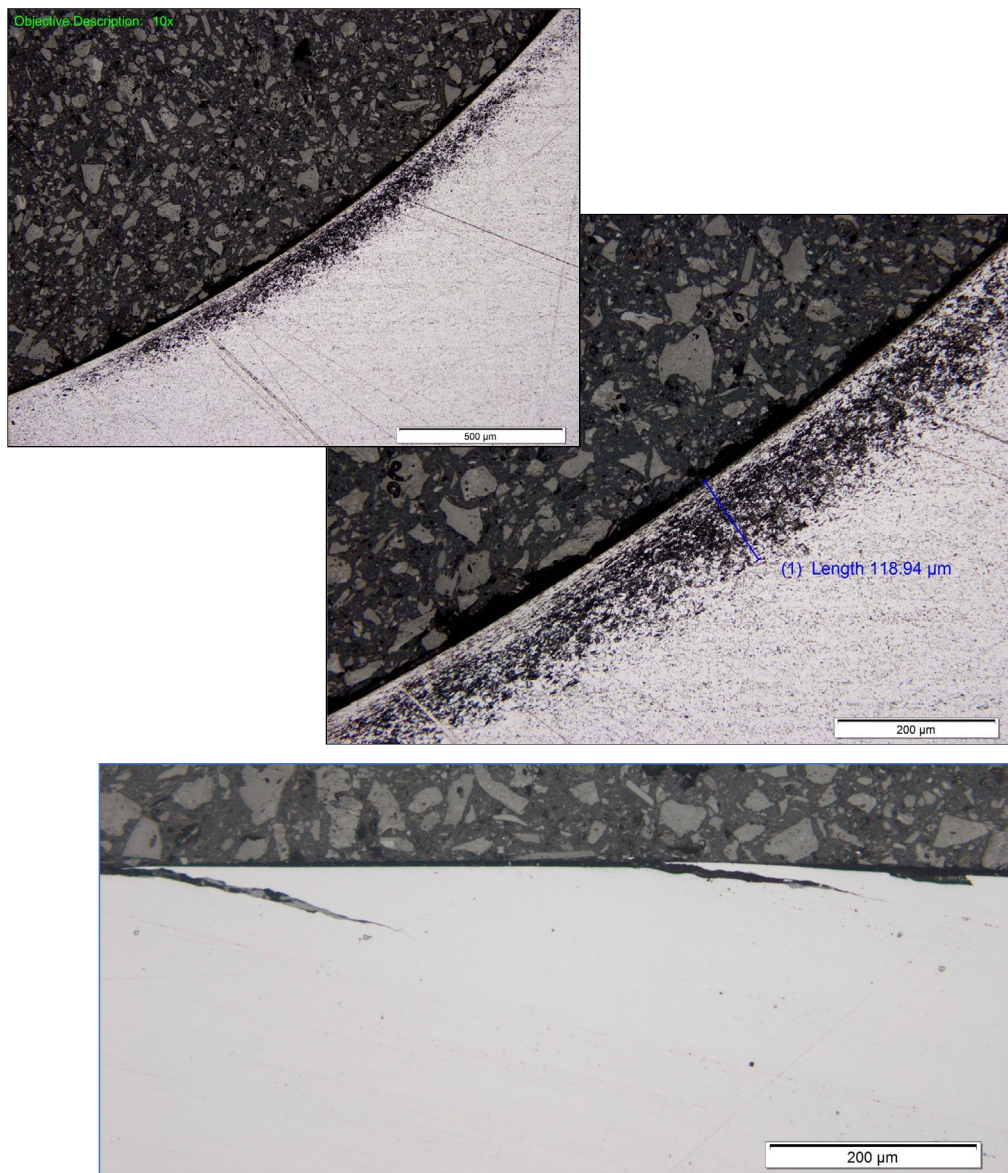


**Figure 79**

DER layer identified on the radial section and surface cracks shown on circumferential section of the inner race, inboard side

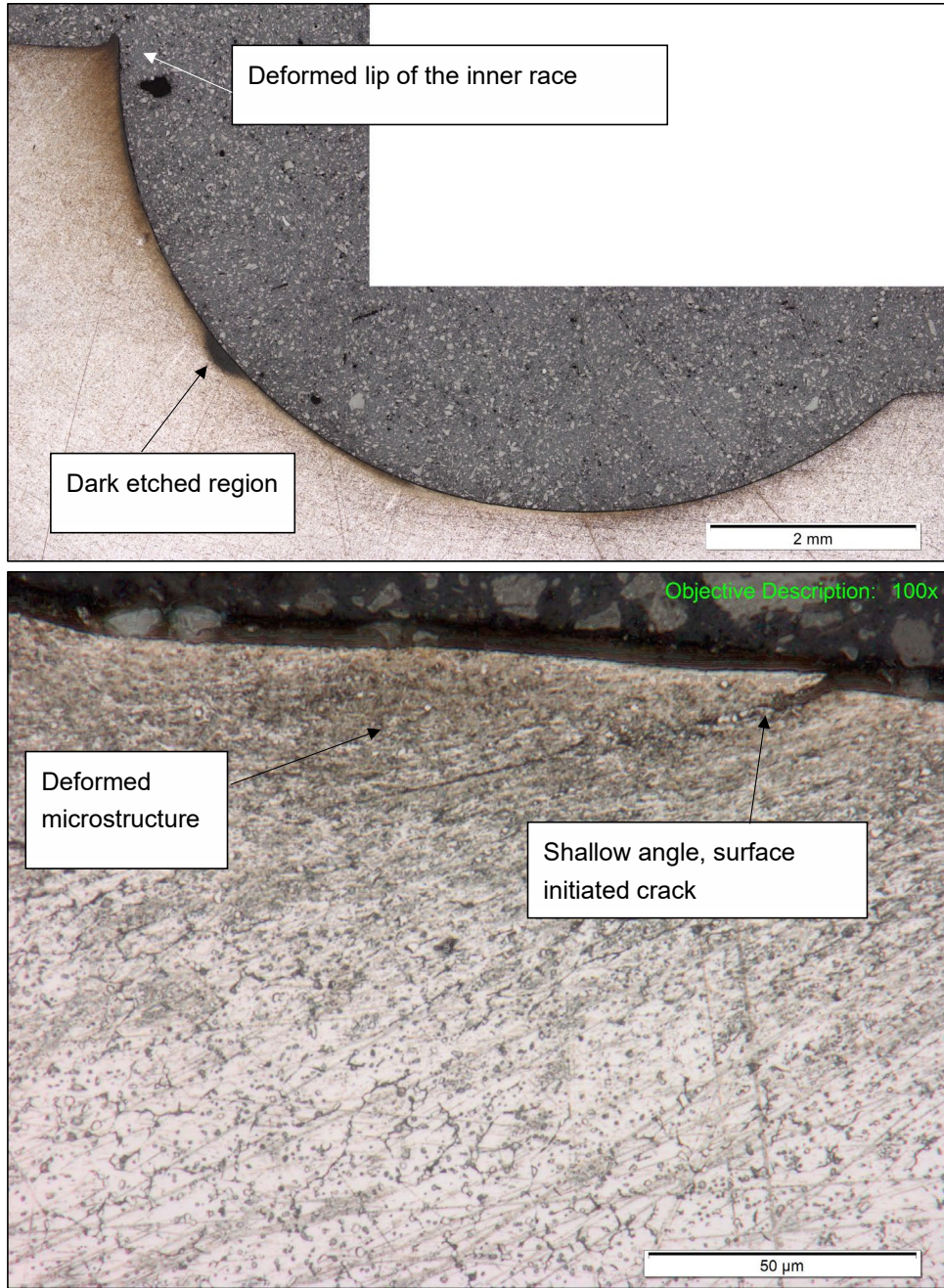


**Figure 80**

Outboard inner race radial section showing DER and circumferential section showing surface initiated crack

#### 1.16.1.4 Review of AW169 flight test and rig test bearing contact pressures

The data recorded during the AW169 flight test load survey<sup>65</sup> for axial load (TH1) and bending moment were requested by the investigation and provided by the helicopter manufacturer. This consisted of over 1,600 individual flight test manoeuvres from 47 test flights. For each manoeuvre the resulting highest (positive and negative) static and oscillating fatigue load, highest (positive and negative) individual static and dynamic load and highest (positive and negative) total load (combined static and dynamic) was provided. For the bending moment data, this was provided for both 'NRL' and 'PRL' at both 'BB1' and 'BB2'. This data was manually referenced and sorted, to match the helicopter flight test variables for the applicable flight test with the resulting axial load and bending moment data for each manoeuvre test point.

The contact pressure between the bearing rolling elements and the inner and outer races is generated by a combination of the bearing preload and the external axial and bending moment loads acting on the bearing. The bearing manufacturer analysed the contact pressure reached for several combinations of the ratio of axial load to bending moment ( $F_a/M$ ) against axial load ( $F_a$ ). This analysis showed contact pressure reached a similar level to the highest value considered in the development spectrum at axial loads above 7,000N, for each of the considered ratios. To prioritise assessment of the flight test points likely to generate the highest contact pressures, the test data was reviewed and the test points which had an axial load greater than 7,000N were selected as an initial cut, resulting in 95 test points of interest.<sup>66</sup>

For these test points, the approximate bending moment at the bearing needed to be calculated from the individual bending moments recorded at 'BB1' and 'BB2'. This was done independently by the investigation using professional beam analysis software. The bending moment and location data for 'BB1' and 'BB2' were input into a calculation, along with the simplified actuator shaft geometry and material properties to estimate the effective 'PRL' and 'NRL' bending moments at the bearing.

This analysis identified a number of bearing bending moments (PRL and/or NRL) which were greater than the largest bending moment considered in the AW169/189 development spectrum of 42.4 Nm<sup>67</sup>, but lower than was considered by the AW139 development spectrum.<sup>68</sup>

65 See [section 1.6.6](#) for a full description.

66 It is possible high contact pressures were also generated in test points with axial loads below 7,000N, but given resource constraints the analysis was targeted at identifying where contact pressures were equal to or exceeded the development spectrum, rather than a comprehensive review of all the test data.

67 See [Table 4](#) for the full development load spectrum. The highest bending moment, axial loads and contact pressures are highlighted in the table.

68 See [Table 1](#) for the AW139 load spectrum, The highest bending moment is highlighted.

This subset of 37 data points was provided to the bearing manufacturer to input into their current and most accurate bearing model simulation tool to assess the resulting contact pressure and  $PV_{max}$ :

Individual bearings are not certified as a discrete component, they are only assessed for suitability within the system application under consideration, in this case the tail rotor control system. PV is a figure which can be used as a guide to the performance demand on a bearing within a specific application. Calculated as the product of contact pressure and bearing velocity ( $P \times V$ ), it can be considered as a relative indication of how much ‘duress’ the bearing is under in different operating conditions, to allow a simple and direct comparison for different load profiles and operating speeds. As the contact pressure varies across the race profile (Figure 87),  $PV_{max}$  is often used to reference the highest PV figure calculated across the profile. However, it is not intended to be used as an absolute threshold for acceptance or rejection of the bearing. The data below is provided solely to allow comparisons between the development spectrum, flight test data and rig test data, with the same region of values highlighted in yellow on each summary graph.

The full results for the 37 flight test data points are provided in [Appendix E](#) but summary graphs are shown below (Figure 81 and 82).

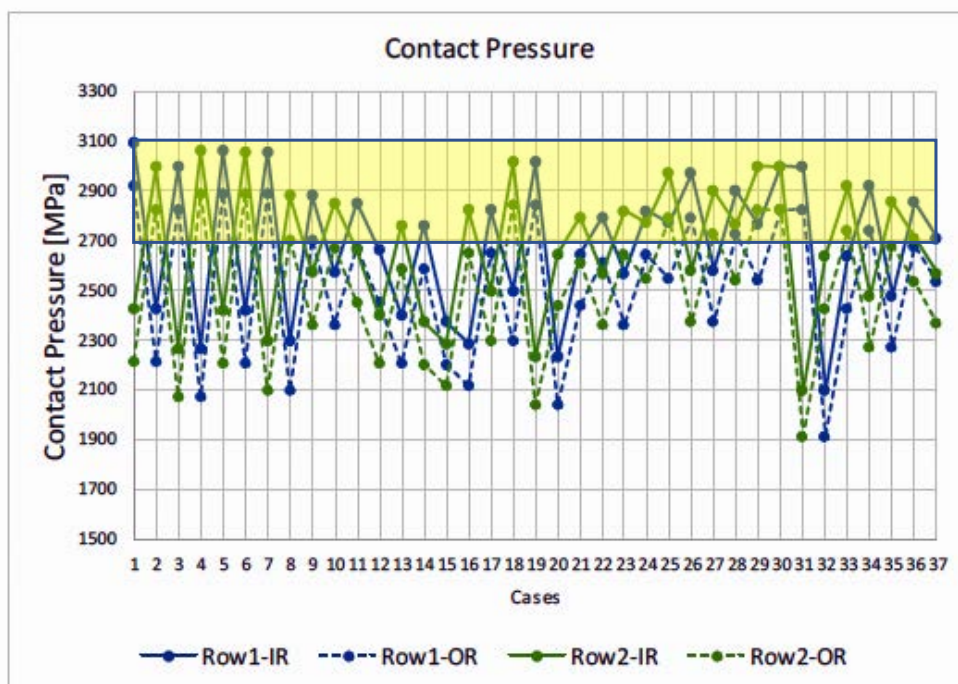


**Figure 81**  
Significant flight test points calculated contact pressures

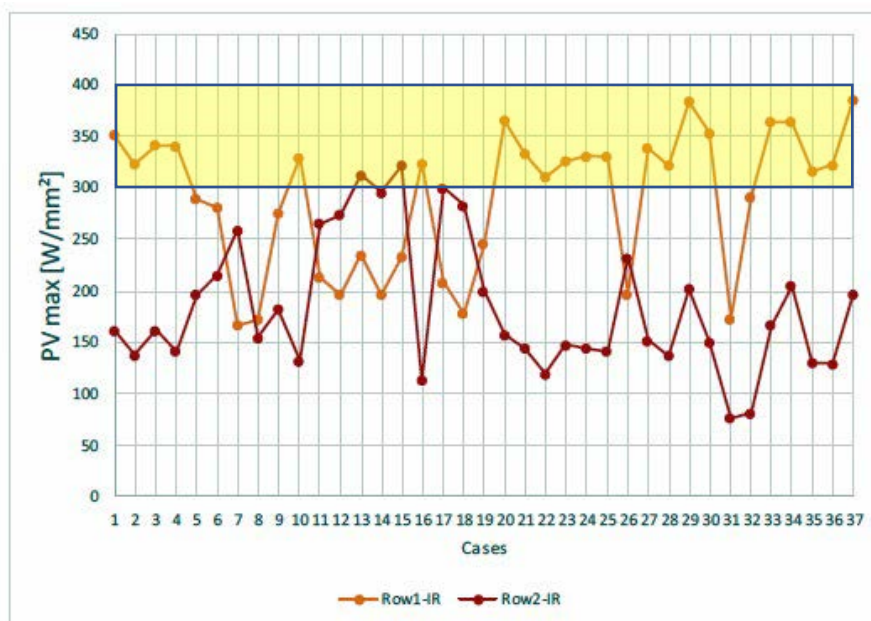


**Figure 82**

Significant flight test points calculated  $PV_{max}$

As a comparison the maximum contact pressure in the bearing certification specification was stated as 3,340 MPa, with a  $PV_{max}$  of 440 on the inner ring for the extreme axial load case of 13,300N FZ (axial load) and 34.4 Nm Bending Moment (Table 4). However, this contact pressure was calculated using the less accurate modelling software available at the time the AW169 was developed.

Reassessment of the contact pressure using the current, more accurate, simulation software gave a revised contact pressure of 3,100 MPa and  $PV_{max}$  of 400 for this load case<sup>69</sup> (the top line of each yellow highlighted box), showing it to be comparable to the highest contact pressures identified in the flight test results, which were achieved with much lower axial loads around 7,000N to 8,000N as shown in Figure 81 and [Appendix E](#).

In order to provide a reference to compare with these figures from flight test, the intended test loads from the last rig test (Table 7) conducted by the helicopter manufacturer were also input into the current bearing model simulation software. This is significant because the rig test demonstrated that the loads applied during the test were sufficient to cause the same deterioration and damage as seen in the accident and other in-service bearings<sup>70</sup>.

<sup>69</sup> Documented in the bearing manufacturer's report TR 11220-22-1 issue C.

<sup>70</sup> See [section 1.16.1.3](#) for detailed description of the test and results.

Cond.	OR Speed [rpm]	Load spectrum for test		
		% Occur.	F <sub>z</sub> [N]	M [N.m]
1	1406	6	14000	42
2	1406	8	10000	42
3	1406	20	7800	42
4	1406	26	6300	42
5	1406	40	4500	42

**Table 7**

Rig test load spectrum

The resulting contact pressures and PV<sub>max</sub> factors were calculated. (Figure 83 and 84).

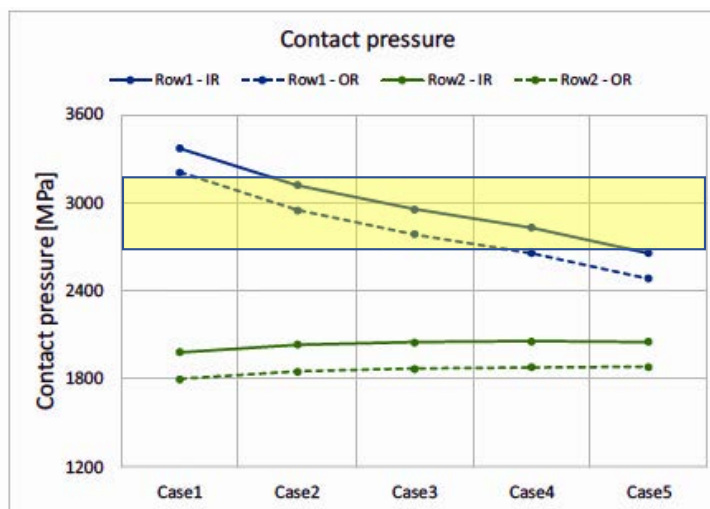


**Figure 83**

Rig test calculated contact pressures

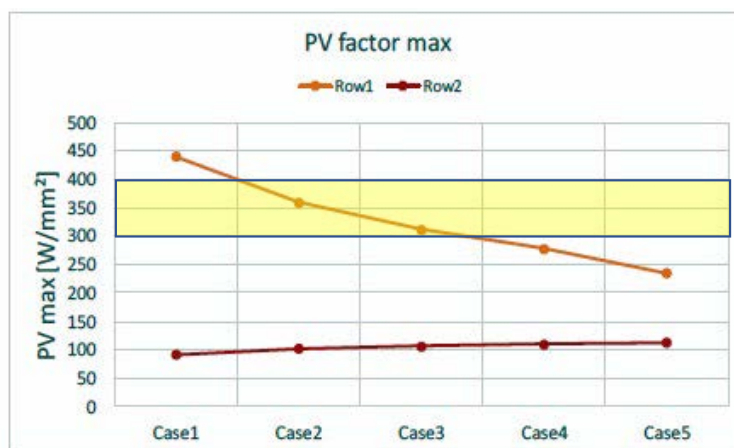


**Figure 84**

Rig test calculated PV<sub>max</sub>

However, as described in [section 1.16.1.3](#) the actual loads applied during the test itself in some cases varied from the planned test point values. In order to give a more accurate assessment of the actual loads used in the rig test, the average for the highest three load cases (positive and negative) was calculated (Table 6 and Table 8) to give a representation of the test as a whole and these were provided to the bearing manufacturer to reassess the contact pressures. The results are presented below (Figures 85 and 86).

Factual Information

	Axial Load (N)	Approx. bearing bending moment NRL (Nm)	Approx. bearing bending moment PRL (Nm)
Case 1	13,834.01	-10.5	-2.25
Case 2	-10,684.6	20.4	-20.6
Case 3	9,703.204	-5.9	-9.5
Case 4	-7,605.67	15.6	-19.6
Case 5	7,956.766	-4.64	-10.4
Case 6	-5,980.96	12.7	-18.1

**Table 8**

Load cases considered by the analysis of averaged test data

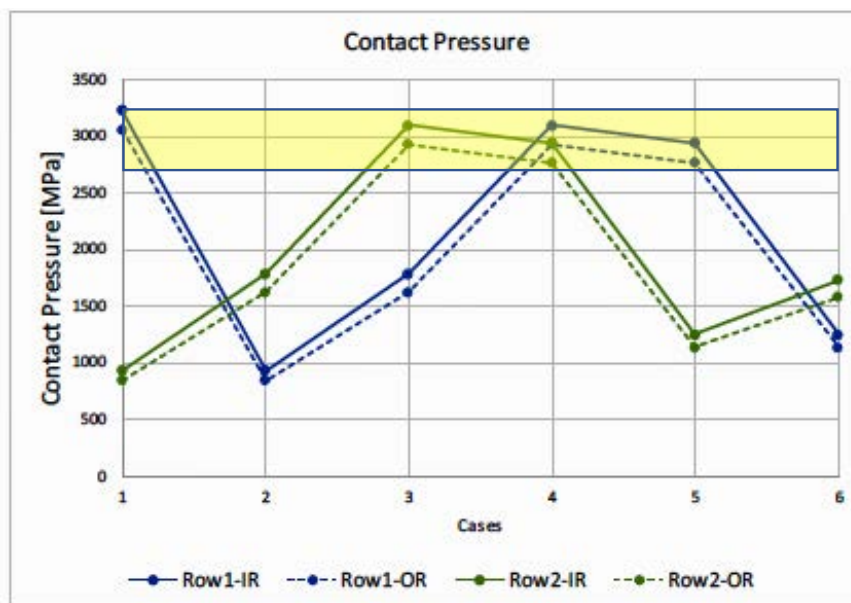


**Figure 85**

Rig test actual contact pressure (averaged data)

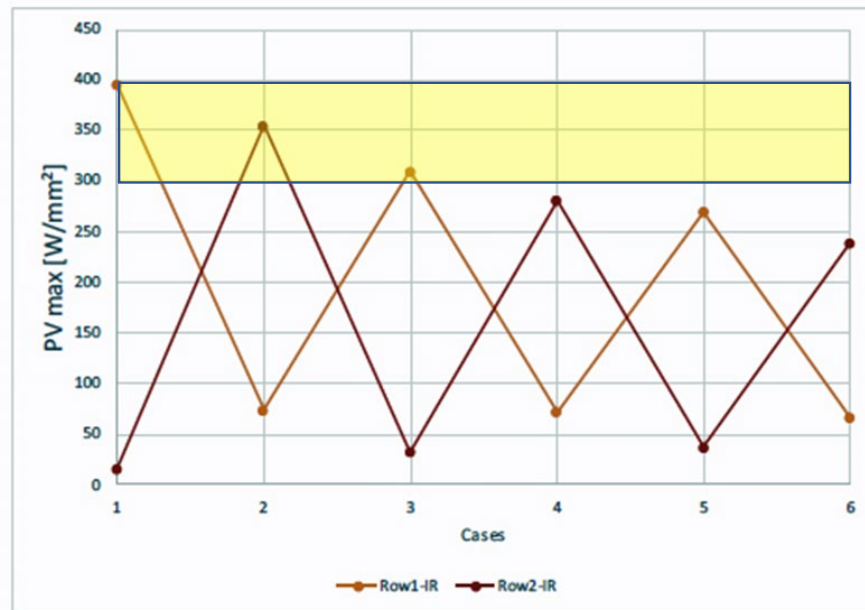


**Figure 86**

Rig test actual  $PV_{max}$  (averaged data)

Again, most of these load cases are comparable with the contact pressures and  $PV_{max}$  calculated for the flight test data group.

None of the contact pressures generated by the actual test load conditions were in excess of the contact pressures considered by the original development load spectrum, as calculated by the standard of bearing modelling software available at that time. However, the highest actual test point contact pressure was higher than the highest contact pressure in the development spectrum after it was reassessed with the latest standard of bearing modelling software now available.

The bearing manufacturer was also able to calculate the pressure and PV distribution relative to the curvature of the inner race (Figure 87).

The graphs and illustration of the inner race profile in Figure 87 show how contact pressure and PV vary across the race profile and where the peak values occur ( $PV_{max}$ ). The location of these peak values correlates closely with where the first evidence of surface initiated rolling contact fatigue appeared on the inner races of bearing s/n 16141 used in the rig test, shown in Figures 76, 79 and 80<sup>71</sup>. And the inner races of bearing s/n 14134 which was removed from service, shown in Figures 46 and 50<sup>72</sup>.

71 See [section 1.16.1.3](#) for a full description of the bearing condition.

72 See [section 1.12.5](#) for a full description of the bearing condition.

The significance of this data comparison is explained further in the analysis [section 2.9.3](#) - Review of flight and rig test data.

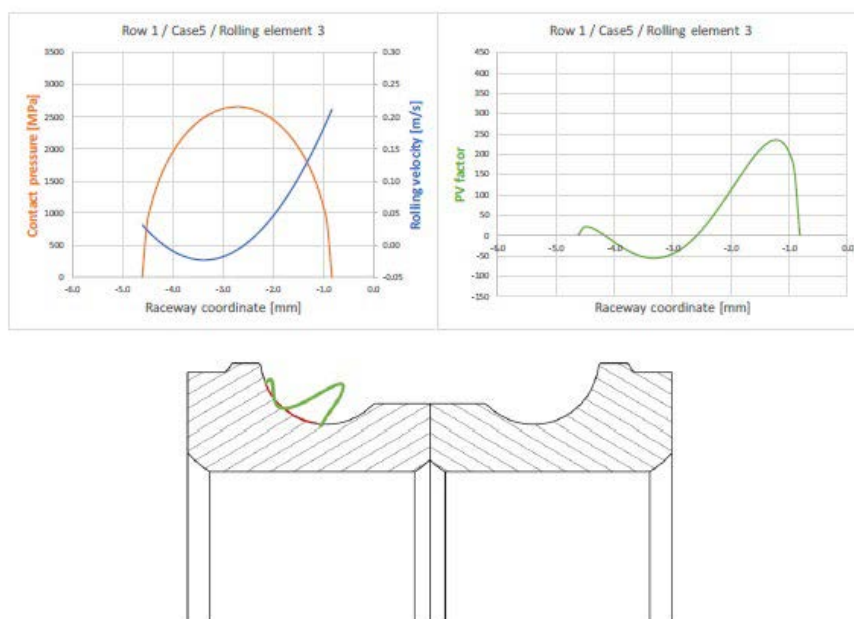


**Figure 87**

PV distribution relative to the inner race curvature

### 1.16.2 Impact assessment

The helicopter manufacturer carried out an assessment of the deceleration loads experienced during the impact sequence using recorded and calculated data provided by the AAIB. The assessment considered the loads on the helicopter's structure in the region of the fuel tanks and rear row of passenger seats. It also considered the possible differences had the helicopter's landing gear been extended.

The assessment identified that with the landing gear extended, there was no significant decrease in the forces transmitted through the helicopter's structure. The manufacturer stated that this was because the calculated rate of deceleration and the forces involved exceeded the landing gear's ability to react, deform and dissipate the impact energy.

In reality the impact sequence was highly dynamic, but in order to estimate the deceleration loads, based on an analysis of recorded data, the assessment determined that the helicopter initially struck the ground with  $19.77^\circ$  of nose up pitch and  $29.88^\circ$  of left roll (Figure 88).

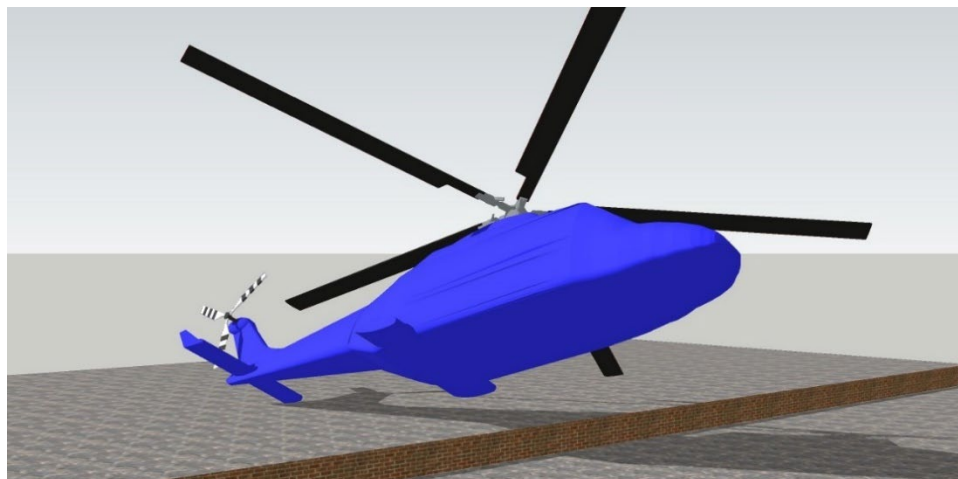


**Figure 88**

Illustration of initial impact attitude

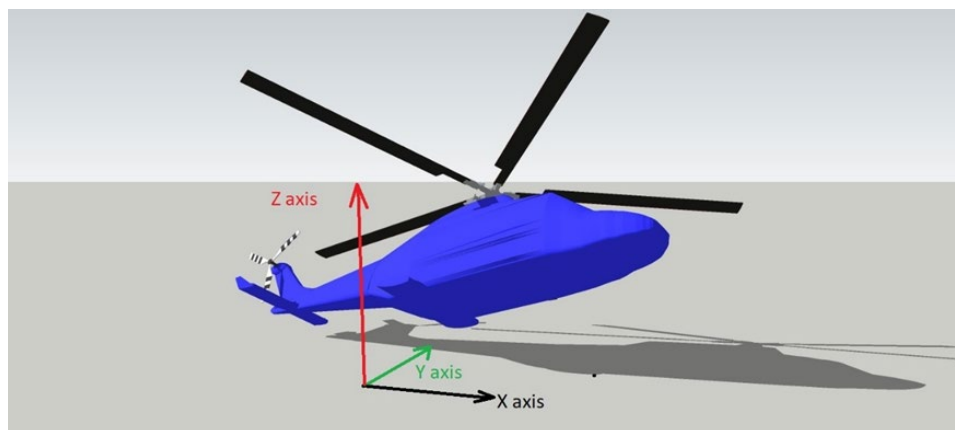
The deceleration loads were then calculated at three points, A1, A2 and A3 (Figure 89).



**Figure 89**

Impact load calculation positions  
(original image courtesy of the manufacturer)

The maximum and minimum accelerations in the vertical (Z), lateral (Y) and horizontal (X) axes and the time they occurred after the initial impact were calculated (Figure 90 and Table 9). These indicated that G-VSKP had probably been subjected to loads which exceeded its design limits. The helicopter's attitude and the highly dynamic nature of the impact and subsequent loads meant that it was not possible to determine the absolute margin by which the design limits were exceeded.

**Figure 90**

Axis convention used for impact assessment calculation

Position		X Axis	Y Axis	Z Axis
A1	Maximum	+48.05g @ 0.03s	+31.57g @ 0.027s	+32.871g @ 0.028s
	Minimum	-46.18g @ 0.026s	-40.14g @ 0.029s	-41.87g @ 0.0314s
A2	Maximum	+29.25g @ 0.022s	35.81g @ 0.31s	+46.08g @ 0.0265s
	Minimum	-29.36g @ 0.024s	-30.31g @ 0.0325s	-41.76g @ 0.023s
A3	Maximum	+73.99g @ 0.0315s	152.39g @ 0.0294s	+86.85g @ 0.0239s
	Minimum	-92.11g @ 0.018s	-33.72g @ 0.0205s	-122.3g @ 0.0279s

**Table 9**

Calculated maximum and minimum impact accelerations

The simulation showed that the impact with the step would result in localised crushing of the lower fuselage and significant damage to the fuel tank supporting structure, with elements of damaged structure being driven into the space occupied by the fuel tank bladders causing numerous penetrations of the bladders. This was consistent with the damage observed during the examination of the helicopter wreckage.

### 1.16.3 Flight simulator trials

The investigation team used the manufacturer's flight simulator facilities to investigate the symptoms of the control failure experienced by G-VSKP. The trials were also an opportunity to gain an understanding of what cues might have been available to the pilot and what challenges he faced in recognising and responding to the emergency. During these trials the investigation used a variety of flight and response parameters to explore their effect on scenario outcomes.

The trials revealed that G-VSKP experienced a divergent and disorientating failure with no system-generated cues to alert the pilot to its nature. Despite the pilot's application of full left pedal to counter the uncommanded rotation, the helicopter continued yawing right. With nose-down pitch and right bank applied at the time of failure, the helicopter quickly diverged in all three axes. In the trials, even with the collective lever fully lowered within one second of the failure, the remaining torque imbalance resulted in peak yaw rates exceeding 100°/s. The trials indicated that in the time and height available to the accident pilot it was not possible to regain positive control of the helicopter's trajectory.

While primarily exploring post-failure controllability factors, a secondary aim of the trials was to compare a standard Cat A profile with that of the accident flight. The observed 600-700 ft/min average rate of climb on the accident flight required a higher main rotor torque setting than would have been needed for a 300 ft/min climb. For similar collective lever intervention times, while peak yaw rates and aircraft instability were slightly elevated at the higher torque setting, the trials indicated this did not significantly influence the post-failure controllability of the helicopter.

A detailed account of the flight simulator trials is included at [Appendix B](#).

#### 1.16.4 Manufacturer's additional flight mechanics analysis

The manufacturer performed additional flight mechanics analysis using flightlab software in order to consider if a different control input sequence after the failure could have enabled a lower vertical speed at impact. The details provided by the manufacturer are included in [Appendix J](#). The simulation followed the event up to the instant of failure using the FDR data. Immediately after the failure the control logic simulated inputs to limit the pitch and roll motions, and 1.5 seconds<sup>73,74</sup> after the failure, the collective lever was fully lowered. The collective lever was fully raised at a simulated height of approximately 100 ft. When the collective lever was lowered, cyclic control inputs to minimise pitch and roll motions continued. The engines were not shut down. The analysis plots provided by the manufacturer do not show any of the simulated lateral motion of the helicopter. The manufacturer concluded from this analysis that it was possible to:

73 According to FAA Advisory Circular 29-2C (AC 29-2C) Annex B *Airworthiness Guidance for Rotorcraft Instrument Flight*, 1.5s is the suggested pilot response time that may be used during testing of automatic flight guidance and control systems for an 'attentive-hands-on' phase of flight. Available at AC 29-2C with changes 1-8 (faa.gov) [accessed 5 May 2023].

74 The FAA stated that the AC 29-2C 'response,' or 'delay' times, are used solely for flight test demonstration of compliance and had been harmonised with other regulatory authorities, including the EASA and that they are meant to serve as a mechanism for test pilots to conduct evaluations.

- Limit the yaw rate and maintain pitch and roll attitudes within manageable limits.
- Avoid the disengagement of the AFCS and thus maintain at least the basic stabilisation along the entire event (by avoiding the saturation of the yaw rate channel above 128°/s).
- Decrease the rate of descent at impact to values around 1950 ft/min.

## 1.17 Organisational and management information

### 1.17.1 Requirements for non-commercial operations with complex aircraft

European Union Commission Regulation No. 965/2012<sup>75</sup>, including its subsequent amendments, regulates the operation of aircraft subject to the EASA regulatory framework. Specifically, Annex VI (Part-NCC) of that regulation applies to non-commercial operations with complex motor-powered aircraft.

#### 1.17.1.1 Complex helicopters

Under the EASA regulatory framework, a helicopter is considered complex if it is certificated:

- for a maximum takeoff mass exceeding 3,175 kg, or
- for a maximum passenger seating configuration of more than nine, or
- for operation with a minimum crew of at least two pilots.

G-VSKP was considered a complex helicopter because its maximum takeoff mass exceeded 3,175 kg and it was certificated for a maximum of 11 passengers.

#### 1.17.1.2 Part-NCC Operator requirements

Part-NCC requires operators of complex aircraft to adhere to the same essential requirements as commercial air transport operators but the rules are proportionate - instead of holding an Air Operator's Certificate, operators must submit a declaration to the member state's competent authority<sup>76</sup> about their operation.

<sup>75</sup> Commission Regulation (EU) No 965/2012 ('Air Operations Regulation'). Available at <https://www.easa.europa.eu/document-library/regulations/commission-regulation-eu-no-9652012> [accessed 28 July 2023].

<sup>76</sup> UK CAA for aircraft registered and/or operated from within the UK.

NCC operators need to comply with the Air Operations Regulation, in particular the detailed requirements in its Annex III (Part-ORO - Organisation Requirements) and Annex VI (Part-NCC), and their pilots must hold a valid licence in accordance with Commission Regulation (EU) No 1178/2011 laying down requirements on aircrew licensing. NCC operators are further required to:

- have an Operations Manual,
- have a management system corresponding to the size of the operator and the nature and complexity of its activities,
- have an approved Minimum Equipment List for each aircraft,
- complete and submit a declaration to the competent authority, detailing the aircraft type, operational and continued airworthiness requirements and any approvals held, and
- ensure that the pilot(s) flying the aircraft hold(s) a Part-FCL licence issued under Commission Regulation (EU) No 1178/2011.

The operator of G-VSKP was compliant with these requirements and had added G-VSKP to their Part-NCC declaration to the CAA with effect from 13 October 2017.

The helicopter was not operating with an active Flight Data Monitoring<sup>77</sup> system and, under Part-NCC regulations, it was not required to.

#### 1.17.2 Congested area operations

The LCFC training ground and King Power Stadium were within an area designated as a congested area and special permission was required to fly into them. The aircraft operator had been granted delegated authority from the CAA to conduct congested area take offs and landing in accordance with procedures set out in their operations manual which included the requirement to conduct a site survey to establish that safe operations were achievable.

The two landing sites in Leicester had been surveyed in accordance with the requirement, thereby providing pilots of G-VSKP with the appropriate permission to operate into the sites. A requirement of the congested area permission for G-VSKP was that operations at these sites were to comply with Cat A profiles to mitigate the risk of engine failures during takeoff and landing.

<sup>77</sup> A system used to monitor aircraft operations, capturing flight parameters in a similar way to accident data recorders. System thresholds can be set for a given flight profile. Should a flight deviate beyond expected parameters the system would alert the operator, thus prompting a review of the flight.

### 1.17.3 Operational oversight

Data from G-VSKP's previous flights from the stadium showed that the rate of climb had exceeded 300 ft/min and turns had been commenced below  $V_Y$  on previous occasions. It was not possible to establish the reason for the rate of climb exceedances or what prompted turns below  $V_Y$ .

For NCC operations, individual owners and operators must conduct an appropriate level of ongoing operational oversight. G-VSKP's operator's operations manual stipulated that surveyed landing sites, such as the King Power Stadium, should be '*re-surveyed at intervals of not more than 12 months.*' The investigation found evidence that the site had been resurveyed by the pilot within the preceding 12 months.

Pilots using the operator's congested area permissions framework were required to submit an after-flight report each time they operated into surveyed sites. G-VSKP's pilot had complied with this requirement.

Data from the CAA indicated that there were in excess of 780 helicopters<sup>78</sup>, of many different types, in the UK onshore sector. Most of these were introduced under legacy, rather than EASA, certification standards. Most helicopters currently operating in the UK are not equipped with FDM systems. The diverse nature and scope of onshore helicopter operations poses a challenge for the development of FDM algorithms which rely on detecting operational parameters that are outliers when compared with a 'normal' flight profile.

As part of their NCC oversight strategy the CAA had initiated a 4-year rolling programme of operator audits in compliance with Part-ARO<sup>79</sup> requirements for the oversight of declared organisations.

## 1.18 Additional information

### 1.18.1 AW109 Cat A profile

A witness, with experience of flying Cat A profiles on both the AW169 and AW109 types, suggested to the investigation that the pilot's greater familiarity with the AW109 helicopter could explain the relatively high rate of climb seen during the stadium departure. The equivalent Cat A profile for the AW109 required a climb at  $500\pm 100$  ft/min.

<sup>78</sup> CAA presentation to the RAeS Onshore Helicopter Symposium, Hamilton Place, London, July 2019.

<sup>79</sup> EASA Part-ARO - Authority for Air Operations. Available at <https://www.easa.europa.eu/acceptable-means-compliance-and-guidance-material-group/part-aro-authority-requirements-air> (accessed 28 July 2023)

### 1.18.2 Reported drone sightings

Several witnesses came forward to report “drone” activity around the stadium after the match.

Leicestershire Police operate a Small Unmanned Surveillance Aircraft (SUSA) which is employed for crowd surveillance and intelligence gathering on match days. The SUSA was airborne at the end of the match. Activity is coordinated by a tactical controller located with the Silver Commander in the stadium’s match-day operations room.

All the witness reports of drone activity correlated with known police SUSA operations after the end of the football match. The police aircraft was on the ground when G-VSKP arrived into the stadium and its operations had finished by the time the helicopter departed. There were no reported drone sightings during the period that G-VSKP was airborne on the accident flight.

### 1.18.3 Research regarding pilot response to helicopter tail rotor emergencies

As part of a trial undertaken on behalf of the CAA and published in 1997<sup>80</sup>, pilot response time<sup>81</sup> to tail rotor drive failures was measured during routine training sorties with civil pilots in an Aérospatiale Super Puma simulator. The failure was injected during level flight at 2,000 ft and the first cue available to the pilots was yaw to the left of approximately 80°/s. This research was considered relevant because the failure symptoms and the required pilot response were similar to the accident circumstances. The study report does not detail the terrain below the helicopter when the failure was injected. The study defined ‘detection time’ as the time between the onset of the failure and the initiation of a response using the collective lever. Yaw pedal response was not reported. Data on detection time was collected from 35 pilots who were not expecting the failure. It ranged from 0.58 s to 3.21 s and the mean was 1.53 s. The study also collected ‘total reaction time’ which was defined as the time between the initiation of the failure and the completion of lowering the collective. Total reaction times ranged from 3.26 s to 8.26 s and the mean was 4.9 s.

80 Chappelow, J.W. and Smith, P.R. (1997). *Pilot Intervention Times in Helicopter Emergencies: Final report*. PLSD/CHS/HS3/CR97020/1.0. DERA

81 The time taken to detect an event, identify what it is, decide on a response and execute that response. In the case of this research, the time between the onset of the yaw which was the first symptom of the failure and the time when the collective reached the minimum point.

#### 1.18.4 Startle and surprise

Startle is a *'brief, fast and highly physiological reaction to a sudden, intense or threatening stimulus'*<sup>82</sup>. A startle response occurs immediately in response to a startling stimulus and can impair pilot responses for a short period of time, usually between 0.3 and 1.5 s<sup>83</sup>.

Surprise is: *'an emotional and cognitive response to unexpected events that are (momentarily) difficult to explain, forcing a person to change his or her understanding of the problem.'* Surprise often follows a startle response if the cause of the stimulus that triggered the startle is not understood. Experimental studies looking at the effects of surprise on the flight deck have shown for example, delayed initiation of responses<sup>84</sup> and incorrect or incomplete application of procedures<sup>85</sup>.

#### 1.18.5 Critical Part

Critical parts are defined by CS 29.602 as:

*'A critical part is a part, the failure of which could have a catastrophic effect upon the rotorcraft, and for which critical characteristics have been identified which must be controlled to ensure the required level of integrity.'*

Critical parts are identified by the manufacturer through conducting a Preliminary System Safety Assessment, typically using Functional Hazard Analysis (FHA) and Failure Modes and Effects Analysis (FMEA) techniques. These techniques attempt to anticipate all the ways in which a system may fail in operation, the probability of failure occurrence and the severity of the effect of the failure. Catastrophic failure for the TRA was defined in the FMEA as resulting in the loss of the helicopter, the death of multiple occupants or the death or incapacitation of the flight crew. The current definition in CS AMC 29.1309 is any failure that prevents the continued safe flight and landing of the rotorcraft.

82 Landman, A., Groen, E.L., van Passen, M.M. Bronkhorst, A. & Mulder, M. (2017) 'Dealing with unexpected events on the flight deck: A conceptual model of startle and surprise' in Human Factors, Vol 59 pp 1161-1172.

83 Martin, W., Murray, P. & Bates, P. (2012) 'The effects of startle of pilots during critical events: a case study analysis' Proceedings of 30<sup>th</sup> EAPP Conference: Aviation Psychology & Applied Human Factors – working towards zero accidents.

84 Martin, W.L., Murray, P.S., Bates, P.R., & Lee, P.S. (2016) 'A flight simulator study of the impairment effects of startle on pilots during unexpected critical events.' Aviation Psychology and Applied Human Factors, Vol 6, pp24-32

85 Casner, S.M., Geven, R.W. & Williams, K.T. (2013) 'the effectiveness of airline pilot training for abnormal events.' Human Factors, Vol 55, pp-477-485.

### 1.18.6 Rolling Contact Fatigue (RCF)<sup>86</sup>

RCF is a type of surface damage that results from repeated rolling or rolling and sliding contact between curved surfaces, typically the race and ball in a bearing. RCF can be considered comparable to conventional material fatigue to the extent that it results from alternating stress action, in the case of bearings this is referred to as contact or Hertz<sup>87</sup> stress. Contact stress comes from the forces acting on the rolling elements of the bearing pushing them onto the race surface. This results in an area of material conformity (deformation), which creates a small contact area or 'footprint' to produce a contact pressure on the race. For deep groove ball bearings this contact area is typically an ellipse shape.

Over the lifetime of the bearing RCF will result in cracks forming in the race material, which then propagate and due to repeated contact stress will result in material loss.

This is typically characterised by cracks which initiate in a region of higher stress at a subsurface level and grow upwards towards the surface (Figure 91).

Bearings operating with adequate lubrication, a correct operating temperature, a suitable load level and contact points with pure rolling motion (rather than sliding) will eventually fail due to RCF given enough time. The life of a rolling bearing is defined as the number of revolutions the bearing can perform before incipient macropitting (material loss) occurs. The life is referred to as the  $L_{10}$  life, because it is a statistical prediction that gives a 90% reliability that similar bearings will achieve the same number of revolutions given the same operating conditions. However, RCF can also result in the premature failure of the bearing under less than optimum conditions.

Macropitting is macroscale damage often described as pitting, initial pitting, destructive pitting, flaking, spalling, scabbing and fatigue wear. It results from the subsurface growth of fatigue cracks, which may have a surface or subsurface origin and have a distinctive appearance. Fully developed macropits (with a diameter much larger than their depth) show discrete walls and a floor that intersects the surface at a steep or shallow angle depending on whether they initiate at the surface (shallow  $\leq 30^\circ$ ) or subsurface (steep  $\geq 40^\circ$ ) (Figure 92).

86 This section includes paraphrased and condensed extracts and figures 90 and 91 from the publication 'Rolling Contact Fatigue – Review and Case study' by Dr N Symonds. British Crown Copyright 2004/ MOD.

87 The analytical method of determining the contact stresses for two non-conforming objects was developed by Heinrich Hertz in 1882.

Factual Information

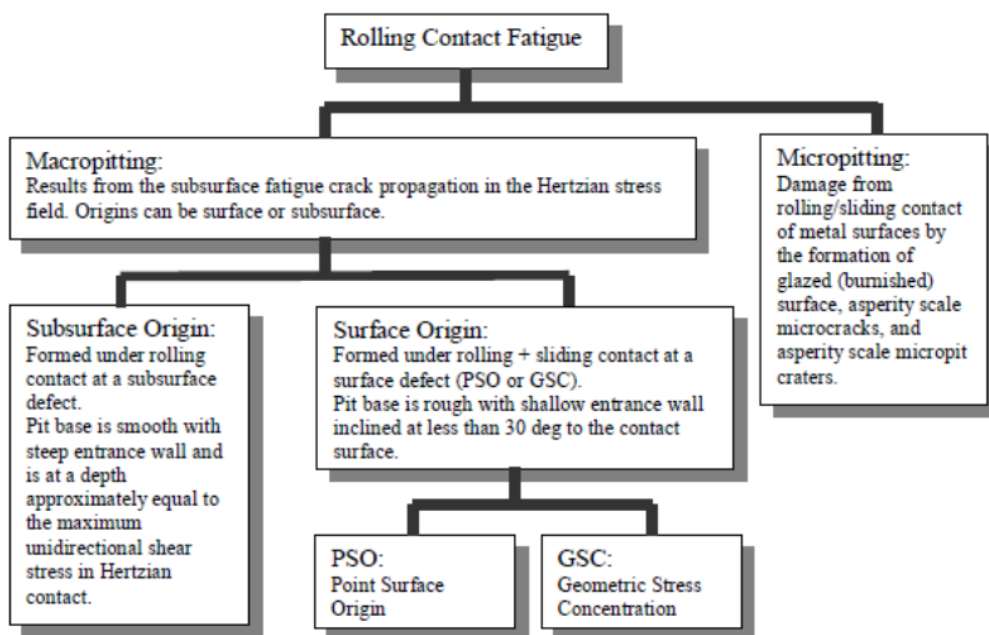


**Figure 91**  
RCF, key features and divisions

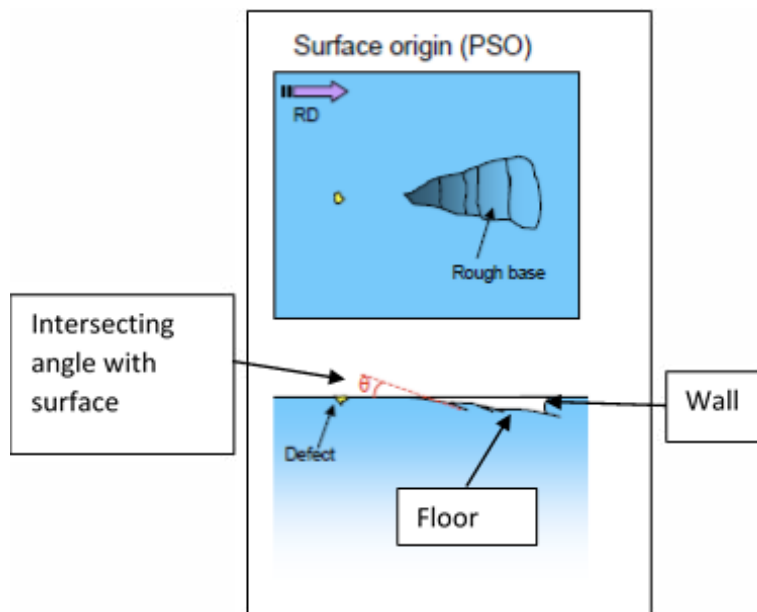


**Figure 92**  
Illustration of typical surface origin macropitting

The bearing races are also subject to forces acting in a plane which is parallel to the race surface and perpendicular to the forces pushing the rolling elements into the race. The stress generated in the race material by these forces is called shear stress. The position of maximum shear stress is normally located just

below the surface at Hertzian depths. Sliding (rather than rolling) balls can significantly alter the stress distribution in the surface and near-surface material of a bearing race. As the tangential forces and thermal gradient caused by friction from a sliding ball increase the magnitude of the alternating shear stress, it moves nearer to the ball/race contact area causing premature crack initiation to occur at the surface and the crack to extend downwards into the material. Once surface macropitting has initiated, the bearing becomes noisy and rough running. If allowed to continue to operate, catastrophic failure of the bearing will follow.

Maintaining adequate lubricant to prevent sliding is an important aspect of avoiding premature failure.

In a rolling bearing, such as the tail rotor duplex bearing, the balls and bearing races are nonconforming<sup>88</sup>. Consequently, the bearing load is concentrated where the ball and race come into contact. Under these pressures the balls and race elastically deform so that their surfaces conform to each other over a very small area creating the conditions for elastohydrodynamic lubrication (EHL). In a ceramic hybrid bearing, the extreme hardness of the ceramic balls means they conform less than a conventional steel ball bearing, resulting in a smaller contact area and higher contact pressures.

#### 1.18.7 Grease lubrication<sup>89</sup>

Grease is formed from a base oil, mixed with a thickener. The grease used in the tail rotor bearing is Aeroshell Grease 22, which is a clay-based grease with a synthetic hydrocarbon base oil. Other additives can be used in grease manufacture depending on the application, for example antioxidants, which extend the life of the grease, and others to reduce operating friction and improve load carrying. AeroShell Grease 22 is formulated and approved to meet US Military specifications MIL PRF 81322G and MIL PRF 24508B. The grease change process is strictly managed and the grease is subject to regular performance review to maintain its Qualified Product Listing on the US Military Approval Portal (QPD - Qualified Products Database (dla.mil)).

---

88 A nonconforming contact is one in which the shapes of the bodies are dissimilar so that under zero load they only touch at a point.

89 Adapted from Grease Lubrication in Rolling Bearings – Piet M. Lugt. and the SKF Evolution magazine article *Grease lubrication mechanisms in rolling bearing systems* (skf.com)

### *Phases in grease lubrication*

Grease lubrication is a dynamic process that can be divided approximately into three phases.

The duplex bearing used in the tail rotor is fully filled at manufacture, so the grease is located between the rolling elements. Once in operation, this leads to high churning losses during start-up or running-in and can result in excess grease being pushed past the bearing seals to form a grease 'collar' around the outside of the bearing face. During this phase, called the churning phase, the grease will be pushed from the races into the unswept volume of the bearing (onto the seals or the bearing race shoulders) or will end up attached to the cage. This phase can last up to 24 hours of operation and is characterised by higher friction, leading to increased operating temperatures and, as the churning phase progresses, potentially some degradation of the lubricant which is retained on the races.

In the second phase, known as the bleeding phase, the bearing reaches a steady state, with the reservoirs of grease in these non-race locations slowly providing the races with lubricant either by bleeding oil from the grease thickener or by shear<sup>90</sup>. The lubricating films on the bearing races are governed by a feed and loss mechanism in which they are fed by grease from the reservoirs but also lose lubricant due to side flow from the contact between the ball and the race and due to oxidation. This may lead to lubricant starvation, especially in sealed bearings where the grease reservoirs are smaller. Another feed mechanism is occasional replenishment caused by softening of the grease close to the ball/race contact due to local heat development, resulting from occasional film breakdown.

At some point, the reservoirs will be empty or deteriorated to the point that replenishment can no longer happen. This is the final phase, resulting in severe film breakdown, called the end of grease life, which subsequently leads to bearing damage and failure.

### *Grease reservoir formation*

The rate at which the reservoir formation will take place is governed by the flow properties of the grease, also called its rheological properties. This will also determine the physical degradation of the grease.

Lubricating grease shows visco-elastic behaviour, meaning that the viscosity of the grease is a function of both shear and shear rate. The viscosity is very high at low shear rates. This means that the resistance to flow will be very high

---

<sup>90</sup> The mechanical action of two surfaces moving parallel to each other.

if the grease is not touched – ie when it is located in the unswept volume. This is termed the consistency of the grease. During the churning phase the grease may lose some of its consistency. The extent to which this occurs is called the mechanical stability of the grease.

The viscosity of lubricating grease is so high at very low shear rates that only creep flow will occur, and the grease has an apparently solid behaviour. The opposite of this is shear thinning, which is when the grease viscosity decreases substantially with increasing rates of shear.

At very high shear rates the grease viscosity may approach the base oil viscosity. Such high shear rates occur in the lubricating films between rolling elements and races. Together with oil bleeding, this is the reason why the film thickness in grease-lubricated bearings is usually calculated using the base oil viscosity ( $\eta_{oil}$ ).

#### *Film thickness*

A lubricating grease will only provide a long bearing service life if a sufficiently thick film is developed, separating the rolling elements (balls) from the races. Both base oil and thickener are known to enter the bearing race. The lubricating film thickness in grease-lubricated bearings is determined by boundary layers formed by thickener material ( $h_R$ ) and by the hydrodynamic action of the base oil ( $h_{EHL}$ ) (elastohydrodynamic lubrication). The film thickness ( $h_T$ ) is therefore:

$$h_T = h_R + h_{EHL}$$

Grease-lubricated bearings often run under so-called starved lubrication conditions where only very thin layers of oil are available and where the film thickness is primarily a function of the thickness of these oil layers. The change in thickness of these layers is caused by the difference between the feed and loss flow rates of lubricant into or out of the raceways. The oil on the race rolling surface is lost due to the transverse flow caused by the high contact pressure between the balls and the race. Some replenishment may take place by creep flow and oil bleeding but this will be a very slow process. Shear from the relative rotation of the cage and race and drag due to the balls spinning as well as rolling, will probably have a greater effect in drawing in fresh grease from the reservoirs. At higher temperatures oxidation and evaporation will also have an impact on the film thickness resulting in lubricant being lost. Higher temperatures will also change the viscosity and lubricity of the grease.

### *Dynamic behaviour*

Starved lubrication will cause a decrease in film thickness that will proceed until the bearing is no longer properly lubricated. Temporary collapses of the lubricant film layer result in direct contact between the ball and race, causing bearing damage.

These are referred to as 'events' and are identified by a rise in temperature. They do not follow a regular or predictable pattern and can vary in duration. The film thickness will subsequently increase again, often as a result of the heat generated softening the surrounding grease and allowing it to flow. This results in sufficient lubrication and a reduction in temperature until the next event takes place. This sequence may occur a number of times, depending on the ability of the grease to recover following an event, which is a function of the ability of the grease to maintain its fluidity. Where the outer ring of the bearing rotates, this can also have a detrimental effect on the grease by resulting in higher temperatures, increased grease flow and accelerated oil bleeding.

### *Grease life*

Grease life is defined by the point in time where the grease can no longer lubricate the bearing and is indicated by a permanent rise in operating temperature. This time may be very long and therefore difficult to measure in a bearing test rig. To accelerate such a test, the outer ring of the test bearing is heated, which accelerates the ageing process and reduces the viscosity of the grease. Grease life is also affected by the rotational speed of the cage. For the same bearing rotational speed, outer ring rotation causes a higher cage rotational speed, than inner ring rotation.

### *Effect of load on Grease Life*

Bearing load shortens grease life more than would be expected based on EHL film thickness theory alone. Where varying loads occur, bearing manufacturers will often use penalty factors for higher loads to reduce the expected grease life compared to constant low load applications. The effect of load also increases with increased bearing speed. The magnitude of bearing load has a small effect on fully flooded lubricant film thickness, but has a large effect on starvation rate, contact size, grease degradation and damage during starvation events.

### *Safe operating temperature*

Lubricating greases are developed to operate in a limited temperature window. The maximum temperature, called the high temperature limit (HTL), is determined from the dropping point when the grease loses its structure

irreversibly. The safe maximum temperature is lower and is called the high temperature performance limit (HTPL); for safety reasons the HTPL is reduced by 15-20°C.

The low temperature limit (LTL) is determined by the temperature at which the grease will enable the bearing to start up without difficulty. It is usually measured by a start-up torque test. The safe minimum temperature therefore is higher and is called the low temperature performance limit (LTPL). In the zone between these safe temperatures the grease life is a function of temperature where, as a rule of thumb, grease life halves with every 15°C temperature increase. AeroShell Grease 22, has a useful operating range of -54°C to +177°C.

### *Grease life models*

Various models exist that can be used to predict grease life. All models are empirical, based on grease life tests. Grease life is defined as the grease  $L_{10}$  life; the time at which 10% of a large population of bearings have failed. For sealed bearings such as the tail rotor bearing, under normal circumstances, the grease life would be expected to be higher than the service life of the bearing.

### *Ageing*

Both the mechanical and chemical properties of the grease will change while the grease is exposed to milling and oxidation in the bearing. The type of degradation depends on the operating conditions: physical ageing dominates at lower temperatures and higher speeds, whereas chemical ageing dominates at high temperatures. Physical ageing results in a change to the grease's rheological properties, which results in leakage, reduced bleeding properties and a reduction in its ability to replenish the contact area between the balls and the race. Chemical ageing is primarily caused by oxidation.

Antioxidants slow this process but when these are consumed, oxidation leads to a loss of lubricant. Oxidation results in the formation of volatile products within the grease which then evaporate resulting in the formation of a lacquer which no longer lubricates the bearing.

### *Choice of grease*

Grease manufacturers provide a specification for the different types of grease that they produce. The selection of a specific grease for a specific bearing application is done by the bearing and helicopter manufacturers in parallel. The grease manufacturer is typically not involved in this process beyond providing guidance on the general suitability of their products to different applications. For the tail rotor duplex bearing the choice of AeroShell 22 grease was primarily

made by the helicopter manufacturer, who had extensive experience of using it in other bearing applications across their range of helicopters. The suitability of the grease was confirmed by the bearing manufacturer, based on their assessment of the load spectrum provided by the helicopter manufacturer.

#### 1.18.8 Dark Etched Region

During destructive examination of the various bearings under investigation, sections of the bearing were subjected to a standard metallurgy technique of polishing and chemical etching to reveal features within the microstructure of the steel. The Dark Etched Region (DER) was identified after using Vilella's reagent on the bearing sections. It is a recognised feature in metallurgy, indicative of microstructural change as a result of the cyclic passage of the balls over the surface of the bearing. It is most heavily concentrated at a depth corresponding to the maximum shear stress and consists of a ferritic phase<sup>91</sup> containing non-uniformly distributed excess carbon content. It was also identified in this failure mode as being a precursor to the appearance of cracks on the bearing surface due to rolling contact fatigue.

#### 1.18.9 Avionics simulator – yaw rate effects

The helicopter manufacturer has an avionics test bed. This replicates the interconnected avionic systems from the helicopter.

It allows the evaluation of how the systems react to different conditions. This was used to verify how the helicopter avionic systems reacted to an invalid yaw rate.

The ADAHRS units supply the FCC channels with yaw rate data, amongst many other parameters. The data bus can only represent yaw rates between  $-128^{\circ}/s$  and  $128^{\circ}/s$ . Outside of this range the data on the bus is flagged as invalid. The effects of this were explored using the avionics simulator.

The start condition for the test was both autopilots engaged in attitude mode, with no warnings or cautions. Invalid yaw rate data was simulated for the output of the ADAHRUs. This resulted in the AP1 and AP2 switch lights on the AFCS control panel extinguishing and an aural "AUTOPILOT AUTOPILOT" message in the headset, repeated twice. The Crew Alerting System showed three amber caution messages: '1-2 AP OFF', 'AP AHRS1 FAIL' and 'AP AHRS 2 FAIL'. The autopilot indications on the PFD switched from ATT<sup>92</sup> to green boxes. The other attitude and air data related indications, originating from the ADAHRUs, were unaffected.

91 Ferrite is a body centred cubic structure phase of iron which exists below temperatures of  $912^{\circ}C$ .

92 'Attitude hold' autopilot mode.

#### 1.18.10 Flight mechanics simulation

The helicopter manufacturer developed models that relate control inputs to resultant aircraft orientation and motion.

The manufacturer had determined, through modelling and testing, that the bearing failure would result in the tail rotor actuator moving to its full extent in the same direction and with the same speed as was active when the control input became disconnected. This fault was injected into various simulation models with different actuator speeds to establish when the resultant modelled behaviour best matched the recorded motion of the accident flight. There were limitations to this process, including the accuracy of the derived yaw rates from the flight data and the validity of the modelling outside of the certified envelope. Of the fault profiles tested, the accident was best replicated, particularly during the initial period following failure of the bearing, with the actuator taking 2.5 seconds to drive the tail rotor to  $-10^\circ$  of pitch.

#### 1.18.11 Vibration monitoring of the duplex bearing

The manufacturer determined that the current TVM sensor set would not assist in vibration monitoring of the duplex bearing. They carried out rig tests to establish a method for integrating the monitoring of the duplex bearing into the vibration health monitoring system.

For an effective system, the location of the accelerometer must be subject to vibration from the failing component. The algorithms applied to the sensor data must also be properly configured to detect the changes in vibration characteristics. Rig testing of the tail rotor systems was carried out to evaluate different locations for the sensor and the benefit of different algorithms.

Figure 93 shows some of the accelerometer locations evaluated on a test rig. The rig was run with a normal bearing, a bearing with no grease and a damaged bearing. The signals acquired at sensors located at both ends of the rod were similar. Signals acquired on the lever, shown as A05 and A06 (Figure 93), retained a similar vibration pattern.

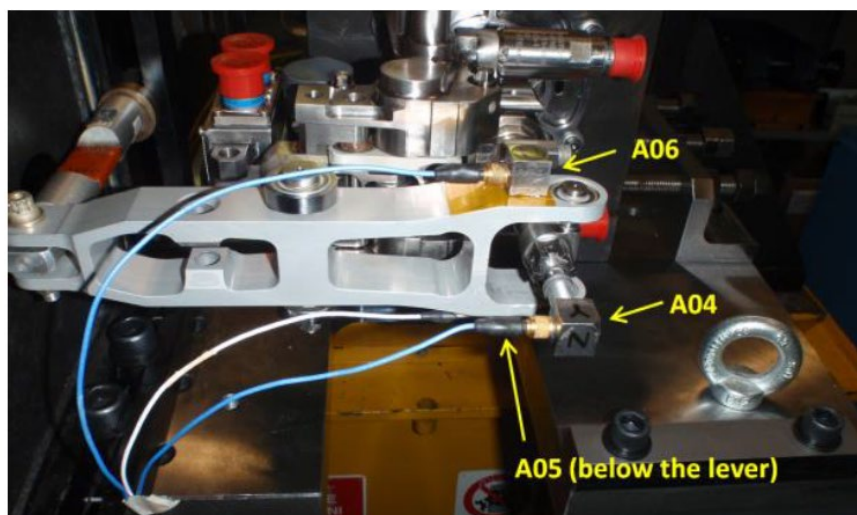


**Figure 93**

Sensor location testing.

(The actuator is approximately upside down compared to the helicopter mounted orientation)

The Health Indicator algorithms were applied to the gathered data. The most reactive to the degradation were linked to low frequency energy, though others also detected issues. It was decided that all their standard bearing Health Indicators would be used on the helicopter, coupled to a new sensor on the lever in the A06 location (Figure 94). Field experience would determine which are the most effective Health Indicators in practice.

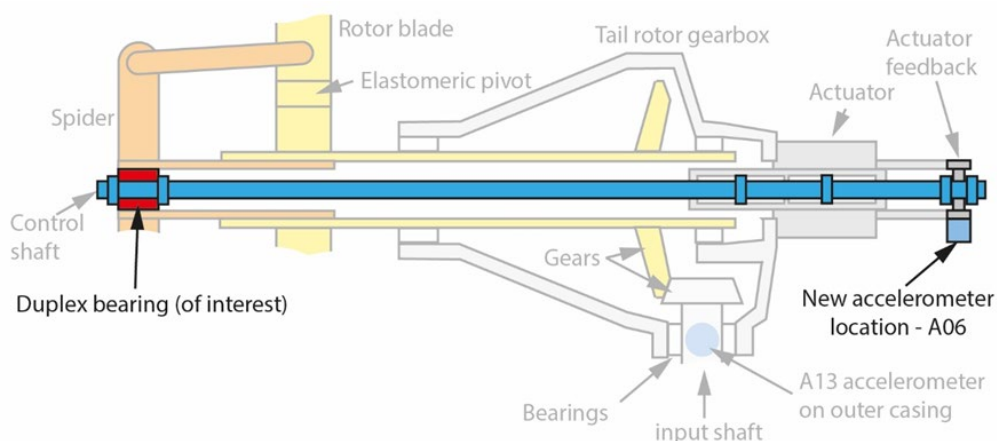
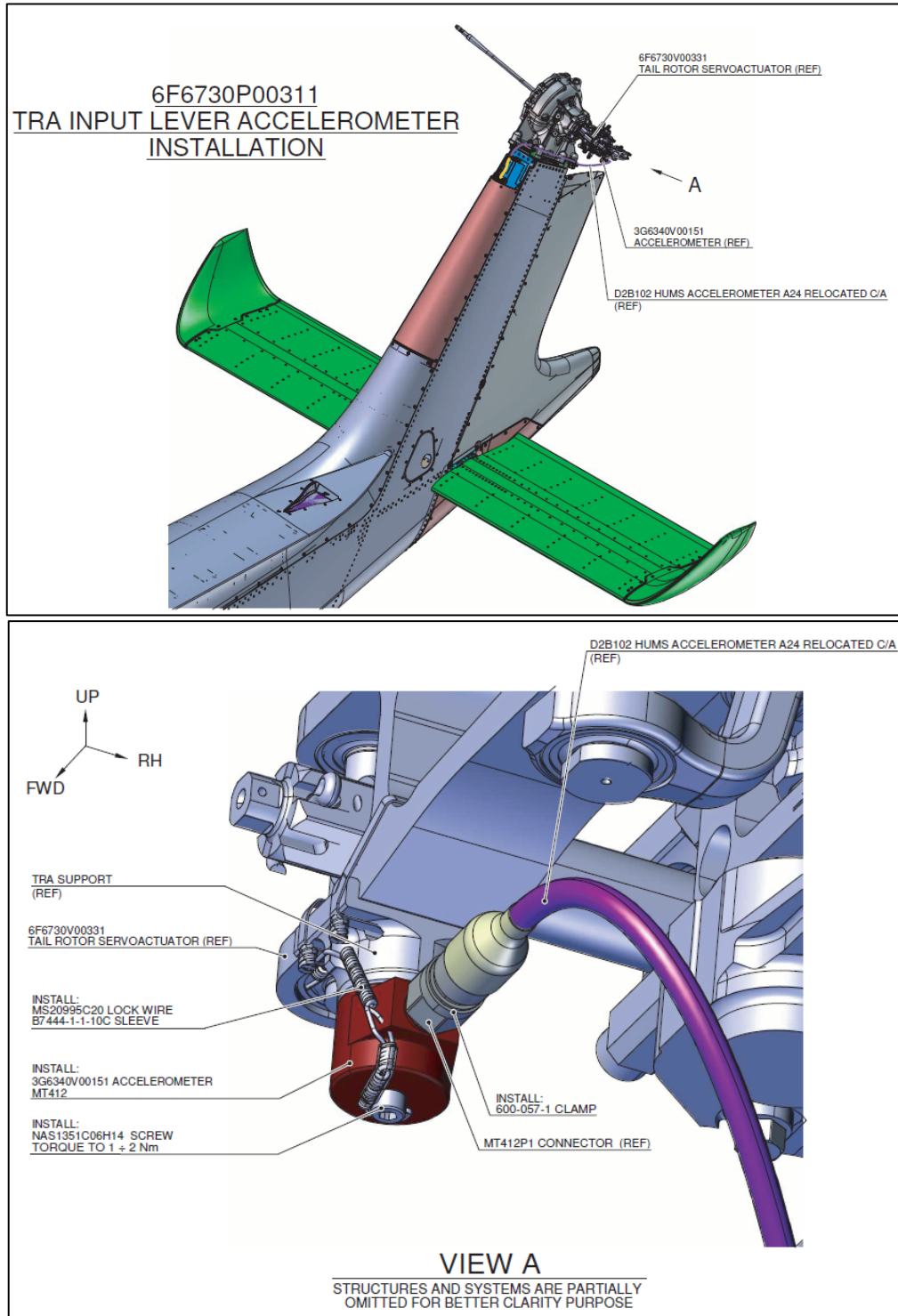


**Figure 94**

Simple schematic of the new accelerometer location relative to the duplex bearing of interest



Factual  
Information

**Figure 95**

Extracts from manufacturer's modification document SB 169-140  
(Image courtesy of the manufacturer)

### *Safety action*

The helicopter manufacturer issued a letter to the AW169 customers and operators, reference PSE/2019/0373, dated 16 July 2019 and Service Bulletin. N°169-140, dated 30 July 2019. The letter described recent enhancements of the HUMS '*dedicated to the monitoring of the Tail Rotor (TR) Duplex Bearing area.*'

These detail the relocation of an accelerometer to the TR actuator lever assembly feeding into the onboard vibration monitoring systems (Figure 95). The change is on production aircraft and available for retrofit through the Service Bulletin.

The systems were put in place for transferring the new data to Heliwise and the manufacturer is providing a free of charge data analysis service for this new data. The letter stated that '*Customers and Operators are strongly recommended to regularly upload HUMS data on the servers to ensure a timely and effective trend monitoring.*'

#### 1.18.12 Previous accidents

##### *LN-OJF*

On 29 April 2016, the main rotor of an Airbus Helicopters EC 225 LP Super Puma, registration LN-OJF, detached in-flight. The helicopter was transporting oil workers and was enroute from the Gullfaks B platform in the North Sea to Bergen Airport in Norway.

The subsequent investigation by the Norwegian Safety Investigation Authority (NSIA)<sup>93</sup> revealed that the accident was a result of a fatigue fracture in one of the eight second stage planet gears in the epicyclic module of the main rotor gearbox (MGB). The fatigue fracture initiated from a surface micro-pit in the upper outer race of the bearing, propagating subsurface while producing a limited quantity of particles from spalling, before turning towards the gear teeth and fracturing the rim of the gear without being detected.

The investigation found that the combination of material properties, surface treatment, design, operational loading environment and debris gave rise to a failure mode which was not previously anticipated or assessed.

The design of the EC 225 LP satisfied the requirements in place at the time of certification in 2004. However, the NSIA found weaknesses in the EASA Certification Specifications for Large Helicopters (CS 29).

93 [Report on the air accident near Turøy, Øygarden municipality, Hordaland county, Norway 29 April 2016 with Airbus Helicopters EC 225 LP, LN-OJF, operated by CHC Helikopter Service AS | nsia](#) (accessed 28 July 2023)

The accident had clear similarities to an Airbus Helicopters AS 332 L2 Super Puma accident off the coast of Scotland in 2009 (G-REDL)<sup>94</sup>. This accident was investigated by the AAIB and was also identified to be the result of fatigue fracture in a second stage planet gear; however, the post-investigation actions were not sufficient to prevent another main rotor loss.

The NSIA investigation into the LN-OJF accident found that only a few second stage planet gears ever reached their intended operational time before being rejected during overhaul inspections or non-scheduled MGB removals. The parts rejected against predefined maintenance criteria were not routinely examined and analysed by the helicopter manufacturer in order to understand the full nature of any damage and its effect on continued airworthiness. The NSIA made the following recommendation:

*'Safety recommendation SL No. 2018/08T*

*The Accident Investigation Board Norway recommends that the European Aviation Safety Agency (EASA) review and improve the existing provisions and procedures applicable to critical parts on helicopters in order to ensure design assumptions are correct throughout its service life.'*

#### *B-MHJ*

B-MHJ<sup>95</sup> was an AgustaWestland AW139 that ditched at Victoria Harbour, Hong Kong on 3 July 2010. The accident occurred because the tail rotor assembly detached from the helicopter. This happened shortly after takeoff when the helicopter was climbing over water at approximately 350 ft AMSL and 70 kt. It was a two-pilot operation. The initial symptoms of the failure were *'a loud bang from the rear of the helicopter'* and *'airframe vibrations'* along with a loss of authority of the yaw pedals. The report states that the commander *'immediately'* put the helicopter into autorotation and the outcome was a controlled ditching. All occupants survived. The total time between the first symptoms of the failure and the touchdown was 16 seconds.

94 <https://www.gov.uk/aaib-reports/2-2011-aerospatiale-eurocopter-as332-l2-super-puma-g-redl-1-april-2009> (accessed 28 July 2023)

95 Hong Kong Special Administrative Region Civil Aviation Department (2014). Report on the accident to AgustaWestland AW139 Registration B-MHJ operated by East Asia Airlines Limited at Hong Kong Victoria Harbour on 3 July 2010. [https://www.cad.gov.hk/reports/B-MHJ%20Accident%20Final%20Report\\_2%20June%202014\\_Consolidated.pdf](https://www.cad.gov.hk/reports/B-MHJ%20Accident%20Final%20Report_2%20June%202014_Consolidated.pdf) [Accessed on 28 July 2023]

### PR-SEK

PR-SEK<sup>96</sup> was an AW139 that crashed in the Campos Basin in Brazil on 19 August 2011 due to the tail rotor assembly detaching from the helicopter.

The failure occurred when the helicopter was in a stabilised climb over water with the autopilot engaged at 130 kt. It was a two-pilot operation. The initial symptoms of the failure were abnormal noise and ‘abrupt’ yaw to the right and roll to the left. For the purpose of determining response time, this was assumed to be the point in time when the pilots were first alerted to a problem<sup>97</sup>. The failure resulted in significant lateral and longitudinal accelerations. The autopilot responded initially with a left pedal input to oppose the yaw and the pilot made cyclic control inputs and began to lower the collective 1.2 – 1.7 s after the first symptoms of the failure. This initial movement of the collective was then reversed, and the pilot began to lower the collective again about 4.5 to 5 s after the first symptoms of the failure, completing the input about 5 to 5.5 s after the onset of the failure. The pilot achieved zero yaw rate and a stabilised autorotation, but the helicopter became uncontrollable due to the loss of both hydraulic systems and crashed into the sea. All occupants suffered fatal injuries.

### G-WNSR

G-WNSR<sup>98</sup> was a Sikorsky S-92A that suffered uncommanded yaw twice due to a failure of the tail rotor pitch change shaft bearing during a flight on 28 December 2016 from Aberdeen to several offshore installations. The first time was during lift-off from an offshore installation. As the helicopter lifted, it yawed unexpectedly to the right and the pilot immediately started increasing the left pedal input to oppose the developing yaw. Full pedal was reached after about three seconds. After a further two seconds, about five seconds after the uncommanded yaw began, the pilot began to lower the collective. The second occasion was during landing at another installation and the response in terms of starting the lower the collective was faster (about 1.5 s after the uncommanded yaw began).

[Appendix C](#) summarises this information from previous events alongside the research findings discussed above.

96 Centro de Investigação e Prevenção de Acidentes Aeronáuticos (CENIPA) 2015, Final report A-546/CENIPA/2015. [http://sistema.cenipa.aer.mil.br/cenipa/paginas/relatorios/rf/en/RF\\_A-546CENIPA2015\\_PR-SEK\\_-\\_English\\_Final.pdf?fbclid=IwAR3T-enQCNrc5nucpMuNO1hwhZU\\_yU6sLUNM2aNjdNi47js4WXXOeQfpGtY](http://sistema.cenipa.aer.mil.br/cenipa/paginas/relatorios/rf/en/RF_A-546CENIPA2015_PR-SEK_-_English_Final.pdf?fbclid=IwAR3T-enQCNrc5nucpMuNO1hwhZU_yU6sLUNM2aNjdNi47js4WXXOeQfpGtY) [Accessed on 7 January 2021]

97 Reported in Table a on page 10 of the report as 19:48:05. All other times highlighted here were measured from this point on Figure 1 of the CENIPA report on page 12. The sample rate for collective position is 0.5 s.

98 [Aircraft Accident Report AAR 1/2018 - G-WNSR, 28 December 2016 - GOV.UK \(www.gov.uk\)](#) (accessed 29 July 2023)

### 1.18.13 Rule Making Tasks (RMT) 128 and 712

As a result of the recommendations from the LN-OJF investigation and other associated safety investigations, EASA initiated rulemaking task 128 to consider changes to CS 27 and CS 29. RMT 712 was initiated to improve and modernise the regulations relating to safety assessment of systems and to harmonise with proposed changes to the FAA regulations.

In February 2022, EASA issued Notice of Proposed Amendment (NPA) 2022-01. This proposed several amendments to CS-27 and CS-29, including changes to CS 29.602 which addresses critical parts. The proposed new text amended 'shall' to 'must' for paragraph b and introduced the concept of a Continued Integrity Verification Programme (CIVP). The NPA also proposed the introduction of a new Acceptable Means of Compliance (AMC) guidance for CS 29.602.

The NPA also contained the proposed amendment to CS 29 introducing an AMC for CS 29.571 Fatigue evaluation of flight structure, which introduced consideration of rolling contact fatigue in the design of rotor drive systems.

It also proposed changes to the AMC for CS 29.1309 to increase the focus on detecting errors in the development process. Further changes were subsequently introduced to the CS 29.1309 regulation text. These removed specific requirements relating to how the safety assessment must be carried out, but also introduced the requirement for no catastrophic failures from a single cause.

The full text extracts of the NPA relating to these changes can be found in [Appendix G](#).

Comment Response Document (CRD) 2022-01 was issued in February 2023 detailing the comments received in response to NPA 2022/01 and documenting EASA's decision whether to accept or reject them. As a result of these comments, EASA decided to withdraw the proposed changes to CS 29.602, stating it required further review with stakeholders.

The remaining changes were introduced into Amendment 11 of CS-29 issued in Feb 2023. The final wording of the relevant extracts is included in [Appendix I](#).

#### 1.18.14 Certification Specifications for Engines (CS-E)

The EASA design requirements relating to engines are contained within a dedicated set of Certification Specifications referred to as CS-E.

Turbine engines have several components whose failure is assessed as resulting in a hazardous engine effect, which qualifies them as critical parts<sup>99</sup>. However, as these components are not Principal Structural Elements their assessment, testing and the control of fatigue life, resulting in a hard life limit on the aircraft, is addressed by regulation CS-E.515 - Engine Critical Parts. The full wording of CS-E 515 is contained in [Appendix F](#) of this report. The life limit of these components is classed as an airworthiness limitation and is contained in the Airworthiness Limitations Section (ALS) of the instructions for continued airworthiness for the aircraft on which the engine is installed.

---

<sup>99</sup> See [section 1.18.5](#) for the equivalent CS 29 definition of critical parts.

## 2 Analysis

### 2.1 General

The helicopter was compliant with all applicable airworthiness requirements, had been correctly maintained and was appropriately certified for release to service prior to the accident flight.

After taking off from the King Power Stadium, while climbing through a height of approximately 250 ft, the helicopter pitched nose-down and, shortly afterwards, entered a gentle right turn in response to the pilot's control inputs. Moments after the helicopter became established in the turn, a divergent and accelerating uncontrollable right yaw rate developed. As the yaw rate increased it induced uncommanded pitch and roll deviations and rendered directional control of the helicopter's flight path impossible.

The physical evidence recovered from the accident site confirmed that the loss of yaw control of the helicopter resulted from failures in the tail rotor control system, which physically disconnected it from the pilot's control inputs on the yaw pedals. The subsequent rotation of the helicopter was driven by the unopposed torque couple from the main rotor combined with the additional thrust from the tail rotor as its blades moved unrestricted to their physical limit of travel, resulting in a negative blade pitch angle. This sequence of events was initiated by the seizure of the tail rotor duplex bearing.

### 2.2 Helicopter operation

G-VSKP was a corporately owned helicopter which was operating under a third-party operator's Part-NCC declaration to the CAA. The operator was compliant with the requirements of Part-NCC and its associated regulations. Under Part-NCC regulations G-VSKP was not required to be equipped with an active FDM system. Operations into the LCFC training ground and the King Power Stadium were conducted under the auspices of the operator's delegated congested area permission issued by the CAA.

The accident pilot was an independent contractor providing pilot services to the owner. At the time of the accident, he held a valid ATPL(H), was a current TRI on the AW169 and was the pilot in command of G-VSKP.

While not yet a qualified helicopter pilot, the front seat passenger was commercially licensed to fly fixed wing aircraft. She was familiar with G-VSKP and had previously flown it under the supervision of the accident pilot.

Prior to the flight the pilot appeared to be in good spirits and had been witnessed carrying out flight planning for the accident flight while at the stadium.

The investigation did not find any operational causes for the accident.

### 2.3 Stadium departure

Permission to operate into the King Power Stadium was conditional on the use of Cat A flight profiles to mitigate against the risk of engine failure. The pilot was required to follow the Ground and Elevated Heliport/Helideck Variable TDP Procedure as specified in the AW169 RFM. This required a maximum 300 ft/min rate of climb and was designed to assure safe performance margins should one engine fail at a critical stage in the departure.

While the investigation was not able to determine the actual TDP height used on the accident flight, the helicopter was above an appropriate height of 215 ft when the pilot lowered its nose and committed to a CTO.

The accident flight departure differed from the published RFM Cat A profile to the following extent:

- The rate of climb during the rearward climb exceeded 300 ft/min.
- The helicopter's landing gear was raised at a speed below  $V_Y$ .

While the accident flight departure was flown at a higher rate of climb than specified in the AW169 RFM, simulator trials indicated that the consequent additional main rotor torque did not significantly influence the post-failure controllability of the helicopter.

Had the helicopter suffered an engine failure below 215 ft, a controlled landing back into the stadium may not have been assured.

Cockpit voice recording revealed that the pilot had asked the front seat passenger to select the landing gear up, indicating that he did not take his hand off the collective lever to do so himself. The call to raise the landing gear came after the pilot had committed to the CTO. The investigation did not consider raising the helicopter's landing gear before reaching climb speed to be a contributory factor in the accident or in its survivability.

The performance analysis for the stadium operation, derived from RFM performance tables, assumed an 85 ft height loss during the transition to a climb following an engine failure above TDP. While not explicitly prohibited by the RFM Cat A procedure profile, a turn commenced below  $V_Y$  could have affected obstacle clearance during a single engine CTO.

G-VSKP entered a low angle of bank turn (approximately 10-15°) while still below  $V_Y$  but approximately 85 ft above TDP and 170 ft above the 130 ft minimum obstacle clearance height for the departure. In a 15° angle of bank turn the vertical component of the helicopter's main rotor thrust would have been reduced by approximately 3-4%<sup>1</sup>.

While recognising that entering a turn below  $V_Y$  was outwith the manufacturer's guidance for the Cat A procedure being flown, given the low angle of bank and additional obstacle clearance margin at entry to the turn, the investigation considered that it did not compromise the safety of the helicopter while both engines were operating normally. It was also determined that, given the helicopter's height at turn entry and assuming the pilot would have rolled out of the turn to maximise the vertical component of rotor thrust if an engine had subsequently failed, the required obstacle clearance margin would likely still have been achieved.

In this specific case the recorded data showed the tail rotor failure sequence was precipitated by the pedal input initiating the turn. However, pedal inputs during this phase of flight are common and could have been made for any other potential reason, for example to compensate for a variable crosswind.

As such, the investigation concluded that the pilot choosing to enter a turn below  $V_Y$  was not of itself a factor in the accident.

Based on the evidence available, it was not possible to determine why the departure differed from the RFM procedure. A witness suggested that the rate of climb exceedance could have been due to the pilot's greater familiarity with the AW109 Cat A departure profile, but the investigation could not objectively establish if this was the case.

## 2.4 Emergency handling

### *Emergency procedure*

Due to there being no certification requirement, the AW169 RFM did not contain guidance for the specific tail rotor pitch control runaway failure experienced by G-VSKP. The LTE drill contained within the RFM details two scenarios, '*in the hover*' and '*in forward flight*.' G-VSKP was climbing in a dynamic transition from rearward to forward flight and had entered a turn at the time of failure. Training scenarios for various malfunctions were available in the simulator but there were none that related directly to this failure mode. The AW169 type rating course was not required to include training for failures involving tail rotor pitch control runaway. Without a specific drill for the encountered failure, applying the LTE

<sup>1</sup> Vertical component of thrust in a 15° banked turn derived by  $\text{Cos}(15^\circ) = 0.9659 = 96.59\%$  of the total main rotor thrust.

emergency procedure would have been an appropriate response by the pilot. Shutting down the engines as part of the LTE drill would have removed the engine-derived component of the de-stabilising torque, but not that component generated by the tail rotor at maximum negative pitch. Given the rate at which the yaw divergence developed, the dynamic and disorientating behaviour of the helicopter, and the limited time and height available, the investigation considered it was not unreasonable for the pilot to concentrate on flying the helicopter rather than diverting his attention inside in an attempt to locate and operate the engine rotary controls.

#### *Pilot response time*

A pilot can only begin to take action when they have recognised the need to act and identified an appropriate emergency procedure to follow. As discussed above, the pilot performed the most appropriate actions available.

The accident pilot reacted to the uncommanded yaw in less than one second by attempting to oppose it with the pedals. The next action, lowering the collective, was initiated about five seconds after full left pedal was applied and was completed over the course of about two seconds. The point when full left pedal was applied and had no effect was considered to be the moment that the pilot could definitely recognise the need to take additional action.

Data from previous tail-rotor failure accidents shows that pilots immediately reacted to the uncommanded yaw using the pedals. Data from these accidents and from research show that the next action of lowering the collective is more variable. In the B-MHJ and PR-SEK accidents the pilots faced no obstructions in their landing area and in the G-WNSR event the helicopter had only just lifted off so lowering the collective was probably a clear course of action. This would likely have helped the pilots to act quickly in comparison to being faced with an ambiguous situation.

When the failure occurred in this accident, the helicopter was above, or close to being above, the stadium roof. In that position, with the heading and pitch angle that the helicopter had at the time, the pilot would have had a view of the stadium roof. This was an imposing structure with substantial vertical supports above the main roof line. It is possible that the pilot decided to wait before lowering the collective in an effort to avoid descending onto the stadium structure.

If the pilot did not decide to wait, a combination of adverse performance shaping factors was present which may have had the effect of lengthening his response time:

- Startle in response to the unexpected and dramatic uncommanded yaw.
- Surprise and confusion indicated by the pilot's comment "I'VE NO IDEA WHAT'S GOING ON". The symptoms of the failure in that phase of flight had never been experienced by him before.
- Disorientation due to the effects of the rapid yawing, pitching and rolling of the helicopter on his visual and vestibular sensory organs.

There are no sources of evidence to tell the investigation more about the accident pilot's thought processes or capability to respond in that moment. Taking everything into account, the G-VSKP pilot's response was considered to be within the range expected given the circumstances. A similar amount of time could be required for any pilot to initiate the appropriate response but a lengthy response results in more instability and even more challenge for a pilot. Training and procedures can improve response times, but they will always be vulnerable to performance shaping factors like startle. Given the large variation of pilot response times, rapid pilot response should not be relied on when assessing risks and designing procedures associated with such failures.

#### *Post-failure controllability*

Lowering the collective after the failure reduced the de-stabilising main rotor torque but also had the effect of reducing lift from the rotor blades and the helicopter began to descend rapidly. With its tail rotor pitch at the full extent of its travel, G-VSKP maintained a high residual yaw rate during the descent.

The simulator trials conducted at the helicopter manufacturer's facilities showed that the greater the time taken to lower the collective, the greater the peak yaw rate and the magnitude of associated pitch and roll deviations. However, regardless of how quickly the collective was lowered, it was not possible to achieve effective directional control of the flightpath following a tail rotor pitch runaway in simulated flight conditions representative of the accident.

The manufacturer also performed additional flight mechanics analysis where computer generated control inputs designed to limit the pitch and roll motions began immediately after the failure, the collective was lowered after 1.5 seconds and the collective was raised at the best possible moment. The manufacturer

concluded that it was possible to limit yaw, pitch and roll motions, avoid the disengagement of the AFCS and reduce the rate of descent at impact by instantly applying optimal control inputs.

Whilst it may have been theoretically possible to achieve a more stable attitude and lower rate of descent at impact with the ground, the simulator trials and flight mechanics analysis were not valid representations of real pilot performance in an unexpected and confusing failure situation. In the flight mechanics analysis a 1.5 second interval was incorporated to simulate pilot response time. As discussed above, the response times of line pilots in real emergency situations can be expected to be variable and longer than those used in the simulations. The pilot response times suggested in AC 29-2C are for the purpose of standardisation during testing of AFCS systems and are not a performance standard for pilots.

Immediately from the point of failure, the flight mechanics analysis was 'flown' by a computer model that does not replicate the limitations of real human performance in terms of ability to judge the magnitude and direction of the helicopter's motion and respond to it. Therefore, the model was able to make optimal control inputs that are unlikely to be possible for a real pilot encountering a situation for the first time. Similarly, the model was able to make iterative calculations to judge the optimal moment to raise the collective which was not possible for the accident pilot.

In the accident flight, after the failure but before the collective was lowered, the helicopter was lifted away from the stadium roof on an off-vertical yawing axis. No lateral motion information was included in the flight mechanics analysis, but the control inputs presented would have provided less time for the helicopter to move away from the roof and would likely have resulted in a descent axis that was closer to vertical. Given the helicopter was likely above the stadium roof at the point of the failure, in this theoretical scenario the helicopter may have been more likely to collide with the roof structure or land closer to the stadium where there were more people.

In the latter stages of the descent the accident pilot raised the collective to cushion the impact. The investigation could not determine what cues were available to the pilot, or find any documented guidance that might have helped him assess when to begin raising the collective, or the degree to which this reduced the rate of descent. The investigation did not determine to what extent pitch, roll and yaw instability might have affected the pilot's judgement of height during the descent. Nonetheless, at night, in a highly unstable helicopter which was yawing uncontrollably and descending rapidly in close proximity to buildings, the pilot managed to cushion the descent sufficiently to render the initial impact survivable for at least four of the five occupants.

The investigation found that, in the prevailing circumstances, the loss of yaw control was irrecoverable. Theoretical analysis presented by the manufacturer suggests it may have been possible to maintain a more stable attitude and achieve a lower rate of descent. However, this is not representative of real pilot performance and would not necessarily have improved the outcome.

## 2.5 External operational factors

### *Meteorological*

There were no observed adverse weather phenomena that would have affected the departure and, on the observed climb heading, the crosswind component was within limits for the departure.

### *Drone activity*

None of the drone activity observed by witnesses in the vicinity of the stadium occurred during the time when G-VSKP was airborne on the accident flight. The investigation found no evidence that drone activity was relevant to the accident and evidence from the rest of the investigation was not consistent with mid-air collision as a causal factor.

## 2.6 Accident flight recorded data

The recorded data did not indicate any system status problems before takeoff.

After the helicopter climbed out from the stadium a rapidly increasing yaw rate developed, contrary to the pilot's pedal inputs. The recorded data indicated that the helicopter yaw rate reached 200°/s within approximately 7 seconds of the helicopter failing to respond to yaw control inputs. The derived yaw rate peaked at 209°/s. With this yaw rate, the longitudinal forces experienced by the pilot would have been in excess of 3 g in the forward direction. The yaw rate reduced to approximately 150°/s after the collective was lowered, but this still far exceeded what might be experienced or considered controllable in routine flight.

The helicopter behaviour was modelled by the manufacturer with different failure scenarios based on the physical evidence. The modelled reactions to disconnecting the tail rotor actuator arm and driving the rotor blade pitch to -10° over 2.5 seconds correlated well with the recorded data. However, there were limitations in both the recorded flight data and the modelling data. As such, it was not possible to determine with certainty the maximum tail rotor blade pitch achieved, given that the primary yaw stops were no longer effective in limiting the range of movement.

Prior to impact, the collective was pulled up, the rotor speed dropped and the engine torques ramped up to compensate. This reduced the descent rate prior to impact.

There was a period of approximately 14 seconds between the initial loss of tail rotor control and the impact with the ground.

### *Alerts*

'AP AHRS1 FAIL' and 'AP AHRS 2 FAIL' cautions were flagged during the accident flight. The autopilot systems use motion data from the ADAHRS units. Within approximately 4 seconds of the onset of the failure the yaw rate exceeded  $128^{\circ}/s$ , the maximum yaw rate value that the ADAHRS units can send to the autopilots. After this, the yaw rate data became invalid and the autopilots disconnected and flagged cautions against the two ADAHRS. The disconnection of the autopilot and 'AP AHRS1(2) FAIL' cautions are therefore not failures as such but a functional system being exposed to yaw rates it was not designed to handle.

Other warnings and cautions were issued. A 'ROTOR LOW' warning was triggered as the rotor speed briefly dropped by more than the 2% allowable with two engines running. With a nominal  $N_R$  of 103%, the main rotor is rotating at 348 rpm, nearly  $2100^{\circ}/s$ . The yaw rate of the helicopter itself peaked at approximately 10% of this, which is an unusual control situation. The  $N_R$  reduction was minor and was quickly recovered. The collective was lowered shortly after this.

Oil pressure alerts were generated for the main gearbox and engines. The oil systems for each engine and the main gearbox are separate. The alerts were likely triggered due to the effects of the yaw-rate-induced forces on the oil distribution and sensing of each of the three oil systems. The gearbox and engines did not fail.

The DAFR recorded a problem with ADAHRS1 for the last two seconds of flight. The cause of this is not known. The NVM from the ADAHRU records internal problems only. It did flag a failure, but time alignment indicated that it was likely later, possibly at impact. The cause of the DAFR recorded failure is not known and not considered relevant to the accident sequence.

## **2.7 Loss of tail rotor control**

The accident sequence began with a deterioration over time of the duplex bearing which connected the rotating tail rotor assembly with the non-rotating tail rotor actuator control shaft. Eventually the bearing became so damaged that the rotating outer race and the static inner race of the bearing became

seized. The tail rotor system is driven at high torque by the main helicopter gearbox, which in turn is driven by the engines. When the bearing seized, the torque from the tail rotor drive system was transmitted through the bearing to the actuator control shaft, causing it to rotate at high speed.

Immediately prior to the control shaft starting to rotate, the pilot had applied an input on the right yaw pedal. This resulted in the tail rotor actuator control shaft starting to move to the right, pushing out the spider assembly which, via the pitch link connection, reduced the tail rotor blade pitch.

The locking nut at the actuator end of the control shaft clamped the pin carrier to the outer shaft of the hydraulic actuator, with the pin in the carrier providing the pivoting connection to the control system linked to the pilot's pedals. The now rotating inner shaft had enough torque to break the locking wire and shear the installed split pin on the nut. Continued axial movement of the control shaft under hydraulic pressure maintained the contact pressure between the nut and the pin carrier, allowing the threaded portion of the shaft to 'unscrew' completely from the nut<sup>2</sup>. In the process, friction heated the nut sufficiently for localized melting to occur, effectively welding it to the pin carrier. Both the nut and pin carrier were pushed off the end of the control shaft as it continued to move (Figure 96).

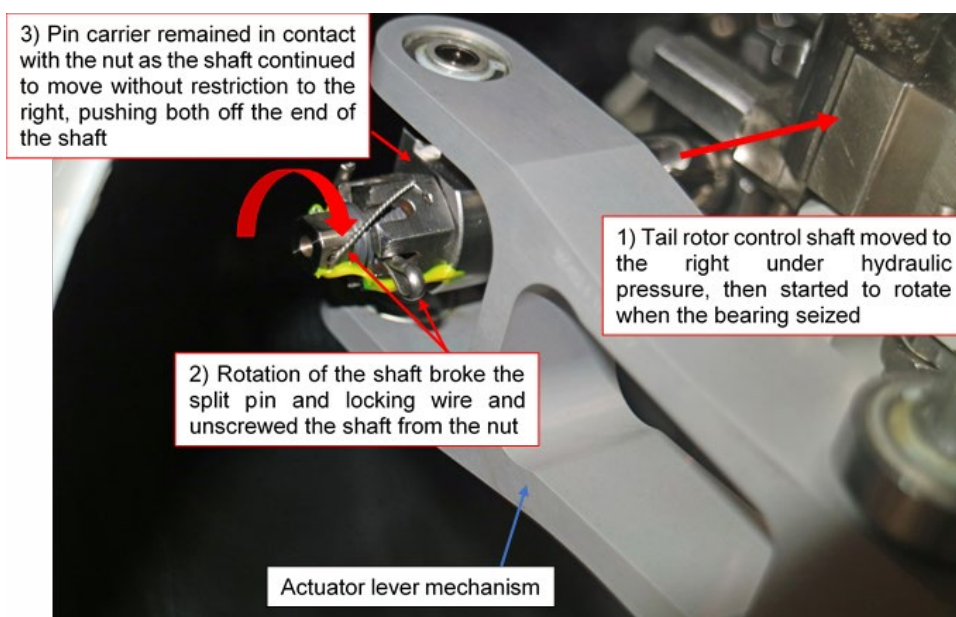


**Figure 96**

Sequence of disconnection of the TRA control shaft from the pilot's controls

<sup>2</sup> The rotation of the control shaft also resulted in the tightening of the locking nut at the bearing end, leading to the high torque figure found during disassembly.

The actuator lever mechanism is designed to act as mechanical feedback for the hydraulic actuator, closing off hydraulic pressure once the movement of the control shaft matches the pilot's pedal input. As the lever was now completely disconnected from the control shaft, the shaft continued to move under hydraulic pressure without restriction. The primary control stops for the yaw system, which normally limited the range of travel of the tail rotor blades, were located on the pilot's side of the disconnect and so become ineffective. This allowed the control shaft to continue moving until it reached the full range of travel physically possible for the blades. The result was an increasing rate of right yaw, driven by the now unresisted main rotor torque couple and the torque generated by the force from the negative pitch angle of the tail-rotor blades.

The pilot tried to apply a left yaw pedal input to stop the rotation but due to the physical disconnection, had no possible means of controlling the tail rotor. The pilot reduced the collective input to reduce the torque generated by the main rotor; while this reduced the rate of rotation of the helicopter, it remained uncontrollably high until impact.

This sequence of events was verified during the subsequent tail rotor rig testing, which demonstrated that the locking nut would 'unscrew' once the bearing began to seize with an input load present on the control shaft.

## 2.8 Crashworthiness and survivability

Information provided by the helicopter manufacturer confirmed that the AW169, including the cabin configuration installed in G-VSKP, met the emergency landing and crashworthiness requirements of CS 29 Amendment 2 when the helicopter type was certified.

The examination of the impact absorption mechanisms of the rear passenger seats that were occupied on the accident flight found that they had operated and reached the limit of their travel. This confirmed that the helicopter and its occupants had been subjected to vertical deceleration forces greater than the 30g design limit of the seat impact absorption mechanisms.

The highly dynamic nature of the impact meant that it was not possible to make a direct comparison between the requirements of CS 29 and the forces experienced during the accident. However, the impact analysis calculations, supported by the physical condition of the crashworthiness safety features and fuselage structure, indicate that the impact forces probably exceeded the design specifications of the helicopter.

Despite the magnitude of the impact forces, post-mortem examination showed that four of the five occupants survived the initial impact. Their reported injuries

would, however, have prevented them from being able to escape from the helicopter without external assistance, given the position in which it came to rest.

The analysis also showed that the presence of the concrete step produced localised crushing of the lower fuselage and structure supporting the fuel tank bladders. The damage observed to the lower fuselage on the accident site confirmed that elements of this damaged structure had penetrated the fuel tank bladders.

### *Fire and rescue*

The helicopter came to rest on its left side. The impact with the step had resulted in the release of fuel which then pooled around the helicopter. Given the final orientation of the helicopter and the damage it sustained during the impact sequence, there would have been several potential ignition sources including the engines, damaged navigation and anti-collision lights and other damaged electrical circuits. Evidence shows that the fire had already taken hold when the first emergency services vehicle arrived on site, approximately one minute after the impact. Statements from the police officers who were first on the scene stated that the fire appeared to have progressed forward from the rear of the helicopter.

With the helicopter resting on its side and the fire having taken hold, the first responders were unable to reach the uppermost, right side to gain access to either the cockpit or cabin. They attempted to gain access to the cockpit by breaking the windscreen but as this was designed to withstand a high-speed bird strike, it could not be broken with the equipment available to them. Specialist equipment would have been needed to break or cut the windscreen. The intensity of the fire increased rapidly preventing further rescue attempts. The post-mortems confirmed that the surviving occupants would have quickly succumbed to inhalation of the products of combustion.

The area in which the helicopter struck the ground was the only area close to the stadium which did not contain people, cars or other structures. Given that the pilot had no control over the horizontal trajectory of the helicopter, any change in the timing of the loss of control or the pilot's response could have resulted in third party casualties and additional collateral damage on the ground.

## 2.9 Duplex Bearing failure

### *Accident bearing*

Analysis of the findings from the detailed lab investigation of the accident bearing (s/n 14126) confirmed that the inner and outer races of both sides of the bearing had become damaged by Rolling Contact Fatigue (RCF).

The damage was most extreme on the inner race of the inboard side. The RCF resulted in surface initiated crack growth and led to material loss on the rolling surface of the race. This was likely to have resulted from a high shear stress at the surface of the race material, as evidenced by the surface initiation, material flow and Dark Etched Region (DER) evident on the sectioned races. Evidence from the material analysis and lab work showed that significant heat was generated by the increasing friction between the balls and the race, degrading the grease further until it eventually became dry carbon powder and creating a heat affected zone of changed material properties in the race material closest to the surface. The lack of lubrication then increased the amount of heat generated and the rate at which damage accumulated on the race surfaces.

Whilst a small amount of grease was found around the slider adjacent to the inner race seal, this was consistent with excess grease extruding from the bearing in early operation and was also seen in other bearings removed from service and used in rig tests. The inner race and inboard side seal were found disturbed following removal from the wreckage. However, wear marks on the inside surface of the seal showed that it had been in contact with the cage in operation and it had likely been disturbed by movement of the inner race during the process of extracting the bearing from the wreckage.

Analysis of the failed cages showed that the increasingly erratic rotation speed of the individual balls around the race surfaces caused them to contact the cage and transferred loads to the cage structure which it was not designed to tolerate. This resulted in heavy wear around the cage pockets and subsequent fatigue cracking and failure of the cage structure. Once the cage failed, the now unrestrained balls were able to migrate across a larger area of the race surface spreading the damage.

Inspection of the surface of the inner race showed that large sections of the surface material had been released (macropitting) as crack growth increased. This material had then been ground into powder by the action of the balls and mixed with powdered copper, released from wear to the cage, and the powdered carbon from the grease. The powder mix was then compressed back onto the surface of the race by the contact pressure from the balls, creating a new rolling surface.

RCF then restarted the process of crack growth on the much less homogenous powder coated surface, resulting in larger sections of material being released and re-laid. The profiling of the race surface showed that this created high spots above the normal surface level. As the ceramic ball material was much harder than the race material, their geometry had not been as significantly affected by wear during this process. Eventually the clearance between the balls and the inner and outer races was compromised by the material deposition process and the bearing seized.

#### *Bearings removed from service by continued airworthiness actions*

The selection of bearings investigated after they had been removed from service for failing the mandatory inspection Service Bulletin checks, showed the chronological sequence of deterioration of the bearing in more detail.

Bearing s/n 14134 showed the early stages of RCF damage to the bearing inboard inner race. The grease had deteriorated, due to temperature and mechanical ageing, from a moist lubricant to a tacky residue. Evidence of the increased temperature was also observed in the presence of a zone of heat induced material property change under the running surface of the bearing race. Small crack features were developing on the race running surface, demonstrating the initial phase of surface initiated cracking and material loss. The location of the cracks was consistent with the location of highest contact pressure and PV calculated by the bearing manufacturer's simulation software. The bearing cage was intact, limiting the area of damage on the race.

Whilst the service life of the bearing was appreciably more than the accident bearing (1,117 hours vs 330 hours respectively), this was still short of the discard life of the bearing (2,400 hours) and significantly less than the  $L_{10}$  life (12,882 hours), suggesting that it was subject to a premature failure mechanism rather than routine end of life RCF. This is supported by the surface initiation of the cracks and presence of a DER close to the surface, both consistent with the accident bearing, and when compared to more typical Hertzian subsurface initiated cracking due to routine accumulated operating life.

Bearing s/n 15119 demonstrated a more advanced stage of deterioration. The cracks had developed to the point of significant material loss leaving extensive macropitting on the race surface. The cage was cracked and worn in the pockets and a lip worn around the inner circumference of the inboard cage, indicating a change from the intended smooth rolling mechanism of the balls and allowing the cage to diverge from the normal running line of the balls on the race<sup>3</sup>. The spalling on the ceramic balls from the outboard race suggests truncation had

3 A further example of this can be seen in the bearing used for the manufacturer's rig test documented in [section 1.16.1.3](#).

taken place, this was supported by the wider arc of microstructure damage seen on the outboard inner race. Truncation occurs when the balls migrate to run on the corner of the race surface, significantly increasing the point contact pressure on the balls. Spalling on the surface of the balls is the next stage from traction cracking (crazing seen on the accident bearing), where material is lost as a result of crack growth. The bearing races showed the same surface initiated cracking, shallow DER and heat induced zone of material property change as the previous bearings. The analysis of the race material showed evidence of the balls sliding rather than rolling.

Bearing s/n 13123 displayed a level of damage to the bearing where significant material loss had occurred as areas of macropitting joined together around the surface of the races. The condition of the grease, which had turned to carbon powder shows high temperatures had occurred in the bearing.

However, this bearing did not exhibit the DER below the race surface, indicating that it had not experienced the same level of shear forces from the balls sliding rather than rolling, as with the other bearings inspected. The heavy wear in a single cage pocket and the heavy spalling of a single ball relative to the others, suggests this failure was more likely to have been caused by a problem with the individual ball, possibly an inclusion as evidenced by the particle of iron oxide reportedly found embedded in the ball material.

Whilst there was disagreement between the various lab analysis reports about the cause of the spalling, the similarities to bearing s/n 17115, suggest the mechanism may have been the same, although the inclusion in that case was a different material and was closer to the surface, which accounts for the difference in rate of progression of the bearing damage<sup>4</sup>.

While bearing s/n 14125 was not independently assessed, the physical evidence recorded by the manufacturer demonstrated a similar level of degradation as s/n 15119 and similar features to those seen on the accident bearing.

The grease had degraded until it became powder and the damage had developed to the point of creating macropitting on the inner race surfaces. The cage had failed in fatigue and was worn in the pockets and in a step around the inner circumference of the wide end on one of the rows. This indicated a change from the intended smooth rolling mechanism of the balls and allowed a divergence from the normal running line of the balls on the race. The spalling on the ceramic ball from the side of the bearing where the cage had been displaced by wear from contact with the inner race, suggests this was caused by truncation. Again supported by the wider arc of microstructure damage

---

4 This failure mode was dealt with separately to this investigation by the manufacturer and the EASA as a continuing airworthiness issue.

seen on the inner race surface. The bearing races showed the same surface initiated cracking, shallow DER and heat induced zone of material property change as the other bearings. This evidence was consistent with high surface shear forces resulting from the balls sliding rather than rolling.

#### 2.9.1 Investigation-requested endurance rig test

The bearing (s/n 19189) did not exhibit any external evidence of distress during the rig test run, such as triggering a temperature alert, and the results from the detailed lab investigation of the bearing showed no evidence of surface level fatigue damage. However, the grease condition was consistent with localised operating temperatures higher than the external thermocouples recorded. The presence of the DER below the inner race surface only on the loaded side of the bearing, showed that the microstructural change was a result of the load applied.

The depth of the DER was also similar to that seen on other bearings inspected where surface initiated cracking had subsequently developed. However, this evidence of initial bearing race damage was all to a significantly lesser extent than identified on the other bearings investigated.

As the only test parameter that was applied to the bearing was a consistent load it is reasonable to conclude that the initiation of the material properties change on the loaded race was directly related to the operating load applied. However, the bearing manufacturer's review of contact pressure between the rolling elements and the race surface (conducted after the test was done) showed that a combination of 8,000 N axial load and 16 Nm bending moment did not generate a sufficiently high contact pressure in the bearing to trigger the rate of damage progression seen in the other bearings.

#### 2.9.2 Manufacturer's subsequent rig test

The final rig test carried out by the helicopter manufacturer applied higher loads, through a combination of high axial and bending moment loads, compared to the endurance test requested by the investigation and loaded the bearing cyclically, with varying load magnitudes, alternating loads directions and cooling periods between each cycle. The test spectrum was initially defined to certify the new all steel modification standard bearing and as such needed to reflect the high axial and bending moment loads recorded on both the AW189 and the AW169. The test was then repeated using a hybrid bearing of the type fitted to the accident helicopter, but the manufacturer also elected to remove the inboard seal to explore the effect of this on bearing performance.

### *Grease loss*

The bearing (s/n 16141) was inspected on three occasions during the test sequence. This identified that a 'collar' of extruded grease was present on the side with the seal removed. The grease was extruded within the first 290 operating hours and the quantity did not increase further during the test. The bearing continued to operate for a significant period with recorded temperatures below any of the threshold limits, despite the reduced grease content. The extruded grease was recovered and weighed at 3.3 g.

This was slightly more than the original certification endurance test for the AW169, which lost 2.38 g, and the certification endurance test for the AW189, which lost 2.86 g. With the seal not in place to act as a boundary, additional grease may have been extracted during the recovery process, which would otherwise have been below the seal had it been present. Despite this and given that the seal was completely removed for this test, the loss of grease was not extreme in comparison with other tests conducted. It also showed that removal of the seal did not result in a complete loss of grease, as would have been required to replicate the results of earlier rig tests, where the grease was intentionally removed in its entirety to expedite the failure of the bearing. The loss of some grease past the seals is accepted as normal during the churning phase of bearings which are initially fully filled with grease.

### *Observations during the test*

The temperature data recorded that there was a notable and consistent temperature rise on the side of the bearing which was under load. The larger the load, the greater the temperature rise. As the race rolling surfaces deteriorated, progressively higher temperatures were recorded. These temperature increases were the result of increased friction due to the increased contact pressure between the races and the balls under load, but subsequently added to by the increased friction resulting from deterioration of the grease and the balls travelling over the damaged race surfaces. The test was allowed to continue with peak temperatures of 400°C recorded, at which point a torque load was transferred by the bearing, indicating it was starting to seize.

### *Bearing damage*

The laboratory investigation of the bearing confirmed that both sides of the bearing showed the same rolling contact fatigue features seen in the accident bearing and the other bearings removed from service. Heavy wear on the outboard cage demonstrated how this resulted in the cage being displaced, allowing truncation of the balls. The bearing contained powdered grease and there was evidence of the transfer of copper onto the inner race running

surface. The inner races displayed a heat affected zone and shallow DER as well as regions of deformed microstructure with surface initiated cracks.

The compressed nature of the cracks, the increased levels of plastic deformation and smearing on the outboard inner race, suggest that the sequence of failure had progressed further than seen in the other bearings inspected after removal from service. Despite being the side of the bearing with the seal still fitted, the damage on the outboard side of the bearing had progressed further than the inboard side which had the seal removed. This demonstrated that seal damage or displacement during installation or in service was unlikely to be a factor in the deterioration of the bearing with this specific failure mode.

The low-level transfer of drive torque detected at the end of the rig test showed that the bearing had reached the stage of incipient seizure. However, the damage seen in the bearing had not yet progressed to the stages of fracturing the cage and extensive replacement of the running surface seen in the accident bearing. It is therefore likely that the bearing would have continued to operate, albeit in an increasingly distressed state, for a further period before the damage reached the extent seen on the accident bearing and complete seizure and full transfer of drive torque into the control rod occurred.

The high loads were only applied for short durations, with the load direction reversed immediately afterwards. This allowed the temperature of the unloaded side of the bearing to decrease before the next reapplication of load. The test was also run at the lower AW189 tail rotor speed rather than the maximum AW169 speed, used in all the other rig tests. These mitigations would have an effect in slowing down the rate of deterioration of the bearing. The test data recorded during the test showed that the axial loads applied varied from the planned test spectrum. The average negative loads, which loaded the inboard race were lower than the average positive loads on the outboard race. This was reflected in the level of damage progression seen on the two races.

### 2.9.3 Conclusions from the bearing investigation

#### *Potential causes of bearing failure eliminated*

There are a number of basic factors which can potentially cause a bearing to fail prematurely.

Given the vast experience of operating bearings across many industrial applications, these have been extensively researched and documented and were considered in detail by the investigation.

The investigation benefitted from inspecting several bearings either removed from service or following rig tests. This facilitated the compilation of factors that

were common to the accident bearing and all the similar damaged bearings, and allowed the elimination of those factors which were inconsistent with this group of bearings.

Whilst not an exhaustive list, the following significant factors were considered and eliminated.

Two of the damaged bearings reported were either confirmed or likely to have been caused by manufacturing issues with the balls and were characterised by the extensive spalling of the individual ball affected. These were included in the report to document the differences in the physical evidence, most notably the lack of a DER, to show they were not the same as the accident bearing or bearings s/n 14125 and s/n 15119 and to highlight the consistency of the damage to this group of bearings.

The bearing material properties and dimensions were assessed in the bearings inspected and any variations confirmed to be a consequence of the damage process. Preload was explored by various rig tests and found not to be a significant factor in isolation. The metallurgy showed that the RCF damage was surface initiated and caused by high surface shear stress from the balls sliding. This was not consistent with a random low life failure due to Hertzian fatigue in a bearing operating normally.

Truncation of the balls due to movement of the cage was demonstrated to be a consequence of the failure process on the bearings where this occurred. No evidence supporting truncation as an initiating cause was present on these bearings and evidence of truncation was not found on the accident bearing or consistently across all the bearings which showed the same damage characteristics as the accident bearing.

The investigation considered a grease specification or contamination issue, but it was confirmed that the grease quality is strictly controlled and reviewed to meet Military Specification standards. Each batch of grease was used in multiple hundreds of bearings, which is inconsistent with the numbers of failing bearings identified and the variations in initiation time and time to failure seen across the damaged bearings. No evidence was found to suggest that the grease used in the damaged bearings did not perform in accordance with its specification. Where grease degradation occurred it most likely resulted either from prematurely reaching the end of its useful life due to the high operating contact pressures within the bearing or due to exposure to operating temperatures which exceeded its specification limits.

Water contamination of the bearing during the manufacturing process was also considered, particularly in relation to the application method and use of

preservation oil on the bearing components. There was no evidence identified that this had occurred or was a likely risk and a significant amount of evidence that contradicted it as a possible factor.

The investigation found that there were extensive safeguards within the manufacturing process to avoid contamination of the oil and had it been a problem it would have affected many thousands of other components, which was not the case.

No evidence of water contamination or corrosion has been identified on any of the bearings inspected by the investigation and no generic issues of this nature have been reported by the bearing or helicopter manufacturer on this bearing part number.

The compatibility of the preservation oil with the grease has been reviewed and confirmed by the bearing manufacturer with the grease manufacturer. Contamination of bearings at manufacture was not consistent with the variation in bearing lives observed across the damaged bearings considered by the investigation, where the highest life bearing had the lowest level of damage. An issue present at manufacture would likely have resulted in a consistent rate of deterioration and time to failure across all the bearings.

A more general review of the bearing manufacturing process, including findings from a quality audit conducted by the helicopter manufacturer after the accident, found no evidence to suggest that the actual manufacturing process had caused or contributed to the premature failures of the accident bearing and the bearings with the same failure characteristics.

Extensive leakage from the bearing of low viscosity grease was not consistent with the evidence from the specification of the grease nor from the rig tests which took the bearings up to between 400 and 600 °C. Rather, the tests demonstrated that most of the grease was retained and degraded to carbon powder when subjected to these high temperatures. This was also consistent with temperature experiments on the grease conducted by the helicopter manufacturer to facilitate a baseline assessment of grease condition.

Grease extrusion around the bearing seal during the 'churning phase' leading to a ring of grease around the face of the bearing was confirmed to be normal. This was supported by a number of independent sources of evidence, including reference texts published by recognised industry experts on bearing lubrication, articles published by the bearing manufacturer and a test report issued by the helicopter manufacturer. The AW169/AW189 bearing is unusual in having 100% of the free volume filled with grease. The normal industry standard as quoted in the bearing manufacturer's product catalogue

is 25-35%. The AW139 bearing has a minimum grease content specification of 33%. When applied to the AW169 bearing this suggests that up to 4 g of grease can be extruded with no adverse effect. The rig test referenced by the helicopter manufacturer's report operated a bearing with intact seals and nominal grease content for over 1,000 hours with evidence of grease extrusion around the seal described as 'typical' by the report; no damage was identified on this bearing. Similarly, both certification endurance tests resulted in grease extrusion, but the bearings were still deemed serviceable by the bearing manufacturer.

The final rig test conducted by the manufacturer, where the seal on one side of the bearing was completely removed, showed the damage was worse on the side with the seal still in place and the largest amount of grease (powder) retained.

However, even with the seal completely removed, the amount of grease expelled was not extreme and only slightly greater than the amount of grease expelled in other rig tests. The grease was also extruded early in the test consistent with the initial churning phase, but the recorded bearing temperature remained well below the grease specification operating temperature limits for close to 700 hours of testing. No additional grease was lost before the bearing temperatures started to rise towards the end of the test. These timelines were not consistent with the accident time to failure of 330 hours.

None of the damaged bearings removed from service were found to have missing or significantly displaced seals. Most displayed wear marks on the inner surface of the seals consistent with in situ contact between the seals and the cage. The accident bearing demonstrated the same wear marks. Displacement of the seal found after removal was consistent with displacement of the adjacent inner race resulting from the separation process of the control shaft from the tail rotor wreckage.

#### *Identified cause of bearing failure*

By contrast, a significant amount of common supporting evidence was identified across the group of bearings found with the same damage characteristics as the accident bearing. This provided coherent evidence that these bearings and the accident bearing had suffered the same early onset, surface initiated, rolling contact fatigue, consistent with high contact pressure resulting from operating loads.

The installed, but unloaded bearing is designed to operate with a constant baseline contact pressure between the balls and the races, controlled by the preload on the bearing. When an additional external axial load and/or bending

moment are experienced by the bearing due to the tail rotor hydraulic actuator reacting or overcoming the inertial, elastomeric and aerodynamic loads generated by the tail rotor blades during manoeuvres in different operating conditions, this increases the contact pressure between the balls and the race, within the side of the bearing reacting the load.

Research has shown that the ceramic balls used in hybrid bearings result in a contact pressure approximately 12% higher than steel balls under the same load.

This is because the hard ceramic balls deform less under pressure creating a contact 'footprint' between the balls and the race surface that is smaller than with steel balls. The balls and races are normally separated by a thin layer or film of grease that lubricates the contact area and reduces the friction. This is referred to as elastohydrodynamic lubrication. The thickness of this grease layer and hence the effectiveness of the lubrication provided, is affected by a number of factors, but most significantly by the contact pressure it is subject to and by the temperature, which affects its viscosity.

Grease that is heavily worked by the mechanical effects of a high contact pressure and the chemical changes which result from high operating temperatures due to increased friction, will degrade more rapidly than would otherwise be the case in a less extreme environment; this is referred to as ageing. As the grease degrades it reduces its effectiveness as a lubricant. This even applies to grease which is working exactly as defined by its specification. Where this is anticipated or monitored by design, the grease can be replaced at appropriate intervals. With sealed bearings, such as the tail rotor duplex bearing, this is not possible and is mitigated by selecting a grease which won't reach the end of its effective life prior to replacement of the bearing. However, accurately predicting this effective life is dependent on a full understanding of the bearing maximum contact pressures, temperatures and load cycle durations likely to be encountered in operation.

Loss of lubrication effectiveness either by momentary reductions in film thickness, which can result in lubrication starvation events, or by degradation of the grease, or by a combination of both, increases friction between the bearing race and the balls, leading to a further increase in temperature. This cycle also results in an increase in the amount that the balls slide which creates high shear stresses at the surface of the bearing race material, further increasing the temperature. Initially the increase in surface shear stress will manifest as subsurface microstructural change but this will progress under continued high stress to form distinctive surface initiated cracks and material loss, which also increases friction. This cyclic process eventually causes sufficient damage to the bearing race surface that it results in a self-perpetuating downward spiral of

reducing lubrication effectiveness, increasing friction, temperature and damage to the bearing until it seizes (Figure 97).

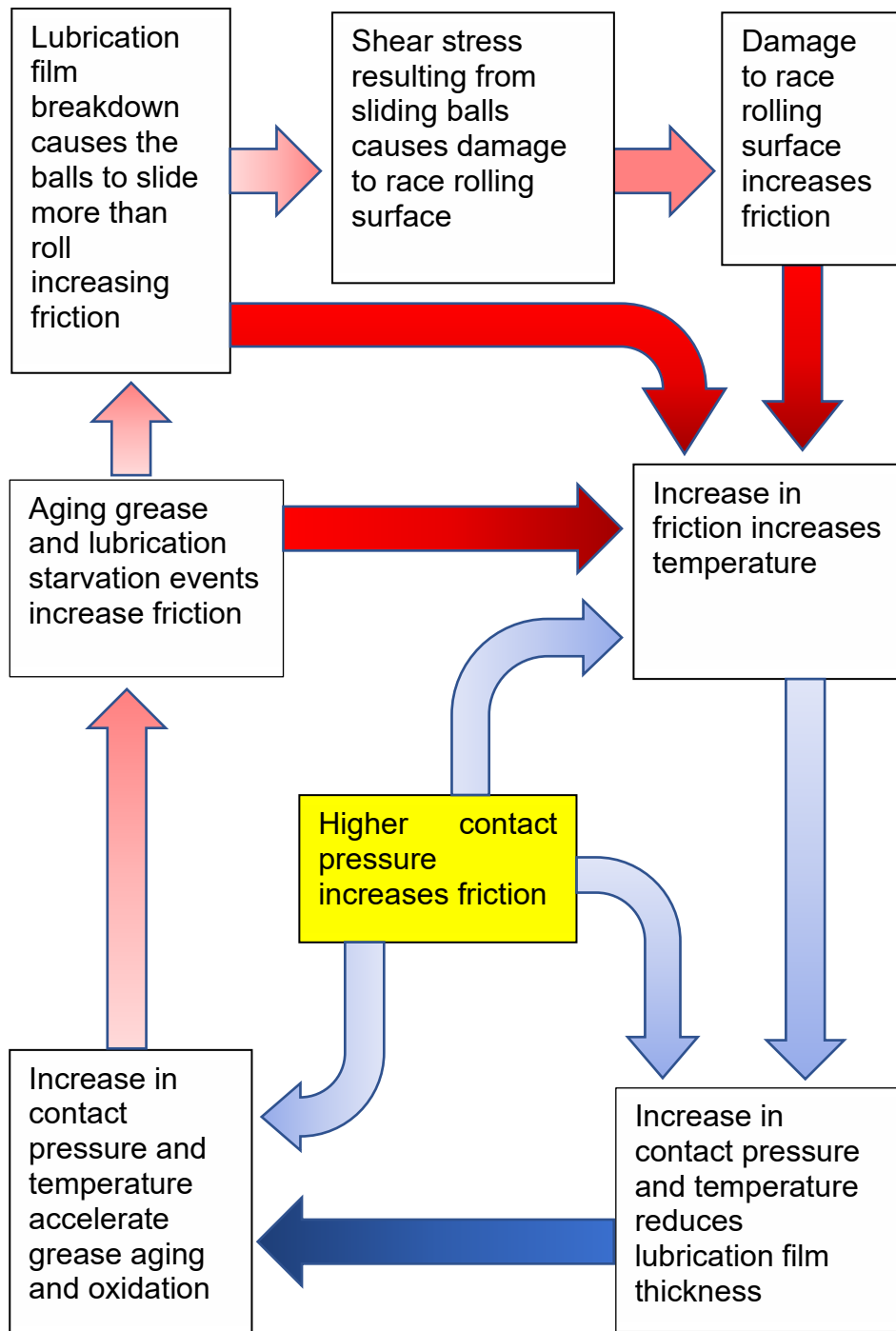


**Figure 97**

Cycle of increasing friction, grease deterioration and surface damage in bearings due to high contact pressure, resulting in premature failure

Analysis

The degradation of the grease, seen to various extents across all the bearings inspected, was indicative of the high mechanical work and the increasing temperature due to increases in friction. While there is the possibility of rapid grease deterioration in the churning phase of the bearing's operation, given that only a limited number of bearings have been identified with damage and all bearings experience this phase, it can only act as a potential contributory or exacerbating factor to the main issue of degradation caused by high mechanical work and friction.

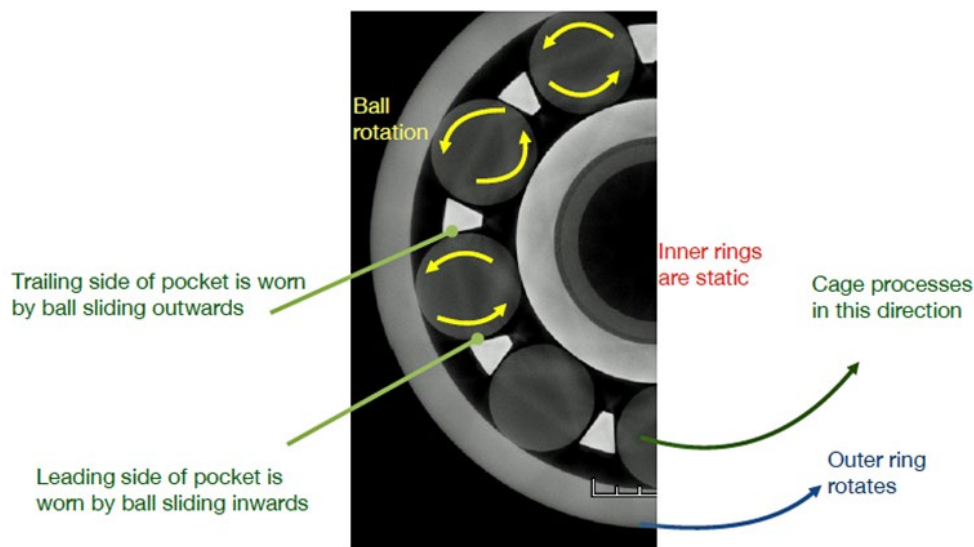
The presence of a DER just below the race surface was characteristic of the high shear stress closer to the surface than Hertzian theory would predict, caused by the increased amount that the balls were sliding rather than rolling. The DER was not present on bearing s/n 13123, which suffered a similar degradation sequence and level of distress, but due to a different failure cause. It was, however, present on the bearing from the final rig test, where the only variable test parameter introduced which would negatively impact on the bearing's performance was a high operating contact pressure, resulting from high applied axial and bending moment loads.

As seen across all of the bearings, once fatigue cracks developed on the race surface, the friction and thus heat increased as the balls rolled or slid over the rough surface, further increasing the stresses on the race material and changing the microstructure of the material within a heat affected zone below the race surface, making it softer and less durable. This continued to degrade the grease further, eventually completely removing its capacity to lubricate the bearing and accelerating the rate of RCF damage, leading to more significant macropitting and material loss.

The final sequence to failure, only seen to its fullest extent in the accident bearing, occurred as debris released by the RCF damage was ground to powder and re-laid to form an unstable new race surface that continued to break up. This represented the final stage of the bearing's life until the dimensional clearances reduced sufficiently for the bearing to seize completely (Figure 100).

#### *Cage damage and wear*

The damage and wear to the cages was also indicative of this failure mechanism and was consistent across the accident bearing, the bearings removed from service and the rig test bearing. Figure 98 shows how the balls and cage rotate within the bearing, resulting in wear to the cage.

**Figure 98**

### Rotation of balls and cage within the bearing

The geometry of the bearing inner and outer races results in an angled spin axis for the balls. The scoring and witness marks within the pockets confirmed that the balls had been in contact with the sides of the pockets, resulting in a friction force that pushed the cage towards the seal, causing the narrow ends of the cages to be forced against the balls and the wide ends against the inner ring.

This force occurred whenever the cage rotational speed varied relative to the balls (Figure 99), but may also have been exacerbated by the bending moments acting on the bearing.

On the accident bearing the outboard cage, although fractured through three pockets at the narrow end, remained in one piece, whereas the inboard cage had broken completely into two sections. Where the fracture surfaces were not smeared, it was possible to identify fracture features consistent with fatigue. Momentary but repeated speed differences between the balls and the cage, driven by disruption to the procession of the balls, resulted in contact between the balls and the cage and generated tension across the pockets, creating the cyclic loading required to drive the fractures. Once the inboard cage broke into two sections it moved outwards against the outer race due to inertia, resulting in the wear mark on the outward side of the narrow end of the cage.

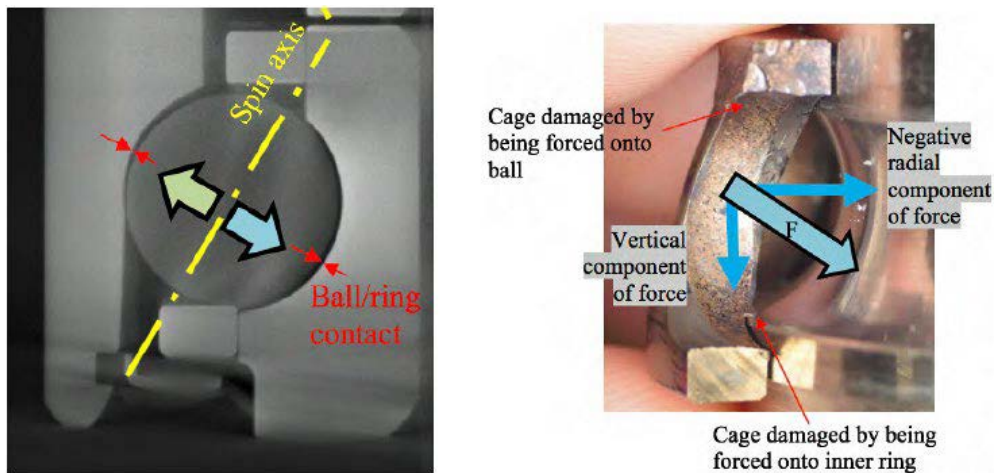


**Figure 99**

Ball spin axis and force generated by friction between the balls and the cage pocket

The disruptions in the procession of the balls were caused by lubrication failure events, resulting in the balls sliding rather than rolling. Once macropitting was present on the rolling surface, the increased friction as the ball rolled over the pitting would have exacerbated this.

Movement of the cages due to wear or failure allowed the balls to run on the edge of the race causing truncation and spalling and to move across the race surface extending the area of damage.

	Inner race	Balls	Cage	Outer race	Grease
1	Witness mark band from passage of balls.	The ceramic balls impart a loading and traction force on the inner ring.			The friction forces locally heat the bearing making the grease work harder, the grease is pushed out of the contact.
2	A dark etched region (DER) is formed under the raceway as the microstructure is changed.			Although loaded by the balls, the geometry of the contact reduces the local stress, no DER yet.	Grease, goes from brown to black, becomes thicker and sticky in consistency, with lumps. Some separation of the oil and thickener material.
3	Surface traction creates grain-flow and microcracks.	Increased friction at contact with inner ring, some sliding	Creation of witness marks within cage pockets.	Witness mark band from passage of balls. Ball sliding wear marks.	

Analysis

	Inner race	Balls	Cage	Outer race	Grease
4	RCF macro-cracking and creation of ring debris. Heating of inner ring affecting bulk microstructure (Heat affected zone and softening). Damage progresses with time creating increasingly rough running surface for balls.	The balls display crazing from heat and traction forces, lots more sliding and stopping of individual balls.	Cage slows relatively to individual balls (caused by other balls sliding). Friction between spinning balls and cage pocket forces cage towards seal, resulting in cage deformation and wear.	DER formed below the race surface. Grain flow at surface leading to RCF micro-cracking and micro pitting. Surface becomes rougher and produces debris.	Grease continues to degrade.  The friction present heats the grease fully degrading its properties, eventually turning it to dust.
5	Cage debris are free to move about the bearing, becoming adhered to the race rolling surface.		Cyclic loading of cage pockets by uneven ball procession drive fatigue cracks through narrow and wide ends of cage pockets		
6	A mix of cage, race and grease debris become over-rolled by the balls which are no longer constrained by the cage. A hybrid alloy material is deposited over the race surface.	With the cage broken the path the balls can take becomes more erratic and less confined. The balls run over the hybrid material rolling in more layers of debris.	Two pockets completely fail. Cage breaks into two sections, inertia throws them against the outer ring. Lots of cage debris is created adding to the mix of ring debris and remaining grease.	With the failure of the cage, the ball path is no longer stable and so can lead to plastic deformation of edge of raceway.	
7	Large subsurface cracks form within the weak hybrid layer of material, breaking out large chunks and re-depositing them.	Balls impart RCF loading conditions on the surface and subsurface of the hybrid material.	The cage continues to produce large amounts of debris. Hybrid debris flakes transfer to the cage pockets.	Hybrid debris flakes transfer to the outer race rolling surface and are over-rolled.	
8	A full race width piece of hybrid material fails through subsurface RCF. The chunk of material enters the pathway of the next ball.	The next ball cannot fit within the gap between the two raceways with the additional chunk of hybrid debris present. The ball stops relatively to the outer ring, applying torque to the normally stationary inner race.	The cage section with the jammed ball stops. The second cage section stops when it meets the first section. The bearing is seized	The locked bearing applies torque through the bearing housing, sliding the outer race within its housing.	
9	The torque on the inner race drives the rotation of the TRA control shaft.			The torque between the outer race and the housing is reduced by the rotation of the shaft.	

Figure 100

Figure showing failure sequence of the bearing

### *Review of flight and rig test data*

The data referred to in this section of the analysis can be found in [section 1.16.1.4](#).

Analysis of the flight test load survey data for axial load<sup>5</sup> and bending moment (M) confirmed a cluster of manoeuvres that generated bending moments higher than the largest moment considered by the bearing manufacturer in the development load spectrum, but which occurred in combination with axial load magnitudes that were approximately half the highest axial load considered within the development spectrum. All the cases occurred on flights which were conducted within the approved operating envelope for production helicopters, though some were recorded during higher altitude or specialist equipment test flights. However, the conclusion drawn in the test reports by the helicopter manufacturer for these flights was that the loads were matched or were less severe than those recorded during lower altitude, basic flights and as such they were not unique to those flight conditions.

When the combinations of medium (7-8 kN) axial loads and high bending moments recorded during these manoeuvres were assessed using the bearing manufacturer's current computational model, the inner race contact pressure and  $PV_{\max}$  were the same as with the most extreme axial load (13 kN) case in the development spectrum (3,100 MPa).

The contact pressure and  $PV_{\max}$  for the selected flight test manoeuvres were also similar to those which occurred under the actual (averaged) loads (combined axial and bending moment) applied during the manufacturer's rig test. As can be seen in the comparison of the highlighted areas on the summary graphs in [section 1.16.1.4](#). This is significant because the rig test generated the same damage characteristics seen in the accident bearing and others removed from service. It is therefore possible to conclude that the contact pressures which generated damage during the rig test can also be experienced by the bearing during operation of the helicopter in routine manoeuvres, though likely only under a limited set of operational circumstances.

The manoeuvres completed during the load survey test flights were a limited set of tightly defined individual test points. The axial and bending moment loads of interest were recorded during the dynamic entry and exit of the manoeuvres, as well as during the steady state 'on condition' part of the test point. Only the highest test point conditions were analysed during the investigation. The flight tests did not measure loads during dynamic combinations of manoeuvres and were necessarily flown in calm, low wind speed conditions, rather than the turbulent, gusting wind conditions that may be experienced in service.

<sup>5</sup> Also referred to as  $F_z$ ,  $F_a$  or TH1.

It is likely that what might be considered as less severe individual manoeuvres or combinations of manoeuvres, when flown in 'real world' conditions during the normal operation of the helicopter, can generate combinations of bending moment and axial load that result in the same or greater bearing contact pressures than the flight test and rig test points analysed by the investigation in [section 1.16.1.4](#) or considered by the original development load spectrum for the bearing (Table 4).

The accident helicopter was a production standard model and therefore not fitted with the sensors installed on the instrumented prototype airframes used for flight testing by the manufacturer. As such, it was not possible to determine exactly what axial loads, bending moments or contact pressures the accident bearing had experienced in service.

Some of the specific flight test points identified by the analysis which generated high contact pressures, related to simulated wind speeds from adverse directions<sup>6</sup>, ground taxiing and from autorotation manoeuvres. The flight recorder data recovered from the accident helicopter only provided a 25 hour snapshot of the 330 hours which the helicopter had been operated. But it did include evidence that the pilot practised autorotations, as would be expected of a commercial pilot maintaining currency in emergency procedures, and that the helicopter was taxied on the ground. Due to the shape of the football stadium, takeoffs could only be done in one of two directions orientated along the long axis of the pitch. The helicopter could potentially have been exposed to adverse wind directions as it emerged above the stadium roof, but this was not recorded in the flight data or journey logs. The helicopter was locked into this specific routine during the football season, differentiating it from other roles, such as offshore transport or Helicopter Emergency Medical Services (HEMS).

Without recorded data evidence for the whole life of the helicopter nor onboard load measuring or recording equipment, it was not possible to determine with certainty that the specific manoeuvres identified by the flight test analysis had been experienced by the accident helicopter, or whether other routine manoeuvres and flight conditions experienced by the helicopter had resulted in similar or greater contact pressures to those identified in flight and rig testing.

The ESUM data showed 12 transient exceedances of the RFM transmission maximum continuous torque limit. Seven of these events occurred prior to delivery of G-VSKP. The maximum torque reached was 109% for a duration of approximately 60 seconds. The Type Certificate Data Sheet (TCDS) for the AW169<sup>7</sup> provides an all-engines operating maximum torque limitation of 111%

6 See [section 1.6.5.2](#) for further explanation of adverse wind directions.

7 <https://www.easa.europa.eu/sites/default/files/dfu/AW169-TCDS%20R-509%20Issue1.pdf> (Accessed 3 July 2023)

for a duration of 5 minutes. It was therefore concluded that, while the ESUM data showed 12 transient exceedances of RFM limits the TCDS limits had not been exceeded.

No evidence was identified in 25 hours of recorded data recovered by the investigation that G-VSKP had been flown outside the approved envelope for the AW169 for that period. All the high contact pressure manoeuvres identified from the flight test data were also within the approved envelope for type certification. As such, there was no evidence to suggest that the accident duplex bearing had experienced, or had failed as a result of being subjected to, manoeuvres that were not approved for the AW169 in normal operation.

Although the contact pressures considered by the bearing manufacturer in the original development load spectrum during their development analysis were similar in magnitude to those which led to the failure in the rig test and subsequently highlighted by analysis of the flight test loads, they were considered in a different context by the bearing manufacturer at the time. The  $L_{10}$  analysis considered a theoretical distribution of contact pressures and durations across the life of the bearing based on an eventual failure by routine Hertzian RCF. This did not provide any guarantee that those high contact pressures could be sustained repetitively in a dynamic real world operating environment where bearing performance is also dependent on the response of the lubrication to sustained mechanical loading and elevated operating temperatures, potentially leading to lubrication film breakdown, surface shear loads and surface initiated cracking due to premature RCF.

When all the evidence available to the investigation was considered as a whole, including the very specific damage to the cages and races seen across all the bearings, the rig test results and the comparative flight and rig test contact pressure data analysis, it was concluded likely that the accident helicopter tail rotor duplex bearing failed due to premature grease deterioration and accumulation of race damage caused by high contact pressures, resulting from routinely conducted manoeuvres within the approved operating envelope of the helicopter.

#### *Variation in bearing time to failure*

There was significant variation in the operating lives of the bearings examined in this investigation. The extent of damage observed was not consistent with a simple relationship of increasing flight hours, with the accident bearing showing the maximum level of distress, whilst having the lowest service life<sup>8</sup>.

---

8 Bearing s/n 17115 is excluded from this, given that the failure mode was confirmed as being different from the accident bearing.

Analysis of the evidence available suggests that only a limited subset of manoeuvres generated combined loads sufficient to cause contact pressures within the bearing, that over time resulted in grease deterioration and race damage. The inherent flexibility in helicopter manoeuvres and diversity of atmospheric conditions in which they operate, results in significant potential variability in the duration, magnitude and frequency of exposure to the potentially damaging contact pressures associated with this subset of manoeuvres. These differences in the timing and severity of exposure to high contact pressures for each individual helicopter affected, resulted in significant potential variation in the accrued bearing life at which accumulation of damage was initiated, the rate at which the damage progressed towards failure and the extent of the damage observable at the time when they were inspected, following removal from service due to a maintenance inspection or as the result of an incident or accident.

In addition to the bearings chosen to be part of the investigation, it is possible that others removed from service over this period had developed damage to some degree but were either not returned to the manufacturer or were not subjected to the same disassembly inspection to identify and document the damage. It is also likely some helicopters in the AW169 and AW189 fleet were not subject to manoeuvres which generated bearing contact pressures sufficient to cause premature damage, as evidenced by the endurance rig test, or were subjected to these high contact pressure manoeuvres, but not to an extent sufficient to progress the cycle of grease deterioration far enough to result in observable damage, prior to the bearing being removed at the required discard life or replaced by the new standard of bearing. All these factors in combination may help to explain why only a relatively small number of tail rotor hybrid bearings operated in AW169s and AW189s either failed or were confirmed to have suffered damage.

Analysis of the tail rotor rotational speed from the 25 hours of flight data available to the investigation, also shows that the accident helicopter operated, as expected, in 'PLUS' mode for the majority of this time with some occasional reversions to 'BACKUP' mode. This resulted in approximately 75% of the tail rotor bearing's recorded operation being at rotational speeds above that used by the bearing manufacturer for their original and subsequent performance analysis of the bearing or by the helicopter manufacturer during their final rig test. Analysis of the 216 hours of ESUM data also showed similar extensive but expected operation of the tail rotor above 100% rpm. The majority occurring around 103% rpm, but with transients up to a maximum of 106%. Whilst these operational rotational speeds were well within the limits for the bearing, when combined with the other factors affecting contact pressure, they would have contributed to the duress the bearing was under, as illustrated by the PV factor. It is unlikely that this was significant in its contribution to the initiation

of the failure but may have accelerated the rate of damage accumulation within the accident bearing when compared to others in service or used in the final rig test.

### *Assessment of bearing certification requirements and testing*

#### *TDH rig tests*

TDH rig endurance tests were carried out during both the AW189 and AW169 development and were used as the main tests to validate that the bearing could operate satisfactorily, albeit the tail rotor duplex bearing was just one of many components being assessed in the rotor drive and control systems.

A visual only inspection of the condition of the bearings after the test, determined they were in good condition and this was considered sufficient by the manufacturer and the airworthiness authority to satisfy the certification requirement. The axial load sample data provided to the investigation showed similar magnitudes to the development load spectrum. Due to the high data sampling rate, it wasn't practical within the limitations of the investigation to calculate the bearing bending moments experienced, though given the test was inherently static, it is unlikely that they would have reached the levels recorded during the dynamic manoeuvres of flight test. As such, it was not possible to assess the contact pressures within the bearing to allow a comparison with the subsequent investigation rig testing. However, the lack of wear or damage seen during the visual inspection of the TDH test bearings, along with the condition of the grease, suggest the contact pressures and local temperatures of the inner races were not particularly high and less than the rig test which resulted in failure of the bearing.

#### *Flight test*

The original flight test programme used four flight test helicopters on the AW169 and five on the AW189. Several of the tail rotor duplex bearings fitted to these helicopters were replaced during the programme, for various reasons. As a result, the highest life achieved on a single bearing prior to certification was 558 hours, compared to the discard life of 2,400 hours. One of these bearings was removed from an AW169 flight test helicopter during a routine maintenance inspection for what was initially considered rough operation. This was the same inspection process which detected the failing bearings during the post-accident in-service inspections. However, the cause for removal during flight test was subsequently dismissed as inaccurate and the bearing was not investigated further, highlighting the subjective nature of the inspection criteria. The manufacturer confirmed that at the conclusion of the pre-certification flight test programme of both the AW189 and the AW169,

the installed duplex bearings remained fitted to the flight test helicopters. As such, none of the bearings removed during either helicopter type's pre-certification flight test programme were inspected for condition by the bearing manufacturer, neither were the bearings inspected after the pre-certification flight test programme had been completed.

Whilst at least some of the bearings would have experienced high contact pressures during the flight testing, it is likely that the very limited exposure duration to test manoeuvres which generated those high contact pressures, the multiple prototype airframes used for the testing and the limited total flight times on each bearing meant that the damage, if present, was not sufficient to have been detected by the on-wing inspections. The possible exception to this was the AW169 bearing removed for rough operation but as this was not investigated further, the evidence was lost.

Whilst the flight test load survey results were assessed by the helicopter manufacturer, this was primarily from a component fatigue life perspective, rather than to validate the load spectrum supplied to the bearing manufacturer during initial approval of the bearing for this application. The bearing manufacturer was not provided with any of the flight test data. They were the only party that had the specialist proprietary computer model to calculate the contact pressures resulting from the various axial load and bearing bending moment combinations recorded in flight. As such, a comparison of bearing contact pressures experienced during flight test with the original predicted design load spectrum contact pressures, was not carried out before the helicopter type designs were approved by the airworthiness authority and the AW189 and AW169 models entered service.

There was no requirement for the helicopter manufacturer to share the flight test data with the bearing manufacturer, as nothing in the airworthiness regulations requires flight data to be used to validate the accuracy of the theoretical load spectrum analysis for bearings. The bearing manufacturer had highlighted in their design document summarising their analysis of the theoretical load spectrum provided by the helicopter manufacturer, that the contact pressures were high for this bearing design. Their stated understanding was that the provided load spectrum included a safety margin in the maximum load cases and as such had confirmed the bearing was acceptable for the application. Had they been provided with the flight test data, it is possible they may have realised that this was not the case, given the actual flight loads recorded.

As the helicopter manufacturer ultimately decides the final build standard of their product, it was not possible to state definitively whether raising such concerns would have resulted in changes to the design in this specific case. However, the lack of regulatory requirements or guidance requiring both parties

to conduct a formal post-test review, contributed to the fact that no opportunity was ever provided to at least consider the continued suitability of the bearing in this application.

There is always the potential for theoretical loads analysis to underestimate the loads which occur in practice. This was the case with the initial AW149/AW189 bearing load spectrum (Table 2). Where subcontract suppliers hold the sole expertise to analyse the significance of this for the component they design and qualify against a specification, it is essential that the type design manufacturer shares all the subsequent data obtained from the installed rig and flight tests during development. This provides the opportunity for a 'closed loop' validation by the specialist manufacturer of their component within the system application in which it will be used. This is particularly significant for critical parts, where component failure has catastrophic implications. The following Safety Recommendation is made:

#### **Safety Recommendation 2023-018**

It is recommended that the European Union Aviation Safety Agency amend Certification Specification 29.602 to require type design manufacturers to provide the results of all relevant system and flight testing to any supplier who retains the sole expertise to assess the performance and reliability of components identified as critical parts within a specific system application, to verify that such components can safely meet the in-service operational demands, prior to the certification of the overall system.

#### *Rolling Contact Fatigue*

There are currently no explicit requirements within the CS 29 regulations defining how rolling contact fatigue should be addressed within the design process or any compliance test activity for any type of bearing, even though bearings are being used in critical safety applications on helicopters.

Following the LN-OJF accident and the subsequent Norwegian Safety Investigation Authority findings and recommendations, the European Union airworthiness authority undertook to review RCF as part of RMT 128 and an NPA was issued in February 2022, with various proposed amendments to CS 29, which were eventually included in Amendment 11 of CS 29 in February 2023.

The amendment to the AMC for CS 29.571 offers an improvement by providing guidance to manufacturers to at least consider rolling contact fatigue within their analysis. However, this regulation is aimed at Principal Structural Element

(PSE) components within a power drivetrain, rather than critical components within a control system, such as the duplex tail rotor bearing. The tail rotor which included the duplex bearing was certified to CS 29.547, so the manufacturer would not have considered CS 29.571 during the tail rotor design process. Only the Acceptable Means of Compliance has been amended rather than the regulation and this only states RCF should be considered during the analysis, as such it does not introduce any specific criteria, which must be met and demonstrated during certification, to ensure an appropriate minimum safety standard when dealing with components whose failure is assessed as catastrophic or hazardous. The mitigating actions it proposes are also aimed at drivetrain systems and include techniques such as magnetic chip detection, which is associated with a liquid oil lubrication system rather than an individual, sealed, grease lubricated component. The action taken to date does not adequately address the issue highlighted by this investigation of the lack of regulatory requirements specifically addressing the risk of catastrophic failure due to premature rolling contact fatigue in bearings identified as critical parts.

As such, the following Safety Recommendation is made:

#### **Safety Recommendation 2023-019**

It is recommended that the European Union Aviation Safety Agency introduce additional requirements to Certification Specification 29 to specifically address premature rolling contact fatigue failure across the full operating spectrum and service life of bearings used in safety critical applications.

#### 2.9.4 Associated factors

##### *Critical parts*

Although not causal to this accident, the tail rotor bearing has an ambiguous airworthiness status.

Currently only life limits and associated latent failure inspections deemed Critical Maintenance Requirements (CMR) for principal structural elements, identified under CS 29.571 and CS 29.573, are mandated by the regulations to be listed as airworthiness limitations in the ALS, which in this case is Chapter Four of the Approved Maintenance Planning Information (AMPI) manual. Other critical parts, whose failure is just as catastrophic for the helicopter, but which do not fit under this definition are just considered to have discard lives, which are managed as scheduled maintenance tasks in a different section of the AMPI (Chapter Five). Whilst the helicopter manufacturer and airworthiness authority argued that at a basic level all tasks and limits contained in the AMPI

are necessary for the continued airworthiness of the helicopter and discard lives are enforced, the difference in status of these components and the way they are considered and described in the AMPI, despite them having the same safety criticality, creates ambiguity. This is exemplified by the introduction to Chapter Five of the AMPI which states '*This section gives the recommended time limits requirements for the components of the helicopter*'. In contrast the ALS section of Chapter Four is clear that the life limits are an airworthiness requirement and can't be varied, even going to the extent of applying life limit reductions, where the operation of the helicopter is considered more severe than that used for the original life assessment analysis.

On the AW169 and AW189 the bearing manufacturer stated that a maximum service life was necessary given the magnitude of the load spectrum compared to the AW139, but the helicopter manufacturer maintained their approach from the AW139. Although development of the AW169 AMPI used an MPD process for assessing scheduled maintenance tasks, which added a degree of independent assessment, the basic regulatory analysis which fed this process was still conducted by the helicopter manufacturer and followed the historical precedence of the AW139 experience. The mitigating actions taken after the first failure of a tail rotor bearing on the AW139 took place in 2012, the same time the AW169 and AW189 bearings were being developed. The introduction of a discard life at that time was not mandated as the cause of the AW139 bearing failure was not confirmed and the change was precautionary. The helicopter manufacturer has subsequently amended the AW139 bearing discard life to 2,400 hours to be consistent with the maintenance task which removes the bearing. This was effectively mandated by an Airworthiness Directive from the European Union airworthiness authority, which required bearings with a higher or equal life to be removed from service and has continued the ambiguity over whether this is an airworthiness limitation or not.

The duplex bearing was identified as a critical part, as defined by CS 29.602, by the helicopter manufacturer because its failure was assessed as catastrophic, an assessment which has been validated by the circumstances of this accident. Analysis by its manufacturer of the bearing against the development load spectrum has also determined that it would have a finite life in this application, the mitigation for which is replacement before it reaches its anticipated failure life. The airworthiness considerations for non-structural critical parts are identified through assessment to demonstrate compliance with CS 29.602, but this regulation does not currently address life limits or their equivalent status to the ALS limits identified to comply with CS 29.571. As such, no specific rules or guidance are available to manufacturers to provide clarity on this issue.

A similar requirement does exist within CS-E dealing with critical parts on engines, where the level of detail in the regulation relating to assessment and

control of airworthiness limitations for critical parts is far greater than is provided in CS 29.602, even though they address the same catastrophic risk. The component life limits generated by the analysis to comply with this regulation are also required to be listed as airworthiness limitations in the ALS for the aircraft. CS-E.515 is provided in [Appendix F](#) for comparison. The following Safety Recommendations are made:

**Safety Recommendation 2023-020**

It is recommended that the European Union Aviation Safety Agency amend Certification Specification 29.602 to define the airworthiness status of life limits on non-structural critical parts and how they should be controlled in service.

**Safety Recommendation 2023-021**

It is recommended that the European Union Aviation Safety Agency define the airworthiness status of life limits and how they should be controlled for existing non-structural critical parts approved to Certification Specification 29.602 requirements, already in service.

The classification of the tail rotor duplex bearing as a critical part by the helicopter manufacturer meant that additional control measures were introduced during manufacture and installation of the bearing and required that duplicate and recorded inspections be carried out during maintenance. However, prior to the accident, there was no requirement in place, either regulatory or from the manufacturer, to conduct a sample assessment of the bearing condition after removal from service for any of the AW139, AW189 or AW169 fleets. This could have helped to validate the assumptions used for the calculated  $L_{10}$  life and discard time calculations by flagging up potential premature degradation issues. Time expired and rejected bearings were instead disposed of directly by operators, resulting in valuable evidence being lost. This issue of inspecting critical parts following rejection from service is an ongoing concern that has been identified in several previous accident investigations, including the investigation into LN-OJF, where a similar finding and recommendation was made<sup>9</sup>.

In response, the European Union airworthiness authority included a proposed amendment to CS 29.602 in NPA 2022-01, which introduced the concept of a Continued Integrity Verification Programme (CIVP). Whilst the basic principle of requiring a CIVP was a positive step in the right direction, the proposed wording of the amendment was confusing in that it specifically replaced 'shall' for 'must' in the changes to paragraph b of the regulation but reverted to 'shall' again for the new paragraph introducing the CIVP, suggesting a difference in their interpretation. The European Union official policy document on the use of English language suggests that 'shall' and 'must' are interchangeable in

<sup>9</sup> [Section 1.18.13](#) refers.

a regulatory context. However, the proposed wording of the complimentary AMC, introduced to support the regulation change, stated that a list of data sources 'can' be used to support the CIVP rather than 'must' be used, introducing an element of choice.

*'(2) The following data can be used to support the CIVP:*

- (i) analysis of occurrence reports;*
- (ii) analysis of unscheduled removal rates;*
- (iii) results of scheduled maintenance;*
- (iv) strip reports / analysis at overhaul;*
- (v) post-TC development and maturity tests;*
- (vi) additional inspection (non-destructive and/or destructive) and testing on selected high time or rejected components;*
- (vii) feedback from lead customers;'*

It went on to state:

*'The assessments required by the CIVP, as described above, should be performed at suitable periods through the complete life of the subject component types, considering the types of operation, environment and ageing effects expected. To meet this objective, an evaluation will need to be performed on at least one sample of each component at each major inspection interval or overhaul, and at retirement time, as applicable.*

*In addition, the applicant should consider scheduling early evaluation opportunities to confirm the suitability of the inspection intervals scheduled at entry into service.'*

This again was a positive improvement from the previous position of no requirement at all, but the wording still introduced an element of choice about when sampling should be completed and to what extent. It suggested that inspections are driven by expected ageing, not to identify or respond to unexpected issues. It set a low bar for time expired sampling and did not address inspection of premature failures. Given the significance of the failure of critical parts, mandating a clear, consistent standard is a proportionate response. Such an approach would be consistent with the way critical parts are

controlled in engines as defined by CS-E; the relevant content of CS-E.515 can be viewed in [Appendix F](#) for comparison.

The proposed change continued to have an element of ambiguity regarding the airworthiness approach to critical parts and raised doubts about whether the suggested CVP would in practice achieve the necessary level of validation from service run components. The other concern relating to the proposed amendment was that it only addressed the issue for new design helicopters, not existing helicopters already in service.

In February 2023 the proposed regulation amendments were withdrawn by EASA, following their review of comments received from the industry during the consultation process for the NPA. Although EASA have committed to continue to review potential regulation change, at the time of writing no further proposals have been put forward and the concern remains unaddressed.

Therefore, the following Safety Recommendations are made:

#### **Safety Recommendation 2023-022**

It is recommended that the European Union Aviation Safety Agency amend Certification Specification 29.602 to require manufacturers to implement a comprehensive post-removal from service assessment programme for critical parts. The findings from this should be used to ensure that reliability and life assumptions in the certification risk analysis for the critical part or the system in which it operates remain valid.

#### **Safety Recommendation 2023-023**

It is recommended that the European Union Aviation Safety Agency require manufacturers to retrospectively implement a comprehensive post-removal from service assessment programme for critical parts, approved to Certification Specification 29.602 requirements, already in service. The findings from this should be used to ensure that the reliability and life assumptions in the certification risk analysis for the critical part or the system in which it operates remain valid.

Starting with a theoretical load spectrum, calculation of a bearing  $L_{10}$  life<sup>10</sup> to define a service discard time, is a statistical process, based on best practice developed from industry experience. It cannot be accurately or repeatably demonstrated by a single test due to the variability of individual results. This

<sup>10</sup> See [section 1.18.6](#) for further detail.

theoretical calculation is based on ideal operating conditions, in terms of lubrication, contamination and other environmental factors leading to eventual failure due to routine, Hertzian rolling contact fatigue. Even assuming the theoretical assessment of the loads and operating conditions used to calculate the  $L_{10}$  life prove completely accurate in operation, by definition 10% of the bearings will likely still fail at a different life to that calculated. The  $L_{10}$  life of the AW169/AW189 bearing was reduced significantly to give an in-service discard time, which was based on the experience of the bearing manufacturer. The reduction from a 12,882 hour calculated  $L_{10}$  life to a 2,400 hour discard life, is indicative of the inherent variability in the way this theoretical assessment is made.

Only by virtue of its location in the tail rotor, the bearing was included in the tail rotor structural load analysis conducted to a set of load considerations listed in CS 29.547, though this just requires the structure to 'withstand' the prescribed limit loads. For the duplex bearing this translated to a limited set of seven theoretical load conditions. The only stated consideration in this development load spectrum regarding safety margins was related to static axial loads, where standard structural safety margins of limit and ultimate axial load were considered. Whilst the bearing manufacturer commented on the contact pressure generated by the static limit and ultimate axial load in the design spectrum provided to them, the use of any safety factor for the combined dynamic loads in this process was ambiguous and not clearly defined. As there are no specific regulations governing this process for non-PSE components such as the duplex bearing, there is no industry standard for what safety margin should be applied to the theoretical bearing dynamic load spectrum. In the case of the tail rotor bearing, the flight test loads demonstrated that there was little, if any, margin for the effect of contact pressure on bearings by the full spectrum of combinations of dynamic loads. Depending on what other regulations a non-structural critical part is subject to, there may not be any applicable loads analysis requirements or guidance at all.

The exposure durations for each of the load conditions used to calculate the  $L_{10}$  life, and thus discard time of the bearing, are also an approximation using an amalgamated flight profile, combining all the different roles the helicopter can be used for. This produces an estimated percentage of the operating life occurring at the various loads from the maximum to zero. Unlike Chapter Four airworthiness limitations in the AMPI, in practice there is:

- No requirement to operate in accordance with this profile.
- No in-service monitoring of actual operating profiles.
- No penalty life tariff applied to the tail rotor bearings for helicopters which operate for longer at higher loads and contact pressures.

As with the other aspects relating to management of critical parts, the example of how this is covered in much greater depth by the regulation CS-E.515 for engines, can be found in [Appendix F](#). The following Safety Recommendation is made:

**Safety Recommendation 2023-024**

It is recommended that the European Union Aviation Safety Agency amend Certification Specification 29.602 to provide guidance and set minimum standards for the calculation of design load spectrums for non-structural critical parts. They must encompass, with an appropriate and defined safety margin, the highest individual operating load and combination of dynamic operating loads, and the longest duration of exposure to such loads that can be experienced in operation.

*System safety analysis*

The certification process for the tail rotor system conducted by the helicopter manufacturer identified that the consequences of failure of the duplex bearing would be potentially catastrophic, but it did not correctly identify the mechanism by which this would eventually occur. Compliance with the various certification requirements during development did offer opportunities to identify and mitigate the failure sequence seen in the accident, but these opportunities were not realised at the time.

The failure mitigation recommended by the bearing manufacturer and employed by the helicopter manufacturer to prevent in-service failure of the duplex bearing, was a repetitive 400 hour subjective inspection for wear and smooth rotation of the bearing and a 2,400 hour discard time for the bearing.

Given that the bearing was a sealed unit and could not be checked internally, the maintenance inspection, even if carried out identically each time, would only have been able to identify gross issues with the bearing and was less reliable in outcome than a task with empirical acceptance and rejection criteria. Failure of the accident bearing, and others rejected in service, demonstrated that the 400 hour interval was too infrequent to address all possible causes of bearing degradation before they became catastrophic.

Though the failure analysis work conducted by the manufacturer of the helicopter identified that the failure of the duplex bearing and the castellated locking nut on the bearing end of the TRA control shaft would be catastrophic and the TRA manufacturer identified that failure of the castellated locking nut on the actuator end leading to loss of feedback control would be catastrophic; the

failure mechanism of the shaft rotating in the opposite direction to the thread on the actuator end locking nut, resulting in it 'unscrewing', was not identified as a potential outcome.

The AW139 was designed to have a left-hand thread on the actuator shaft and locking feature, to prevent it unscrewing if the actuator shaft rotated following a bearing failure. This suggests that the failure mode had been considered as part of the AW139 development. An AW139 bearing failure in 2012 demonstrated that this design successfully prevented the actuator shaft from unscrewing from the pin holder.

Whilst the subsequent bearing failure still resulted in a disconnection of the pilot's controls from the tail rotor blades, it allowed the actuator feedback system to remain connected, resulting in the blades moving to a relatively neutral position rather than driving to an extreme position as seen in this accident. This was all known to the helicopter manufacturer at the time the AW169 and AW189 tail rotor actuator was being developed, but the experience from the AW139 appears not to have crossed between product design teams or to the subcontract supplier of the actuator. The modification introducing a left-hand thread on the actuator has subsequently been introduced into service by the helicopter manufacturer on the AW169 and AW189 post-accident. Whilst this change alone may not have prevented the accident, it directly addresses a step within the accident sequence and the airworthiness authority considered it significant enough to mandate the change.

In a similar manner the castellated locking nuts on both ends of the shaft were identified as safety critical, requiring double locking features to comply with CS 29.607. However, the safety locking features employed were generic to vibration related issues. As such, they were not designed to prevent the locking nut from unscrewing against rotation driven by tail rotor drive torque during the accident sequence.

The existing certification requirements in CS 29.547 and CS 29.1309 and their Acceptable Means of Compliance (AMC) guidance, require a design assessment and failure analysis to be conducted to identify hazardous and catastrophic component failures within the tail rotor and its control system and minimise their occurrence to an acceptable level of probability. Indeed, the latest version of CS 29.1309 now goes further to state that no catastrophic failure should occur from a single cause.

Under the current interpretation of these regulations, the European Union airworthiness authority confirmed that there was no requirement to further assess the consequences of any component failure once that failure is classified as catastrophic. However, the failure of the duplex bearing and

the release of the castellated locking nut in this accident only became catastrophic when the consequences of that failure affected the surrounding system in which they operated.

As this accident demonstrates, where a bearing failure can lead directly to a catastrophic outcome, it is not enough to rely solely on statistically derived mitigations such as  $L_{10}$  life and the inspection efficacy and interval. It is just as important to try to mitigate the severity of the outcome as well as minimising occurrence. Manufacturers can employ additional techniques such as vibration and temperature or condition monitoring, along with a more in-depth and integrated failure analysis of the wider system to identify potential mechanical design changes, such as redundancy and damage or failure tolerant features, in combination with the statistical analysis. For example, the testing carried out during this investigation has shown that torque sensors on the control shaft can detect the initial transfer of torque by the bearing due to incipient seizure, before the damage reaches a stage where the bearing seizes completely and catastrophically, offering a potential early warning indication.

The safety actions introduced by the helicopter manufacturer and mandated by the airworthiness authority after the accident, show that aspects of this approach have subsequently been taken to retain the airworthiness of the AW169 and AW189 fleet. Lessons learnt from this should be incorporated into certification requirements to prevent future accidents. The change to the AMC for CS 29.571 in CS 29, Amendment 11 recommends taking a fail-safe approach to critical component design, but this is only aimed at structural components rather than control systems. This does not go far enough to address the need to review the entire system for mitigation options for failures initially assessed as catastrophic. This regulation was also not considered as part of the demonstration of compliance for either the tail rotor (including the duplex bearing) or the tail rotor hydraulic actuator.

The following Safety Recommendation is made:

#### **Safety Recommendation 2023-025**

It is recommended that the European Union Aviation Safety Agency amend the relevant requirements of Certification Specification 29 and their Acceptable Means of Compliance to emphasise that, where potentially catastrophic failure modes are identified, rather than rely solely on statistical analysis to address the risk, the wider system should also be reviewed for practical mitigation options, such as early warning systems and failure tolerant design, in order to mitigate the severity of the outcome as well as the likelihood of occurrence.

## 2.10 Safety Actions

The helicopter manufacturer took immediate steps following the accident to introduce inspections of the tail rotor duplex bearing on both AW169 and AW189 helicopters in service. These were mandated by EASA Airworthiness Directives.

Emergency AD 2018-0241-E was issued 7 November 2018 and referenced ASB 169-120 and 189-213 on 5 and 6 November 2018. It mandated a one-time visual inspection of the servo-actuator installation to identify movement of the castellated locking nut.

Emergency AD 2018-0250-E was issued on 19 November 2018. In addition to the requirements of the first AD, a precautionary one-off inspection of the duplex bearing was added.

The helicopter manufacturer then published ASB 169-125 and ASB 189-214 on 21 November 2018. Consequently, the EASA issued Emergency AD 2018-0252-E to mandate them. This introduced a one-time inspection and breakaway torque check of the duplex bearing and inspection and reinstallation of the servo-actuator castellated locking nut.

It was then determined that repetitive inspections of the duplex bearing were necessary for continued monitoring of the fleet. The helicopter manufacturer published ASB 169-126 and ASB 189-217 accordingly, and EASA issued Emergency AD 2018-0261-E on 30 November 2018 to mandate these inspections.

In the period following the introduction of these inspections, tail rotor system rig tests were being conducted by the helicopter manufacturer (see [section 1.16.1](#)). The test results showed that as the duplex bearing degraded, its operating temperature increased consistently.

A modification was developed by the helicopter manufacturer to install and repetitively inspect a thermal strip on the bearing end of the tail rotor actuator control shaft. This was introduced in ASB 169-135 and ASB 189-224 and mandated by the EASA through the issue of AD 2019-0023 on 1 February 2019.

Operator feedback from the repetitive tail rotor inspections allowed improved techniques to be developed and the helicopter manufacturer published ASB 169-148 and 189-237 on 29 May 2019, to provide instructions for more in-depth inspections of the duplex

bearing. The EASA issued AD 2019-0121 on 3 June 2019 to require accomplishment of these actions. Later revised to AD 2019-0121(R1).

The helicopter manufacturer introduced into service a modification to the Vibration Health Monitoring (VHM) system fitted to the AW169 and AW189 by issuing SB 169-140 and SB 189-227. The modification relocated an existing accelerometer sensor on the tail to the servo-actuator control lever, to allow monitoring of the vibration signature of the duplex bearing and provide an optional aid for the continued airworthiness of the fleet.

Whilst the modification itself was not mandated, the reporting of data from helicopters with the modification installed, was mandated. This requirement was included in EASAAD 2019-0193 issued 7 August 2019, which also included all the other inspection requirements and superseded AD 2019-0121(R1).

Modifications were introduced into service to address the findings of the investigation.

In early 2020, the helicopter manufacturer issued modification Service Bulletins 169-153 and 189-249. These introduced a new standard of tail rotor actuator. The control shaft now has a left-hand thread on the castellated lock nut and an additional washer fitted to the actuator end of the shaft. The EASA then issued Airworthiness Directive 2020-0048 on 6 March 2020, which superseded AD 2019-0193. This AD mandated the fitment of the new standard control actuator, with one-way interchangeability<sup>11</sup>. Fitting of the modified actuator alleviated the requirement to conduct an inspection of the castellated lock nut every 10 flight hours. All the additional inspections were retained in the new AD.

The final change by the manufacturer was to develop a new tail rotor duplex bearing introduced into service by Service Bulletins 169-162 and 189-254 on 4 August 2020.

Replacement with the new bearing was required within 400 flight hours or 4 calendar months of the SB issue date. The new bearing replaced the ceramic balls with steel balls. The new bearing had an introductory life limit of 400 flight hours. The Service Bulletin also

11 The old part number actuator can be replaced by the new part number actuator, but not the other way around.

required time expired bearings to be returned to the manufacturer for inspection following replacement.

Service Bulletins 169-178 and 189-272 were also issued on 4 August 2020 to increase the inspection intervals for the new bearing. The 10 hour repeat inspections of the thermal strip and the bearing were extended to 50 hour repeat inspections. While the 20 and 50 hour checks were extended to 100 hours, the 200 hour check was reduced to 100 hours.

EASA issued AD 2020-0197 on 10 September 2020 to mandate the SBs for fitment of the new bearing design and to extend the inspection intervals.

The day after the accident the operator took the following safety action:

All the operator's other company operated AW169 were grounded and, in accordance with their SMS procedure, did not resume operations until 30 November 2018, at which point the operator was satisfied that sufficient action had been taken to establish continuing airworthiness of the helicopter.

## 2.11 Operational oversight

Onshore helicopter operations are diverse in both their nature and the number of different types used. This diversity poses a challenge for the development of meaningful FDM algorithms that might compliment the operational supervision of helicopters, such as the AW169 type, equipped with FDM-capable systems. With such a widespread footprint, the airworthiness authority relies on operators to maintain effective tactical oversight of these operations. Without active and effective in-cockpit monitoring systems, comprehensive day-to-day oversight of single-pilot helicopter operations is impractical.

## 2.12 HUMS

The AW169 helicopter's systems incorporate vibration monitoring functions that are used in conjunction with Heliwise, a ground-based system, to detect the degradation of key components in the transmission system. The system gathers vibration data using accelerometers located strategically for the target components. The sample rates and Health Index or Health Indicator (HI) process algorithms are tuned to the target components. The trends in the HI results can be tracked using Heliwise as it is these rather than the absolute values, that indicate problems. The duplex bearing was not being monitored by this system.

The nearest sensor to the failed bearing was not in a location conducive to detecting these failures. Even had it sensed vibrations of concern, the operator did not, nor were they required to, upload the data for analysis after each flight. The manufacturer has introduced a new accelerometer at a location suitable for monitoring the tail rotor duplex bearing, with associated additional data gathering and processing updates. When installed, upload of the data recorded from it to the Heliwise system is mandated, but installation of the new sensor is optional.

The raw data from the accident flight was lost but the processed data was recovered. Historical HUMS data was also available. The last upload from G-VSKP to the Heliwise system provided helicopter data from 11 September 2018 to 28 September 2018. The manufacturer reviewed the available data for any issues and determined that no maintenance actions would have been triggered.

## 3 Conclusions

### 3.1 Findings

1. G-VSKP was operated out of Fairoaks Airport in compliance with the requirements for non-commercial operations with complex motor-powered aircraft established in Commission Regulation (EU) No 965/2012, in particular in Annex VI (Part-NCC).
2. The pilot was correctly licensed and qualified to conduct the flight.
3. The congested area permission for operations at the King Power Stadium required a Cat A departure to mitigate the risk of engine failure.
4. The average rate of climb during the accident flight rearwards climb exceeded the Cat A profile's parameters but the additional torque demand did not materially affect the post-failure controllability of the helicopter.
5. The helicopter was above an appropriate TDP height when the pilot committed to a CTO.
6. When above TDP height, but before completing the Cat A procedure acceleration profile, the pilot initiated a turn to the right while transitioning to forward flight.
7. A right yaw pedal input during the turn initiation resulted in the tail rotor actuator control shaft moving to the right under hydraulic pressure from the actuator.
8. The tail rotor duplex bearing seized resulting in the tail rotor actuator control shaft, driven by the high torque tail rotor drive system, rotating at high speed.
9. The axial movement of the tail rotor actuator control shaft maintained contact pressure between the pin carrier and the lock nut, causing the nut and pin carrier to friction weld together.
10. Both secondary locking features on the castellated locking nut at the actuator end of the shaft failed under the torque from the rotating shaft, and the control shaft unscrewed from the nut.

11. Once the control shaft was detached from the pin carrier, the feedback mechanism of the hydraulic control system became ineffective, and the control shaft continued to move under hydraulic pressure until the pitch of the tail rotor blades reached its physical limit of travel.
12. The rate of yaw of the helicopter continued to increase rapidly due to the unopposed main rotor torque couple and negative tail rotor blade pitch angle.
13. The pilot's yaw control pedals became ineffective after the TRA control shaft detached, resulting in the pilot being unable to control the direction or rate of yaw of the helicopter.
14. Without effective yaw control the pilot was unable to control the horizontal trajectory of the helicopter.
15. Cross-coupling of forces generated around the helicopter's normal axis by the high yaw rate, led to large deviations in pitch and roll.
16. Startle, surprise, disorientation and reduced visual cues due to the darkness were likely to have been performance shaping factors for the pilot response time; nonetheless, it was within the range expected considering simulator research, previous accidents and the circumstances when the failure occurred.
17. The position of the helicopter above the stadium roof at the point of loss of yaw control, may also have influenced the pilot's response.
18. The pilot lowered the collective to reduce main rotor thrust, thereby reducing its contribution to the destabilising torque which was driving the departure in yaw.
19. With the collective lowered the helicopter no longer had enough lift to maintain height and began to descend.
20. As the helicopter approached the ground, the pilot reduced the rate of descent by fully raising the collective lever.
21. The helicopter struck the ground across a 0.5 m step in the concrete surface of an area of rough ground and came to rest on its left side.
22. The analysis of the impact forces, experienced by the helicopter when it struck the step, indicated that they probably exceeded the design requirements of the helicopter.

23. The impact absorption features of the passenger cabin seats operated as designed and their condition indicated that the vertical deceleration force experienced by the passengers exceeded 30 g.
24. All the occupants suffered significant impact injuries; for one occupant these were likely to have been fatal.
25. Impact with the step resulted in disruption of the helicopter's fuel tanks allowing fuel to pool around the fuselage. This subsequently ignited.
26. The damage caused to the helicopter and its orientation provided numerous potential ignition sources for the leaking fuel.
27. First responders arrived at the accident site within one minute of the helicopter striking the ground and attempted to gain access to the cockpit and cabin. They were unable to do so due to the orientation of the fuselage, the strength of the cockpit windscreen and the rapid increase in the intensity of the fire.
28. The helicopter was rapidly engulfed by fire and the occupants who survived the initial impact died from inhaling the products of combustion.
29. Simulator trials confirmed to the investigation that the loss of yaw control was irrecoverable.
30. The helicopter was compliant with all applicable airworthiness requirements, had been correctly maintained and was appropriately certified for release to service prior to the accident flight.
31. The condition of the tail rotor duplex bearing could not have been predicted or identified by existing maintenance requirements prior to the accident.
32. The condition of the tail rotor duplex bearing began to deteriorate well before the accident flight.
33. An increase in contact pressure and temperature within the bearing races from a combination of axial and bending moment loads likely resulted in lubrication starvation events and degradation of the grease through aging.
34. High contact pressures and deterioration of the grease likely contributed to increased sliding of the ceramic balls leading to high surface shear stress and the development of surface initiated rolling contact fatigue.

35. The surface initiation of the cracks, shallow DER and the zone of changed material properties directly below the race surface were all indicative of the ceramic balls sliding rather than rolling.
36. The rolling contact fatigue resulted in distinctive surface initiated cracking which then progressed to extensive liberation of the race surface material.
37. The increased friction between the balls and the damaged race surface resulted in further heat generation which degraded the grease until it became powdered carbon and created a zone of changed material properties below the race surface.
38. The erratic movement of the balls across the rolling surface placed high loads on the bearing cage, resulting in wear and fatigue fractures.
39. Failure of the cage allowed the balls to move unrestrained across the race surface increasing the extent of the damage.
40. Released material from the cage and race surfaces was ground to dust by the action of the balls and combined with the carbon dust to be re-laid as a new rolling surface for the race.
41. The non-homogeneous and extensively cracked new rolling surface suffered further rolling contact fatigue, causing large sections of material to be released.
42. Eventually the dimensional clearances were reduced by the released material to the extent that the bearing seized.
43. Once the level of damage reached a certain threshold it became self-perpetuating under all operational loads, with an accelerating rate of progression towards ultimate failure of the bearing.
44. Rig test data analysis conducted during the investigation identified that high contact pressures within the bearing were sufficient to initiate a damage cycle that could result in incipient seizure of the bearing before the discard life of 2,400 hours.<sup>1</sup>

---

<sup>1</sup> The 2,400 hour life was based on assessment of the original development load spectrum. The highest actual contact pressure during the test was higher than the highest development spectrum contact pressure after the spectrum had been reassessed using the latest standard of modelling software. See [section 1.16.1.4](#).

45. Rig and flight test data analysis identified that a limited subset of manoeuvres within the normal operating envelope of the helicopter generated combined loads sufficient to cause potentially damaging contact pressures within the bearing.
46. Based on all the evidence available, it was likely that the accident helicopter tail rotor duplex bearing failed due to premature grease deterioration and accumulation of race damage, caused by high contact pressures, resulting from routinely conducted manoeuvres within the approved operating envelope of the helicopter.
47. The extent of damage observed on all the bearings investigated was not consistent with a simple relationship with increasing flight hours: the accident bearing showed the maximum level of distress, whilst having the lowest service life.
48. The inherent flexibility in helicopter manoeuvres and diversity of atmospheric conditions in which they operate, results in significant potential variability in the duration, magnitude and frequency of exposure to the potentially damaging contact pressures associated with this subset of manoeuvres.
49. These differences in the timing and severity of exposure to high contact pressures, for each individual helicopter affected, resulted in significant potential variation in the accrued bearing life at which accumulation of damage was initiated, the rate at which the damage progressed towards failure and the extent of the damage observable at the time when they were inspected, following removal from service due to a maintenance inspection or as the result of an incident or accident.
50. In addition to the bearings chosen to be part of the investigation, it's possible that others removed from service had developed damage to some degree but were either not returned to the manufacturer or were not subjected to the same disassembly inspection to identify and document the damage.
51. Some helicopters in the AW169 and AW189 fleet may never have been subject to manoeuvres which generated contact pressures sufficient to cause premature damage, prior to the bearing being removed at the required discard life or replaced by the new standard bearing.
52. Findings 46-49 in combination may help to explain why only a relatively small number of tail rotor hybrid bearings operated in AW169s and AW189s either failed or were confirmed to have suffered damage.

53. Certification testing for the tail rotor duplex bearing on both the AW169 and AW189 was compliant with the regulatory requirements.
54. There were no certification design or test requirements explicitly addressing rolling contact fatigue in bearings used on helicopters certified to CS 29.
55. The duplex bearings fitted to the flight test helicopters during certification flight testing of the AW169 and AW189 were not removed for detailed inspection at the end of the certification flight test programme, nor were they required to be for certification of the tail rotor control system.
56. The flight test results for tail rotor axial and bending moment loads were not shared with the bearing manufacturer in order to use their proprietary modelling software to validate the original analysis of the theoretical load spectrum and assess the continued suitability of the bearing for this application, nor were they required to be.
57. The failure analysis work conducted by the helicopter manufacturer during certification correctly identified that failure of the duplex bearing by seizure would be catastrophic.
58. The castellated locking nut on the tail rotor actuator end of the control shaft was identified as a catastrophic single point of failure, but only fracture of the nut or release due to vibration were considered.
59. Once the failure of any component was classified as catastrophic by the manufacturer, no further analysis of the failure mode was required by the airworthiness authority to meet certification requirements.
60. The failure mechanism of the shaft rotating in the opposite direction to the thread on the actuator end locking nut, allowing the pin carrier and nut to be released, was not identified by the AW169 certification analysis as a potential outcome of the bearing seizing.
61. The pin carrier and actuator on the AW139 were designed with a reverse thread to address the risk of bearing seizure and shaft rotation.
62. This failsafe design worked successfully during a tail rotor bearing failure on an AW139 in 2012, around the same time the design of the AW169 and AW189 actuator was being developed.

63. Compliance with the various certification risk assessment requirements during development offered opportunities to identify and mitigate the failure sequence seen in the accident, but these opportunities were not realised at the time, in part due to a reliance on statistical analysis to mitigate risk.
64. Although classed as a critical part, prior to the accident, the manufacturer of the helicopter did not require bearings removed from service to be returned to facilitate an inspection of their condition; nor was there any regulatory requirement or guidance that required them to do so.
65. No requirements or guidance were provided in the regulations about how critical part theoretical load spectrums should be calculated to ensure adequate safety margins.
66. From the extensive accident helicopter flight data recovered, no flight system problems were evident before the accident flight.
67. Logged faults were shown to be nuisance faults, evident on other serviceable aircraft and prior to successful flights.
68. The recorded data showed a number of alerts were triggered during the accident flight and related to the high yaw rate which developed after the tail rotor failure.
69. Of the internally logged system faults that occurred during the accident flight, only one could not be definitively attributed to nuisance issues, the high rotation rate or impact. Time alignment indicated this occurred just prior to impact and was not associated with the bearing failure or flight controllability.
70. The high yaw rate, peaking at 209°/s, would have generated significant forces on the occupants of the cockpit given their distance from the centre of gravity of the helicopter.
71. HUMS was installed capable of identifying increasing vibration trends in key components, but its use was not required for NCC operations.
72. The accelerometers fitted at the time for the purpose of vibration monitoring were not positioned to detect vibrations on the critical bearing that failed and were unlikely to do so.
73. The data from the closest accelerometer to the failed bearing was lost in the fire.

### 3.2 Causal Factors

1. Seizure of the tail rotor duplex bearing initiated a sequence of failures in the tail rotor pitch control mechanism which culminated in the unrecoverable loss of control of the tail rotor blade pitch angle and the blades moving to their physical limit of travel.
2. The unopposed main rotor torque couple and negative tail rotor blade pitch angle resulted in an increasing rate of rotation of the helicopter in yaw, which induced pitch and roll deviations and made effective control of the helicopter's flightpath impossible.
3. The tail rotor duplex bearing likely experienced a combination of dynamic axial and bending moment loads which generated internal contact pressures sufficient to result in lubrication breakdown and the balls sliding across the race surface. This caused premature, surface initiated rolling contact fatigue damage to accumulate until the bearing seized.

### 3.3 Contributory Factors

1. The load survey flight test results were not shared by the helicopter manufacturer with the bearing manufacturer in order to validate the original analysis of the theoretical load spectrum and assess the continued suitability of the bearing for this application, nor were they required to be by the regulatory requirements and guidance.
2. There were no design or test requirements in Certification Specification 29 which explicitly addressed rolling contact fatigue in bearings identified as critical parts; while the certification testing of the duplex bearing met the airworthiness authority's Acceptable Means of Compliance, it was not sufficiently representative of operational demands to identify the failure mode.
3. The manufacturer of the helicopter did not implement a routine inspection requirement for critical part bearings removed from service to review their condition against original design and certification assumptions, nor were they required to by the regulatory requirements and guidance.
4. Although the failure of the duplex bearing was classified as catastrophic in the certification failure analysis, the various failure sequences and possible risk reduction and mitigation measures within the wider tail rotor control system were not fully considered in the certification process; the regulatory guidance stated that this was not required.

## 4 Safety Recommendations and Actions

### 4.1 Safety Recommendations

The following Safety Recommendations were made:

#### **Safety Recommendation 2023-018**

It is recommended that the European Union Aviation Safety Agency amend Certification Specification 29.602 to require type design manufacturers to provide the results of all relevant system and flight testing to any supplier who retains the sole expertise to assess the performance and reliability of components identified as critical parts within a specific system application, to verify that such components can safely meet the in-service operational demands, prior to the certification of the overall system.

#### **Safety Recommendation 2023-019**

It is recommended that the European Union Aviation Safety Agency introduce additional requirements to Certification Specification 29 to specifically address premature rolling contact fatigue failure across the full operating spectrum and service life of bearings used in safety critical applications.

#### **Safety Recommendation 2023-020**

It is recommended that the European Union Aviation Safety Agency amend Certification Specification 29.602 to define the airworthiness status of life limits on non-structural critical parts and how they should be controlled in service.

#### **Safety Recommendation 2023-021**

It is recommended that the European Union Aviation Safety Agency define the airworthiness status of life limits and how they should be controlled for existing non-structural critical parts approved to Certification Specification 29.602 requirements, already in service.

#### **Safety Recommendation 2023-022**

It is recommended that the European Union Aviation Safety Agency amend Certification Specification 29.602 to require manufacturers to implement a comprehensive post removal from service

assessment programme for critical parts. The findings from this should be used to ensure that reliability and life assumptions in the certification risk analysis for the critical part or the system in which it operates remain valid.

#### **Safety Recommendation 2023-023**

It is recommended that the European Union Aviation Safety Agency require manufacturers to retrospectively implement a comprehensive post removal from service assessment programme for critical parts, approved to Certification Specification 29.602 requirements, already in service. The findings from this should be used to ensure that the reliability and life assumptions in the certification risk analysis for the critical part or the system in which it operates remain valid.

#### **Safety Recommendation 2023-024**

It is recommended that the European Union Aviation Safety Agency amend Certification Specification 29.602 to provide guidance and set minimum standards for the calculation of design load spectrums for non-structural critical parts. They must encompass, with an appropriate and defined safety margin, the highest individual operating load and combination of dynamic operating loads, and the longest duration of exposure to such loads that can be experienced in operation.

#### **Safety Recommendation 2023-025**

It is recommended that the European Union Aviation Safety Agency amend the relevant requirements of Certification Specification 29 and their Acceptable Means of Compliance to emphasise that where potentially catastrophic failure modes are identified, rather than rely solely on statistical analysis to address the risk, the wider system should also be reviewed for practical mitigation options, such as early warning systems and failure tolerant design, in order to mitigate the severity of the outcome as well as the likelihood of occurrence.

## 4.2 Safety action

This report presents the following safety actions:

### Safety action by the airworthiness authority

Emergency AD 2018-0241-E was issued 7 November 2018 to mandate ASB 169-120 and 189-213. This required a one-time visual inspection of the servo-actuator installation to identify movement of the castellated locking nut.

Emergency AD 2018-0250-E was issued on 19 November 2018. In addition to the requirements of the first AD, a precautionary one-off inspection of the duplex bearing was introduced.

EASA issued Emergency AD 2018-0252-E on 21 November 2018 to mandate ASB 169-125 and ASB 189-214. This introduced a one-time inspection and breakaway torque check of the duplex bearing, inspection and reinstallation of the servo-actuator castellated locking nut.

EASA issued Emergency AD 2018-0261-E on 30 November 2018 to mandate ASB 169-126 and ASB 189-217 to introduce repeat inspections.

EASA issued AD 2019-0023 on 1 February 2019 to mandate ASB 169-135 and ASB 189-224. These introduced a modification developed by the helicopter manufacturer to install and repetitively inspect a thermal strip on the bearing end of the tail rotor actuator control shaft.

EASA issued AD 2019-0121 on 3 June 2019, later revised to AD 2019-0121(R1), to require accomplishment of ASB 169-148 and 189-237, which provided instructions for more in-depth inspections of the duplex bearing.

EASA issued AD 2019-0193 on 7 August 2019, which mandated reporting from the new Vibration Health Monitoring modification introduced by the helicopter manufacturer, it also included all the other inspection requirements and superseded AD 2019-0121(R1).

The EASA issued Airworthiness Directive 2020-0048 on 6 March 2020, which superseded AD 2019-0193. This AD

mandated the fitment of the new standard control actuator, with one-way interchangeability<sup>1</sup>. Fitting of the modified actuator alleviated the requirement to conduct an inspection of the lock nut every 10 flight hours. All the additional inspections were retained in the new AD.

EASA issued AD 2020-0197 on 24 September 2020 to mandate the replacement of the tail rotor duplex bearing with a new design which used steel ball bearings rather than ceramic. The new bearing was introduced with a life limit of 400 flight hours. This allowed an extension of the inspection intervals on the thermal strip and bearing.

### **Safety action by the helicopter manufacturer**

ASB 169-120 and 189-213 were issued on by the helicopter manufacturer. This required a one-time visual inspection of the servo-actuator installation to identify movement of the locking nut.

The helicopter manufacturer published ASB 169-125 and ASB 189-214. This introduced a one-time inspection and breakaway torque check of the duplex bearing, inspection and reinstallation of the servo-actuator castellated nut.

The helicopter manufacturer published ASB 169-126 and ASB 189-217 to introduce repeat inspections of the bearing and lock nut.

A modification was developed by the helicopter manufacturer to install and repetitively inspect a thermal strip on the bearing end of the tail rotor actuator control shaft. This was introduced in ASB 169-135 and ASB 189-224.

Operator feedback from the repetitive tail rotor inspections allowed improved techniques to be developed and the helicopter manufacturer published ASB 169-148 and 189-237, to provide instructions for more in-depth inspections of the duplex bearing.

The helicopter manufacturer introduced into service a modification to the Vibration Health Monitoring (VHM) system fitted to the AW169 and AW189 by issuing SBs 169-140 and 189-227. The modification relocated an existing accelerometer sensor on the

<sup>1</sup> The old part number actuator can be replaced by the new part number actuator, but not the other way around.

tail to the servo-actuator control lever, to allow monitoring of the vibration signature of the duplex bearing as an optional aid to continued airworthiness.

In early 2020 the helicopter manufacturer issued modification Service Bulletins 169-153 and 189-249. These introduced a new standard of tail rotor actuator with a left-hand thread on the castellated lock nut and a washer, fitted to the actuator end of the shaft.

The manufacturer introduced a new tail rotor duplex bearing into service by issuing Service Bulletins 169-162 and 189-254 on 4 August 2020. Replacement with the new bearing was required within 400 flight hours or 4 calendar months of the SB issue date. The new bearing replaced the ceramic balls with steel balls. The new bearing had an introductory life limit of 400 flight hours. The Service Bulletin also required time expired bearings to be returned to the manufacturer for inspection following replacement.

Service Bulletins 169-178 and 189-272 were also issued on 4 August 2020 to increase the inspection intervals for the new bearing. The 10 hour repeat inspections of the thermal strip and the bearing were extended to 50 hour repeat inspections. While the 20 and 50 hour checks were extended to 100 hours and the 200 hour check reduced to 100 hours.

#### **Safety action by the helicopter operator**

The operator grounded all company operated AW169 the day after the accident and, in accordance with its SMS procedure, did not resume operations until the 30 November 2018 when they were satisfied that sufficient action had been taken to establish the airworthiness of the aircraft.

**Intentionally left blank**

Unless otherwise indicated, recommendations in this report are addressed to the appropriate regulatory authorities having responsibility for the matters with which the recommendation is concerned. It is for those authorities to decide what action is taken. In the United Kingdom the responsible authority is the Civil Aviation Authority, Aviation House, Beehive Ringroad, Crawley, West Sussex, RH6 0YR.



Aircraft Accident Report 1/2023

Report on the accident to  
**Leonardo AW169, G-VSKP**  
at King Power Stadium, Leicester  
on 27 October 2018